



University
of Glasgow

Higgs, Martin Robert (2008) *The role of the herpes simplex virus type 1 UL33 protein in DNA packaging*.
PhD thesis.

<http://theses.gla.ac.uk/315/>

Copyright and moral rights for this thesis are retained by the author

A copy can be downloaded for personal non-commercial research or study, without prior permission or charge

This thesis cannot be reproduced or quoted extensively from without first obtaining permission in writing from the Author

The content must not be changed in any way or sold commercially in any format or medium without the formal permission of the Author

When referring to this work, full bibliographic details including the author, title, awarding institution and date of the thesis must be given

**THE ROLE OF THE HERPES
SIMPLEX VIRUS TYPE 1 UL33
PROTEIN IN DNA PACKAGING**

by

Martin Robert Higgs

A thesis presented for the degree of Doctor of Philosophy in the Faculty of Biomedical
and Life Sciences at the University of Glasgow

MRC Virology Unit
Institute of Virology
Church Street
Glasgow
G11 5JR

June 2008

Abstract

The UL33 gene of herpes simplex virus type 1 (HSV-1) encodes a 130 amino acid (aa) protein that is essential for the cleavage of concatemeric viral DNA into monomeric genomes and their packaging into preformed capsids. Several lines of evidence have suggested that UL33, along with the UL15 and UL28 gene products, forms part of a terminase enzyme responsible for catalysing this process.

This thesis describes the creation and characterisation of a number of UL33 insertion mutants in an effort to examine structure-function relationships within this protein and gain further insights into its function. Sixteen distinct mutants, encoding polypeptides with 5 aa insertions located at 14 separate positions throughout the protein, were generated. The abilities of these mutants to complement the DNA packaging and growth defects of viruses lacking functional copies of UL33 (the null mutant *Δ*UL33 and the temperature sensitive mutant *ts1233*) were examined. Nine of the mutants were defective in both assays, and the capacity of all 16 mutants to support DNA packaging correlated precisely with their ability to complement virus growth. Regions of UL33 sensitive to insertion displayed a high degree of sequence conservation with UL33 homologues of other herpesviruses.

In agreement with previous reports, a direct interaction between UL33 and UL28 was demonstrated in immunofluorescence and immunoprecipitation assays. Although all sixteen mutants appeared to interact with UL28 in co-immunoprecipitation experiments, four of the insertion mutants were defective in co-localisation with UL28 in immunofluorescence assays. Interestingly, of these four mutants, three supported DNA packaging to wt levels. Similar experiments confirmed that UL33 interacts directly with UL15, and immunofluorescence assays indicated that none of the mutants was impaired in this interaction.

Novel interactions were also demonstrated between UL33 and the HSV-1 DNA packaging proteins UL6 and UL25. UL6 forms a portal vertex through which DNA is inserted into capsids, whilst UL25 is thought to play a structural role in stabilising capsids upon addition of DNA and is required only during the latter stages of encapsidation. All sixteen UL33 mutants were again able to interact with both partners in immunofluorescence assays. Of the remaining HSV-1 proteins necessary for genome encapsidation, neither UL17 nor UL32 interacted with UL33.

Immunofluorescence studies of virally infected cells revealed that UL15 was necessary for the localisation of the remaining terminase components (UL28 and UL33) to nuclear sites of viral DNA replication, where packaging occurs. This is consistent with a model originally proposed by Yang *et al.* (*J. Virol.* **81**:6419-6433, 2007), who suggested that a nuclear localisation signal within UL15 was necessary for the nuclear import of the terminase complex. Similar experiments revealed that, in the absence of UL6, none of the terminase components localised to replication compartments (RCs), suggesting that UL6 might be required for retaining the terminase at sites of DNA packaging.

Together, the data presented in this thesis are consistent with UL33 forming part of the HSV-1 terminase via its interactions with UL15 and UL28. It is also possible that UL33 contributes to the transient interaction of terminase with the portal protein, UL6, during packaging. Although the interaction between UL33 and UL25 warrants further examination, it could be relevant to the mechanism by which UL25 is recruited to capsids and functions at the late stages of the head-filling process.

Surprisingly, no clear evidence was obtained that any of the 16 mutants was defective in

interactions with UL6, UL15, UL25 or UL28. It is therefore not yet possible to conclude whether the observed interactions of UL33 with these four proteins are essential for viral DNA packaging. By the same token, the reason(s) why nine of the 16 mutants are defective in DNA packaging remains unclear, but does not appear to be associated with their ability to form known protein-protein interactions or to localise to sites of DNA packaging. The development of cell free systems and biochemical assays will be an important step in further characterising these proteins.

Table of contents

Abstract.....	2
Table of contents.....	5
List of figures and tables	12
Acknowledgements	17
Author's Declaration	17
Definitions.....	18
Chapter 1: Introduction.....	22
Section 1.1 The <i>Herpesviridae</i>	22
1.1.1 Definition of herpesviruses.....	22
1.1.2 Classification of the herpesviruses	23
1.1.3 Human herpesviruses and associated infection	25
1.1.4 Genomes.....	26
1.1.5 Capsids	29
1.1.6 Tegument.....	30
1.1.7 Envelope.....	30
Section 1.2 HSV-1 lytic replication	31
1.2.1 Genome structure.....	31
1.2.2 Attachment and entry	31
1.2.3 Genome circularisation.....	35
1.2.4 Regulation of gene expression.....	35
1.2.5 DNA replication	38
1.2.6 Capsid assembly and encapsidation	40
1.2.7 Replication compartments	40
1.2.8 Maturation and egress.....	41

Section 1.3	Viral DNA packaging	43
1.3.1	DNA packaging in dsDNA bacteriophage.....	43
1.3.2	HSV-1 DNA cleavage and packaging	57
Section 1.4	HSV-1 packaging proteins	66
1.4.1	UL6.....	66
1.4.2	UL17.....	68
1.4.3	UL32.....	69
1.4.4	UL25.....	70
1.4.5	UL12.....	72
1.4.6	UL15.....	73
1.4.7	UL28.....	75
1.4.8	UL33.....	76
1.4.9	The HSV-1 terminase: UL15, UL28 and UL33	79
1.4.10	DNA packaging as a drug target.....	83
Section 1.5	Aims	84
Chapter 2:	Materials and methods	86
Section 2.1	Materials.....	86
2.1.1	Chemicals and reagents.....	86
2.1.2	Stock solutions	86
2.1.3	Enzymes.....	89
2.1.4	Cells and culture media.....	89
2.1.5	Antibiotics	90
2.1.6	Viruses.....	91
2.1.7	Baculoviruses.....	91
2.1.8	Bacterial strains	92
2.1.9	Plasmids	92

2.1.10	Radiochemicals	93
2.1.11	Oligonucleotides	93
2.1.12	Antibodies	94
2.1.13	Miscellaneous reagents	95
2.1.14	Computer software	96
Section 2.2	Methods	96
2.2.1	DNA manipulation and analysis	96
2.2.2	Maintenance and manipulation of <i>E. coli</i>	99
2.2.3	DNA preparation	100
2.2.4	DNA sequencing	101
2.2.5	Cell culture and production of virus stocks	102
2.2.6	Creation of recombinant baculoviruses	104
2.2.7	Transfection of mammalian cells	106
2.2.8	Transient packaging assay	107
2.2.9	Southern Blotting and hybridisation	108
2.2.10	Complementation yield assay	109
2.2.11	Immunoprecipitation	110
2.2.12	Subcellular fractionation	111
2.2.13	Western blotting	112
2.2.14	Immunofluorescence	112
Chapter 3:	Using insertional mutagenesis to study UL33	114
Section 3.1	Introduction	114
Section 3.2	Creation and characterisation of UL33 insertional mutants	114
3.2.1	Insertional mutagenesis and identification of mutants	119
3.2.2	Sequencing of UL33 insertional mutants	121
3.2.3	Expression and localisation of mutated UL33 proteins	125

Section 3.3	Ability of UL33 insertional mutants to complement the growth of UL33 mutant viruses	129
3.3.1	Complementation yield analysis using <i>ts1233</i>	129
3.3.2	Complementation yield analysis using <i>dUL33</i>	135
Section 3.4	Ability of UL33 insertion mutants to support amplicon packaging	138
3.4.1	Amplicon packaging using <i>ts1233</i> helper virus	140
3.4.2	Packaging of <i>ts1233</i> genomes in the presence of mutated UL33 proteins	144
3.4.3	Amplicon packaging using <i>dUL33</i>	145
3.4.4	Packaging of <i>dUL33</i> genomes by UL33 mutants.....	150
3.4.5	Ability of mutants to inhibit wt HSV-1 packaging.....	150
Section 3.5	Discussion	155
3.5.1	Isolation and initial characterisation of mutants	155
3.5.2	Ability of mutants to support DNA packaging and complement virus growth	155
Chapter 4:	Interaction of wt and mutated UL33 proteins with the terminase components UL15 and UL28.....	162
Section 4.1	Introduction	162
Section 4.2	Interaction of wt and mutated UL33 proteins with UL15.....	162
4.2.1	UL15 and UL33 interact in recombinant baculovirus-infected cells	163
4.2.2	UL15 and UL33 interact in HSV-1 infected cells.....	166
4.2.3	Immunofluorescence assay for the interaction of wt UL33 with UL15pp65.....	168
4.2.4	Ability of mutated UL33 proteins to interact with UL15-pp65	169
Section 4.3	Interaction of wt and mutated UL33 proteins with UL28.....	172
4.3.1	UL28 and UL33 interact in recombinant baculovirus-infected cells	173
4.3.2	UL28 and UL33 interact in HSV-1-infected cells.....	173

4.3.3	Immunofluorescence assay for the interaction of wt UL33 with UL28-cMyc....	176
4.3.4	Ability of mutated UL33 proteins to interact with UL28-cMyc.....	181
4.3.5	Creation of recombinant baculoviruses expressing mutated UL33 proteins.	184
4.3.6	Ability of mutated UL33 proteins to interact with UL28 in insect cells	186
Section 4.4	Characterisation of UL33 internal deletion mutants.....	187
4.4.1	Ability of $\Delta 1$ and $\Delta 2$ to support DNA packaging and mutant virus growth	189
4.4.2	Immunofluorescence assay for the interaction of $\Delta 1$ and $\Delta 2$ with UL15-pp65	192
4.4.3	Immunofluorescence assay for the interaction of $\Delta 1$ and $\Delta 2$ with UL28-cMyc.	197
4.4.4	Localisation of the UL15-UL28-UL33 complex in transfected cells.....	199
Section 4.5	Discussion	201
4.5.1	Interaction between UL15 and UL33.....	201
4.5.2	Interaction between UL28 and UL33.....	203
Chapter 5:	Interaction of wt and mutated UL33 with other packaging proteins.....	207
Section 5.1	Introduction	207
Section 5.2	Interactions of UL33 with UL6 and UL6in269	207
5.2.1	Co-immunoprecipitation of UL6 and UL33 from HSV-1 infected cells	208
5.2.2	Co-immunoprecipitation of UL6 and UL33 from recombinant baculovirus- infected insect cells	208
5.2.3	Co-localisation of wt UL6 and UL33-HIS ₆ in transfected cells.....	210
5.2.4	Immunofluorescence assay for the interaction of wt UL33 with UL6.....	212
5.2.5	Ability of mutated UL33 proteins to interact with wt UL6	215
5.2.6	Immunofluorescence assay for the interaction of wt UL33 with UL6in269.	217
5.2.7	Ability of mutated UL33 proteins to interact with UL6in269	219

Section 5.3	Interaction of UL33 with UL17	222
5.3.1	Immunoprecipitation analysis of UL17 and UL33 from HSV-1 infected cells...	222
5.3.2	Immunoprecipitation analysis of UL17 and UL33 from recombinant baculovirus-infected insect cells.....	222
5.3.3	Sub-cellular localisation of UL17 and UL33 in transfected cells.....	224
Section 5.4	Interaction of UL33 with UL25	224
5.4.1	Co-immunoprecipitation of UL25 and UL33 from HSV-1 infected cells.....	227
5.4.2	Co-immunoprecipitation of UL25 and UL33 in recombinant baculovirus- infected insect cells	227
5.4.3	Co-localisation of UL25 and UL33 in transfected cells.....	230
5.4.4	Co-localisation of UL25 and mutated UL33 proteins in transfected cells.....	232
Section 5.5	Interactions of UL33 with UL32	232
5.5.1	Immunoprecipitation of UL32 and UL33 from HSV-1-infected cells.....	232
5.5.2	Immunoprecipitation of UL32 and UL33 from baculovirus-infected insect cells	235
5.5.3	Sub-cellular localisation of UL32 and UL33 in transfected cells.....	235
Section 5.6	Discussion	238
5.6.1	UL33 interacts with UL6.....	238
5.6.2	UL33 interacts with UL25.....	241
5.6.3	UL33 interacts with neither UL17 nor UL32.....	244
Chapter 6:	The localisation of terminase proteins to viral replication compartments	247
Section 6.1	Introduction	247
Section 6.2	Visualisation of the terminase proteins in infected cells.....	247
6.2.1	Visualisation of UL15, UL28 and UL33 in infected cells.....	248

Section 6.3	Ability of wt and mutated UL33 proteins to localise to RCs.....	251
6.3.1	Localisation of transiently transfected UL33 in <i>dUL33</i> -infected cells.....	251
6.3.2	Ability of mutated UL33 proteins to localise to RCs.....	253
Section 6.4	The role of UL15, UL28 and UL33 in localising the terminase components to replication compartments	255
6.4.1	Localisation of putative terminase components in cells infected with viruses lacking functional copies of UL15, UL28 and UL33.....	255
6.4.2	Western blot analysis of cells infected with S648, gCB and <i>dUL33</i>	259
6.4.3	Subcellular location of UL28 and UL33 in the absence of UL15	261
6.4.4	UL15 supplied <i>in trans</i> is sufficient to restore the localisation of UL28 and UL33 to RCs in S648-infected cells.....	263
Section 6.5	Localisation of UL6 in HSV-1-infected cells	266
6.5.1	UL6 localises to RCs early during viral infection.....	266
6.5.2	UL6 is necessary for the localisation of the putative terminase to RCs	268
6.5.3	UL6 localisation to RCs is unaffected by the absence of the putative terminase subunits.....	270
Section 6.6	Discussion	270
6.6.1	Localisation of wt UL6, UL15, UL28 and UL33 to RCs.....	270
6.6.2	The mechanism of terminase localisation to RCs.....	272
6.6.3	Localisation of mutated UL33 proteins to RCs.....	275
Chapter 7:	Conclusions.....	276
Section 7.1	Future perspectives	284
References	287

List of figures and tables

	Page:
Figure 1.1: Genome structures within the herpesviruses	27
Figure 1.2: HSV-1 genome structure and isomers	32
Figure 1.3: Structure of the λ bacteriophage <i>cos</i> site	48
Figure 1.4: A mechanism for λ bacteriophage DNA packaging	52
Figure 1.5: A model for HSV-1 DNA packaging	58
Figure 1.6: Pathways of HSV-1 capsid assembly	61
Figure 1.7: The HSV-1 strain 17 <i>syn+ a</i> sequence	65
Figure 3.1: Nucleotide alignment of pUL33 with related herpes simplex virus sequences	116
Figure 3.2: Principles of the MGS transposition system	117
Figure 3.3: Screening for insertions within the UL33 gene	120
Figure 3.4: Mapping positions of insertion within UL33 by restriction digest	122
Figure 3.5: Position and sequence of 15 bp insertions within the UL33 gene	123
Figure 3.6: Positions and sequence of 5 aa insertions in the UL33 protein	124
Figure 3.7: Analysis of mutated polypeptide expression in transfected cells	126
Figure 3.8: Localisation of the UL33 protein in transfected cells	128
Figure 3.9: The cellular localisation of mutated UL33 proteins in transfected cells	130
Figure 3.10: Ability of mutants to complement <i>ts1233</i> growth	133
Figure 3.11: Western analysis of UL33 expression in the <i>ts1233</i> complementation assay	134
Figure 3.12: Ability of mutants to complement <i>dUL33</i> growth	136
Figure 3.13: Western analysis of UL33 expression in the <i>dUL33</i> complementation assay	137
Figure 3.14: The amplicon packaging assay	139
Figure 3.15: Ability of UL33 mutants to package amplicon DNA in the presence of <i>ts1233</i>	141

Figure 3.16: Ability of UL33 mutants to package <i>wt</i> 1233 genomes.....	146
Figure 3.17: Ability of UL33 mutants to package amplicon DNA in the presence of <i>d</i> UL33	147
Figure 3.18: Ability of UL33 mutants to package <i>d</i> UL33 genomes.....	151
Figure 3.19: Ability of mutants to act as dominant negative DNA packaging inhibitors ..	153
Figure 3.20: The position of UL33 insertional mutants relative to amino acids conserved amongst the <i>alphaherpesvirinae</i>	157
Figure 3.21: The position of 5 aa inserts relative to the predicted secondary structure of UL33	160
Figure 4.1: Co-immunoprecipitation of UL15 and UL33 from recombinant baculovirus- infected cells.....	164
Figure 4.2: Co-immunoprecipitation of UL15 and UL33 from HSV-1-infected cells.....	167
Figure 4.3: Co-localisation of UL15-pp65 and UL33 in transfected cells.	170
Figure 4.4: Subcellular localisation of UL15-pp65 and mutated UL33 proteins in transfected cells	171
Figure 4.5: Co-immunoprecipitation of UL28 and UL33 from recombinant baculovirus- infected cells.....	174
Figure 4.6: Co-immunoprecipitation of UL28 and UL33 from HSV-1-infected cells.....	177
Figure 4.7: Co-localisation of UL28-cMyc and UL33 in transfected cells.....	178
Figure 4.8: Intracellular distribution of UL28-cMyc and UL9 in transfected cells.....	180
Figure 4.9: Subcellular localisation of UL28-cMyc and mutated UL33 proteins in transfected cells	182
Figure 4.10: Principles of the Bac-to-Bac Baculovirus expression system	185
Figure 4.11: Interaction of mutated UL33 proteins with UL28 in recombinant baculovirus- infected cells.....	188
Figure 4.12: Sequences of proteins encoded by p Δ 1 and p Δ 2	190

Figure 4.13: Ability of UL33 internal deletion mutants to support DNA packaging and <i>d</i> UL33 growth.....	191
Figure 4.14: Expression of UL33 internal deletion mutants.....	193
Figure 4.15: Ability of UL33 internal deletion mutants to interact with UL15-pp65	195
Figure 4.16: Subcellular distribution of internal UL33 deletion mutants and UL9 in transfected cells	196
Figure 4.17: Ability of UL33 internal deletion mutants to interact with UL28-cMyc.....	198
Figure 4.18: Localisation of the UL15-UL28-UL33 complexes in transfected cells	200
Figure 4.19: The position of $\Delta 1$ and $\Delta 2$ relative to amino acids conserved amongst the <i>alphaherpesvirinae</i>	205
Figure 5.1: Co-immunoprecipitation of UL6 and UL33 from HSV-1 infected cells.....	209
Figure 5.2: Co-immunoprecipitation of UL6 and UL33 from recombinant baculovirus-infected cells.....	211
Figure 5.3: Co-localisation of UL6 and UL33-HIS ₆ in transfected cells	213
Figure 5.4: Co-localisation of UL6 and UL33 in transfected cells.....	214
Figure 5.5: Co-localisation of UL6 and mutated UL33 proteins in transfected cells.....	216
Figure 5.6: Co-localisation of UL6 ⁱⁿ²⁶⁹ and UL33 in transfected cells	218
Figure 5.7: Intracellular localisation of UL6 ⁱⁿ²⁶⁹ and UL9 in transfected cells.....	220
Figure 5.8: Co-localisation of UL6 ⁱⁿ²⁶⁹ and mutated UL33 proteins in transfected cells	221
Figure 5.9: Immunoprecipitation of UL17 and UL33 from HSV-1-infected cells.....	223
Figure 5.10: Immunoprecipitation of UL17 and UL33 from recombinant baculovirus-infected cells.....	225
Figure 5.11: Intracellular localisation of UL17 and UL33 in transfected cells	226
Figure 5.12: Co-immunoprecipitation of UL25 and UL33 from HSV-1 infected cells.....	228
Figure 5.13: Co-immunoprecipitation of UL25 and UL33 from recombinant baculovirus-infected cells.....	229

Figure 5.14: Co-localisation of UL25 and UL33 in transfected cells.....	231
Figure 5.15: Intracellular localisation of UL25 and UL9 in transfected cells	233
Figure 5.16: Co-localisation of UL25 and mutated UL33 proteins in transfected cells.....	234
Figure 5.17: Immunoprecipitation of UL32 and UL33 from HSV-1-infected cells	236
Figure 5.18: Immunoprecipitation of UL32 and UL33 from recombinant baculovirus- infected cells.....	237
Figure 5.19: Intracellular localisation of UL32 and UL33 in transfected cells	239
Figure 5.20: The location of the proposed UL17-UL25 heterodimer on C-capsids (from Trus <i>et al.</i> , 2007).....	243
Figure 6.1: Visualisation of the terminase components in HSV-1-infected cells.....	249
Figure 6.2: Localisation of transiently expressed UL33 in Δ UL33-infected cells	252
Figure 6.3: Localisation of mutated UL33 proteins in Δ UL33-infected cells.....	254
Figure 6.4: Localisation of the terminase components in cells infected with viruses lacking UL15, UL28 or UL33.....	257
Figure 6.5: Western blot analysis of cells infected with viruses lacking UL15, UL28 or UL33	260
Figure 6.6: The subcellular location of UL28 and UL33 in the absence of UL15	262
Figure 6.7: Supply of UL15 <i>in trans</i> restores the ability of UL28 and UL33 to.....	264
Figure 6.8: UL6 co-localises with ICP8 in HSV-1 infected cells.....	267
Figure 6.9: UL6 is required for the localisation of terminase components to RCs.....	269
Figure 6.10: Localisation of UL6 to RCs is independent of UL15, UL28 and UL33	271
Figure 7.1: A model for terminase assembly on the capsid portal.....	281

	Page
Table 3.1: Quantification of amplicon packaging in the presence of <i>ts1233</i>	143
Table 3.2: Quantification of amplicon packaging in the presence of <i>dlUL33</i>	149
Table 3.3: Quantification of dominant-negative packaging assays	154
Table 4.1: Ability of UL33 mutants to interact with UL28-cMyc in an immunofluorescence assay.....	183
Table 5.1: A summary of previously identified protein-protein interactions involving UL33 homologues from EBV, KSHV and VZV.....	246
Table 7.1: Summary of the properties of the UL33 insertion and deletion mutants	277

Acknowledgements

I would like to thank Professor Duncan McGeoch for allowing me the opportunity to work within the MRC Virology Unit.

I am also indebted to Dr Nigel Stow for his tireless enthusiasm and guidance, and for his observations during the preparation of this thesis.

Thanks must also go to the past and present members of lab 201, especially Maureen O'Hara, Mary Murphy, Dr Blair Strang and Dr Valerie Preston, for their support, discussions and advice during my period in the lab. Similarly, heartfelt appreciation goes to my friends and fellow 'inmates' of the quiet room who provided invaluable support during the preparation of this thesis.

My lasting gratitude must go to the members of my family, especially my parents, for their support during difficult times. Finally, my deepest love and thanks to Claire, who, despite her own experiences, was helpful, supportive and encouraging throughout the course of my studies.

Author's Declaration

The author was the recipient of a Medical Research Council Studentship. Except where stated, the work presented in this thesis was carried out by the author.

Definitions

μCi	- microcurie
μg	- microgram
μl	- microlitre
μM	- micromolar
μm	- micrometer
aa	- amino acid
AcMNPV	- <i>Autographa californica</i> multicapsid nucleopolyhedrovirus
ADP	- adenosine diphosphate
ATP	- adenosine triphosphate
ATPase	- adenosine triphosphatase
bp	- base pair
BHK (cells)	- baby hamster kidney (cells)
CAV	- cell associated virus
CIP	- calf intestinal phosphatase
CLB	- cell lysis buffer
CRV	- cell released virus
Cy5	- cyanine-5
dATP	- 2' –deoxyadenosine-5'-triphosphate
dCTP	- 2' –deoxycytidine-5'-triphosphate
dGTP	- 2' –deoxyguanosine-5'-triphosphate
DMEM	- Dulbecco's modified Eagle's medium
DMSO	- dimethylsulphoxide
DNA	- deoxyribonucleic acid
DNase	- deoxyribonuclease
ds	- double stranded
dTTP	- 2' –deoxythymidine-5'-triphosphate
<i>E. coli</i>	- <i>Escherichia coli</i>
EBV	- Epstein-Barr virus
EDTA	- ethylenediaminetetra-acetic acid
EtBr	- ethidium bromide
FCS	- foetal calf serum

FITC	- fluorescein isothiocyanate
GMEM	- Glasgow's modified Eagle's medium
GPCMV	- guinea pig cytomegalovirus
GST	- glutathione-S-transferase
HCMV	- human cytomegalovirus
HeBS	- hepes buffered saline
hepes	- N-[2,-hydroxyethyl]piperazine-H ⁺ -[2-ethane sulphonic acid]
HHV-6	- human herpesvirus 6
HHV-7	- human herpesvirus 7
HHV-8	- human herpesvirus 8
HSV-1	- herpes simplex virus type 1
HSV-2	- herpes simplex virus type 2
h	- hours
h.p.i.	- hours post infection
h.p.t.	- hours post transfection
HRP	- horseradish peroxidase
IE	- immediate early
IHF	- integration host factor
kbp	- kilobase pairs
kDa	- kilo daltons
KSHV	- Kaposi's sarcoma associated herpesvirus (HHV-8)
LB	- L-broth
M	- molar
MBP	- maltose binding protein
MCS	- multiple cloning site
mg	- milligram
MIEP	- major immediate early promoter
min	- minutes
ml	- millilitre
mM	- millimolar
mm	- millimetre
NBCS	- newborn calf serum
nm	- nanometre
NPT	- non-permissive temperature
NP40	- nonidet NP40 detergent

NTB	- nick-translation buffer
°C	- degrees Celsius
ORF	- open reading frame
P _i	- inorganic phosphate
p.f.u.	- plaque forming unit
PBS	- phosphate buffered saline
PMSF	- phenylmethylsulphonyl fluoride
PRV	- pseudorabies virus
PT	- permissive temperature
PVDF	- polyvinylidene fluoride
RCs	- replication compartments
RNA	- ribonucleic acid
RNase	- ribonuclease
rpm	- revolutions per minute
RSB	- reticulocyte standard buffer
RSC	- rabbit skin cell
SDS	- sodium dodecyl sulphate
SDS-PAGE	- SDS- polyacrylamide gel electrophoresis
sec	- second
Sf21 (cells)	- <i>Spodoptera frugiperda</i> strain 21 (cells)
ss	- single stranded
SSC	- standard saline citrate
TEMED	- N,N,N',N'-tetra-methyl-ethylene diamine
Tris	- 2-amino-2(hydroxymethyl)-1,3-propanediol
Triton X-100	- octyl phenoxy polyethoxy ethanol
ts	- temperature sensitive
TBS	- Tris buffered saline
U	- units
UV	- ultra violet
V	- volts
v/v	- volume ÷ volume
VZV	- varicella zoster virus
w/v	- weight ÷ volume
wt	- wild type
X-Gal	- 5-bromo-4-chloro-3-indolyl-(D-galacto pyranoside)

Amino acids

Alanine	Ala	A	Leucine	Leu	L
Arginine	Arg	R	Lysine	Lys	K
Asparagine	Asn	N	Methionine	Met	M
Aspartate	Asp	D	Phenylalanine	Phe	F
Cysteine	Cys	C	Proline	Pro	P
Glutamate	Glu	E	Serine	Ser	S
Glutamine	Gln	Q	Threonine	Thr	T
Glycine	Gly	G	Tryptophan	Trp	W
Histidine	His	H	Tyrosine	Tyr	Y
Isoleucine	Ile	I	Valine	Val	V

Chapter 1: Introduction

The work presented in this thesis relates to the role that the herpes simplex virus type 1 (HSV-1) UL33 protein plays in packaging viral DNA into the capsid. In the following introduction, the general properties of the herpesvirus family are discussed, followed by an outline of the HSV-1 life cycle. The well-characterised process of DNA packaging in bacteriophage is then examined in detail. Finally, the literature relating to HSV-1 DNA packaging is reviewed, especially with regard to UL33 and its role as a putative component of the viral terminase enzyme.

Section 1.1 The *Herpesviridae*

1.1.1 Definition of herpesviruses

Herpesviruses are large double-stranded DNA viruses that have historically been defined by the architecture of their virions. A large linear dsDNA genome is contained within an icosahedral capsid shell, which is in turn surrounded by a proteinaceous tegument layer, and encased by a lipid bilayer containing several virally encoded proteins. Over 100 members of the *Herpesviridae* have been identified in a wide range of vertebrate species (reptiles, mammals, birds, amphibians and fish), together with a single virus able to infect several related marine bivalve species (Arzul *et al.*, 2001; Davison *et al.*, 2005).

Natural infection by herpesviruses generally causes only limited disease, and is usually restricted to a single host. Members of the family exhibit several common characteristics:

1. All encode proteins involved in the synthesis of nucleic acid and metabolism of nucleotides, such as DNA polymerase and helicase-primase enzymes. Furthermore, all herpesviruses encode enzymes involved in protein processing (e.g. kinases and proteases).
2. Many members of the family have been demonstrated to establish and maintain a

persistent infection in their natural hosts, termed latency. Latent genomes exist as circular episomes, with only a subset of viral genes undergoing transcription. Reactivation of latent virus leads to productive infection and associated disease.

3. Productive infection leading to virion release invariably results in death of the host cell.
4. The processes of viral DNA synthesis, capsid assembly and encapsidation of viral genomes occur within the nuclei of infected cells. Further particle maturation occurs within the cytoplasm.

1.1.2 Classification of the herpesviruses

On the basis of both phylogenetic and biological attributes, herpesviruses are currently divided into three groups within the family *Herpesviridae*. It is proposed that these groups are reclassified as the families *Herpesviridae*, *Alloherpesviridae* and *Malacoberpesviridae* within the new order *Herpesvirales* (Davison, 2002; Davison *et al.*, 2005; McGeoch *et al.*, 2006).

The first group (proposed to become the *Herpesviridae*) comprises viruses infecting mammalian, reptilian and avian hosts, and is split into three subfamilies:

- (i) *Alphaherpesvirinae*: (including herpes simplex virus types 1 and 2, varicella zoster virus and pseudorabies virus). These viruses are neurotropic, and establish latency in neuronal ganglia proximal to the initial site of infection. They exhibit broad host species and cell type range, and replicate efficiently and rapidly in cell culture.
- (ii) *Betaherpesvirinae*: (including human cytomegalovirus, guinea pig cytomegalovirus, human herpesviruses -6 and -7 and murine cytomegalovirus). Replication of these viruses in tissue culture is somewhat slower than for *alphaherpesvirinae*, and they display a more restricted host cell range. Latent infection is established in monocytes and spleen cells.
- (iii) *Gammaherpesvirinae*: (including Kaposi's sarcoma associated herpesvirus and Epstein Barr virus). Viruses in this subfamily exhibit lymphotropism, and life cycles vary in length.

The host cell range of these viruses is more limited than either of the other two sub-families. Moreover, infections tend to be restricted to a single species, with latency established in cells of the lymphatic system.

The existence of a subset of 'core' genes conserved amongst all three subfamilies of the *herpesviridae* has been interpreted as evidence for a common evolutionary origin. Study of amino acid alignments of the protein complement encoded by these viruses demonstrated that *alpha*-, *beta*- and *gamma-herpesvirinae* exhibit extensive evidence of co-evolution with their hosts. It is postulated that this co-evolution explains the limited host cell range of many members of the family (McGeoch *et al.*, 2000; McGeoch, 2001; McGeoch & Gatherer, 2005)

The second group, forming the proposed family *Alloherpesviridae*, includes viruses able to infect bony fish and amphibians. Demonstration of a common ancestry between these viruses and those infecting mammalian/avian hosts has been problematic, mainly due to the extensive divergence of viral proteins (reviewed by Davison, 2002). Nevertheless, similarities between the two groups in terms of capsid structure and maturation suggest a common origin (Davison & Davison, 1995; Booy *et al.*, 1996).

The third proposed group, the *Malacoherpesviridae*, contains only one virus: ostreid herpesvirus (OsHV), which is able to infect several marine bivalve species (Arzul *et al.*, 2001; Davison *et al.*, 2005). Analysis revealed that none of the proteins encoded by OsHV exhibited sequence similarity to any known herpesvirus structural protein. However, cryo-electron microscopy studies showed that OsHV capsids exhibit characteristic herpesvirus T=16 symmetry, and are structurally very similar to the capsids of other herpesviruses (Davison *et al.*, 2005).

1.1.3 Human herpesviruses and associated infection

Eight human herpesviruses have been isolated and characterised thus far, with representatives within each of the three *herpesviridae* subfamilies outlined above. In general, infections are usually asymptomatic and not life threatening. Although rare, interspecies transmission of herpesviruses can cause serious disease. For example, a non-human alphaherpesvirus, B virus (cercopithicine herpesvirus-1; genus *Simplexvirus*), has been attributed as the cause of several human fatalities. B virus is endemic in macaques but is able to infect humans in a highly pathogenic fashion, and if untreated can give rise to serious disease with a high mortality rate (reviewed by Benson *et al.*, 1989).

Humans are the natural hosts of three members of the *alphaherpesvirinae*. Herpes simplex virus type 1 (HSV-1; genus *Simplexvirus*) has been extensively studied and is the prototype virus for this subfamily. Initial infection can occur at a number of sites (mainly at or near the mouth), with latency established in trigeminal sensory neurons innervating the site of infection (reviewed by Hagglund & Roizman, 2004; Efstathiou & Preston, 2005). Re-activation of the virus from latency leads to cold sore lesions at or near the primary site of infection. HSV-2 (genus *Simplexvirus*) is closely related to HSV-1 and causes disease clinically indistinguishable from HSV-1 infection, but is primarily associated with genital infections. Infection with varicella-zoster virus (VZV; genus *Varicellovirus*) is associated with chickenpox in children, causing the appearance of small vesicles that rupture and scab over and that are frequently associated with intense itching (varicella). Latent infection is established in neurons, and reactivation within adulthood leads to the condition known as shingles (zoster).

Three members of the *betaherpesvirinae* are also able to infect humans. Human cytomegalovirus (HCMV; genus *Cytomegalovirus*) is the prototype species within this

subfamily, and has been comprehensively studied. Infection is usually asymptomatic. However, acute disease is noted in individuals unable to mount a successful immune response, such as the immunocompromised and those infected via transplacental transmission. Thus, HCMV is a major cause of neonatal disease resulting from congenital infection, mainly characterised by damage to the brain and nervous system. Infection of immunocompromised individuals is often associated with retinitis. Latent infection by HCMV occurs in peripheral blood monocytes (reviewed by Sinclair & Sissons, 2006). Human herpesviruses -6 and -7 have been identified more recently, and are less well studied. Both are members of the *Roseolovirus* genus, and are closely related in terms of both genomes and gene products. Both HHV-6 and HHV-7 have been identified as causative agents of exanthema subitum, a febrile illness observed in infants and children associated with a rash.

The gammaherpesvirus Epstein-Barr virus (EBV) is the causative agent of infectious mononucleosis in many infected adolescents, and is a member of the *Lymphocryptovirus* genus. It has also been implicated in nasopharyngeal carcinoma, Hodgkin's disease and Burkitt lymphoma. However, other factors also contribute to these diseases. EBV establishes latent infections in B-lymphocytes. A second gammaherpesvirus, Kaposi's-Sarcoma associated herpesvirus (KSHV; genus *Rhadinovirus*), is the most recently identified human herpesvirus. It is the causative agent of Kaposi's Sarcoma, an endothelial lesion that frequently occurs as a complication of HIV infection.

1.1.4 Genomes

Herpesvirus genomes are linear, dsDNA molecules, ranging in length between 120-250 kbp and encoding approximately 70-220 proteins. Herpesvirus genomes differ by the presence and arrangement of terminal and internal repeat sequences and can be divided into seven groups on the basis of their genome structure (Davison & Davison, 1995) (**Figure 1.1**).

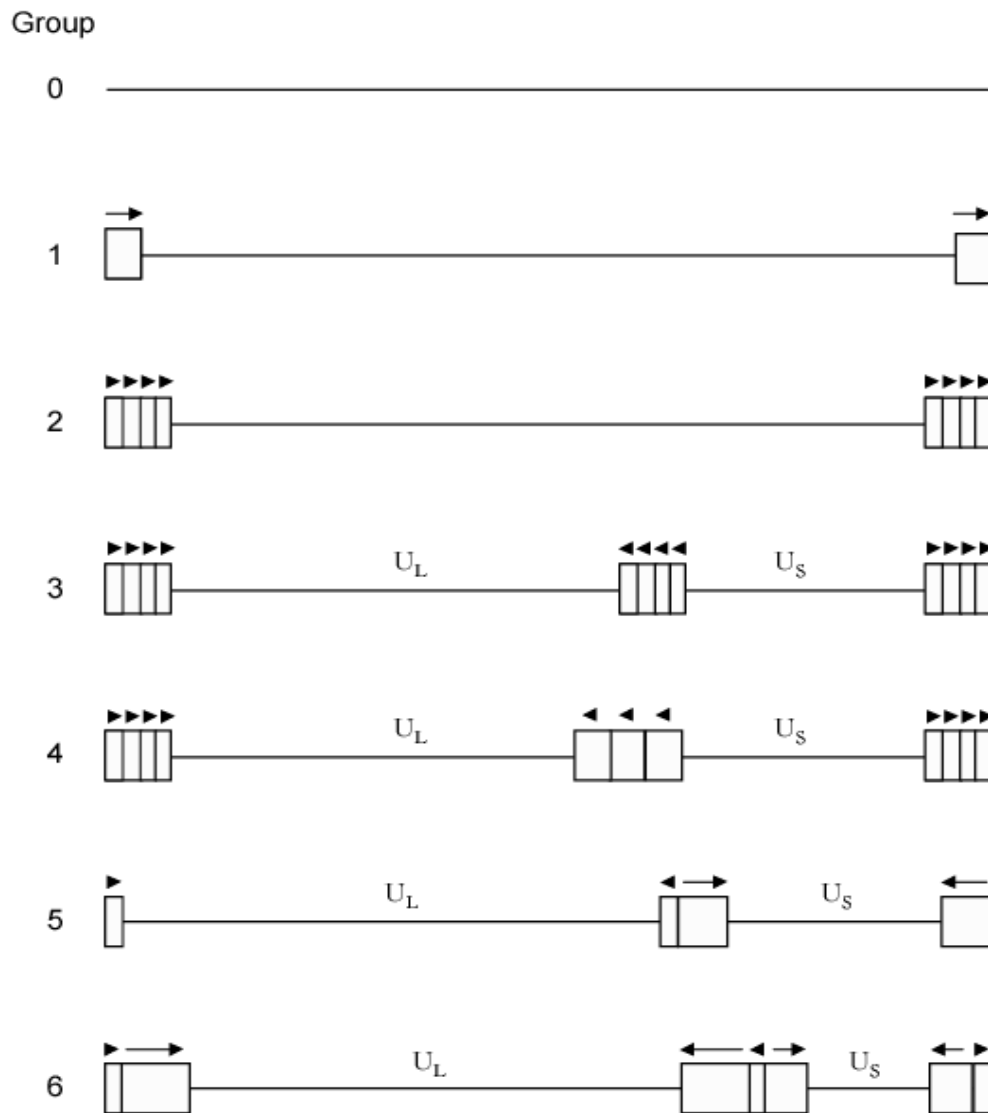


Fig. 1.1: Genome structures within the herpesviruses.

The various genome structures found within the herpesviruses are represented above (not to scale). Unique coding regions are designated by a single line, whilst repeat regions are signified by boxes. The orientation of repeat sequences is indicated by an arrow. Adapted from Davison and McGeoch (1985) and Roizman *et al.* (1992).

The simplest genome arrangement observed in herpesviruses is typified by tupaia (tree shrew) herpesvirus (group 0; Koch *et al.*, 1985). Such genomes contain no terminal or internal repeats, and consist of a single unique region. Group 1 genomes contain single directly repeated units at each terminus of a single unique region and are epitomized by HHV-6 and CCV (Davison, 1992; Gompels *et al.*, 1995). Group 2 genomes, represented by Herpesvirus saimiri, contain multiple copies of a direct repeat at each terminus (Albrecht *et al.*, 1992). Group 3 genomes are similar in structure to those of group 2, but in addition contain internal multiple copies of the repeats in the opposite orientation. This, as observed in the genome of Cottontail rabbit herpesvirus (Cebrain *et al.*, 1989), leads to the generation of two unique regions, denoted U_L and U_S (long and short unique regions respectively). Group 4 genomes also contain both internal and terminal repeated sequences. However, as observed in the case of EBV, the internal repeats of group 4 genomes are unrelated to the terminal repeats (Given & Kieff, 1979). The genome of VZV is representative of group 5 genomes, with inverted repeats surrounding U_L distinct from those surrounding U_S (Davison & Scott, 1986). Moreover, the repeats flanking U_S are much longer than those adjacent to U_L , giving rise to the ability of U_S to invert at high frequency relative to U_L through recombination. The most complex genomes (group 6), typified by HSV-1 and HCMV, are essentially similar to group 5 except that the repeats flanking U_L are longer (Roizman, 1979). The terminal and internal repeats flanking U_L are referred to as TR_L and IR_L , whilst those flanking U_S are TR_S and IR_S . High frequency inversion of the L ($TR_L-U_L-IR_L$) and S ($IR_S-U_S-TR_S$) segments generates four genomic isomers in equimolar amounts (see Figure 1.2). Group 6 genomes also contain a short direct repeat at the termini (the *a* sequence) that is additionally present in inverted orientation at the junction of the L and S segments.

The role of these four isomeric forms in virus replication is unknown. Indeed,

immobilisation of U_L and U_S relative to each other has no effect on HSV-1 replication (Jenkins & Roizman, 1986). Herpesvirus genomes contain sequences at their termini required for the packaging of DNA into preformed capsids (see section 1.3.2.2).

1.1.5 Capsids

Despite considerable variations in genome length, all herpesvirus genomes are packaged into morphologically similar capsid shells 125-130 nm in diameter (Schrag *et al.*, 1989; Booy *et al.*, 1991; Butcher *et al.*, 1998). Herpesviruses with widely divergent capsid protein sequences exhibit remarkably similar capsid structures (Booy *et al.*, 1996). Examination of HCMV capsids by cryo-electron microscopy demonstrated that encapsidation of the large (230 kbp) HCMV genome is achieved through a higher packaged DNA density than HSV-1, together with a slightly larger capsid volume (Bhella *et al.*, 2000). Herpesvirus capsids display $T=16$ icosahedral symmetry with the icosahedral capsid shell of 162 capsomers comprised of 150 hexamers and 12 pentamers. The capsomers are assembled around a proteinaceous scaffold that is cleaved and released during capsid maturation. Groups of three capsomers are separated by a heterotrimeric “triplex” complex, composed of two viral proteins.

Several forms of capsid are observed in the nuclei of cells infected with herpesviruses, and can be distinguished by electron microscopy and sucrose gradient centrifugation. Three angularised forms of capsids, A-, B- and C-, can be isolated from infected cells, and retain the same shell composition whilst differing as to their contents. C-capsids contain viral genomes and are able to mature into infectious virions. Both A- and B- capsids lack DNA but A-capsids are devoid of both DNA and protein, whilst B-capsids retain cleaved scaffold (reviewed by Homa & Brown, 1997).

Procapsids contain the same capsid shell proteins surrounding a core of uncleaved scaffold.

They are more spherical than A-, B- or C-capsids, and the shell has a more porous structure. During infection the spherical procapsids give rise to A-, B- and C-capsids. Both A- and B-capsids are considered dead end products (the former resulting from abortive packaging events), and only C-capsids can mature into infectious virus particles. The processes of capsid assembly and maturation in HSV-1 are dealt with in more detail in section 1.3.2.1.

1.1.6 Tegument

Within mature herpes virions, capsids are surrounded by a proteinaceous layer known as the tegument, which consists of at least 15 viral proteins. The tegument has long been considered to be amorphous. However, more recent study suggests that, due to interaction with the capsid, a portion of the innermost tegument layer displays icosahedral symmetry (Zhou *et al.*, 1999). Functions of tegument proteins vary, but include viral gene transactivation, DNA packaging, degradation of host mRNA and structural components of the virion (Spear & Roizman, 1972; Heine *et al.*, 1974; McLauchlan *et al.*, 1992; Salmon & Baines, 1998; Thurlow *et al.*, 2005).

1.1.7 Envelope

In virions, the capsid and tegument are enveloped by a lipid bilayer studded with virally encoded glycoproteins. It is thought that this membrane originates from the trans-Golgi network (TGN), after a complex process of primary envelopment at the outer nuclear membrane, cytoplasmic de-envelopment and secondary envelopment at the TGN (reviewed by Mettenleiter, 2002).

Several virally encoded glycoproteins protrude from the envelope, and are visible as spikes by electron microscopy. The precise number of glycoproteins encoded varies from virus to virus, but they are thought to have multiple roles including virus entry and virion

maturation. The glycoproteins encoded by HSV-1 are described in section 1.2.2.

Section 1.2 HSV-1 lytic replication

1.2.1 Genome structure

The linear double-stranded HSV-1 genome is 152 kbp in length, and is classified as a group 6 genome. Two covalently linked segments, L and S, comprise the genome, and each contains a unique coding region, known correspondingly as U_L and U_S (**Figure 1.2**). The U_L and U_S regions, 107.9 and 13 kbp in length respectively, together encode at least 71 proteins. Inverted repeats flank the unique sequences, with U_L flanked by TR_L and IR_L , and U_S flanked by TR_S and IR_S . These inverted repeats allow the inversion of U_L and U_S with respect to each other, generating four distinct equimolar isomers of the genome (Figure 1.2 panel B). Three ORFs are situated within these repeat regions, two within R_L and one in R_S (McGeoch *et al.*, 1988; Dolan *et al.*, 1998).

At the genomic termini lie direct repeats of a 250-500 bp sequence known as the *a* sequence, with one or more copies at the L terminus and a single copy at the S terminus. One or more inverted copies of the *a* sequence also lie at the junction between the L and S segments. Those regions of R_L and R_S excluding the *a* sequence are respectively known as *b* and *c* sequences. The genome of HSV-1 can therefore be represented as $a_m b-U_L-b' a'_n c'-U_S-ca$, where inverted sequences are indicated by ' and both *n* and *m* are variable (Figure 1.2). The *a* sequence contains the *cis*-acting sequences necessary for cleavage and packaging of the HSV-1 genome, and is discussed in more detail in section 1.3.2.2.

1.2.2 Attachment and entry

HSV-1 encodes at least eleven glycoproteins (gB, gC, gD, gE, gG, gH, gI, gJ, gK, gL and gM), of which several (gC, gE, gG, gI, gJ and gK) are dispensable in cell culture.

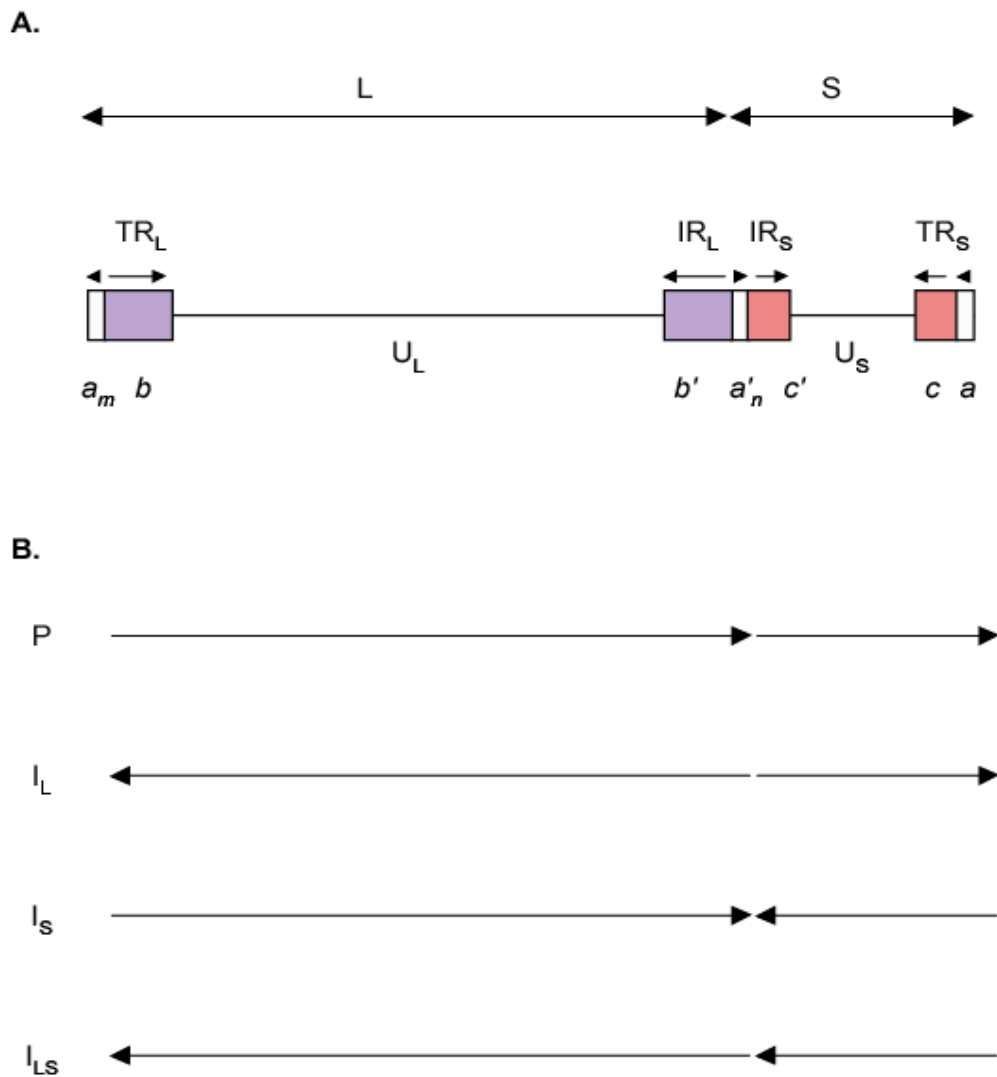


Fig. 1.2: HSV-1 genome structure and isomers.

A. The HSV-1 genome (not to scale). The unique coding regions U_L and U_S are denoted by lines, and the flanking repeats R_L and R_S indicated by boxes. Regions of R_L and R_S lacking the a sequence are denoted b and c respectively. Terminal (TR_L and TR_S) and internal repeats (IR_L and IR_S) are inverted with respect to each other, with relative orientations denoted by arrows. At least one copy of the a sequence, required for DNA encapsidation, is present at each terminus, and in inverted orientation between IR_L and IR_S . m and n indicate that there may be multiple a sequences at the L terminus and at the joint between L and S.

B. Genomic isomers of HSV-1. Inversion of U_L and U_S relative to each other gives rise to four genomic isomers. P = prototype; I_L = inverted U_L ; I_S = inverted U_S ; I_{LS} = inverted U_L and U_S .

Glycoproteins play several roles in the HSV-1 life cycle: attachment to the cell surface and mediation of fusion, stimulation of cell-to-cell spread, and promotion of secondary envelopment (de Zarate *et al.*, 2004; Farnsworth & Johnson, 2006; Farnsworth *et al.*, 2007).

Glycoproteins gB and gC have been implicated in binding incoming virus to the cell.

However, binding has been demonstrated to be reversible, and bound virus eluted from the cell surface is still infectious, suggesting that binding and fusion are distinct events. (Bender *et al.*, 2005) showed that both soluble gB and anti-HSV-1 gB antibodies blocked virus binding. Whilst gC is dispensable in cell culture, it has been demonstrated to increase HSV-1 binding efficiency almost 10-fold. Many herpesviruses bind to cells via heparan sulphate, which is thought to promote entry by allowing viral glycoproteins close proximity to the appropriate entry receptors (reviewed by Spear & Longnecker, 2003).

Three classes of cellular entry receptor for HSV-1 have been identified by expression of the respective genes on cells deficient in endogenous HSV-1 receptors (e.g. Chinese hamster ovary (CHO) cells). Herpesvirus entry mediator (HVEM) is a member of the TNF receptor family, and has been demonstrated to co-immunoprecipitate with gH and gD, and to trigger virus-liposome fusion at acidic pH (Perez *et al.*, 2005; Whitbeck *et al.*, 2006). Two related members of the immunoglobulin family (nectin-1 and -2) have also been identified as HSV-1 receptors. In addition, expression of the human B5 membrane protein in porcine cells rendered them permissive for HSV-1 infection, suggesting that B5 comprised a third class of HSV-1 receptor (Perez *et al.*, 2005). It was also demonstrated that HSV-1 could infect non-permissive CHO cells in the absence of endogenous HSV-1 receptors when grown on permissive BHK cells, suggesting that an acquired host-cell infectivity factor may also contribute to virus entry (Conner *et al.*, 2005).

A subset of four HSV-1 glycoproteins (gB, gD, gH and gL) has been shown to participate in the fusion of virus and cell membranes. Together, these critical glycoproteins are thought to act in concert to promote fusion. Binding of gD to a cellular receptor likely acts as a trigger to fusion, although precise mechanisms have yet to be elucidated. It is thought that once gD binds its cellular receptor, a conformational change permits its interaction with gH/gL and gB thereby promoting fusion.

Three entry pathways have been proposed for HSV-1. Initial studies suggested that the membrane of HSV-1 fused directly with the cellular membrane of Vero and Hep2 cells. However, in CHO and HeLa cells, HSV-1 entry has been observed to occur by endocytosis and subsequent acidification of virus-containing endosomes. A third pathway, proposed more recently, suggested that endocytic entry could occur in the absence of endosomal acidification, although a functional gD-receptor was still required (Milne *et al.*, 2005).

Entry releases the capsid and tegument into the cytoplasm. Capsids, complexed with a subset of the tegument proteins, are transported to the nucleus via microtubules (Sodeik *et al.*, 1997; Mabit *et al.*, 2002). This transport is mediated by the cellular motor protein dynein (Kristensson *et al.*, 1986; Dohner *et al.*, 2002), although the precise mechanism of interaction between virus and motor is not understood. Investigations using PRV concluded that the tegument proteins UL36, UL37 and US3 were likely candidates to interact with dynein (Granzow *et al.*, 2005). Studies have also identified two cellular kinases, P-I-3 kinase and focal adhesion kinase, as being important for virus trafficking to the nucleus (Nicola & Straus, 2004; Cheshenko *et al.*, 2005).

After transport to the nucleus, capsids dock with the nuclear pore complex (NPC).

Diffusion of the capsid through nuclear pores is precluded by the large capsid size: thus

genome entry into the nucleus is dependent upon release of DNA through the NPC.

Uncoating of the viral genome at the NPC has been demonstrated to involve the host cellular import factors importin- β and Ran-GTP (Smith & Helenius, 2004). Studies using atomic force microscopy suggested that the genome is released into the nucleus as a condensed rod (Shahin *et al.*, 2006).

1.2.3 Genome circularisation

It has traditionally been thought that, soon after entry to the nucleus, linear HSV-1 genomes circularise in order to act as templates for DNA replication (Poffenberger & Roizman, 1985; Garber *et al.*, 1993; Hwang & Bogner, 2002). However, Jackson & DeLuca (2003) provided data suggesting that linear, not circular, genomes act as the template for DNA synthesis. This demanded a re-appraisal of how and when the linear HSV-1 genomes circularises. Recent studies have confirmed that circularisation occurs rapidly upon infection, that circularised molecules acts as templates for DNA synthesis, and that the cellular protein RCC1 is involved in this process (Strang & Stow, 2005; Strang & Stow, 2007). The host proteins DNA ligase IV and its cofactor XRCC4 have also been implicated in HSV-1 circularisation and replication, possibly through direct ligation of incoming genomic termini (Muylaert & Elias, 2007).

1.2.4 Regulation of gene expression

HSV-1 genes are transcribed in a tightly regulated temporal cascade, and are designated as immediate-early (IE; α), early (E; β) or late (L; γ) genes according to their transcription pattern and the structure of their promoter regions. The transcription of the five IE genes (ICP0, ICP4, ICP22, ICP27, and ICP47) is stimulated by the action of the tegument protein VP16. Together with two cellular proteins, Oct-1 and HCF, VP16 is able to recruit host transcription factors to the promoters of IE genes and initiate transcription (Kristie & Roizman, 1987; Gerster & Roeder, 1988; O'Hare *et al.*, 1988). Indeed, VP16 acts as an

efficient transcriptional activator in both yeast and mammalian cells (Cousens *et al.*, 1989). HCF is required for the nuclear import of VP16 after virus entry and tegument release (LaBoissiere & O'Hare, 2000). The majority of the IE gene products play regulatory roles in the transcription of β class genes. Expression of IE genes peaks at around 4 hours post-infection, but the genes remain expressed throughout lytic infection.

The HSV-1 ICP0 protein has been demonstrated to be a promiscuous transcriptional transactivator, able to initiate transcription from HSV and heterologous promoters (reviewed in Everett, 2000; Hagglund & Roizman, 2004). An accumulating body of evidence suggests that ICP0 functions to lift cellular repression of viral transcription, and that this repression is in part mediated by the cellular proteins PML and SP100 (Everett, 2006; Everett *et al.*, 2007). ICP0 has been demonstrated to initiate the degradation of PML by the ubiquitin-proteasome pathway, leading to disruption of nuclear substructures known as ND10 domains (Everett *et al.*, 1998; Chelbi-Alix & de The, 1999; Everett, 2006). This is dependent upon the presence of a functional RING-finger motif present within the N-terminus of ICP0.

The HSV-1 ICP4 protein is able to both positively and negatively regulate viral gene transcription, and activates most of the early and late viral genes. In the absence of ICP4, post- α gene expression is blocked. In line with its role as a transcriptional modulator, ICP4 is able to interact with multiple transcription factors, and bind DNA. Although the precise mechanism by which ICP4 activates transcription of early and late genes is unclear, evidence suggests that ICP4 enhances the binding of transcription factors to sites on viral promoters (Grondin & DeLuca, 2000). ICP4 is also able to repress transcription of several viral genes including its own by binding directly to specific sites in the promoter region (Leopardi *et al.*, 1995).

ICP47, whilst expressed with IE kinetics, has no role in regulating viral gene expression. Rather, ICP47 abrogates the presentation of viral antigens by major histocompatibility complex class-I molecules on the surface of infected cells, thus helping to minimize the acquired immune response (reviewed by Vossen *et al.*, 2002).

As well as being transcriptional transactivators of β gene expression, several IE genes can also act to regulate gene expression at the post-transcriptional level. For example, ICP27 acts to suppress host cell protein synthesis during HSV-1 infection, whilst maintaining translation of viral mRNAs. ICP27 achieves this through the shuttling of unspliced viral mRNA from the nucleus to cytoplasm (Mears & Rice, 1996; Sandri-Goldin, 1998). Moreover, ICP27 sequesters proteins involved in spliced mRNA export, and recruits these proteins to unspliced viral mRNAs, resulting in their export into the cytoplasm (Fontaine-Rodriguez *et al.*, 2004; Sandri-Goldin, 2004; Brandon Chen *et al.*, 2005). As only four lytic HSV-1 genes are spliced, this has a minimal effect on viral gene translation. Three of the four spliced HSV-1 genes are expressed from IE promoters before maximal splicing inhibition, and the fourth, UL15, is expressed as a late (γ_2) transcript. It is postulated that UL15 may either be spliced by an alternative mechanism not affected by ICP27, or inhibition of splicing by ICP27 may be short-lived (Weir, 2001).

Genes expressed with early (β) kinetics are primarily involved in DNA replication and nucleotide metabolism. Transcription of these genes occurs before DNA synthesis and is dependent on the expression of IE genes, notably functional ICP4 (reviewed by Weir, 2001).

Late, or γ , genes fall into two distinct classes dependent upon the kinetics of expression.

Leaky-late genes (γ_1) are expressed prior to viral DNA synthesis, but require this process to reach maximal expression levels, whilst true-late (γ_2) genes require the onset of DNA synthesis for transcription. Genes in these classes encode many virion components and proteins involved in capsid assembly, encapsidation and virion maturation. Functional ICP27 and ICP4 are required for late gene expression (reviewed by Weir, 2001).

1.2.5 DNA replication

HSV-1 DNA replication and the functions of the replication proteins have been reviewed by Boemher & Lehman (1997) and Lehman & Boemher (1999).

Replication of HSV-1 DNA is dependent upon *cis* acting sequences, acting as origins of replication, and a number of virally-encoded *trans*-acting proteins. HSV-1 encodes two related origins utilised during lytic infection, termed ori_L and ori_S . These sites confer upon plasmids the ability to replicate in the presence of the essential proteins described below. Two copies of ori_S and one of ori_L are found within a viral genome, with ori_L present near the centre of the U_L region (Spaete & Frenkel, 1985), and two identical copies of ori_S within the IR_S and TR_S regions. The reasons for possessing three origins of two types remain unclear, as deletion of either ori_L or both copies of ori_S does not significantly impair replication in tissue culture (Balliet *et al.*, 2005).

HSV-1 also encodes seven *trans*-acting proteins (UL9, UL29 (ICP8), UL42, UL30, UL5, UL8, UL52) whose functions are directly involved in DNA replication. It is now known that UL9 encodes the origin binding protein, UL29 (ICP8) is the ssDNA binding protein, UL30 and UL42 form the viral DNA polymerase, and UL5, UL8 and UL52 together comprise the helicase/primase complex. A brief description of each protein is given below.

UL29 encodes a single-stranded DNA binding protein, ICP8, which acts as a helix

destabilising protein at the replication forks. UL9 encodes the HSV-1 origin binding protein, which exists as a homodimer, and is able to bind specifically to sequences within ori_S and ori_L in a cooperative manner. Furthermore, UL9 encodes an ATP-dependent helicase activity, which is stimulated by ICP8. UL30 and UL42 form the heterodimeric DNA polymerase complex. Polymerase activity is associated with the UL30 subunit, whilst UL42 acts as an accessory factor to enhance polymerase activity. The helicase/primase complex of HSV-1 is comprised of the gene products of UL5, UL8 and UL52. UL5 specifies the helicase activity of the complex, but this activity is dependent upon the co-expression of UL52. Similarly, UL52 exhibits a primase activity, but only in the presence of UL5. UL8 is not necessary for either function *per se*, but enhances both activities. Together with UL9, ICP8 appears to distort the DNA surrounding the origin. The helicase activity of UL9 then unwinds the origin, and the resulting ssDNA is coated with ICP8. This allows the viral DNA polymerase (UL30 and UL42) and helicase-primase complex (UL5, UL8 and UL52) to access the DNA, and establish a viral replication fork.

DNA replication is thought to initially proceed by an origin-dependent *theta* mechanism, in which circular templates are amplified. Decatenation of these circular genomes is presumably mediated by host cell topoisomerases. Analysis using a mutant with a temperature-sensitive lesion in UL9 demonstrated that once DNA synthesis has begun UL9 is no longer required; this suggested that origin-dependent DNA initiation is a single event (Schildgen *et al.*, 2005). However, the *theta* mode of DNA replication has never been reconstituted *in vitro*. DNA replication is then thought to switch to an origin-independent rolling-circle mechanism, although the mechanism by which replication switches from one mode to another is unknown. Neither an HSV-1 origin nor UL9 are required for rolling circle replication *in vitro*. Indeed it has been demonstrated that, in the presence of ori_S , rolling circle replication is inhibited by the addition of UL9. Rolling circle replication

generates long DNA concatemers, consisting of genomes arranged in a head-to-tail fashion, that act as substrates for the encapsidation process. Importantly, concatemeric molecules may also be formed by recombination (reviewed by Wilkinson & Weller, 2003).

Late in DNA replication viral genomes recombine at high frequency, giving rise to branched molecules that must be resolved before encapsidation. The nuclease encoded by the HSV-1 UL12 gene, described in further detail in section 1.4.5, is thought to play a key role in resolving these branched molecules prior to cleavage and packaging.

1.2.6 Capsid assembly and encapsidation

After DNA replication, concatemeric DNA is cleaved into genome lengths and packaged into procapsids in a tightly coupled process (see section 1.3.2). The products of DNA packaging are angularised nuclear C-capsids, which are the precursors of infectious viral particles.

1.2.7 Replication compartments

Very early in infection, incoming viral genomes are visualised in the nucleus by fluorescence *in-situ* hybridisation as discrete dots surrounded by nuclear substructures known as ND10 bodies, with new ND10s assembling around incoming viral genomes (Everett & Murray, 2005; Everett, 2006). However, as infection progresses, components of the ND10s are degraded by a mechanism dependent upon the viral protein ICP0 (Everett *et al.*, 1998). This permits the recruitment of viral and cellular proteins required for the initial transcription of the genome.

Following synthesis of the viral DNA replication proteins, DNA synthesis commences. Subsequent rounds of transcription and protein recruitment lead to the formation of replication compartments (RCs), which are the sites for DNA replication, encapsidation

and capsid assembly. Several viral factors required for DNA synthesis, transcription, capsid assembly and DNA packaging have been demonstrated to localise to RCs (Ward *et al.*, 1996; Phelan *et al.*, 1997; de Bruyn Kops *et al.*, 1998; Lamberti & Weller, 1998; Yu & Weller, 1998a; Geisen *et al.*, 2000a). Amongst these factors is the HSV-1 ssDNA binding protein ICP8 (encoded by the UL29 gene), which, due to its interaction with replication forks during viral DNA replication, has seen widespread use as a marker for RCs (Quinlan *et al.*, 1984). Manifold cellular proteins involved in DNA damage repair, recombination and chromatin remodelling have also been demonstrated to interact with ICP8 in RCs (Fontaine-Rodriguez *et al.*, 2004). Several cellular chaperones have additionally been identified at sites proximal to RCs, including Hsc70, Hsp90 and Hsp40 (Burch & Weller, 2004). Together, it is postulated that these cellular factors play crucial roles in the replication of HSV-1. As infection progresses, replication compartments enlarge to eventually fill most of the nucleus, and host chromatin is marginalised (Randall & Dinwoodie, 1986; Simpson-Holley *et al.*, 2005).

1.2.8 Maturation and egress

After DNA encapsidation, C-capsids are targeted to the nuclear periphery, possibly utilising nuclear actin to facilitate transport (Forest *et al.*, 2005). The release of C-capsids into the cytoplasm is precluded by degradation of the nuclear lamina. Through the actions of UL31, UL34 and US3, the nuclear lamina is disrupted, allowing capsids to access and bind to the inner nuclear membrane through an unknown mechanism (Mettenleiter, 2002; Liang & Baines, 2005; Simpson-Holley *et al.*, 2005; Bjerke & Roller, 2006). Both UL31 and UL34 are thought to be critical for the envelopment of C-capsids at the inner nuclear membrane, and are incorporated into the virion during budding into the perinuclear space, suggesting a possible role in de-envelopment (Reynolds *et al.*, 2002; Mettenleiter, 2004).

Exit of capsids from the nucleus is generally accepted to occur via a complex pathway

involving envelopment of capsids as they bud through the inner nuclear membrane into the perinuclear space and subsequent de-envelopment as the capsid fuses with the outer nuclear membrane and is released into the cytoplasm. Several HSV-1 proteins have been implicated in this process. For example, UL51 is thought to play a role in exit of capsids from the perinuclear space (Nozawa *et al.*, 2005).

Subsequently, capsids gain both tegument and lipid envelope at the trans-Golgi network (TGN) or related post-endoplasmic reticulum compartments. Recruitment of tegument proteins to the immature virion is mediated by several crucial interactions. For example, it has been shown that incorporation of VP22 and VP16 into the tegument requires interaction between these partners, and is specifically dependent upon the C-terminal domain of VP22 (Hafezi *et al.*, 2005; Mouzakis *et al.*, 2005).

HSV-1 glycoproteins, as with their cellular counterparts, are synthesised at the endoplasmic reticulum, and travel via the Golgi apparatus to reach the final site of re-envelopment. Mutation of highly conserved motifs within the cytoplasmic domain of HSV-1 gB have been demonstrated to inhibit trafficking to the TGN, implicating these motifs in intracellular sorting (de Zarate *et al.*, 2004). Evidence also suggests that successful re-envelopment requires interaction between tegument proteins and the cytosolic tails of viral glycoproteins (reviewed in Mettenleiter, 2004). Trafficking of viral glycoproteins to the TGN is thought to occur independently of capsid egress (Turcotte *et al.*, 2005).

Recently, Leuzinger *et al.* (2005) suggested that, in stark contrast to the model described above, capsids might exit the nucleus via enlarged nuclear pores and never undergo primary envelopment at the nuclear membrane. Furthermore, they proposed that naked cytoplasmic capsids were capable of budding into any membrane, accounting for previous

observations of virions in the perinuclear space. However, this appears irreconcilable with the phenotype of viruses lacking UL36 and UL37 (reviewed by Mettenleiter, 2004). These viruses exhibit an accumulation of naked cytoplasmic capsids, although virions are still observed in the perinuclear space. Together, this suggests that budding into these different compartments requires different factors, and is inconsistent with the proposals of Leuzinger and co-workers (Mettenleiter & Minson, 2006).

Once tegumentation and secondary envelopment have occurred, virions contained in endosomal compartments are directed to the plasma membrane and infectious virus is released by exocytosis. Evidence suggests that direct cell-to-cell spread of HSV-1 is also important in viral dissemination (reviewed by Johnson & Huber, 2002). Together with the glycoproteins gB, gD and gH/gL, the heterodimeric gE/gI complex is involved in mediating cell-to-cell spread. It seems that gE/gI functions by targeting enveloped virions from the TGN to the lateral or basolateral surface of cells, permitting virus release into the space between cells (Farnsworth & Johnson, 2006).

Section 1.3 Viral DNA packaging

Compared to our understanding of the processes surrounding DNA replication, knowledge of viral genome packaging in herpesviruses is less well advanced. However, several parallels have been drawn with the analogous process in dsDNA bacterial viruses or bacteriophage, which have been extensively studied. Indeed, similarities between the encapsidation processes, amongst other parallels, have revealed a possible common ancestry between herpesviruses and bacteriophage (Booy *et al.*, 1991; Davison, 1992; Przech *et al.*, 2003; Trus *et al.*, 2004; Baker *et al.*, 2005).

1.3.1 DNA packaging in dsDNA bacteriophage

A considerable amount of information is available about the structure, life cycle and

biochemistry of bacteriophage. Based upon the organisation of the virus genome, phage with linear dsDNA genomes can be divided into three groups: 1) Linear genomes with unique terminal sequences e.g. λ and T3; 2) Linear circularly permuted genomes e.g. P22 and T4; 3) Genomes with terminally attached proteins or with host sequences e.g. ϕ 29 and Mu phage (reviewed in Fujisawa & Morita, 1997). The packaging characteristics of several phage are discussed below, focusing on those linear dsDNA phage (such as T4 and λ) that most resemble herpesviruses in their packaging mechanisms.

DNA replication of group 1 and 2 phage genomes generally results in the accumulation of concatemeric molecules. Monomeric genomes are cleaved from these concatemeric intermediates and packaged into preformed proheads. Several central features, crucial for DNA packaging, are conserved amongst most dsDNA phage. Linear genomes are packaged into a preformed protein prohead, which displays 5-fold rotational symmetry, through a unique vertex known as the portal vertex. At this portal vertex, DNA enters through a non-head protein known as the connector, which exhibits 12-fold rotational symmetry. Although the connector is required for DNA packaging, it is not thought to play a role in catalysing the cleavage or packaging of DNA *per se*. The structures of several connector proteins have been determined, including those from T7, T4, SPP1, P22, ϵ 15 and ϕ 29 (Simpson *et al.*, 2000; Orlova *et al.*, 2003; Fokine *et al.*, 2004; Tang *et al.*, 2005; Agirrezabala *et al.*, 2005a; Jiang *et al.*, 2006; Lebedev *et al.*, 2007). All connectors studied so far share a similar homo-dodecameric structure with the subunits surrounding a central channel, and exhibiting 12-fold rotational symmetry. This common structure is observed despite the lack of discernable amino acid sequence similarity. In the case of ϕ 29, the connector is closely associated with an RNA transcript, pRNA, which is required for successful DNA packaging.

A packaging enzyme, known as terminase, is fundamental to the phage DNA encapsidation process. To date, all bacteriophage terminases identified have two subunits, designated large and small. Terminases exhibit a DNA-dependent ATPase activity that is thought to provide the energy necessary to drive the thermodynamically unfavourable packaging process. ATP has also been implicated as an allosteric effector of assembly of a functional packaging complex. The functions attributed to the terminase enzyme are separated between the two subunits. The large terminase subunit has been shown to bind the connector proteins of several phage, is responsible for cleaving and translocating DNA, and also contains ATP binding sites. ATP hydrolysis at these sites is thought to drive DNA translocation. Recognition of the phage DNA to be packaged is mediated by the small terminase subunit.

Of note is the presence of several conserved motifs in the large terminase subunit of all phage examined thus far. Consensus sequences known as Walker A and B motifs are present in a large number of enzymes capable of nucleotide binding and hydrolysis (Walker *et al.*, 1982). This includes the large subunits of viral terminases (McClelland *et al.*, 2002; Mitchell & Rao, 2004). A conserved glutamate residue, thought to be involved in ATP hydrolysis, has also been identified. Mutational analysis in T4 has demonstrated the importance of these motifs for functional packaging (Kondabagil *et al.*, 2006). An endonuclease-resolvase motif was also identified in the C-terminus of several phage terminase large subunits, and conserved residues were demonstrated to be crucial for nuclease activity in T5 phage (Ponchon *et al.*, 2006).

Interestingly, phage that produce concatemers differ in the mechanism by which they generate their genomic termini. For a number of bacteriophage, the initial step in packaging involves the recognition of a specific sequence on the concatemer e.g. *pac* or *cos* sites. This

is followed by an initial cleavage event, which is either site-specific (e.g. λ and T3) or sequence-independent (e.g. T1), to create a genomic terminus. DNA is then packaged unidirectionally from the newly generated end into the prohead, by a translocation mechanism thought to be common to all dsDNA phage. A second cleavage event liberates the packaged monomer from the rest of the concatemer. Again, this cleavage may be site-specific as in λ and T3, or non-specific as in T1.

T4 phage employs a slightly different mechanism (reviewed by Rao & Black, 2005). Although long-held that T4 DNA packaging is sequence-independent, more recent evidence suggests that packaging is initiated at or near specific *pac* sites located within the gp16 gene. However, the second cleavage event to terminate packaging occurs only when the head is full, and 102% of a genome length has been packaged. If the T4 packaging process is highly processive, then a single cleavage near a *pac* site followed by multiple rounds of packaging and genome excision would yield a panel of genomes with apparently randomised termini.

Several paradigms have been proposed for the arrangement of packaged DNA in the mature head, although current thinking favours a coaxial spooling model first proposed by (Richards *et al.*, 1973). This proposition can accommodate the liquid crystalline arrangement of packaged DNA observed in phage (Harrison, 1983). Cryo-electron microscopy studies of packaged T7 DNA, along with *in silico* modelling of a spooling mechanism, lend support to this model (Cerritelli *et al.*, 1997; Agirrezabala *et al.*, 2005b). Investigations of the packaged DNA of T4, ϕ 15, ϕ 29 and P22 phage further bear out the coaxial spooling hypothesis (Zhang *et al.*, 2000; Fokine *et al.*, 2004; Jiang *et al.*, 2006; Lander *et al.*, 2006; Xiang *et al.*, 2006). An interesting feature of several of these studies was the presence of packaged DNA within the portal channel, suggesting that the DNA is primed

for release upon attachment to the host.

1.3.1.1 DNA packaging in λ phage

DNA packaging in bacteriophage λ has been extensively studied (Catalano, 2000; Feiss & Catalano, 2005). Since the genomic termini of λ , like HSV-1, are generated from concatemers by sequence-specific cleavage events, lambda packaging is described in detail below.

The λ particle consists of an isometric head containing a linear genome, a tail surrounded by a contractile sheath and a fibre attached to the base of the tail. The genome is 48.5 kbp in length, with complementary single-stranded 12 base termini. Upon infection the genome is circularised by ligation of its cohesive ends. Replication of the linear genome via the *theta* mode of DNA replication, followed by rolling circle replication and recombination, gives rise to concatemers that are the substrates for DNA packaging.

The packaging signal of lambda phage

The minimum *cis*-acting sequence required to initiate and terminate DNA packaging in λ is known as *cos*. Found at the junction between viral genomes within concatemers, *cos* is a 200 bp segment containing several subsites that have specific roles in the recognition, translocation and packaging of viral DNA (**Figure 1.3**).

The *cos* subsite *cosN* contains the cleavage site, and is required for both initiation and termination of packaging. During packaging, the terminase enzyme introduces nicks into the DNA duplex at sites N_1 and N_2 within *cosN* to produce cohesive genome termini. Of the 22 bp in *cosN*, ten of these bases exhibit rotational symmetry. Together with the presence of a leucine zipper motif within the large subunit of the terminase, gpA, this

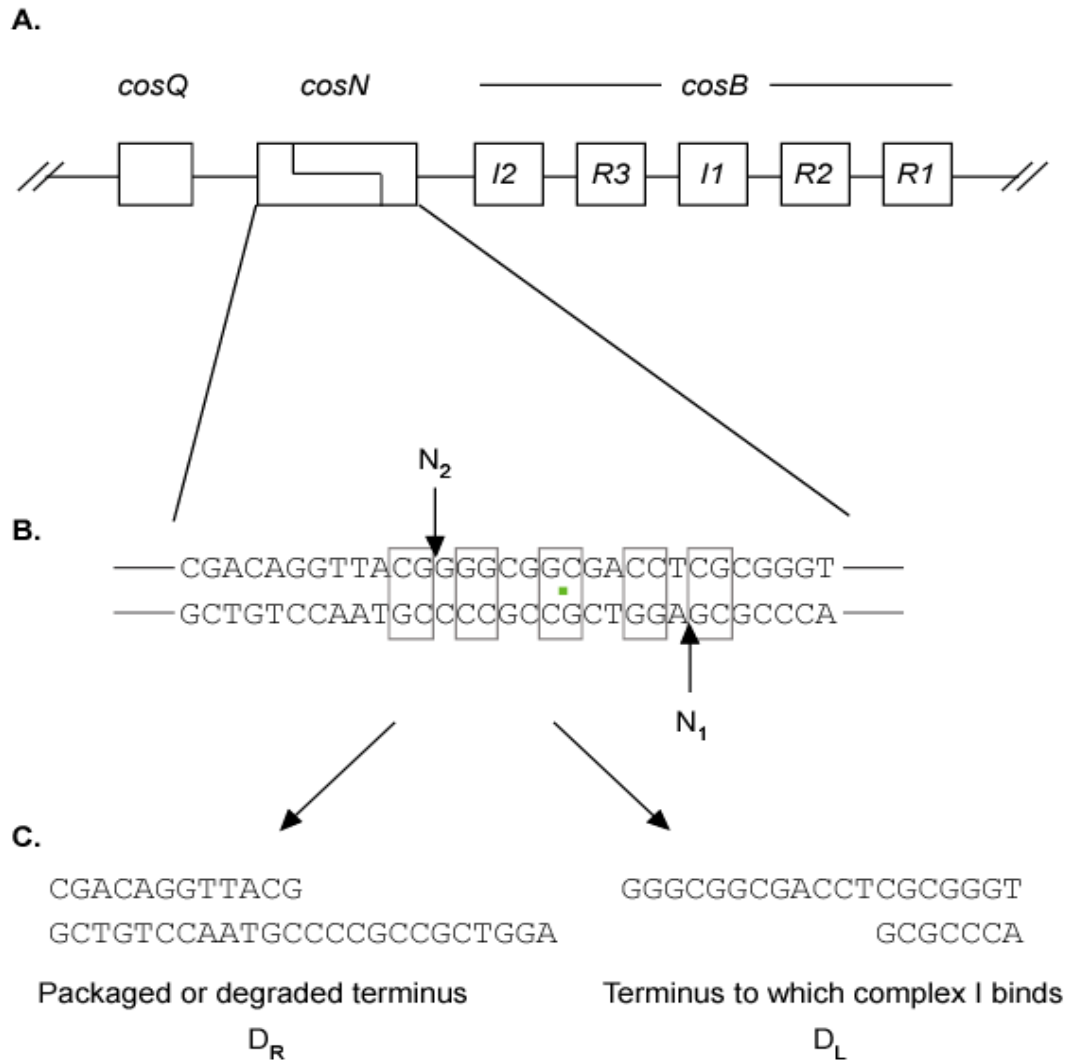


Fig. 1.3: Structure of the λ bacteriophage *cos* site.

A. Structure of the *cos* packaging signal (not to scale). The *cos* sequence lies at the junction between genomes within the λ concatemer. Cleavage during initiation of packaging requires *cosN* and *cosB*, whilst *cosQ*, *I2* and *cosN* are prerequisites for cleavage during termination.

B. Terminase-mediated duplex nicking occurs at two sites within *cosN*, N_1 and N_2 . *cosN* exhibits imperfect rotational symmetry around a central position, denoted by a green dot. Those bases exhibiting rotational symmetry are indicated by boxes.

C indicates the termini released by duplex cleavage. The terminase remains associated with the *cosB*-containing terminus (D_L) to form the translocating complex I.

symmetry has been seen as evidence that gpA binds as a dimer to induce duplex nicking.

The *cosB* subsite is similarly involved in both the initiation and termination of packaging. *cosB* contains three 16 bp repeat elements: R1, R2 and R3, and two consensus binding sites for the protein IHF (integration host factor). IHF is a site-specific DNA binding protein encoded by *E. coli* that has been shown to induce a DNA bend between R2 and R3. It is thought that IHF-induced duplex bending allows the binding of gpNu1 to the R sites of *cosB*, and that these interactions are required to properly position gpA for *cosN* cleavage (Ortega & Catalano, 2006). Faithful nicking of *cosN* by terminase requires ATP and the I2 sequence lying between R3 and *cosN*, in addition to the remainder of *cosB*. Processive packaging by terminase also requires *cosB* to be present.

The third subsite, *cosQ*, is located upstream of *cosN* and is essential for the proper termination of packaging. Mutants of *cosQ* have been shown to correctly initiate packaging, but the termination cleavage event is impaired. In the absence of *cosQ*, packaging proceeds beyond *cosN* until the head is full. Thus, *cosQ* is thought to be involved in stalling the packaging machinery in order to allow cleavage at *cosN*. However, as *cosN* and I2 are also involved in termination of packaging, *cosQ* appears to be only one part of a larger termination signal.

The λ terminase

The lambda terminase consists of two virally encoded subunits, gpA and gpNu1.

Terminase is responsible for a number of functions: recognition of the concatemeric λ DNA substrate; initiation of packaging including nicking of the duplex at *cosN*; translocation of DNA into the prohead and the concomitant hydrolysis of ATP; and termination of packaging by cleavage at *cosN*. At present, the stoichiometry of the *in vivo*

terminase complex is unknown, although recombinant terminase has been purified as a gpA₁•gpNu1₂ holoenzyme (Gaussier *et al.*, 2005). It is proposed that functional terminase is comprised of four heterotrimers, representing a complex of (gpA₁•gpNu1₂)₄ (Maluf *et al.*, 2006).

The viral Nu1 gene encodes the small terminase subunit, gpNu1, which is responsible for recognising concatemeric DNA and promoting the assembly of the terminase complex. Studies using chimeric constructs of λ and phage 21 gpNu1 have identified several domains within the 181aa gpNu1. The N-terminal half of gpNu1 contains the *cosB* binding domain, whilst the C-terminal 40 aa are necessary for interaction with gpA and holoenzyme formation. More recently, a high resolution nuclear mass resonance solution structure has been obtained for the gpNu1 DNA-binding domain (de Beer *et al.*, 2002). This confirmed that the N-terminus of gpNu1 contained a helix-turn-helix motif which mediates gpNu1 binding to *cosB*, and that the DNA-binding domain dimerises about *cosB*. In marked contrast to other small terminase subunits studied, gpNu1 contains ATP and ADP binding sites, and exhibits ATP hydrolysis in the context of the holoenzyme (Gaussier *et al.*, 2005).

gpA, the larger terminase subunit, is the product of viral gene A and is 641 amino acids in length. Several biochemical activities have been attributed to gpA: site-specific endonuclease, DNA-dependent ATPase and DNA helicase activities (Hwang *et al.*, 1996). Moreover, domains have been identified that are crucial for interaction with the connector gpB, and for the interaction with gpNu1. Communication between the N-terminal ATPase and C-terminal nuclease domains of the large terminase subunit has been shown to be critical in T4 phage (Kanamaru *et al.*, 2004).

A conserved Walker motif lies within the C-terminus of gpA (Walker *et al.*, 1982).

However, mutation of crucial amino acids within this motif failed to abolish ATPase activity, but rather simultaneously abrogated helicase and endonuclease activities. Cross-linking studies using a non-hydrolysable ATP analogue instead identified a site within the N-terminus of gpA which bound ATP (Hang *et al.*, 2000). Mutation of surrounding Tyr or Lys residues abrogated ATPase and packaging activities, but did not affect helicase or endonuclease properties. Further analysis revealed that several mutations in this region of gpA perturbed terminase assembly (Dhar & Feiss, 2004). Mutational analysis also confirmed that the translocase domain of gpA is separate from the helicase and nuclease domains.

As previously mentioned, the *E. coli* protein IHF plays a role in DNA packaging, but is not a component of the terminase enzyme. In general, IHF is thought to mediate the recruitment of proteins to nucleoprotein complexes, possibly via its ability to induce 180° bends in DNA duplexes. Viral packaging is decreased in the absence of IHF, suggesting a direct role in encapsidation. Indeed, IHF and gpNu1 binding has shown to be co-operative and sequence-specific, with each protein contributing to the induction of a bend in the viral DNA, about which a functional terminase complex is assembled (Lynch *et al.*, 2003; Gaussier *et al.*, 2005; Ortega & Catalano, 2006).

Packaging mechanism of λ

Utilising information drawn from studies on *cos* and the terminase proteins, a comprehensive model of lambda phage packaging has been proposed (Feiss & Catalano, 2005) (**Figure 1.4**).

(a) Initiation of packaging:

Packaging initiates with assembly of the terminase upon *cosN*. Binding of IHF to the I1 site of *cosB* stimulates duplex bending, and allows the recruitment of four gpA₂•gpNu1₁

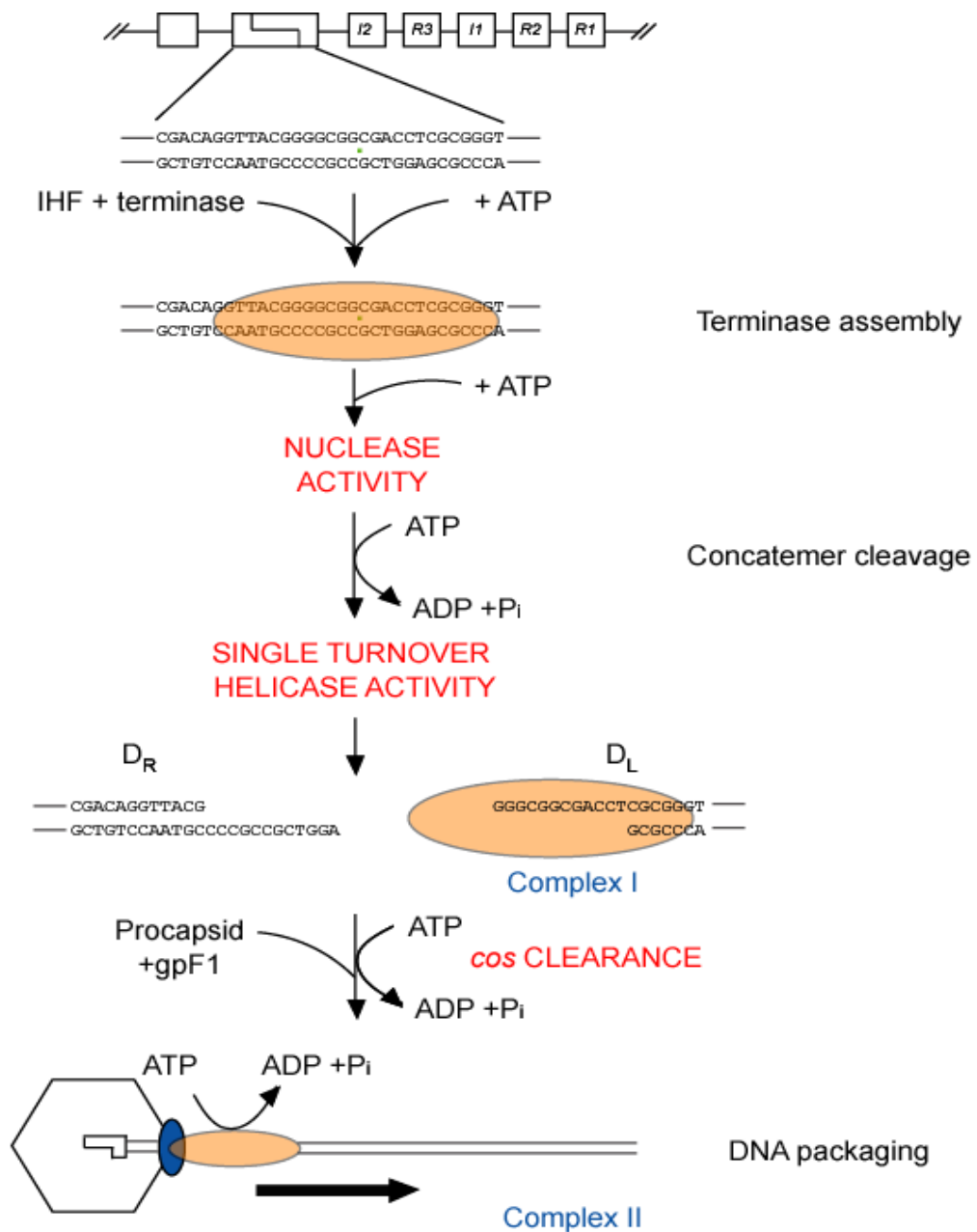


Fig. 1.4: A model for λ bacteriophage DNA packaging.

The terminase holoenzyme, postulated to be a (gpA₁-gpNu₂)₄ complex, assembles upon *cos*, and is represented by an orange oval. Co-operative recruitment of gpA and gpNu1 is mediated by ATP binding. The nuclease activity of terminase is stimulated by ATP, and subsequent hydrolysis to ADP and P_i fuels the helicase reaction to yield complex I. Binding of the gpA subunits of terminase to the portal (blue oval) of the nascent prohead stimulates *cos* clearance and activation of the translocase activity of terminase. DNA translocation is powered by ATP hydrolysis. Recognition of the next downstream *cos* site and subsequent cleavage releases the full head, whilst terminase remains bound to D_L reforming complex I (not shown).

heterotrimers (Maluf *et al.*, 2006; Ortega & Catalano, 2006). Through an interaction between gpNu1 and the R3 and R2 elements of *cosB*, gpA is then recruited to *cosN*, yielding a pre-nicking complex. Binding of ATP to gpNu1 increases its affinity for *cos* DNA, and may play a role in the formation of the pre-nicking complex (Yang & Catalano., 2004).

Subsequently, ATP hydrolysis by the C-terminal ATPase site of gpA allows a conformational rearrangement of the terminase, yielding a complex with nicking and helicase activities. This complex, in the presence of Mg^{2+} , induces nicks within *cosN* at N1 and N2. ATP-dependent strand separation mediated by the helicase activity of gpA leads to release of the right cohesive end (D_R) of the genome, which is subject to degradation by host nucleases. The stable complex of terminase and left cohesive genome end (D_L) is known as complex I, and can be reconstructed *in vitro* (Yang & Catalano, 2003).

Interaction of the prohead with complex I, promoted via the viral gpF1 protein, stimulates a transition to complex II, in which the N-terminal translocating ATPase site of gpA is fully active. In the absence of gpF1, concatemers are not processed to genome length. It is surmised that gpF1 promotes the release of *cos* from the terminase by destabilising complex I.

(b) Translocation of DNA

Complex II is responsible for translocating DNA into the prohead, fuelled by ATP hydrolysis. Several models of translocation have been proposed (see Section 1.3.1.2), but the precise mechanisms involved have not been elucidated.

Packaging of the 48.5 kbp λ genome takes 2-3 minutes *in vivo*, with an estimated two ATP molecules hydrolysed per base pair. Thus packaging of a single genome equates to the hydrolysis of 30,000 ATP molecules min^{-1} terminase $^{-1}$. This is significantly greater than *in*

in vitro rates of ATP hydrolysis demonstrated for purified recombinant λ and T4 terminases (Baumann & Black, 2003; Yang & Catalano, 2003). Therefore, formation of higher-order terminase complexes may be required to hydrolyse ATP at the required rate.

(c) Termination of packaging

Genome packaging is terminated when terminase reaches the next downstream *cos* site. Nicks must be introduced into *cosN*, the cohesive strands separated, and the terminase must dissociate from the full head.

As mentioned previously, *cosQ* is required for the efficient termination of packaging, together with *cosN* and the I2 element. (Feiss & Catalano, 2005) propose that *cosQ* promotes a reorganisation of the terminase to allow cleavage of *cosN* and the correct termination of packaging. Following cleavage, cohesive strands must be separated, in a process thought to be analogous to the formation of complex I.

In several phage, a headful mechanism is thought to mediate the termination of packaging, whereby signals from a “sensor” detects when the capsid is full of DNA and activates the endonuclease activity of terminase. Until recently, the identity of this putative sensor has been elusive. However, studies of T4 phage implicated spooling of DNA about the connector protein (Fokine *et al.*, 2004). Examination of P22 phage revealed that packaging of DNA induces a conformational change within the portal protein, suggesting that this may be the “sensor” by which headful P22 packaging is terminated (Lander *et al.*, 2006).

A feature of many packaging motors acting on concatemeric DNA, including λ , is processivity: once packaging is terminated, a second packaging event is initiated from the terminus generated by the termination cleavage. Thus, terminase must remain associated

with the left cohesive end of the cleaved duplex, in a state thought to resemble complex I, and able to recruit a new prohead and initiate a new round of packaging.

1.3.1.2 Models for DNA translocation in phage

Several paradigms have been proposed to describe the mechanism of genome translocation in ds DNA phage, and are detailed below.

Terminase-mediated translocation model

This model, based on studies in T3 phage, proposes that the terminase is directly responsible for the translocation of DNA (Fujisawa & Morita, 1997). Six copies of the large T3 terminase subunit, gp19, are envisaged to bind to six subunits of the connector complex. It is proposed that each gp19 subunit is bound to the DNA backbone in the presence of ATP, and that this stimulates a DNA-dependent ATPase activity within gp19. Hydrolysis of ATP to ADP and P_i results in a conformational change within gp19, pushing the DNA into the head. Binding of a new ATP molecule stimulates the return of gp19 to its original extended conformation. Movement of the duplex allows the adjacent gp19 molecule to bind, and the cycle is complete. Once this cycle has proceeded six times, 6 ATP molecules will have been hydrolysed and one turn of duplex will have been packaged. This predicted ratio of one ATP molecule for every 1.7 bp packaged is remarkably close to the experimental value observed by Shibata *et al.* (1987).

This model is similar to that proposed for the action of monomeric helicases (Lohman, 1993). Indeed, resolution of the structure of the T4 ATPase gp17 revealed similarity with monomeric helicases, suggesting that T4 packaging proceeded via an inchworm mechanism (Sun *et al.*, 2007). Lambda DNA packaging is also thought to proceed via this mechanism.

Rotating connector model

This model is founded upon a symmetry mismatch between the 12-fold symmetry of the connector and the 5-fold symmetry of the head. The earliest version of this model proposed that ATP hydrolysis stimulates the rotation of the portal with respect to the head, screwing the DNA into the capsid (Hendrix, 1978). This model implies that some part of the connector interacts directly with the DNA helix, analogous to the threading arrangement of a nut (connector) and bolt (DNA). The role of the terminase in this model is not identified, but is presumably to provide energy for the rotation of the portal.

In 2000, Simpson and co-workers revised this model for the phage $\phi 29$. In their model, hydrolysis of ATP by a pentameric ATPase-pRNA complex causes conformational change of the portal. It is proposed that the terminase acts as a stationary stator around the spindle formed by the DNA helix. Rather than the connector rotating continuously around the DNA duplex, each ATP hydrolysis stimulates the portal to occupy a new position on the DNA helix, thus driving encapsidation.

Two recent studies have, however, forced a re-evaluation of these models. Experiments in which the connector protein of T4 was fused to a protein on the outer surface of the capsid, thereby preventing potential connector rotation, elegantly demonstrated that connector rotation was not necessary for packaging in this phage (Baumann *et al.*, 2006). More recently, single particle studies of the portal in $\phi 29$ have excluded portal rotation as the mechanism driving DNA packaging (Hugel *et al.*, 2007).

Osmotic pump model

Originally suggested by Serwer (1988), and later refined (Serwer, 2003), the osmotic pump model proposes that, after initiation of packaging, binding and subsequent hydrolysis of ATP by the terminase releases the DNA from the terminase, allowing translocation to

begin. DNA enters the portal via an osmotic pressure gradient between the lower pressure inside the capsid and higher pressure outside. Packaging is assisted by the packaging motor and putative interactions of DNA with the connector. As DNA is packaged, the osmotic gradient decreases, and it is envisaged that this is sensed by an internal projection of the connector. This stimulates ATP binding by the terminase and subsequent capture of the DNA duplex, and ATP hydrolysis by the larger terminase subunit. Together, it is hypothesised that these events drive contraction of the capsid and the opening of holes in the outer shell, releasing small molecules from the capsid interior, and restoring the osmotic gradient. Packaging continues in this fashion, mediated in the latter stages by interaction of the DNA with the inner capsid surface, until termination.

This model requires that capsids retain the ability to contract upon ATP hydrolysis. Moreover, the capsid must be variably porous and non-porous to small molecules, to allow restoration of the osmotic gradient. These constraints, compounded by indications that the irreversible expansion of T3 prohead is triggered when 25% of the genome is packaged (Shibata *et al.*, 1987), render this model unlikely.

1.3.2 HSV-1 DNA cleavage and packaging

Compared to the wealth of knowledge on bacteriophage DNA packaging, less is known about the analogous process in herpesviruses. Nevertheless, several parallels between bacteriophage and herpesviruses are readily apparent.

A model for herpesvirus DNA packaging, consistent with the current literature, is presented in **Figure 1.5**. Herpesvirus DNA replication results in the accumulation of concatemeric molecules (section 1.2.5) that are the substrate for the DNA packaging process. Concurrently, capsid assembly in the nucleus produces short-lived spherical procapsids that are proposed to be the precursors of mature capsid forms (see 1.3.2.1).

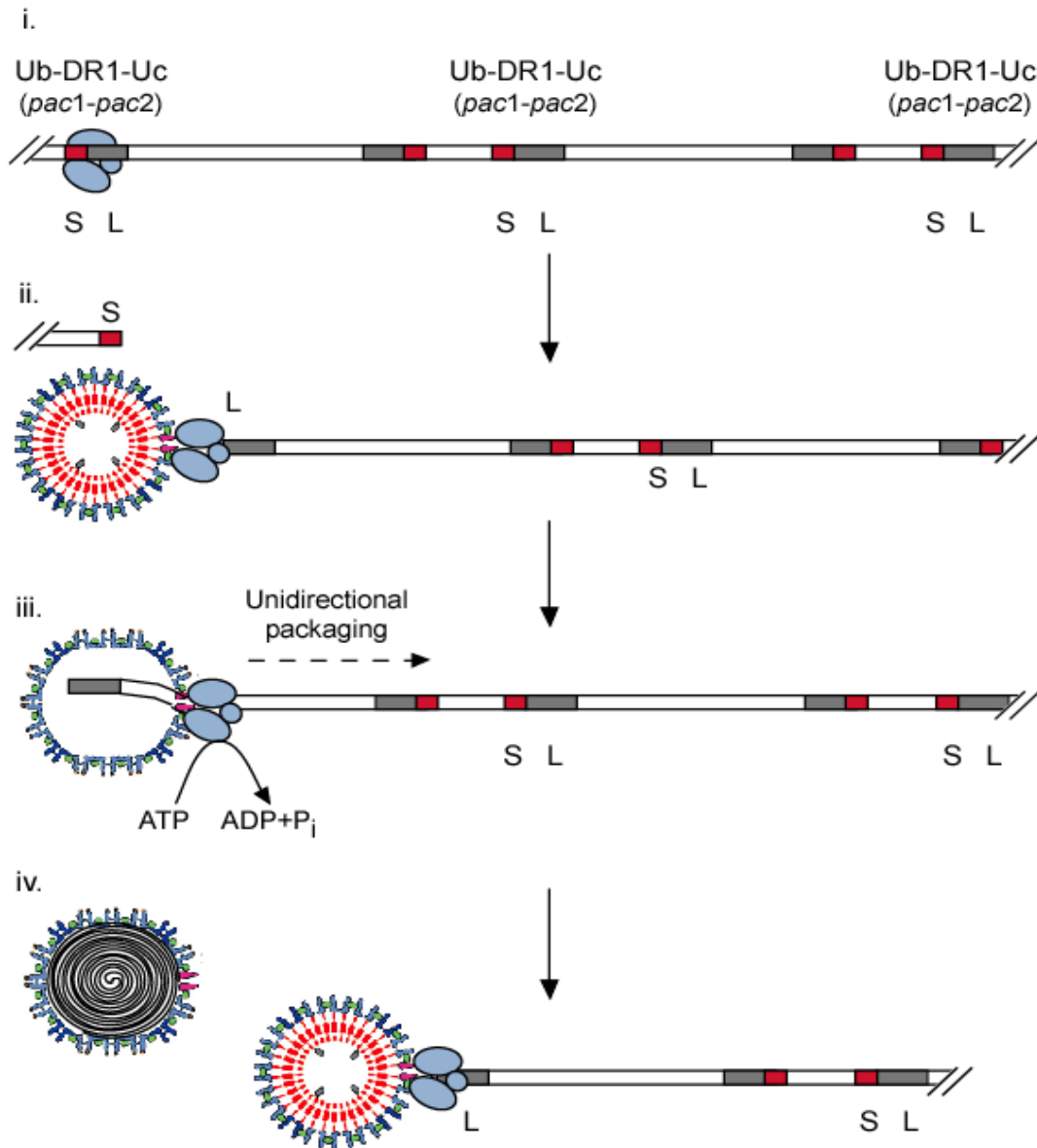


Fig. 1.5: A model for HSV-1 DNA packaging.

(i) Packaging is initiated when the terminase (light blue) recognises the concatemer and assembles at Uc-DR1-Ub sites at the junction between genomes. Terminase-mediated cleavage releases the S terminus (red), and the L terminus (grey) is inserted into the nascent procapsid (ii). The free S terminus is likely to be degraded. (iii) DNA translocation occurs unidirectionally, with the concomitant hydrolysis of ATP, loss of cleaved scaffold and angularisation of the capsid shell. Upon reaching the next similarly orientated downstream Uc-DR1-Ub site, cleavage liberates the packaged genome from the concatemer. Terminase likely remains associated with the L terminus to initiate a further round of packaging (iv).

Packaging is thought to initiate when concatemeric DNA is recognised by a viral terminase and a functional packaging complex is assembled at specific sites upon the concatemer. The duplex is cleaved and DNA translocated through a unique portal vertex into preformed procapsids. A second cleavage event generates a unit length species, and packaging is terminated. As with λ , herpesvirus packaging is processive, with multiple packaging events initiated by a single packaging complex. The terminase acts to recognise the packaging site on concatemeric DNA, recruit the empty capsid, cleave the duplex and hydrolyse ATP to drive translocation of DNA into the capsid. Indeed, depletion of ATP has been shown to inhibit packaging and lead to the accumulation of B capsids containing cleaved scaffold (Dasgupta & Wilson, 1999).

Originally, it was proposed that the DNA was packaged into capsids in a toroidal fashion around a protein core (Furlong *et al.*, 1972). However, more recent studies suggested that packaged DNA is uniformly distributed within C-capsids, and adopts a liquid crystalline conformation closely resembling that observed in bacteriophage (Booy *et al.*, 1991). Gibson & Roizman (1971) proposed that spermine present within capsids was involved in partially neutralising the negatively charged DNA.

The following sections outline current knowledge on the fundamentals of DNA packaging in HSV-1, including the putative roles of several viral proteins in encapsidation. These roles have been surmised from studies on HSV-1 and the herpesviruses HCMV, PRV, GPCMV, KSHV and HHV-6, and also in large part by inference from studies of dsDNA phage. For comprehensive reviews on herpesvirus assembly and packaging, see Homa & Brown (1997), Brown *et al.* (2002) and Baines & Weller (2005).

1.3.2.1 Capsid assembly and maturation

The processes of DNA packaging and capsid maturation are thought to occur concurrently

in infected cells. Co-ordinated assembly of capsid components about a proteinaceous scaffold results in the formation of spherical procapsids that are the precursors of all angularised capsid forms and the substrates for DNA packaging (**Figure 1.6**) (reviewed by Homa & Brown, 1997).

The primary components of the HSV-1 capsid are the major capsid protein VP5 and the triplex proteins VP19C and VP23. The pentons and hexons (collectively known as capsomers) of the capsid shell are composed of five or six copies of VP5 respectively, and together form the floor of the capsid. Two copies of VP23 and a single VP19C molecule make up triplexes that sit above this floor and connect groups of three capsomers. The proteinaceous scaffold about which procapsids are assembled is composed of pre-VP22a protein, encoded by the UL26.5 gene, and full length UL26 protein. These proteins make contact with the inner face of the capsid floor via their C-termini. The UL26 protein contains a protease domain that is responsible for auto-cleavage, generating VP24 (the maturational protease) and VP21 (scaffold domain). During packaging VP24 cleaves pre-VP22a and VP21 near their C-termini, breaking their interaction with the capsid floor. Both cleaved proteins are subsequently released from the capsid as DNA is inserted.

Experiments demonstrated that HSV-1 procapsids could be assembled in insect cells infected with baculoviruses expressing the HSV-1 capsid proteins. Studies using these procapsids indicated that capsid assembly is initiated around the portal protein and proceeds via the stepwise addition of VP5-preVP22a complexes to a growing shell (Newcomb *et al.*, 1999). It was demonstrated that a region of the scaffold protein was crucial in mediating the incorporation of the portal to the capsid (Singer *et al.*, 2005). Furthermore, if assembly was initiated in the absence of the portal protein, subsequent addition of the portal to the growing shell did not enable portal incorporation, suggesting

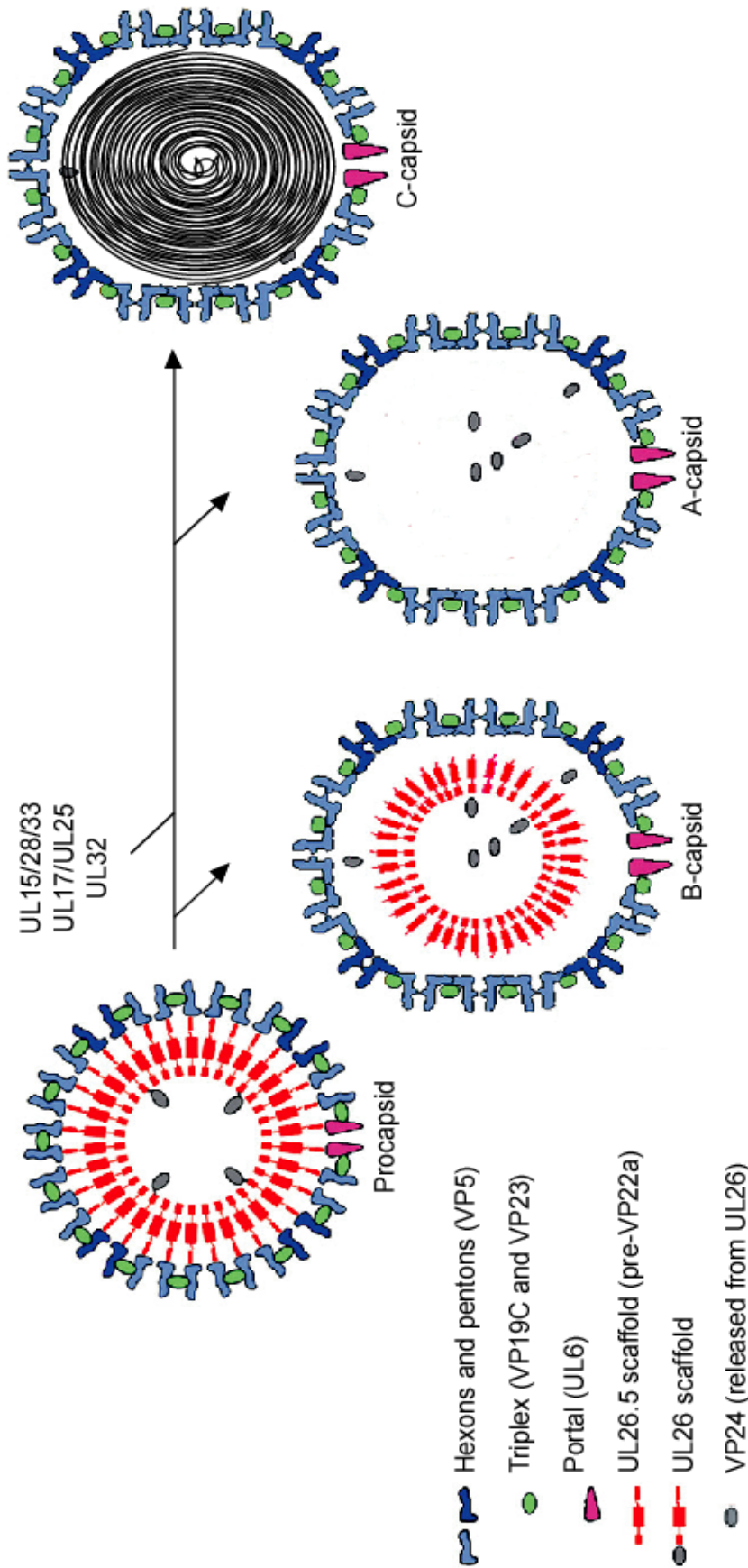


Figure 1.6: Pathways of HSV-1 capsid assembly.

Spherical procapsids are assembled by the stepwise addition of capsid proteins to a growing shell (not shown). Cleavage of the internal scaffold and angularisation of the shell gives rise to B-capsids lacking DNA but which retain the cleaved scaffold. The viral proteins UL15, UL17, UL25, UL28, UL32 and UL33 are necessary for genome encapsidation. It is envisaged that aborted packaging events give rise to A-capsids, which lack both scaffold and DNA. C-capsids are the product of successful packaging events, and can mature into virions. Adapted from Trus *et al.* (2007).

that assembly proceeded by addition of shell components to the portal (Newcomb *et al.*, 2005).

The first evidence that procapsids were the progenitors of angularised B-capsids came from studies by Newcomb *et al.* (1996), who demonstrated that purified HSV-1 procapsids angularised into polyhedral shells upon *in vitro* incubation. Successful maturation of procapsids into C-capsids is tightly coupled to both cleavage of the internal scaffold and DNA packaging.

Analysis of several HSV-1 KOS mutants first demonstrated that cleavage of the internal scaffold is necessary but not sufficient for DNA packaging, and provided insight into the formation of A-capsids containing neither scaffold nor DNA as abortive products of unsuccessful DNA encapsidation (Sherman & Bachenheimer, 1987; Sherman & Bachenheimer, 1988). Studies using *ts1201*, which contains a temperature-sensitive lesion in the UL26 protease, reinforced the importance of scaffold cleavage in DNA encapsidation. At the non-permissive temperature (NPT), large-cored B-capsids containing uncleaved scaffold accumulated in the nucleus of cells infected with *ts1201* (Preston *et al.*, 1983). Upon downshift to the permissive temperature and restoration of protease activity, scaffold protein was cleaved and DNA-containing C-capsids generated (reviewed by Rixon, 1993; Homa & Brown, 1997). B-capsids are envisaged to be angularised shells containing cleaved scaffold that have not undergone a DNA packaging event, and are dead-end products. Empty A-capsids are found in cells infected with viruses able to initiate DNA packaging (e.g. wt HSV-1 and mutants in the UL12 and UL25 genes), but not in cells infected with other DNA packaging mutants. C-capsids containing DNA but lacking an internal scaffold are products of a successful packaging event, and are the only capsids able to undergo nuclear egress and further maturation.

1.3.2.2 The *a* sequence and Uc-DR1-Ub

The *a* sequence of HSV-1 contains the *cis*-acting sequences required for genome cleavage and packaging, and in strain 17syn+ encompasses a region approximately 400 bp in length. A number of direct repeats (DR1 and DR2, and in some strains DR4) and two quasi-unique regions, Ub and Uc, together constitute the *a* sequence (**Figure 1.7**). Each complete *a* sequence is flanked by copies of DR1, with tandem *a* sequences separated by a single copy of DR1. Within the terminal *a* sequences, the Uc motif lies proximal to the L terminus of the genome, whilst Ub lies closest to the S terminus. The two quasi-unique regions are separated by multiple reiterations of DR2 and, if present, DR4.

Within Ub and Uc lie the *pac1* and *pac2* motifs, which contain several elements conserved near the termini of avian and mammalian herpesvirus genomes, and which play crucial roles in DNA packaging (Deiss *et al.*, 1986; Nasserri & Mocarski, 1988; Deng & Dewhurst, 1998; Deng *et al.*, 2004; Feederle *et al.*, 2005). The first hint that packaging signals may be conserved between herpesviruses was provided by studies in which the HSV-1 *a* sequence was functionally replaced by the *a* sequence from HCMV (Spaete & Frenkel, 1985). The *pac1* motifs of Ub are represented by a G+C-rich region, followed by a T-rich element and a second region of high G+C content. The Uc *pac2* motifs comprise a consensus CGCCGCG motif and T-rich and G+C-rich elements (**Figure 1.7**).

During encapsidation, cleavage occurs within DR1, creating genomic termini containing an incomplete DR1 with a 3' overhang of a single base (Mocarski & Roizman, 1982). Upon fusion of termini during circularisation (section 1.2.3), a complete DR1 repeat is regenerated at the centre of a novel Uc-DR1-Ub fragment formed by joining the terminal *a* sequences (**Figure 1.7**). This Uc-DR1-Ub junction has been demonstrated to represent the minimal functional HSV-1 packaging signal (Nasserri & Mocarski, 1988; Hodge & Stow,

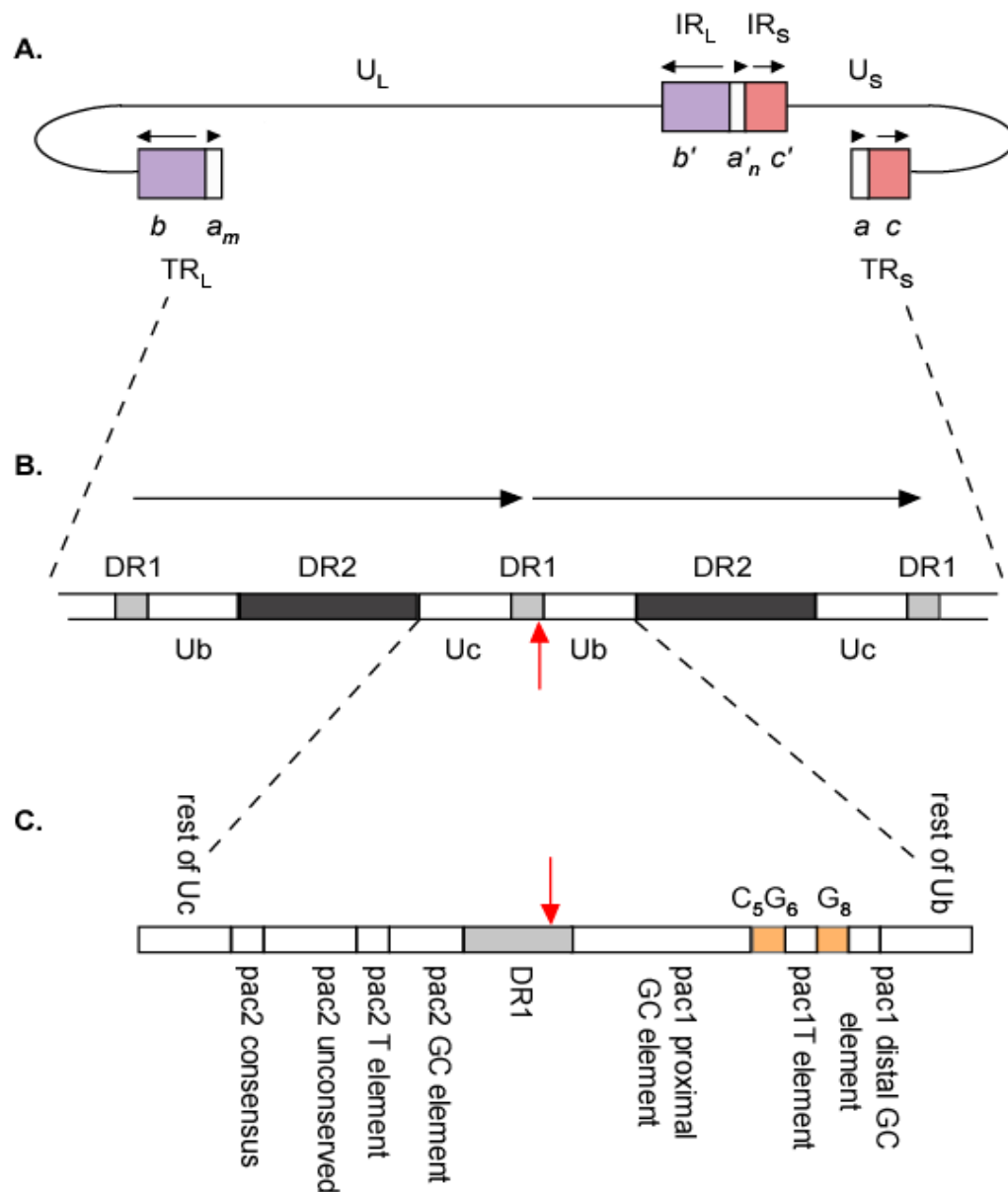


Fig. 1.7: The HSV-1 strain 17 syn+ *a* sequence

A. Ligation of terminal *a* sequences within the HSV-1 genome upon circularisation gives rise to a novel Uc-DR1-Ub fragment (**B**). The relative orientation of the *a* sequences is indicated by black arrows, and the site of concatemer cleavage during encapsidation denoted by red arrows. **C.** Within Uc-DR1-Ub lie the conserved *pac1* and *pac2* motifs, comprised of several sequence elements.

2001).

Traditionally, studies on herpesvirus cleavage packaging signals have employed two approaches. The first is the introduction of putative packaging signals at ectopic sites within viral genomes, and the examination of concatemeric DNA for cleavage at novel sites corresponding to the inserted sequences. However, in many instances, analysis can be complicated by repair of mutated sequences by recombination with wt *a* sequences. The second approach utilises amplicons: plasmids containing both a viral origin of replication (*ori_s*) and a putative packaging signal. The amplicons are transfected into tissue culture cells and helper functions are supplied by wt virus, either via co-transfection of viral DNA or super-infection with virus particles. Amplicon DNA is replicated autonomously and, in the presence of functional packaging signals, is encapsidated. The first demonstration that sub-genomic molecules could be packaged, provided they contain the correct signals, was provided by (Vlazny *et al.*, 1982). Stow *et al.* (1983) demonstrated that encapsidation of amplicon DNA required sequences from either genomic terminus, and concluded that the *a* sequence must therefore contain all the sequences necessary for cleavage and packaging.

Mutation of the *pac1* and *pac2* motifs utilising either of these approaches has allowed the functional importance of packaging elements to be examined. The insertion of mutated *a* sequences into an ectopic site within the strain KOS genome revealed the significance of *pac1* in directing cleavage of the S terminus of HSV-1 (Smiley *et al.*, 1990). Analysis of ectopic mutated copies of *pac1* and *pac2* in the context of the MCMV genome suggested that several elements in both motifs were crucial for successful MCMV DNA packaging (McVoy *et al.*, 1998). Introduction of mutations into HSV-1 *pac1* and *pac2* sequences had profound effects on the propagation and packaging of amplicons containing the mutated sequences. These data led to a model in which signals for the initiation and termination of

packaging are contained within Uc and Ub respectively, and the directions of packaging of the viral genome is from the L terminus to the S terminus (Hodge & Stow, 2001).

Section 1.4 HSV-1 packaging proteins

Six *trans*-acting proteins encoded by HSV-1 (UL6, UL15, UL17, UL28, UL32 and UL33) are absolutely required for DNA cleavage and packaging, but are dispensable for capsid assembly or DNA replication. Viruses lacking functional versions of these proteins exhibit a common phenotype whereby DNase-sensitive concatemers accumulate in infected cells, but DNase-resistant (i.e. encapsidated) viral DNA and genomic termini are absent.

Moreover, these viruses exhibit an absence of C-capsids, together with the accumulation of B-capsids containing cleaved scaffold. These data indicate that these proteins are absolutely required for successful DNA packaging to be initiated. A seventh protein, UL25, is not required for DNA cleavage or the initiation of packaging, but seems to be crucial at the later stages of the packaging process. Similarly, the HSV-1 UL12 gene, encoding an alkaline nuclease, is also required for efficient packaging, although packaging can occur in the absence of functional UL12.

1.4.1 UL6

The 75 kDa UL6 protein has been identified as a component of all three types of mature angular capsids as well as procapsids (Patel & MacLean, 1995; Sheaffer *et al.*, 2001). Initial studies on a virus containing a temperature-sensitive lesion in UL6 revealed its importance in the encapsidation process (Sherman & Bachenheimer, 1987; Sherman & Bachenheimer, 1988). Analysis of UL6-null mutants isolated on complementing cell lines revealed that, in non-complementing cells, viral DNA exists as endless concatemers and B-capsids lacking UL6 accumulate (Patel *et al.*, 1996; Lamberti & Weller, 1998). Recent experiments, in which knock down of the HCMV homologue of UL6 (UL104) using an RNA interference approach led to a decrease in both viral growth and C-capsid formation, confirmed the

importance of UL6 in the packaging process (Dittmer & Bogner, 2006).

Several lines of evidence indicate that the 676 aa UL6 protein forms a dodecameric portal complex at one of the procapsid vertices, structurally and functionally analogous to the connector proteins of bacteriophage. Immunogold labelling of UL6 on B-capsids revealed the deposition of gold particles adjacent to a single capsid vertex. Furthermore, electron microscopy analysis of purified recombinant baculovirus-expressed UL6 complexes revealed heterogeneous ring-like structures, with an estimated mass corresponding to a dodecameric complex of UL6 (Newcomb *et al.*, 2001). Further examination of UL6 expressed from baculovirus-infected insect cells revealed that these rings are polymorphic, exhibiting 11-, 12-, 13- and 14-fold rotational symmetry. It was postulated that the dodecameric form of the complex is incorporated into procapsids, and that the portal projects outwards from the capsid shell (Trus *et al.*, 2004). In agreement with these proposals, tomographic analysis of HSV-1 A-capsids suggested that the majority of the portal may lie outwith the capsid shell (Cardone *et al.*, 2007). However, in stark contrast, evidence from cryotomographic reconstructions of HSV-1 capsids lacking pentons led Chang and colleagues to propose that UL6 formed a portal that lay partially within the capsid shell, in a manner reminiscent to that of ϵ 15 and P22 (Chang *et al.*, 2007). In agreement with this proposal, examination of the KSHV portal by cryotomography revealed that the complex was internally localised (Deng *et al.*, 2007), rather than the outward-protruding model suggested by Trus *et al.* and Cardone *et al.*. It remains to be determined which model is correct.

Recent analysis of a series of UL6 mutants revealed a putative leucine zipper motif within UL6. Mutation of Leu residues within the zipper, or deletion of the entire zipper region, abrogated the ability of mutants to form ring-like structures and to support functional

DNA packaging (Nellissery *et al.*, 2007). Therefore, the zipper may be important for UL6-UL6 interactions involved in ring formation.

By analogy with dsDNA bacteriophage, the portal is also thought to mediate the interaction between terminase and capsid. Indeed, immunofluorescence and co-immunoprecipitation studies revealed that UL6 and the UL15 and UL28 components of the putative HSV-1 terminase interacted (White *et al.*, 2003). This was supported by evidence that in HCMV, the putative portal UL104 and terminase protein UL56 interact, and that this interaction is necessary for DNA packaging to occur (Dittmer *et al.*, 2005).

1.4.2 UL17

The 703 aa UL17 protein has long been recognised as essential for viral replication (Baines & Roizman, 1991). Analysis of null mutants lacking UL17 revealed its involvement in the cleavage and packaging process, and demonstrated the accumulation of B-capsids in the absence of a functional copy of this gene (Salmon & Baines, 1998). Several studies have indicated that UL17 is present in A-, B- and C-capsids, and that more UL17 is present in virions than in capsids. Furthermore, UL17 is also present in L-particles lacking capsids (Salmon & Baines, 1998; Thurlow *et al.*, 2005). Thus, UL17 is unique in being the only HSV-1 DNA packaging protein present in the virion tegument. In contrast, UL17 was reported to be absent from the tegument of PRV, although still crucial for the cleavage and packaging of PRV genomes (Granzow *et al.*, 2005).

Taus and colleagues (1998) demonstrated that, in wt-infected cells, the UL6 protein and major capsid proteins VP5 and pre-VP22a co-localized with ICP8 in replication compartments. However, in the absence of UL17, the major capsid components were not able to co-localize with ICP8, and formed distinct aggregates separate from replication compartments. This suggested that UL17 had a role in targeting capsid components to

replication compartments during infection (Taus *et al.*, 1998).

More recently, it was established that association of UL25, another packaging protein, with angular capsids was dependent upon the presence of UL17. Furthermore, this relationship appeared to be reciprocal; in the absence of UL25, capsids contained two times less UL17 than observed on wt capsids (Thurlow *et al.*, 2006). Since both proteins were detected at multiple locations on the capsid it was hypothesised that they may play a role in stabilising capsids rather than acting directly in the packaging process.

1.4.3 UL32

A virus containing a temperature sensitive lesion in the UL32 gene was isolated in 1973, and later provided the first evidence that UL32 is essential for HSV-1 cleavage and packaging (Schaffer *et al.*, 1973; Sherman & Bachenheimer, 1987). Characterisation of a UL32 insertional mutant, *hr64*, confirmed that UL32 was crucial for cleavage and packaging of viral DNA. In *hr64*-infected non-complementing cells, endless concatemeric DNA and B-capsids accumulated in the nucleus (Lamberti & Weller, 1998).

The UL32 gene encodes a 67 kDa (596 aa) cysteine-rich protein which predominantly accumulates in the cytoplasm of infected cells, although a proportion co-localises with ICP8 in viral replication centres (Chang *et al.*, 1996; Lamberti & Weller, 1998). Chang and co-workers (1996) demonstrated that, contrary to predictions based on the presence of conserved motifs, UL32 was neither a glycoprotein, nor did it encode an aspartyl protease activity. Moreover, they demonstrated that both native and histidine-tagged UL32 bound zinc.

As with UL17, UL32 seems to be important in localising capsids to replication compartments during infection. Examination of infected cells by immunofluorescence

using an anti-hexon antibody revealed that, during wt infection, capsids co-localised with ICP8 in replication compartments. However, in the absence of UL32, capsids were no longer restricted to replication compartments and exhibited diffuse localisation throughout the cell (Lamberti & Weller, 1998).

1.4.4 UL25

Two viruses containing temperature-sensitive lesions in the UL25 gene, *ts1204* and *ts1208*, have been isolated and characterised (Addison *et al.*, 1984). At the NPT, electron microscopy studies revealed that neither virus was capable of assembling C-capsids; instead, an accumulation of B-capsids suggested a packaging defect. In addition, *ts1204* exhibited a very early defect when inoculated onto cells at the NPT, such that no viral gene expression occurred. Subsequent studies have shown that the UL25 lesion of *ts1204* prevents uncoating at the NPT (V. Preston, personal communication).

Studies on the virus KUL25NS, a UL25-null mutant, revealed that in the absence of UL25, genomic DNA was cleaved but that genomes remained DNase-sensitive, confirming that UL25 is required for stable packaging of DNA. Moreover, a lack of functional UL25 led to the accumulation of abortive A-capsids, suggesting that packaging was successfully initiated but not completed (McNab *et al.*, 1998). The authors proposed that UL25 acted as a 'plug' to retain DNA after the completion of packaging, and that this may be mediated by the binding of UL25 to the *a* sequence.

These findings were extended by Stow (2001), who, in contrast, showed that KUL25NS could stably package both amplicon and genomic DNA, albeit inefficiently. Packaging of full-length genomes and amplicon-derived molecules longer than 100 kbp was impaired to a much greater degree than encapsidation of shorter amplicon-derived molecules. Crucially, the L-terminus of the genome was represented in packaged DNA at a significantly higher

level than the S terminus. This is consistent with packaging occurring from L to S, and suggests that UL25 may have an important role in the latter stages of encapsidation (Hodge & Stow, 2001). Stow proposed an alternate late function for UL25 in packaging; that incorporation of UL25 into the capsid during DNA packaging stabilised the capsid and/or the packaging machinery.

Study of purified HSV-1 capsids determined that the 580 aa UL25 protein is predominantly found in C-capsids, with decreasing amounts in A- and B-capsids respectively. In procapsids, very little UL25 was observed, suggesting that UL25 is added as packaging proceeds towards the generation of mature C-capsids (Sheaffer *et al.*, 2001). Experiments with a GFP-tagged UL25 protein demonstrated that UL25 was able to interact with the capsid proteins VP19C and VP5, whilst immunoelectron microscopy studies revealed UL25 associated with both pentons and hexons (Ogasawara *et al.*, 2001). This was confirmed by Newcomb *et al.* (2006), who demonstrated by immunoelectron microscopy that UL25 bound to the capsid vertices. In addition, and in agreement with the hypotheses of McNab and colleagues, Ogasawara *et al.* (2001) demonstrated that UL25 bound the *a* sequence, and thus may act as a 'plug' to anchor DNA inside the capsid. This interaction has however not been confirmed.

Recently, the crystal structure of a truncated form of UL25, lacking the N-terminal 133 amino acids, was resolved (Bowman *et al.*, 2006). The structure reveals a helical core surrounded by flexible loops, consistent with proposals that UL25 binds diverse partners during encapsidation. Sequence comparisons of UL25 homologues identified four conserved clusters of surface residues that were proposed to be involved in protein-protein interactions.

As previously described, binding of UL25 to capsids is thought to be mediated by UL17 (Thurlow *et al.*, 2006). Cryo-electromicroscopy studies of HSV B- and C-capsids revealed a C-capsid specific component (CCSC) not apparent in B-capsids, or in B-capsids purified from a UL25-null virus. On the basis of biochemical data, and fitting of the crystal structure of UL25 into the CCSC mass, it was proposed that the CCSC comprised a UL17-UL25 heterodimer (Cardone *et al.*, 2007). It was speculated that, as DNA is packaged into the capsids, conformational changes expose several sites to which UL17 and UL25 bind. Moreover, it was suggested that the CCSC acts as an allosteric effector to promote nuclear egress of filled capsids.

Recent studies on PRV and HSV-1 have suggested that UL25 may play a role in tegumentation. This conclusion is based on the ability of UL25 to interact with the C-terminus of the large tegument protein, UL36, and that UL25 is required to recruit a fragment representing the C-terminus of UL36 to sites of capsid assembly in the nucleus, allowing its incorporation into capsids (Coller *et al.*, 2007).

1.4.5 UL12

In contrast to the above proteins, the 626 aa alkaline nuclease encoded by UL12 is not essential for DNA packaging. In the absence of a functional alkaline nuclease, however, packaging efficiency is impaired. In viruses lacking functional UL12, an increase in the complexity of branched structures within concatemers was noted and very few C-capsids were present. Together with an increase in the number of abortive A-capsids, these data suggested that capsids containing packaged DNA are unstable in the absence of UL12 (Shao *et al.*, 1993; Martinez *et al.*, 1996). Analysis of the mutant *ambUL12* revealed that the efficiency of both DNA replication and packaging was decreased in the absence of functional UL12 (Porter & Stow, 2004a). Furthermore, the virions produced in the absence of UL12 exhibited high particle: p.f.u. ratios, and contained genomes that were non-

infectious and behaved abnormally in gels (Porter & Stow, 2004b).

Interaction between UL12 and the ssDNA-binding protein ICP8 has been demonstrated, and this interaction promotes strand exchange during recombination and enhances the nuclease activity of UL12 (Reuven *et al.*, 2003; Reuven & Weller, 2005).

Together, these data led to the proposals that in the absence of functional UL12, aberrant branched genomes were packaged, that packaging was aborted at an increased rate, and that DNA-containing capsids matured inefficiently into the cytoplasm. Thus UL12 is thought to resolve the branched intermediates produced during recombination of HSV-1 genomes prior to packaging. Similarly, endonucleases have been implicated in the replication of dsDNA bacteriophage (Vellani & Myers, 2003).

1.4.6 UL15

The first suggestion that the UL15 gene product was involved in cleavage and packaging came in 1992, when Davison observed that the conserved UL15 gene exhibited limited sequence similarity to the gp17 terminase large subunit of T4 bacteriophage. As previously mentioned, UL15 is one of only four spliced genes encoded by HSV-1. However, replacement of the first exon of UL15 with a cDNA copy of the entire gene revealed that separation of the two exons by an intron is not necessary for viral replication (Baines & Roizman, 1992). Subsequently, UL15-null viruses, in which the UL15 gene was either prematurely terminated or replaced with a *lacZ* gene, were generated and characterised. Both viruses were found to be unable to cleave and package DNA when grown on non-complementing cells (Baines *et al.*, 1997; Yu *et al.*, 1997).

Examination of a virus, *ts66.4*, with a temperature sensitive lesion in the UL15 gene similarly demonstrated UL15 to be crucial for DNA cleavage and packaging. At the NPT,

viral DNA was synthesised but not packaged (Poon & Roizman, 1993). Studies on *ts66.4* were extended by Baines and colleagues (1994), who demonstrated that, at the NPT, DNA accumulated as concatemers, thus indicating that functional UL15 was necessary for both cleavage and packaging of viral DNA. In addition, two protein species of 35 kDa and 75 kDa, sharing the same C-terminus, were detected using an antibody raised against UL15 sequences encoded by the second exon of UL15 (Baines *et al.*, 1994). Two publications revealed that the smaller 35 kDa species was derived from distinct in-frame translation of the second exon of UL15, and that the larger species was required for DNA cleavage and packaging (Baines *et al.*, 1997; Yu *et al.*, 1997). In an extension of these studies, Yu and colleagues mapped the initiation codon of the 35 kDa species, termed UL15.5, to Met⁴⁴³ of UL15. They demonstrated that UL15.5 was not required for viral replication or DNA cleavage and packaging (Yu & Weller, 1998a).

Two studies examined the ability of UL15 to associate with angular B and C capsids (Salmon & Baines, 1998; Yu & Weller, 1998b). The former revealed that an 83 kDa protein, postulated to be full-length UL15, was associated with B capsids and virions. The latter study extended these findings, demonstrating that full-length UL15 is present in greater amounts in B-capsids than C-capsids (Yu & Weller, 1998b). In the absence of UL6 or UL28, however, UL15 was unable to associate with B-capsids. Further analysis of virally-infected cells revealed that proteolytic cleavage of UL15 gave rise to two further products of 80 and 79 kDa. Combined with data from a previous study, it was postulated that the 83 kDa UL15 protein associated with capsids via sequences encoded by its N-terminal 509 amino acids, and that cleavage into the smaller forms was tightly associated with encapsidation having taken place (Salmon & Baines, 1998; Salmon *et al.*, 1999).

UL15 has been demonstrated to be present in procapsids in greater amounts than in DNA-

containing C-capsids (Sheaffer *et al.*, 2001). Quantification of the amount of UL15 in angularised capsids by Beard *et al.* (2004) demonstrated that UL15 was predominantly found in A-capsids, with 12 copies of UL15 per A-capsid. In B-capsids, only a single copy of UL15 was observed, and this remained the case even in absence of UL6. It was speculated that a functional packaging complex contained 12 UL15 molecules, as found in abortive A-capsids, and that, as previously described, B-capsids formed by default in the absence of a functional packaging complex (Beard & Baines, 2004). Together, these findings suggest the terminase remains associated with A-capsids after abortion of packaging and DNA release from the terminase. Decreased amounts of UL28 and UL15 in C-capsids are consistent with packaging being processive.

An accumulating body of evidence suggests that UL15 is a component of the viral terminase enzyme, analogous to the terminase of dsDNA bacteriophage (see 1.4.9.)

1.4.7 UL28

Data collected from studies of HSV-1 UL28, and its homologues in PRV and HCMV, have led to the hypothesis that it forms part of the viral terminase complex together with UL15 and UL33 (see 1.4.9).

The first indication that UL28 was involved in the cleavage and packaging process was provided by studies on a temperature-sensitive virus, *ts1203*, containing a lesion in the UL28 gene. At the NPT, neither cleavage nor packaging was observed, and B capsids accumulated in the nuclei of infected cells (Addison *et al.*, 1990). Similarly, cells infected with a temperature-sensitive virus containing a lesion in the C-terminus of UL28 (*tsZ47*) displayed a similar phenotype at the NPT (Cavalcoli *et al.*, 1993). It was demonstrated that *tsZ47* represented a distinct temperature-sensitive mutant that exhibits intragenic complementation with *ts1203*. In support of these findings, studies on a virus lacking the

PRV homologue of UL28, ICP18.5, and two HSV-1 mutants with deletions in UL28, gCB and gCΔ7B, confirmed the necessity for UL28 in the packaging process (Mettenleiter *et al.*, 1993; Tengelsen *et al.*, 1993). On non-complementing cells these viruses exhibited phenotypes similar to viruses lacking other crucial packaging proteins: the accumulation of uncleaved concatemeric DNA and B-capsids in infected cell nuclei.

The first evidence that the 785 aa UL28 polypeptide may be present in viral capsids came from studies on the homologous protein in HCMV, UL56 (Bogner *et al.*, 1993). Subsequent analysis of angular HSV-1 capsids revealed that UL28 is present in B-capsids, but absent from C-capsids (Yu & Weller, 1998b). Sheaffer and co-workers (2001) demonstrated that UL28 was present in procapsids, in greater amounts than observed in C-capsids. Expansion of these findings by Beard *et al.* (2004) established that UL28 is absent from A-capsids, leading to the speculation that, together with viral DNA, UL28 is lost when DNA packaging is aborted.

1.4.8 UL33

To date, three viruses containing mutations in the conserved UL33 gene have been isolated, providing insight into the role of UL33 as a DNA packaging protein. The temperature-sensitive mutant *ts1233* was characterised by Al-Kobaisi *et al.* (1991). The *ts* phenotype of this mutant results from a single amino acid substitution (Ile → Asp at position 17) within the N-terminus of the 130 aa UL33 protein. At the NPT of 39.2 °C, no cleavage or packaging of concatemeric DNA was observed in cells infected with *ts1233*, and a defect in capsid maturation was observed.

A second *ts* virus, *ts8-22*, was recently described and characterised by Yang *et al.* (2008).

The temperature-sensitive phenotype of this virus stems from a single substitution (Thr → Pro) at position 61 of the UL33 protein. At the NPT of 39 °C, neither viral growth nor

encapsidation of viral DNA was observed. Furthermore, B-capsids produced at the NPT failed to exit the nucleus, in agreement with the findings of Al-Kobaisi *et al.* (1991).

The mutant virus UL33⁻, isolated and characterised by Cunningham & Davison (1993) and hereafter referred to as *d*UL33, also contains a mutation within the UL33 ORF. Removal of an *Xba*I site within UL33 by end filling and religation resulted in a frameshift after nucleotide 91 and the subsequent introduction of a novel downstream stop codon at nucleotide 127. The UL33 protein encoded by *d*UL33 therefore contains 42 amino acids: the first thirty amino acids of wt UL33, followed by twelve novel amino acids (ARRALRLARRRA). This mutation rendered the virus unable to propagate unless grown on complementing 20A cells containing the UL33 gene. Further analyses confirmed that UL33 was not detectable in cells infected with this virus, and revealed that on non-complementing cells, *d*UL33 produced only B-capsids and concatemeric DNA (Patel *et al.*, 1996; Reynolds *et al.*, 2000).

In 2000, Reynolds and co-workers also showed that UL33 was expressed with late kinetics (γ_2 class) and partially co-localised with ICP8 in replication compartments at late times during infection. Mutants lacking individual packaging proteins (UL6, UL15, UL17, UL28 and UL32) were reported to exhibit similar localisation of UL33 (Reynolds *et al.*, 2000).

Examination of angularised HSV-1 capsids revealed that UL33 associates with all three types of capsids (Beard & Baines, 2004). An increased amount of UL33 was observed in A-capsids compared to B-capsids, and association of UL33 was sensitive to increasing GuHCl concentrations. Furthermore, binding of UL33 to capsids was reported to be independent of the presence of UL6, UL15 or UL28. It is unknown whether UL33 is able to associate with procapsids.

UL33 has been demonstrated to interact with several viral proteins. An increasing body of evidence suggests that UL33, by virtue of interactions with UL15 and UL28, is a component of the viral terminase complex responsible for genome cleavage and packaging (1.4.9).

Studies of the HSV-2 homologue of UL33 revealed that nuclear localisation of UL33, and the capsid protein VP26, was dependent upon the presence of the HSV-2 UL14 protein in co-transfection assays (Yamauchi *et al.*, 2001). Furthermore, UL14 was demonstrated to share certain characteristics of heat shock proteins, including sharing sequences with several members of the Hsp70 family (Yamauchi *et al.*, 2002). However, in HSV-1, UL14 is not absolutely essential for viral growth but is important for efficient egress of capsids from infected cells (Cunningham *et al.*, 2000). This suggests that HSV-1 UL14 is dispensable for DNA packaging and is unlikely to play a crucial role in the transport of UL33 to the nucleus. Recent studies have demonstrated that HSV-1 UL14 is important for mediating the nuclear import of VP16, and thus may play a role in early viral transcription events (Yamauchi *et al.*, 2008).

Recent analysis of viral proteins in yeast-2-hybrid (Y2H) screens suggested that the KSHV and VZV homologues of UL33 interact with numerous viral partners (Uetz *et al.*, 2006). Proposed partners include, but are not limited to, the homologues of HSV-1 DNA replication proteins UL5 and UL9, the capsid proteins VP23 and VP26, and several proteins involved in nucleotide metabolism. Interestingly, UL33 was also demonstrated to interact with homologues of the packaging proteins UL17 and UL32 in this system (summarised in Table 5.1).

However, several problems are apparent in the study by Uetz and colleagues. Firstly, many conserved and well-characterised interactions, such as those between the DNA helicase-primase accessory factor and origin-binding protein (UL8 and UL9 respectively, McLean *et al.* (1994), were not detected using this experimental approach. Similarly, interactions between the terminase components (UL15-UL28 and UL28-UL33) were not identified.

Furthermore, strong correlation has been observed between protein hydrophobicity and number of protein partners in Y2H screens (Deeds *et al.*, 2006). Thus, several (or all) of the UL33 interactions observed by Uetz and colleagues may be spurious, and mediated non-specifically by hydrophobic residues within UL33. Lastly, recent experiments utilising Y2H screens to examine protein-protein interactions in EBV failed to detect any of the UL33 interactions observed in KSHV or VZV (Calderwood *et al.*, 2007).

1.4.9 The HSV-1 terminase: UL15, UL28 and UL33

A substantial body of evidence has led to the hypothesis that UL15, UL28 and UL33 form a viral terminase enzyme, analogous to that of several dsDNA bacteriophage, and crucial for the encapsidation of viral genomes. In contrast with phage terminases, HSV-1 terminase therefore contains three subunits. At present, the biochemical activities necessary for DNA packaging (e.g. ATPase or nuclease activities) have not been demonstrated for either the complex or individual subunits of the HSV-1 terminase. No cell-free system for HSV-1 DNA packaging currently exists in which to demonstrate terminase function directly.

Distant relatedness between UL15 and the large terminase subunit of T4 bacteriophage, especially conservation of a putative Walker A box ATP-binding motif, first suggested that the conserved UL15 gene was part of an HSV-1 terminase (Davison, 1992). This was further reinforced by mutation of a conserved Gly residue within the Walker A box of UL15, which abrogated DNA cleavage and packaging (Yu & Weller, 1998a). Further

evidence that UL15 encodes a terminase function was provided by mutagenesis studies in which residues conserved between UL15 and the large subunits of phage terminase were mutated (Przech *et al.*, 2003). Generally, these alterations rendered UL15 unable to support cleavage and packaging, although the ability of the mutated proteins to bind to capsids or localise to replication compartments was unperturbed.

Koslowski *et al.* (1997) provided evidence of a direct interaction between UL15 and UL28, by demonstrating that HSV-1 UL15 is capable of re-locating PRV UL28 to the nucleus of co-transfected cells. Deletion mutants revealed that the C-terminal 155 aa of PRV UL28 were important for the interaction with UL15 (Koslowski *et al.*, 1997). When expressed alone, HSV-1 UL28 was present in the cytoplasm. However, in the presence of UL15, both proteins co-localised in the nucleus, suggesting an interaction. This was confirmed by the purification of a UL15-UL28 heterodimer from HSV-1-infected cells (Koslowski *et al.*, 1999). Mutational analysis of UL28 revealed that at least two separate regions of UL28 are responsible for interactions with UL15 (Abbotts *et al.*, 2000). Recently, analysis of a virus containing a lethal insertion in UL28 revealed a second-site mutation within UL15, capable of restoring functional DNA packaging and providing genetic evidence that interaction between the proteins is necessary for encapsidation (Jacobson *et al.*, 2006).

In 2001, Adelman *et al.* (2001) reported that HSV-1 UL28 encoded a DNA-binding activity, by demonstrating that UL28 bound to a novel ssDNA structure formed by the *pac1* motif. The efficiency of UL28 binding to various *pac1* mutants correlated with the ability of similar *pac1* mutants to undergo cleavage in MCMV. These data were consistent with the hypothesis that UL28 was a crucial component of the putative HSV-1 terminase. However, this appears to conflict with the proposal that *pac1* is involved in packaging termination, and the findings that mutants lacking UL28 exhibit defects in initiation of packaging

(Addison *et al.*, 1990; Tengelsen *et al.*, 1993; Hodge & Stow, 2001). It remains possible, however, that UL28 may also interact with sequences required for initiation. Although the binding of HSV-1 UL28 to packaging signals has not been confirmed, a body of evidence from Bogner and colleagues suggests that the homologous HCMV protein, UL56, is able to bind HCMV packaging signals (Bogner *et al.*, 1998; Bogner, 1999).

Experiments in HSV-1-infected mammalian cells and insect cells mixedly infected with recombinant baculoviruses demonstrated that an antibody directed against UL28 was able to co-immunoprecipitate UL15, UL28 and UL33 (Beard *et al.*, 2002). It was additionally shown that UL33 was able to interact independently with UL15 and UL28. Thus it was suggested that a hetero-oligomeric complex of UL15, UL28 and UL33 comprised the HSV-1 terminase.

In contrast to the studies by Beard and co-workers, Yang and Baines (2006) demonstrated that UL28 was necessary to mediate the interaction between UL15 and UL33.

Furthermore, the presence of UL33 enhanced the UL15-UL28 interaction (Jacobson *et al.*, 2006). Linker-based mutagenesis of UL28 revealed that the C-terminus of UL28 was required for its interaction with UL33 (Jacobson *et al.*, 2006). Furthermore, co-immunoprecipitation analysis of cells infected with the UL28-null mutant gCB confirmed that UL15 and UL33 interact only indirectly.

Immunofluorescence and immunoprecipitation assays demonstrated that both UL15 and UL28 could interact with the HSV-1 portal protein UL6, consistent with their role as a terminase (White *et al.*, 2003). This result was confirmed in HSV-1-infected cells by Yang *et al.* (2007). It remains unknown whether UL33 can also interact with UL6.

Yang and colleagues (2007) additionally demonstrated that the UL15-UL28-UL33 complex was assembled in the cytoplasm of infected cells, and that an NLS within UL15 was responsible for import of the complex into the nucleus. UL6 was imported into the nucleus separately from UL15, suggesting that interaction between terminase and portal is a subsequent event (Yang *et al.*, 2007). Characterisation of two viruses, *ts8-22* and *ts66.4*, containing temperature-sensitive lesions in UL33 and UL15 respectively, demonstrated that at the NPT interaction of the thermolabile protein with the remaining members of the terminase complex was diminished (Yang *et al.*, 2008). Furthermore, the lesion within UL33 was sufficient to reduce interaction with UL28 in transient expression assays.

Studies by Bogner and colleagues on the HCMV homologues of UL28 and UL15, UL56 and UL89 respectively, have provided insight into the function of these proteins in the cleavage and packaging process. UL56 has been demonstrated to exhibit ATPase and nuclease activities *in vitro*, and is able to bind both *pac1* and *pac2* sequences (Bogner *et al.*, 1998). An ATPase activity has also been attributed to UL89 *in vitro* (Scheffczik *et al.*, 2002). Further study has revealed that ATP hydrolysis by UL56 is enhanced by UL89 (Hwang & Bogner, 2002) and that mutation of several residues diminishes the ATPase activity of UL56 (Scholz *et al.*, 2003). The structure of UL56 has been resolved by electron microscopy, which revealed a dimer consisting of two ring-like monomers stacked on top of one another (Savva *et al.*, 2004). Interaction between these proteins has been demonstrated in GST pulldown experiments (Thoma *et al.*, 2006). However, not all these findings are necessarily relevant to the HSV-1 proteins. For example, UL56 has been demonstrated to encode an NLS critical for DNA packaging, which is lacking in the homologous HSV-1 UL28 protein (Geisen *et al.*, 2000b). Furthermore, sequence alignments showed that the ATP binding domains identified by Scholz *et al.* (2003) in HCMV UL56 are not retained in HSV-1 UL28.

1.4.10 DNA packaging as a drug target

Due to its unique mechanism and crucial role in the viral life cycle, DNA cleavage and packaging is an attractive target for novel anti-herpesvirus therapeutics (reviewed by Visalli & van Zeijl, 2003). Indeed, several compounds have been described which target proteins known to be crucial for DNA packaging. The first report of therapeutics able to inhibit the cleavage packaging process came in 1998, when it was demonstrated that a benzimidazole ribonucleoside (BDCRB) inhibited cleavage of concatemeric HCMV DNA (Krosky *et al.*, 1998). In addition, resistance to BDCRB was conferred by two mutations within the second exon of the HCMV UL89 gene, which, on the basis of homology to the T4 bacteriophage terminase large subunit, was postulated to encode the endonucleolytic subunit of the HCMV terminase. Furthermore, mutations within both the UL56 and UL89 genes of HCMV (which are crucial for HCMV encapsidation) conferred resistance to a related packaging inhibitor, TCRB (Krosky *et al.*, 1998).

The first packaging inhibitors (WAY-150138 and CL-253824) to inhibit growth of HSV-1, and to a lesser extent HCMV, HSV-2 and VZV, were described by van Zeijl *et al.* (2000). Examination of viral DNA in infected cells treated with these compounds revealed a defect in the cleavage and subsequent encapsidation of DNA. Three independent isolates revealed that resistance mapped to the putative portal protein UL6, and arose from single point mutations in the amino acid sequence. Moreover, when these mutations were individually introduced into wt virus, they were sufficient to mediate drug resistance. These findings were extended by Newcomb & Brown (2002), who demonstrated that WAY-105138 was able to inhibit incorporation of the portal protein UL6 and the putative terminase subunit UL15 into capsids.

More recently, studies of BDCRB have been extended to determine how it inhibits cleavage and packaging. Studies on guinea pig cytomegalovirus (GPCMV) revealed that whilst packaging occurred in the presence of BDCRB, capsids were unable to protect DNA from degradation by DNase, and were unable to exit the nucleus (Nixon & McVoy, 2004). In addition, BDCRB induced the loss of 2.7-4.2 kbp of sequence from the left-hand end of genomes. This led to the proposal that BDCRB induced a premature cleavage event in GPCMV. The scope of these studies was extended to HCMV, where it was noted that BDCRB induced the formation of a 270 kbp species known as monomer+, containing two copies of the short genome segment (McVoy & Nixon, 2005). It was thus hypothesised that BDCRB induces the skipping of cleavage sites in HCMV. Together, these data suggest that BDCRB acts by altering the ability of terminase to recognise packaging signals.

Section 1.5 Aims

Although UL33 has been demonstrated to be part of the putative HSV-1 terminase complex and vital for DNA packaging, its role in the process has yet to be elucidated. The aims of the work set out in this thesis were to examine structural-functional relationships within UL33, and to shed new light on its role in encapsidation of the viral genome.

Initially, a panel of UL33 mutants bearing 5 aa insertions within the UL33 ORF were created to identify regions important for its function. These were tested for their ability to support viral growth and DNA packaging in cells infected with the UL33 mutant viruses *dUL33* and *ts1233* (Al-Kobaisi *et al.*, 1991; Cunningham & Davison, 1993). These experiments revealed that mutations in several regions of UL33 abrogated growth and packaging.

Subsequent studies aimed to determine why several mutants were unable to support DNA

packaging and viral growth. It was postulated that an inability of several mutants to package DNA might be explained by a failure to interact with the putative terminase proteins UL15 and UL28. However, experiments were unable to demonstrate that any of the mutants were defective in their ability to bind either UL15 or UL28. As a result, ensuing experiments focused on the ability of wild type and mutated UL33 proteins to interact with the other DNA packaging proteins. Although novel interactions were detected between UL33 and UL6, and also between UL33 and the UL25 protein, none of the mutants were compromised in their ability to bind either of these proteins.

Finally, in an effort to determine whether the mutated UL33 proteins retained the capacity to localise to sites of viral DNA packaging, their localisation in *Δ*UL33-infected cells was examined. Further experiments aimed to ascertain whether a specific component of the packaging machinery was responsible for the localisation of the terminase complex to sites of viral replication and genome packaging.

Chapter 2: Materials and methods

Section 2.1 Materials

2.1.1 Chemicals and reagents

All chemicals and reagents were purchased from Sigma-Aldrich Co. Ltd, except where stated below:

BDH Laboratory Supplies:	-Dimethylsulphoxide (DMSO)
	-Dimethylformamide (DMF)
Bio-Rad Laboratories:	-Acrylamide
	-Acrylamide: N, N'-methylene-bis acrylamide
	19:1
	-Ammonium persulphate
Melford Laboratories Ltd:	-Caesium chloride
Pierce:	-Surfact-Amps TM NP40

2.1.2 Stock solutions

Alkaline lysis solution I	15 mM Tris-HCl pH 8.0, 10 mM EDTA pH 8.0, 100 µg/ml RNase A
Alkaline lysis solution II	0.2 M NaOH, 1% (w/v) SDS
Alkaline lysis solution III	5 M Potassium acetate, 11.5 ml glacial acetic acid, in a final volume of 100 ml distilled water
β-galactosidase Fix	2% (w/v) formaldehyde and 0.2% (w/v) gluteraldehyde in PBS
β-galactosidase Stain	5 mM potassium ferricyanide, 5 mM potassium ferrocyanide, 2 mM MgCl ₂ , 0.5 mg/ml X-gal solution in PBS.
Blocking Solution	5% (w/v) marvel, 10% (v/v) FCS, 10% (v/v) glycerol, 0.05% (v/v) Tween-20 in PBS
Blot Presoak	6x SSC, 5x Denhardt's solution, 0.1% (w/v)

	SDS, 20 µg/ml denatured calf thymus DNA
Blot Wash	2x SSC, 0.1% (w/v) SDS
Boiling mix	6% (w/v) SDS, 30% (v/v) glycerol, 0.3% (w/v) bromophenol blue, 210 mM β- mercaptoethanol
Cell Lysis Buffer (2x)	20 mM Tris-HCl pH 7.5, 2 mM EDTA, 1.2% (w/v) SDS
Chloroform:Isoamyl alcohol	24 parts chloroform:1 part isoamyl alcohol (v/v)
Denhardt's Solution	0.02% Ficoll 400, 0.02% polyvinyl pyrrolidone, 0.02% bovine serum albumin
DNA Loading Buffer	0.25% (w/v) bromophenol blue, 40% (w/v) sucrose
Denaturing Gel Soak	0.6 M NaCl, 0.2 M NaOH
EZ Buffer	1% (v/v) NP40, 10% (v/v) glycerol, 100 mM Tris-HCl pH 8.0, 100 mM KCl, 0.5 mM PMSF, 1 µM Leupeptin, 1 µM Pepstatin
Formaldehyde Fix	5% (v/v) formaldehyde, 2% (w/v) sucrose in PBS
Fractionation Buffer A	50 mM Tris-HCl pH 8.0, 50 mM NaCl, 1% NP40, 1 mM dithiothreitol, 0.5 mM PMSF
Fractionation Buffer B	50 mM Tris-HCl pH 8.0, 450 mM NaCl, 1% NP40, 1 mM dithiothreitol, 0.5 mM PMSF
HEPES-buffered Saline (HeBS)	137 mM NaCl, 5 mM KCl, 0.7 mM NaH ₂ PO ₄ , 5.5 mM D-glucose, 21 mM HEPES, adjusted to pH 7.05 with NaOH
Hybridisation Mix	6x SSC, 10x Denhardt's solution, 20 mM Tris- HCl pH 7.5, 1 mM EDTA, 0.5% (w/v) SDS, 50 µg/ml denatured calf thymus DNA
LB Medium	170 mM NaCl, 1% (w/v) Bactopectone, 0.5% (w/v) yeast extract
LB-agar	L-Broth plus 1.5% (w/v) agar
Loening's Buffer	40 mM NaH ₂ PO ₄ , 36 mM Tris, 1 mM EDTA
Neutralising Gel Soak	0.6 M NaCl, 1 M Tris-HCl pH 8.0

Nick-translation Buffer (NTB) (10x)	0.5 M Tris-HCl pH 7.5, 0.1 M MgCl ₂ , 10 mM DTT, 0.5 mg/ml BSA
Permeabilisation Buffer	0.5% (v/v) NP40, 10% (w/v) sucrose in PBS
Phosphate-buffered Saline (PBS)	137 mM NaCl, 2.7 mM KCl, 10 mM Na ₂ HPO ₄ , 2 mM KH ₂ PO ₄
Protease	20 mg/ml grade XIV protease
Resolving gel buffer (4x)	1.5 M Tris-HCl pH 8.8, 0.4% (w/v) SDS
Reticulocyte Standard Buffer (RSB)	10 mM Tris-HCl pH 7.5, 10 mM KCl, 1.5 mM MgCl ₂
RNase Mix (200x)	1 mg/ml RNase A, 100,000 U/ml RNase T ₁ in TE
SDS-PAGE tank buffer	52 mM Tris, 53 mM glycine, 0.1% (w/v) SDS
S.O.C. Media	2% (w/v) tryptone, 0.5% (w/v) yeast extract, 10 mM NaCl, 2.5 mM KCl, 10 mM MgCl ₂ , 20 mM glucose
Stacking gel buffer (4x)	488 mM Tris-HCl pH 6.8, 0.4% (w/v) SDS
Standard Saline Citrate (SSC)	150 mM NaCl, 15 mM sodium citrate
Sucrose Reagent	0.25 M sucrose, 2 mM MgCl ₂ , 50 mM Tris-HCl pH 8.0
TE	10 mM Tris-HCl pH 8.0, 1 mM EDTA pH 8
Towbin Buffer	25 mM Tris, 192 mM glycine, 20% (v/v) methanol
Tris-Borate-EDTA (TBE)	90 mM Tris base, 89 mM boric acid, 1 mM EDTA
Tris-Buffered Saline (TBS)	137 mM NaCl, 5 mM KCl, 0.7 mM NaH ₂ PO ₄ , 5.5 mM glucose, 25 mM Tris-HCl pH 7.4
Triton Reagent	0.5% (v/v) Triton-X 100, 62.5 mM EDTA, 50 mM Tris-HCl pH 8.0
Tryptose Phosphate Broth (TP)	0.1 mg/ml tryptose phosphate in PBS
Versene	0.6 mM EDTA, 0.002% phenol red in PBS
X-gal Solution	20 mg/ml X-gal in DMF

2.1.3 Enzymes

All restriction enzymes, and their appropriate buffers, were supplied by New England Biolabs or Roche Diagnostics Ltd. Other enzymes are listed below, together with their suppliers:

Sigma-Aldrich Co. Ltd:	-Protease grade XIV
	-Lysozyme
	-RNase A
	-RNase T ₁
	-DNase I
New England Biolabs:	-DNA polymerase I
	-T4 DNA ligase
	-Calf intestinal phosphatase

2.1.4 Cells and culture media

Baby hamster kidney 21 clone 13 (BHK-C13) cells were used for much of the presented work, and were obtained from the Unit's Cytology Department. BHK-C13-derived 20A cells were acquired from Charles Cunningham (MRC Virology Unit; Cunningham & Davison, 1993). Rabbit skin cells (RSCs) were obtained from Dr Valerie Preston (MRC Virology Unit), and RSC-derived clone 17 cells were acquired from Dr Joel Baines (Cornell University, Ithaca, New York, U.S.A; Baines *et al.*, 1997). African green monkey kidney (Vero) cells were acquired from Dr Valerie Preston. Vero-derived C1 cells were obtained from Dr Fred Homa (University of Pittsburgh, Pittsburgh, U.S.A.; Tengelsen *et al.*, 1993). *Spodoptera frugiperda* (Sf21) cells were obtained from the Unit's Cytology Department.

The following media was used in the cultivation of these cells:

Glasgow's modified Eagle's medium (GMEM)	- Invitrogen Ltd.
Dulbecco's modified Eagle's medium (DMEM)	- Invitrogen Ltd.
TC100	- Invitrogen Ltd.
Foetal Calf Serum (FCS)	- Invitrogen Ltd.
Newborn Calf Serum (NBCS)	- Invitrogen Ltd.
Human Serum (HS)	- MP Biomedicals LLC
Trypsin (10x)	- Invitrogen Ltd.
EPS	- GMEM supplemented with 100 U/ml penicillin and 100 µg/ml streptomycin
EC5	- EPS plus 5% NBCS
BHK/20A growth medium	- EPS plus 10% NBCS and 7% Tryptose phosphate broth
Vero/C1/RSC/clone 17 medium	- DMEM supplemented with 100 U/ml penicillin and 100 µg/ml streptomycin plus 5% FCS
<i>Sf</i> 21 growth media	- TC100 plus 5% FCS, 100 U/ml penicillin and 100 µg/ml streptomycin
EC ₂ HU ₃	- EPS plus 2% FCS and 3% HS
<i>Sf</i> 21 overlay	- 1:25 dilution of Neutral Red in <i>Sf</i> 21 growth media

2.1.5 Antibiotics

The antibiotics used in this study are listed below, together with their suppliers.

Ampicillin (Penbritin)	- SmithKline Beecham Research
------------------------	-------------------------------

Chloramphenicol	- Sigma-Aldrich Co. Ltd
Gentamycin	- Invitrogen Ltd
Kanamycin	- Sigma-Aldrich Co. Ltd
Tetracycline	- Sigma-Aldrich Co. Ltd
Penicillin/Streptomycin	- Invitrogen Ltd

2.1.6 Viruses

Several herpesviruses were used in the course of the experimental work:

HSV-1 strain 17 syn+	- McGeoch <i>et al.</i> (1988)
UL33- (hereafter referred to as <i>dUL33</i>)	- Cunningham & Davison (1992)
<i>ts1233</i>	- Al-Kobaisi <i>et al.</i> (1991)
gCB	- Tengelsen <i>et al.</i> (1993)
S648	- Baines <i>et al.</i> (1997)
<i>lacZ</i> -UL6 ⁻	- Patel <i>et al.</i> (1996)

2.1.7 Baculoviruses

The following baculoviruses were used in co-immunoprecipitation studies, and express the indicated HSV-1 gene under the control of the AcMNPV polyhedrin promoter:

AcUL6	Patel <i>et al.</i> (1996)
AcUL15	Abbotts <i>et al.</i> (2000)
AcUL17	Dr V. Preston (unpublished)
AcUL25	Thurlow <i>et al.</i> (2005)
AcUL28	Abbotts <i>et al.</i> (2000)
AcUL32	Dr A. Patel (unpublished)
AcUL33	Dr N. Stow (unpublished)

2.1.8 Bacterial strains

Plasmids were manipulated and propagated in *E. coli* strain DH5 (XL1-Blue; Stratagene). High efficiency transformations were performed using electrocompetent *E. coli* DH10B (Genehogs; Invitrogen Ltd.). Recombinant baculoviruses were created using electrocompetent *E. coli* DH10Bac cells (Invitrogen Ltd.).

2.1.9 Plasmids

The following plasmids were used in this study and provided by Dr N. Stow, unless otherwise stated:

pAT153	Vector derived from pBR322 containing amp/tet resistance loci (Twigg & Sherratt, 1980).
pCMV10	Mammalian expression vector specifying amp resistance, and containing a MCS flanked by the HCMV major IE promoter and splicing/polyadenylation signals from SV40 (Stow <i>et al.</i> , 1993)
pAS30	The HSV-1 UL6 gene (nucleotides 15120 to 17323) inserted into the MCS of pCMV10 (Patel <i>et al.</i> , 1996).
pE9	The HSV-1 UL9 gene (nucleotides 23261 to 20809) cloned into the MCS of pCMV10 (Stow <i>et al.</i> , 1993)
pElacZ	pCMV10 containing the <i>E. coli lacZ</i> gene
pGX153	Plasmid pAT153 containing the <i>Bam</i> HI P fragment from HSV-1 (Porter & Stow, 2004b)
pIM96	The HSV-1 UL25 gene cloned into the <i>Bam</i> HI site of pCMV10 (Dr V. Preston, MRC Virology Unit)
pJM9	A cDNA fragment equivalent to the spliced mRNA of UL15 in pCMV10 (Abbotts <i>et al.</i> , 2000)
pJM19	pJM9 with the pp65 epitope (ERKTPRVTTGG) added to the C-terminus of the UL15 ORF (Abbotts <i>et al.</i> , 2000)
pMH19	The HSV-1 UL17 gene under the control of the HCMV MIEP (Thurlow <i>et al.</i> , 2005)
pSA1	pAT153 with the HSV-1 ori _s fragment cloned into the <i>Bam</i> HI site,

2.1.12 Antibodies

The following immunological reagents were used in this study, and are listed together with the immunogen used to create the antibody, and the source or supplier:

Antibody	Immunogen	Source/Reference
Rabbit polyclonal antibodies		
R148	Bacterially-expressed UL33-His ₆ purified from inclusion bodies	Dr V. Preston, MRC Virology Unit
R123	Bacterially expressed amino acids 138-785 of UL28	Abbotts <i>et al.</i> (2000)
R605	Bacterially expressed fusion protein, GST-UL15 (amino acids 551-917)	Dr V. Preston, MRC Virology Unit
R1218	Amino acids 154-703 of UL17-MBP fusion protein	Thurlow <i>et al.</i> (2006)
RC12	A peptide displaying amino acids 580-594 of UL32	Dr A. Patel, MRC Virology Unit
R335	Amino acids 342-580 of UL25-GST fusion protein	Thurlow <i>et al.</i> (2006)
R992	Amino acids 379-676 of UL6-MBP fusion protein	Thurlow <i>et al.</i> (2006)
Mouse monoclonal antibodies		
M51(4)	Bacterially expressed UL33-His	Dr V. Preston, MRC Virology Unit
M166	Bacterially expressed UL25-His	Thurlow <i>et al.</i> (2005)
M175	Bacterially expressed UL6-NusA	Thurlow <i>et al.</i> (2005)
M13924	HSV-1 UL9	Stow <i>et al.</i> (1998)
M7381	HSV-1 ICP8 (UL29)	Everett <i>et al.</i> (2004)
M203	Bacterially expressed UL17-NusA	Thurlow <i>et al.</i> (2005)
DM165	Purified HSV-1 VP5 (UL19) protein	McClelland <i>et al.</i> (2002)
Anti-Histone H1	Histone H1 A & B	Upstate Biotechnology

The following epitope-specific mouse monoclonal antibodies were used:

Epitope:

Mouse Anti-c-Myc	Amino acids 408-439 of human p62 ^{c-Myc}	Sigma-Aldrich Co. Ltd.
Mouse Anti-His ₆	His ₆ epitope	Roche Diagnostics Ltd.
Mouse Anti-pp65	HCMV pp65 epitope (HCMV late gene product)	Capricorn Products
Mouse Anti-Actin	Synthetic actin C-terminal epitope (SGPSIVHRKCF)	Sigma-Aldrich Co. Ltd.

Secondary antibodies

Protein A-horseradish peroxidase conjugate	Sigma-Aldrich Co. Ltd.
Goat Anti-mouse IgG-Cy5 conjugate	GE Healthcare
Goat Anti-rabbit IgG-FITC conjugate	Sigma-Aldrich Co. Ltd.

2.1.13 Miscellaneous reagents

The suppliers of miscellaneous reagents were as follows:

Citifluor:	AF1 Mounting Agent
GE Healthcare:	Rainbow markers
	Hybond-XL Membrane
	Hybond-P PVDF Membrane
	G-50 Microspin Columns
	ECL Reagent
	Gammabind-G-Sepharose
Invitrogen:	Lipofectamine Reagent
	Plus Reagent
Kodak Ltd:	X-omat Film
Fujifilm:	Phosphorimager Screens
Sigma-Aldrich Co. Ltd:	Propidium Iodide
	Ethidium Bromide

Protein-A-Sepharose

Phenol

Finzymes: Insertional Mutagenesis Kit

Qiagen: QiaQuick Gel Extraction Kit

2.1.14 Computer software

LOOPP Protein-threading analysis - <http://cbsuapps.tc.cornell.edu/>

Pattern PROFILE analysis - <http://myhits.isb-sib.ch/cgi-bin/index>

Expasy Translate tool (Gasteiger *et al.*, 2003) - <http://expasy.org/tools/dna.html>

PSIPred (Jones, 1999) - <http://bioinf.cs.ucl.ac.uk/psipred/>

GlobPlot (Linding *et al.*, 2003) - <http://globplot.embl.de/>

Quantity One 1-D Analysis software - Bio-Rad Laboratories

Section 2.2 Methods

2.2.1 DNA manipulation and analysis

2.2.1.1 Restriction enzyme digests

One microgram of plasmid DNA was digested with 2.5 U of appropriate restriction enzyme in a final volume of 10 μ l in the presence of 100 μ g/ml BSA and a 1 x concentration of buffer. Digests were incubated at 37 $^{\circ}$ C for two hours. If further modification of the digested plasmid was required, the reaction was extracted once with an equal volume of phenol, once with an equal volume of chloroform: isoamyl alcohol, and the DNA was precipitated with 2.5 volumes of ethanol. Following centrifugation the DNA was re-suspended in TE pH 7.5.

2.2.1.2 Dephosphorylation of vector

To prevent recircularisation during subsequent ligations, vector DNA was dephosphorylated with calf intestinal phosphatase (CIP). One microgram of linearised vector was incubated with 1 U of CIP at 37 °C for two hours. The DNA was then extracted, precipitated, and re-suspended in TE pH 7.5 as described above (2.2.1.1).

2.2.1.3 Agarose gel electrophoresis

TBE buffer or Loening's buffer containing the appropriate percentage of agarose was boiled, and allowed to cool to approximately 60 °C. Ethidium bromide was added to 0.5 µg/ml, and the agarose poured into a mould containing a well-forming comb. Upon setting, the gel was placed in an electrophoresis tank with the appropriate buffer, and DNA samples containing 1 x DNA loading buffer were added to individual wells. Samples were electrophoresed overnight at a constant voltage of 15 V, or for one hour at 100 V, and the DNA visualised using medium-wave UV.

2.2.1.4 Purification of DNA fragments

Plasmid DNA was digested with the appropriate restriction enzyme(s) to liberate the desired fragment, and the fragments separated on a 0.8% TBE gel containing ethidium bromide. DNA was visualised using long-wave UV, and the desired fragment excised. Purification of the DNA fragment from the gel slice was carried out using a Qiagen QIAquick Gel Extraction Kit according to the manufacturer's instructions. Briefly, the volume of the gel slice containing the fragment of interest was calculated, and the slice incubated in three gel volumes of guanidine thiocyanate at 50 °C. After the agarose had dissolved completely, a single gel volume of isopropanol was added. DNA was adsorbed onto an immobilised silica membrane, washed, and bound DNA eluted with 30-50 µl 10 mM Tris-HCl, pH 8.5.

2.2.1.5 Ligation

One microgram each of vector and DNA fragment were incubated with 1 U of T4 DNA ligase in a total volume of 20 μ l of 1X ligation buffer. The reaction was incubated overnight at 4 $^{\circ}$ C, extracted sequentially with phenol and chloroform:isoamyl alcohol, and precipitated with 2.5 volumes of ethanol. DNA was re-suspended in TE pH 7.5.

2.2.1.6 Insertional mutagenesis

Transposition was carried out using a Finnzyme Mutation Generation System according to the manufacturer's instructions. 170 ng of pUL33 was reacted with the MuA transposase and the M1-Cam^R Entranceposon at 30 $^{\circ}$ C for one hour. The transposase was heat-inactivated by incubation at 75 $^{\circ}$ C for ten minutes. Prior to transformation, 1 μ l of the reaction was diluted with 9 μ l H₂O to reduce the salt concentration of the reaction and avoid arcing during electroporation. Ten aliquots of 1 μ l of the diluted mixture were transformed into electrocompetent DH10 *E. coli* as described below (section 2.2.2.1). Transformed bacteria were plated out on ten LB-agar plates containing chloramphenicol and ampicillin, and incubated overnight at 37 $^{\circ}$ C.

Resultant colonies were picked, and plasmid DNA was prepared by alkaline lysis (section 2.2.3.1). Transformants harbouring the transposon were identified by restriction enzyme digestion. To release the transposon, DNA from positive clones was digested with *Nco*I, and 5 ng of DNA was self-ligated. Plasmid DNA from the resulting transformants was isolated by alkaline lysis (section 2.2.3.1). The positions of the resulting 15 bp insertions were identified by restriction enzyme analysis and DNA sequencing (see Chapter 3).

2.2.2 Maintenance and manipulation of *E. coli*

2.2.2.1 Transformation of competent *E. coli*

Chemically competent DH5 cells (XL-1 Blue) were transformed according to the manufacturer's instructions. Briefly, 50 μl of cells were thawed slowly on ice, and between 1 ng and 10 ng of diluted DNA from a ligation reaction was added. Cells were incubated on ice for 30 min, heat shocked at 42 °C for 45 sec, and placed on ice for two min. 450 μl of S.O.C. medium was added to the cells, which were then shaken at 225 rpm, 37 °C for one hour. The cell suspension was diluted 1:10 with S.O.C. medium, and 100 μl was plated onto LB-agar plates containing the appropriate antibiotic. Plates were incubated overnight at 37 °C.

Electro-competent DH10B and DH10Bac cells were transformed according to the manufacturer's instructions. Essentially, 20 μl of cells were thawed slowly on ice, and DNA added as above. The reaction was electroporated using a Hybaid CellShock CS-100 at 1.8 kV. Subsequently 250 μl of S.O.C. was added, and incubated at 37 °C, 225 rpm for one hour. The transformation was then diluted 100-fold with S.O.C. and plated onto LB-agar plates containing the appropriate antibiotics. In the case of transformed DH10Bac cells, the transformation reaction was incubated at 37 °C for four hours at 225 rpm before being plated out on LB-agar and incubated for seventy-two hours.

2.2.2.2 Storage of *E. coli*

Five millilitres of LB medium containing the appropriate antibiotic was inoculated with transformed DH5, DH10 or DH10Bac *E. coli*. Cultures were grown overnight at 37 °C 225 rpm. 900 μl of the resultant culture was added to 100 μl of filtered DMSO, and

stored at -70°C .

2.2.3 DNA preparation

2.2.3.1 Small scale alkaline lysis preparations

Individual colonies of transformed bacteria were picked, and used to inoculate 5 ml of LB containing the appropriate antibiotics. Cultures were incubated overnight at 37°C , 225 rpm. Plasmid DNA was extracted from transformed cells using an alkaline lysis procedure. Essentially, 1.5 ml of the culture was spun down in a sterile eppendorf at $14,100 \times g$ for 2 min, and the pellet resuspended in 100 μl of ice-cold solution I. 200 μl of solution II was added, and the contents of the eppendorf mixed gently by inversion. 150 μl of solution III was added, the sample mixed gently, and centrifuged for 10 min at $14,100 \times g$. The supernatant was transferred to a sterile eppendorf, extracted sequentially with phenol and chloroform:isoamyl alcohol, and ethanol precipitated. The DNA was resuspended in 100 μl TE containing 1 x RNase mix, and stored at -20°C .

2.2.3.2 Large scale plasmid preparation

Starter cultures of 4 ml LB media and 10 μl of bacterial stock containing the desired plasmid were incubated overnight at 225 rpm, 37°C . The overnight cultures were then added to 350 ml LB, and incubated for sixteen hours at 37°C , 225 rpm. Bacteria were pelleted at $10,400 \times g$ for 10 min, and the pellet thoroughly resuspended in 8 ml TE pH 8.0. After centrifugation at $2,990 \times g$ for 5 min at 4°C , the resultant pellet was resuspended in 2 ml sucrose reagent. 400 μl of 20 mg/ml lysozyme was added, and the sample mixed by inversion and incubated at 4°C for 30 min. 3.2 ml of triton reagent and 800 μl of 0.25M EDTA was added, and the sample incubated for a further 15 min at 4°C .

The cell debris was removed by centrifugation at 124,520 x g for 30 min at 4 °C, and the supernatant decanted into a fresh tube. The sample volume was adjusted to 7.5 ml with 200 µl of 10 mg/ml ethidium bromide and distilled water. 7.5 g of caesium chloride was added to a final density of 1.55-1.60 g/ml. The sample was transferred into T1270 centrifuge tubes, topped with liquid paraffin, and centrifuged at 177,325 x g for 36 hours at 15 °C.

The lower of the two bands in the gradient, corresponding to supercoiled plasmid DNA, was removed using an 18 gauge needle and 5 ml syringe. The ethidium bromide was removed by three sequential extractions with equal volumes of isoamyl alcohol. The resultant aqueous phase was dialysed twice for two hours against 3 litres TE, and stored at -20 °C.

2.2.3.3 Determination of plasmid DNA concentration and identity

The final concentration of large and small-scale plasmid stocks was determined by measuring the absorbance at 260 nm, based upon an A_{260} value of 1.0 corresponding to a dsDNA concentration of 50 µg/ml. The identity of the plasmid was confirmed by restriction enzyme digestion.

2.2.4 DNA sequencing

Plasmid DNA was prepared by the alkaline lysis method (2.2.3.1). 100 ng plasmid DNA and 1 µM primer in a final volume of 3 µl were provided for sequencing. DNA sequencing was carried out by Claire Addison and Aidan Dolan in the Institute, using an ABI prism 377 automated sequencer. Sequence traces and read-outs were analysed using Chromas software (v 1.45).

2.2.5 Cell culture and production of virus stocks

2.2.5.1 Mammalian cell culture

Cells were grown in 175 cm² tissue culture flasks containing the appropriate growth media (section 2.1.4). Confluent monolayers were rinsed with versene, trypsinised with 1x trypsin in versene, and re-suspended to a final volume of 10 ml fresh growth media. 5 x10⁶ cells were seeded into 175 cm² flasks containing the appropriate growth media and incubated until confluent in a 5% CO₂ environment at 37 °C.

Every fifth passage after recovery, the complementing cell lines 20A, C1 and clone 17 were grown in media supplemented with 300 µg/ml of G418.

Cells were routinely screened for mycoplasma by the Unit's Cytology Department.

2.2.5.2 Production of herpesvirus stocks

Six 175cm² tissue culture flasks containing BHK or 20A cells at approximately 90% confluency were infected with HSV-1 or *Δ*UL33 respectively at 0.01 p.f.u./cell. In the same way, six 175cm² tissue culture flasks containing either C1 or clone 17 cells were infected with either gCB or S648 respectively. Three days post-infection, infected cells were released into the media by gentle agitation, pooled and centrifuged at 835 x g for 10 min. BHK cells were similarly infected with 0.01 p.f.u./cell *t*1233, and after incubation at 32 °C for four days the cells were harvested and centrifuged as above.

The pellet was re-suspended in 5 ml of EC5, and extensively sonicated. Cellular debris was pelleted by centrifugation at 835 x g for 10 mins, and the resulting pellet was retained as cell-associated virus (CAV; aliquots stored at -70°C).

The supernatant medium was centrifuged at 21,860 x g for 3 h, and the resulting pellet was re-suspended in 5 ml of EC5 to yield cell released virus (CRV). The suspension was sonicated extensively and aliquots stored at -70°C .

2.2.5.3 Determination of viral stock titres

Ten-fold serial dilutions of virus stocks were made in EC5, and 100 μl samples used to infect near-confluent monolayers of the appropriate cell line in 35mm Petri dishes. Plates were incubated at 37°C (32°C in the case of *t*1233) in an atmosphere of 5% CO_2 for 45 minutes. Two millilitres of EC_2Hu_3 were then added and the monolayers incubated at 37°C for three days (four days at 32°C in the case of *t*1233). The overlay was removed and 1 ml of Giemsa stain added for 30 min. The stain was washed off and the number of plaques from each dilution counted. Virus titre was determined by the following calculation:

Titre = number of plaques on 10^{-n} dilution $\times 10^n \times 10$ p.f.u./ml

e.g. 20 plaques on a -5 dilution plate corresponds to $20 \times 10^5 \times 10 = 2 \times 10^7$ p.f.u./ml

2.2.5.4 Insect cell culture

*Sf*21 cells were grown in 175 cm^2 tissue culture flasks containing *Sf*21 growth media. Confluent monolayers were rinsed with fresh media and removed by gentle agitation before being re-suspended to a final volume of 10 ml in fresh growth media.

Approximately 2×10^7 cells were seeded into 175 cm^2 flasks containing fresh media and incubated at 28°C until confluent.

2.2.5.5 Production of baculovirus stocks

Five 175 cm^2 flasks of near-confluent *Sf*21 cells were infected with 1 p.f.u./cell of the desired baculovirus, and incubated for four days at 28°C . Cells were gently tapped into the media, and pelleted by centrifugation at 835 x g for 5 min. The supernatant

was centrifuged at 38,725 x g for 90 min, and re-suspended in 5 ml of *Sf*21 growth media. Virus stocks were sonicated thoroughly and aliquots stored at -70°C .

2.2.5.6 Determination of baculovirus stock titres

Ten-fold dilutions of baculovirus stocks were made in *Sf*21 growth media, and near-confluent monolayers of *Sf*21 cells were inoculated with 100 μl of the diluted stocks. After incubation for one hour at 16°C , the inoculum was removed and 1.5 ml of growth medium containing 1.5% molten agarose was added, and allowed to set. 1.5ml of *Sf*21 medium was then added to each plate, and the monolayers incubated for four days at 28°C . Monolayers were overlaid with 0.5 ml of *Sf*21 overlay (containing Neutral Red) and incubated overnight at 28°C . Plaques were counted and the titre determined as described (section 2.2.5.3).

2.2.6 Creation of recombinant baculoviruses

The creation of recombinant baculoviruses was carried out using the Invitrogen Bacto-Bac™ system (Invitrogen Ltd.), according to the manufacturer's instructions:

2.2.6.1 Generation of recombinant bacmids

One nanogram pFastBac plasmid containing a wt or mutated UL33 gene was transformed into 100 μl of DH10Bac cells as described previously (2.2.2.1). The bacteria were plated on LB plates containing X-gal, kanamycin, gentamycin and tetracycline. After seventy-two hours, bacterial colonies unable to express functional β -galactosidase were identified. These bacteria were re-plated and plates incubated overnight at 37°C . Recombinant bacmid DNA was isolated using a modified alkaline lysis procedure. Essentially, 3 ml of LB was inoculated with a single colony, and incubated overnight at 37°C , 225 rpm. 1.5 ml of the culture was centrifuged at 14,100 x g for 1 min, and the pellet resuspended in 300 μl of ice-cold solution I. Three

hundred microlitres of solution II was added, and the sample incubated at 16 °C for five min. Three hundred microlitres of 3 M potassium acetate (pH 5.5) was slowly added, and the precipitate removed by centrifugation at 14,100 x g for 10 min. The supernatant was mixed with 800 µl of isopropanol, and incubated at 4 °C for 5 min. The DNA was precipitated by centrifugation at 14,100 x g for 15 min, and rinsed twice with 500 µl of 70% ethanol before being air-dried. The pellet was resuspended in 40 µl of TE pH 8.0, and stored at 4 °C.

2.2.6.2 Production of recombinant baculovirus stocks

Transfection of insect cells

Approximately 9×10^5 *Sf21* cells were seeded into 35 mm dishes two hours prior to transfection, and incubated at 28 °C. One microgram of recombinant bacmid was diluted in 200 µl of unsupplemented TC100 media, and combined with 6 µl of Lipofectamine. The resultant lipid-DNA complexes were incubated for 45 min at 16 °C. The media was removed from the *Sf21* monolayers, and the cells were washed once with 2 ml of unsupplemented TC100. Eight hundred microlitres of TC100 was added to each lipid-DNA complex, and the sample was added to the washed monolayers and incubated at 28 °C for five hours. Two millilitres of *Sf21* growth media was then added, and the monolayers incubated at 28 °C for 72 hours.

Harvesting viral progeny and generating high-titre stocks

Once the transfected cells exhibited signs of cell lysis, the media from the monolayers were transferred into fresh tubes. Cells were removed by centrifugation at 500 x g for 5 min at 4 °C, and the resultant supernatant baculovirus stock was stored at 4 °C. Viral titres were determined and high titre baculovirus stocks prepared as described previously (2.2.5.5).

2.2.7 Transfection of mammalian cells

2.2.7.1 Calcium phosphate transfection

35mm Petri dishes were seeded with 1×10^6 cells, and incubated overnight at 37°C , 5% CO_2 . For each monolayer, 12 μg of carrier calf thymus DNA (2 mg/ml) and 1 μg of plasmid DNA was added to 0.5 ml of HeBs and precipitated with 35 μl 2M CaCl_2 . The resulting fine suspension was added to the monolayers, and incubated at 37°C , 5% CO_2 for 45 min. Two millilitres EC5 were then added, and the plates incubated for 4 hours. The monolayers were then washed and exposed to 1 ml of 22.5% DMSO in HeBS for 4 min (Stow & Wilkie, 1976). After two washes, the cells were incubated in 2 ml EC5 for eighteen hours at 37°C , 5% CO_2 .

2.2.7.2 Lipofection

1×10^5 BHK, Vero or rabbit skin cells were seeded on 12 mm^2 coverslips overnight at 37°C , 5% CO_2 . For each monolayer, 0.5 μg of plasmid DNA was diluted in 25 μl of either GMEM or DMEM containing 4 μl of Plus reagent. The sample was incubated for 15 min at RT. One microlitre of Lipofectamine was diluted in 25 μl of GMEM or DMEM, then added to the DNA-Plus complex, and incubated for 15 min at RT.

Meanwhile, the medium was drained off the monolayers and replaced with 250 μl of GMEM or DMEM. The DNA-Plus-Lipofectamine complex was then added, and the cells incubated for three hours at 37°C , 5% CO_2 . 250 μl of appropriate growth media containing 2x the normal serum concentration was then added, and the cells incubated for sixteen hours at 37°C , 5% CO_2 .

2.2.7.3 Staining for β -Gal expression

Monolayers were transfected with pE*lacZ*, either by lipofection or calcium phosphate

precipitation. Eighteen hours post transfection (h.p.t.) the medium was removed and the monolayer washed in PBS. Cells were fixed by the addition of 1 ml β -galactosidase fix for five min, then washed twice with 2 ml PBS. Monolayers were incubated with 1 ml β -galactosidase stain for 6 hours at 37 °C, and the transfection efficiency calculated. Positive (blue) cells were counted in five fields of view, and the average efficiency calculated. Typically, 50% of lipofectamine-treated cells would be transfected, whilst calcium phosphate treated cells had a transfection rate of 5-10%.

2.2.8 Transient packaging assay

2.2.8.1 Transfection and superinfection

Cells were transfected by the calcium phosphate method described above. Six h.p.t. monolayers were infected with helper virus at 5 p.f.u./cell, and incubated for 45 min at 37 °C, 5% CO₂. After virus adsorption, 2 ml of EC5 was added, and incubation continued for eighteen hours at 37 °C, 5% CO₂.

The medium was removed from monolayers, the cells were washed with TBS and scraped into 2 ml of fresh TBS. Harvested cells were divided into two 1ml aliquots in microfuge tubes, and total and packaged DNA was prepared as described below.

2.2.8.2 Preparation of total cellular DNA

One 1 ml aliquot of harvested cells was centrifuged at 14,100 x g for 1 min and the pellet was thoroughly resuspended in 184 μ l RSB with 0.5% NP40. 184 μ l of 2x CLB containing 0.5 mg/ml protease was then added, and the samples incubated for 1 hour at 37 °C. 32 μ l of 4 M NaCl/0.5 M EDTA was then added, and the sample extracted sequentially with phenol and chloroform:isoamyl alcohol. The DNA was ethanol precipitated and resuspended in 100 μ l TE containing 1 x RNase mix.

2.2.8.3 Preparation of DNase resistant DNA

The second aliquot of harvested cells was centrifuged as above, and the cell pellet was resuspended in 184 μ l RSB containing 0.5% NP40 and 200 μ g/ml DNase I and incubated for 20 min at 37 °C. 184 μ l of 2x CLB containing 0.5 mg/ml protease was added, and the samples processed as above. The DNA was resuspended in 50 μ l of TE containing 1 x RNase mix.

2.2.9 Southern Blotting and hybridisation

2.2.9.1 Southern blot transfer

DNA representing the yield from 4×10^5 cells was digested with *Eco*RI and *Dpn*I in a 40 μ l reaction. Digestion was stopped by the addition of 4 μ l 10x DNA loading buffer, the samples loaded onto a 0.8% Loening's buffer agarose gel containing 0.5 μ g/ml ethidium bromide, and electrophoresed overnight at 15-25 V. To confirm that efficient DNase digestion had occurred, and that all the lanes contained equivalent amounts of DNA, a photograph of the gel was taken under medium wave UV.

The gel was soaked in denaturing gel soak for 45 min, followed by immersion in neutralising gel soak for a further 45 min. The DNA was blotted onto a nitrocellulose membrane by capillary transfer in 6 x SSC for 18 hours at room temperature. DNA was then crosslinked by exposure to 120 mJ/cm² UV light, and the membrane blocked with blot pre-soak for one hour at 68 °C. Specific DNA fragments were detected by overnight incubation in 10 ml hybridisation buffer containing the labelled and denatured DNA probe DNA (see section 2.2.9.2 below). After two 45 min washes in blot wash at 68 °C, the membrane was exposed to a phosphorimager screen and analysed using a BioRad Personal Molecular Imager FX in conjunction with Quantity

One software.

2.2.9.2 Preparation of radio-labelled nick-translated DNA

250 ng of plasmid was combined with 20 μCi each of $\alpha\text{-}^{32}\text{P}$ dCTP and $\alpha\text{-}^{32}\text{P}$ dGTP, 2 U of DNA polymerase I and 10^{-7} mg DNase I. The reaction was incubated at 16°C for 90 min in a final volume of 35 μl of 1x NTB (containing 60 μM dATP and 60 μM dTTP).

The reaction mix was fractionated on a Microspin Sephadex G-50 column to separate radio-labelled plasmid from unincorporated nucleotides. The volume of the radio-labelled plasmid eluted from the column was made up to 1 ml with distilled H_2O , and the DNA was denatured by adding 200 μl of 1 M NaOH. After five minutes, the solution was neutralised by the addition of 200 μl of 1 M HCl and the probe was added to 8.6 ml of hybridisation buffer (prewarmed to 68°C) and used immediately.

2.2.9.3 Stripping and re-probing membranes

To remove radiolabelled DNA, nitrocellulose membranes were incubated in 0.1% SDS at 100°C . After two washes in 2x SSC, the stripped membrane was blocked and hybridised to fresh probe as previously described.

2.2.10 Complementation yield assay

Near-confluent monolayers of BHK cells were transfected with 1 μg of plasmid by the calcium phosphate method (2.2.7.1). Six h.p.t. monolayers were superinfected with 5 p.f.u./cell of helper virus, and incubated at 37°C (39.2°C in the case of *ts1233*). After one hour, inoculum was removed and the plates washed once in 0.14 M NaCl, exposed to 0.1 M glycine, 0.14 M NaCl pH 3.0 for 1 min, and washed in EC5 (Rosenthal *et al.*, 1984). Incubation was continued at 37°C (39.2°C for *ts1233*). Eighteen h.p.i. the cells

and media were harvested, sonicated at 4 °C, and stored at -70 °C. Virus progeny titres were determined under conditions permissive for helper virus replication.

2.2.11 Immunoprecipitation

Immunoprecipitation of baculovirus-expressed proteins from *Sf21* cells

35 mm Petri dishes were seeded with 2.5×10^6 *Sf21* cells, and incubated overnight at 28 °C. Monolayers were infected with 5 p.f.u./cell of the appropriate baculovirus(es), and incubated for 48 h at 28 °C. Infected cells were harvested into the media, and centrifuged at 835 x g for 5 min at 4 °C. The cell pellet was washed twice with ice-cold TBS, and resuspended in 350 µl ice cold EZ buffer. After incubation on ice for 30 min, the sample was centrifuged at 44,000 x g for 10 min at 4 °C, and the supernatant (clarified lysate) was retained.

100 µl of clarified lysate was incubated in a microfuge tube with 30 µl of 50% protein-A-sepharose slurry (in PBS) and 5 µl of the appropriate pre-immune serum, and centrifuged for 1 min at 14,100 x g, 4 °C. 5 µl of the appropriate rabbit polyclonal antibody was then added to the precleared supernatant, and the sample incubated on an end-over-end incubator for 3 hours at 4 °C. 50 µl of 50% protein-A-sepharose slurry (in PBS) was added, and the sample incubated at 4 °C for 2 hours. Immune complexes were collected by centrifugation at 14,100 x g for 1 min at 4 °C, and washed four times with 200 µl of ice-cold EZ buffer. After removal of the final wash, 50 µl of boiling mix was added, and the sample incubated at 100 °C for 5 min. Ten microlitres of sample was analysed by SDS-PAGE and western blotting (2.2.12).

Immunoprecipitation of virus-expressed proteins from BHK cells

1×10^7 BHK cells were seeded into 175 cm² flasks and incubated overnight at 37 °C,

5% CO₂. Cells were infected with 5 p.f.u./cell of the appropriate herpesvirus, and incubated for 18 hours at 37 °C, 5% CO₂. Cells were harvested into the media, collected by centrifugation at 835 x g for 5 min at 4 °C, and washed twice with ice-cold TBS. The pellet was resuspended in 500 µl EZ buffer, and incubated for 30 min at 4 °C. Lysates were centrifuged at 44,000 x g, 4 °C for 10 min, and the supernatants pre-cleared with 50 µl of 50% Gammabind-G-sepharose slurry (in PBS) and 5 µl of appropriate pre-immune serum. The sample was then centrifuged for 1 min at 14100 x g, 4 °C, and 200 µl of pre-cleared supernatant incubated with 5 µl of R148. After incubation for 3 hours at 4 °C on an end-over-end incubator, 80 µl of 50% Gammabind-G-sepharose slurry (in PBS) was added, and the sample incubated at 4 °C for 16 hours. Immune complexes were collected by centrifugation and washed as described above, 80 µl of boiling mix added, and the sample incubated for 5 min at 100 °C. Ten microlitres of sample was analysed by SDS-PAGE and western blotting (2.2.12).

2.2.12 Subcellular fractionation

Near-confluent monolayers of BHK cells in 35mm Petri dishes were mock infected or infected with 1 p.f.u./cell of the appropriate virus. Six h.p.i. cells were harvested and washed with ice-cold PBS, and then resuspended in 150 µl of fractionation buffer A. Nuclei were pelleted by centrifugation at 7000 x g for one min at 4 °C, and the resultant supernatant was retained as the cytoplasmic fraction. Nuclei were resuspended in 150 µl of fractionation buffer B for 10 min at 4 °C, and then sonicated for 10 s to yield the nuclear fraction. 150 µl of boiling mix was added to each fraction, the samples boiled and analysed by SDS-PAGE and western blotting (section 2.2.13).

2.2.13 Western blotting

Typically, 35mm Petri dishes of near-confluent BHK cells were transfected or infected as described previously. 20 h.p.t. or 18 h.p.i. monolayers were washed in ice-cold TBS and resuspended in 100 μ l boiling mix. Samples were incubated at 100 °C for 5 min, and the proteins resolved by SDS-PAGE.

10 μ l of sample was analysed on an 8% or a 15% running gel as indicated (39:1 acrylamide: bisacrylamide) with a 5% stacking gel (19:1 acrylamide: bisacrylamide) at 150V in 1 x SDS-PAGE tank buffer using a BioRad MiniProtean III kit. Separated proteins were blotted onto Hybond-P PVDF membranes using a BioRad transfer kit at 100V, 4 °C for two hours in Towbin buffer. Effective blotting was confirmed by the transfer of Rainbow markers onto the membrane.

The membrane was blocked in blocking solution for two hours, and washed twice in PBS supplemented with 0.05% Tween-20 (PBST). Rabbit and mouse primary antibodies were diluted 1:200 and 1:1000 respectively in PBST with 5% Marvel. The membrane was incubated in diluted primary antibody at 4 °C for three hours, and then had three 15 min washes in PBST. The membrane was incubated in a 1:1000 dilution of protein-A-peroxidase in PBST with 5% Marvel. After a further three 15 min washes in PBST, specific bands were detected by the addition of 1 ml ECL mix, and the blot exposed to X-omat autoradiographic film.

2.2.14 Immunofluorescence

13 mm² glass coverslips in tissue culture wells were seeded with 1×10^5 cells, and incubated at 37 °C, 5% CO₂ overnight. Monolayers were transfected with 0.5 μ g of plasmid by lipofection (section 2.2.7.2), and incubated for 16 hours. Alternatively, cells

were infected with 1 p.f.u./cell of the appropriate herpesvirus, and incubated for 6 hours. The cells were then washed twice in PBS, and fixed with 0.5 ml of formaldehyde fix for ten min. After two further washes with PBS, cells were treated with 0.5 ml permeabilisation buffer for ten min. The monolayers were then washed twice with 1ml PBS supplemented with 1% FCS (PBSF). In the case of herpesvirus-infected cells, monolayers were then incubated in PBS containing 10% HS for 30 min to block virus encoded Fc receptors.

Rabbit and mouse primary antibodies were diluted 1:200 and 1:1000 respectively in PBSF. Permeabilised cells were incubated in diluted primary antibody for 1 hour, and then rinsed five times with PBSF. The cells were incubated for 1 hour in the appropriate FITC- or Cy5-conjugated antibody, diluted 1:200 or 1:500 respectively in PBSF. After five further washes in PBSF, coverslips were rinsed once in distilled water, and air-dried. Where appropriate, cells were incubated in 1 μ g/ml propidium iodide before being rinsed in distilled water and dried. Dry coverslips were mounted on glass slides using AF-1 mounting agent, and examined using a Zeiss LSM 510 confocal microscope in conjunction with Zeiss Axioplan 40x and 63x lenses. Laser lines with excitation wavelengths of 488 nm, 545 nm and 633 nm were used to detect the FITC, propidium iodide and Cy5 fluors respectively. The channels were scanned separately with the settings for each channel maintained throughout, and images were compiled in Adobe Photoshop.

Chapter 3: Using insertional mutagenesis to study UL33

Section 3.1 Introduction

Although the central requirement for UL33 in DNA packaging has been known for several years, its precise role is still unclear. Furthermore, it has not yet been subjected to a detailed mutational analysis. The aim of the work presented in this chapter was therefore to create a panel of mutants with which to define regions of UL33 necessary, or dispensable, for DNA packaging. The data describe the generation of a series of UL33 mutants using a random insertional mutagenesis approach, and their subsequent characterisation in terms of ability to support DNA packaging, and to complement growth of viruses lacking functional UL33.

Two UL33 mutant viruses were used. The temperature sensitive mutant *t*1233, isolated by Al-Kobaisi *et al.* (1991), contains a single amino acid substitution within the N-terminus of UL33 and is defective in DNA packaging and growth at the NPT of 39.2 °C. The UL33-null virus *d*UL33 contains a frameshift after nucleotide 91 within the UL33 gene, resulting in introduction of a novel downstream stop codon at nucleotide 127 (Cunningham & Davison, 1993). The UL33 protein of *d*UL33 therefore contains 42 amino acids: the first thirty residues of wt UL33, followed by twelve novel amino acids (ARRALRLARRRA). This renders the virus unable to propagate or package its genome unless grown on complementing cells expressing the wt UL33 gene.

Section 3.2 Creation and characterisation of UL33 insertional mutants

Plasmid pUL33 contains an HSV-1 fragment comprising nucleotides 69,110 to 69,576

which include the UL33 gene, amplified by PCR from HSV-1 strain 17 DNA and cloned as a *Bam*HI fragment into the expression vector pCMV10. This plasmid was generated by Gordon Reid (MRC Virology Unit, Glasgow), who additionally demonstrated that it could complement both growth and DNA packaging of *d*UL33. Within pUL33, the UL33 ORF is encoded by 390 nucleotides and is expressed under the control of the HCMV major immediate early promoter (MIEP).

Sequence analysis (**Figure 3.1**) demonstrated that pUL33 deviates from the published UL33 gene sequence for HSV-1 strain 17 (McGeoch *et al.*, 1988) by the inversion of nucleotides 325 and 326 within the UL33 ORF, resulting in an Ala¹⁰⁹ → Arg¹⁰⁹ change. Comparison of available sequences from other HSV-1 strains and HSV-2 (Dolan *et al.*, 1998; Ushijima *et al.*, 2007) revealed that these nucleotides are invariably inverted with respect to the published HSV-1 strain 17 sequence, and that Arg is consistently present at position 109. Therefore, the sequence reported by McGeoch *et al.* may contain an error within UL33, or might perhaps be derived from sequencing of a mutated clone.

The Mutagenesis Generation System (MGST[™], Finnzyme) allows the random insertion of an artificial transposon encoding the *cat* gene, which confers chloramphenicol resistance (*cam*^R), into a target plasmid (**Figure 3.2**; panel A). Transposition is catalysed in a cell free system by the transposase enzyme of bacteriophage Mu. To facilitate selection of mutated plasmids, products of the transposition are transformed into electrocompetent bacteria and selected for *cam*^R and ampicillin resistance (*amp*^R) genes on the transposon and target plasmid respectively. DNA from the resulting colonies is isolated and cleaved with *Not*I to remove the bulk of the transposon. After digestion, the plasmid DNA is re-circularised, transformed into bacteria and selected for *amp*^R. The resulting plasmids contain 15 bp insertions: a 10 bp remnant of the

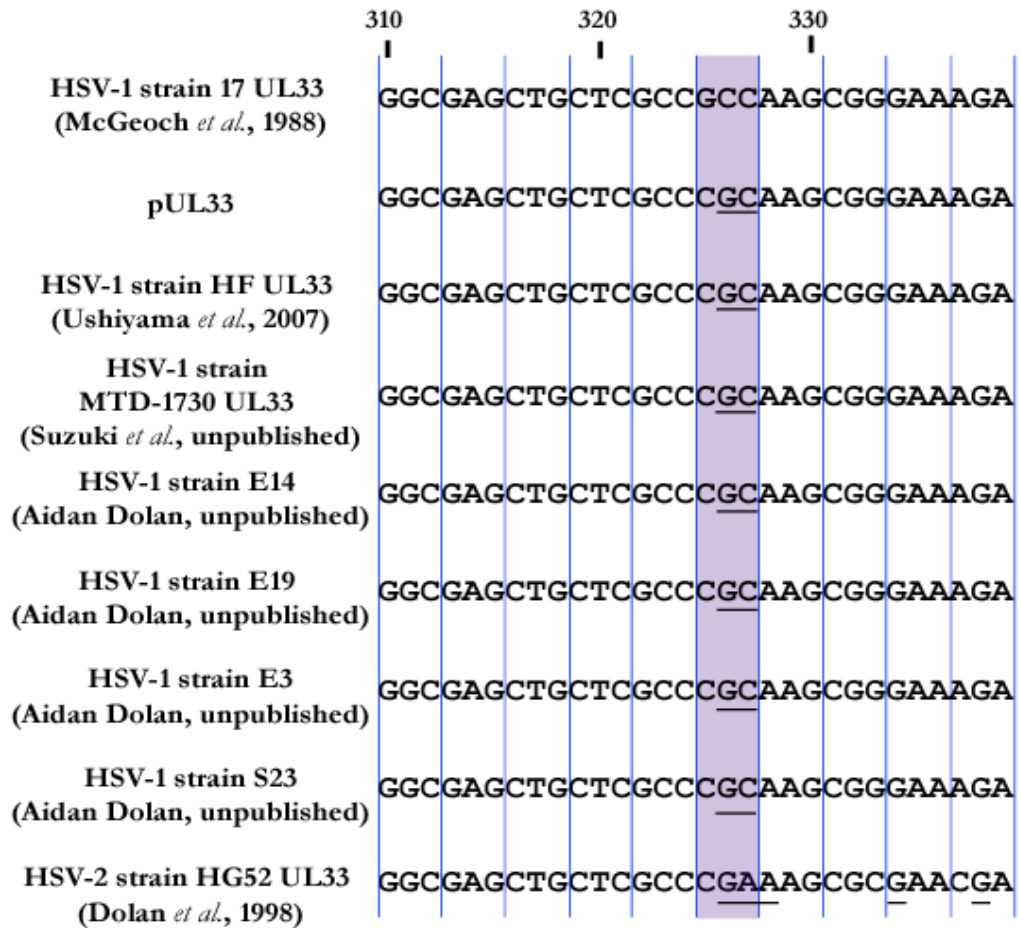


Figure 3.1: Nucleotide alignment of pUL33 with related herpes simplex virus sequences.

The nucleotide sequence of pUL33 was aligned with several UL33 gene sequences using ClustalX. Sequences were obtained from the NCBI Genbank database, and from Aidan Dolan (MRC Virology Unit, Glasgow). The region encoding amino acids 104-113 is shown. Nucleotides are numbered relative to the 'A' of the ATG initiation codon of UL33. Underlined nucleotides represent deviation from the published HSV-1 strain 17 sequence (McGeoch *et al.*, 1988). A blue box indicates the position at which an Ala-Arg substitution was observed relative to the published HSV-1 strain 17 amino acid sequence. Genbank accession numbers: HSV-1 strain 17: X14112; HSV-1 strain HF: DQ899502; HSV-1 strain MTD 1730: AB252866; HSV-2 strain HG52: NC_001798.

A.

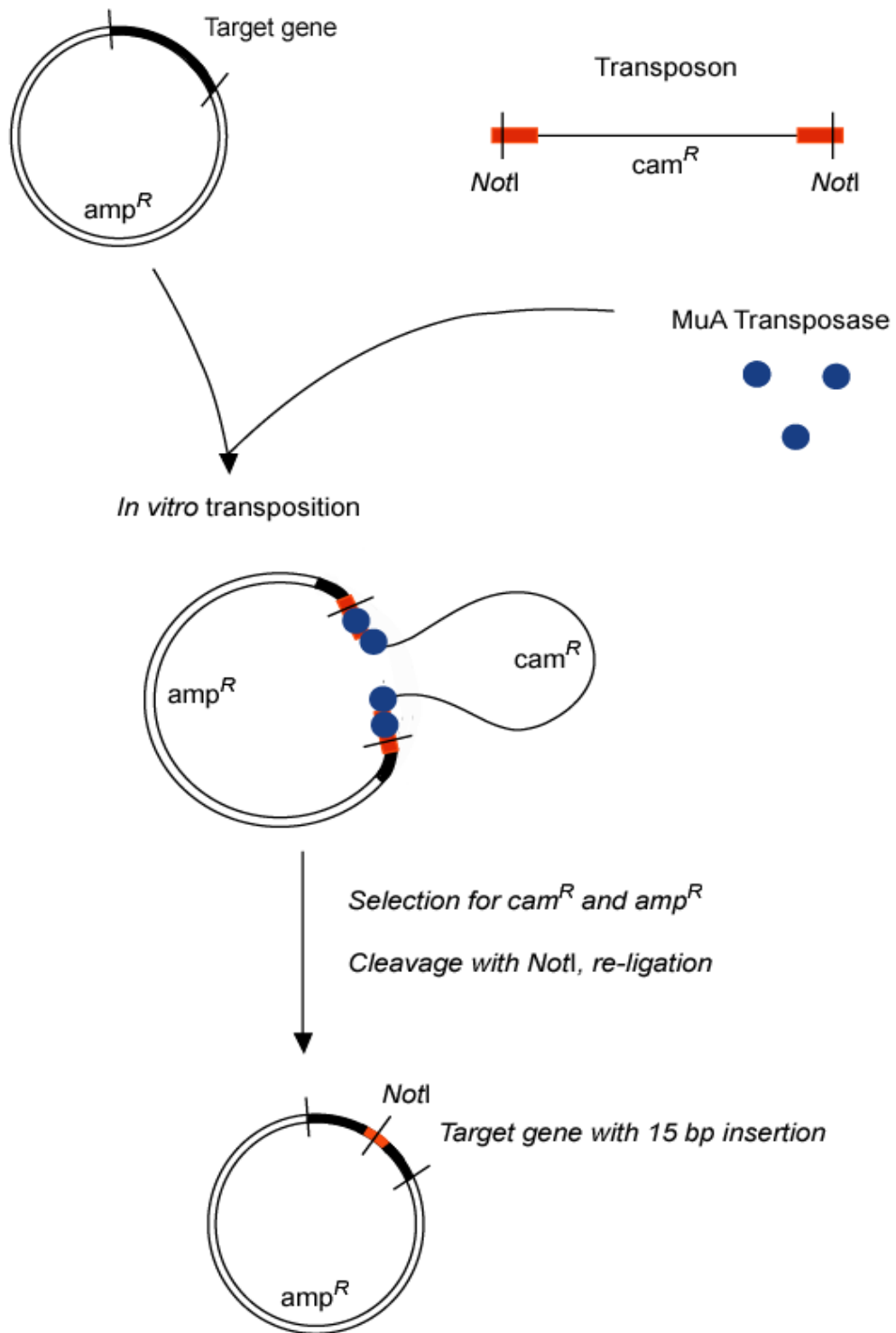


Figure 3.2: Principles of the MGS transposition system

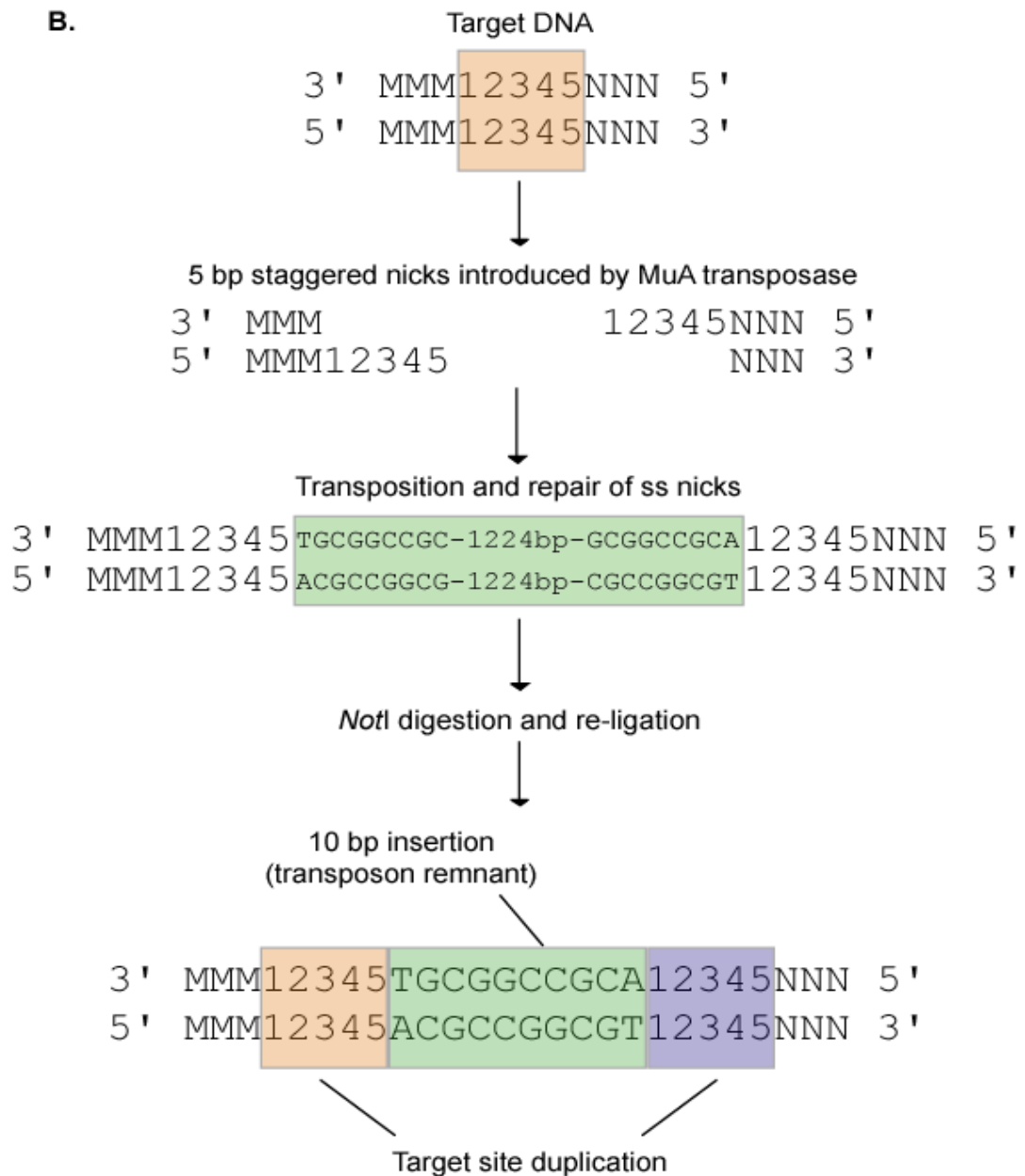


Figure 3.2: Principles of the MGS transposition system.

A. *In vitro* transposition using the MuA transposase facilitates the introduction of a transposon encoding cam^R into the amp^R target plasmid. Insertion can occur within or outwith the gene of interest. Selection for cam^R and amp^R allows the isolation of plasmids containing transposons. Digestion of plasmid DNA with *NotI* releases the transposon, and subsequent re-ligation leaves a 15 bp insert containing a *NotI* site.

B. MuA transposase induces 5 bp staggered nicks at the target site (orange), which are repaired during the latter stages of the transposition reaction, leading to a net duplication of the target nucleotides. The 15 bp insert is composed of a 10 bp remnant of the transposon (green), containing the *NotI* site (GCGGCCGC), and a 5 bp duplication of the target site (purple).

transposon containing a single, unique *NoI* site, and a 5 bp duplication of the target site (**Figure 3.2**; panel B).

3.2.1 Insertional mutagenesis and identification of mutants

Plasmid pUL33 is suitable for use with the MGS without modification since it contains no *NoI* sites. To introduce the transposon into pUL33, an *in vitro* transposition reaction was carried out as described (section 2.2.1.6), and the mixture diluted 1:10 to reduce arcing during electroporation. Following transformation into electrocompetent *E. coli* (strain DH10B) and selection for *cam*^R and *amp*^R, individual colonies (x530) were picked and grown up. Small-scale plasmid DNA preparations were made using an alkaline lysis method (see section 2.2.3.1).

Identification of colonies containing the transposon within the UL33 gene was achieved on the basis of a size change of the UL33-containing fragment, revealed by digesting plasmids with *Bam*HI and separating the fragments by electrophoresis on 0.8% agarose gels. A summary of the screening process and a representative agarose gel of screened plasmids are shown in **Figure 3.3**.

All clones (23) yielding *Bam*HI fragments of 1721 bp and 3834 bp, indicative of transposition within the UL33 fragment, were selected. To remove the bulk of the transposon sequence, aliquots of plasmid DNA were digested with *NoI*. Digested plasmids were re-ligated and transformed into chemically competent DH5 *E. coli*. After selection for *amp*^R individual colonies were picked, and plasmid DNA was isolated using a small scale alkaline lysis procedure. Glycerol stocks of these colonies were also prepared.

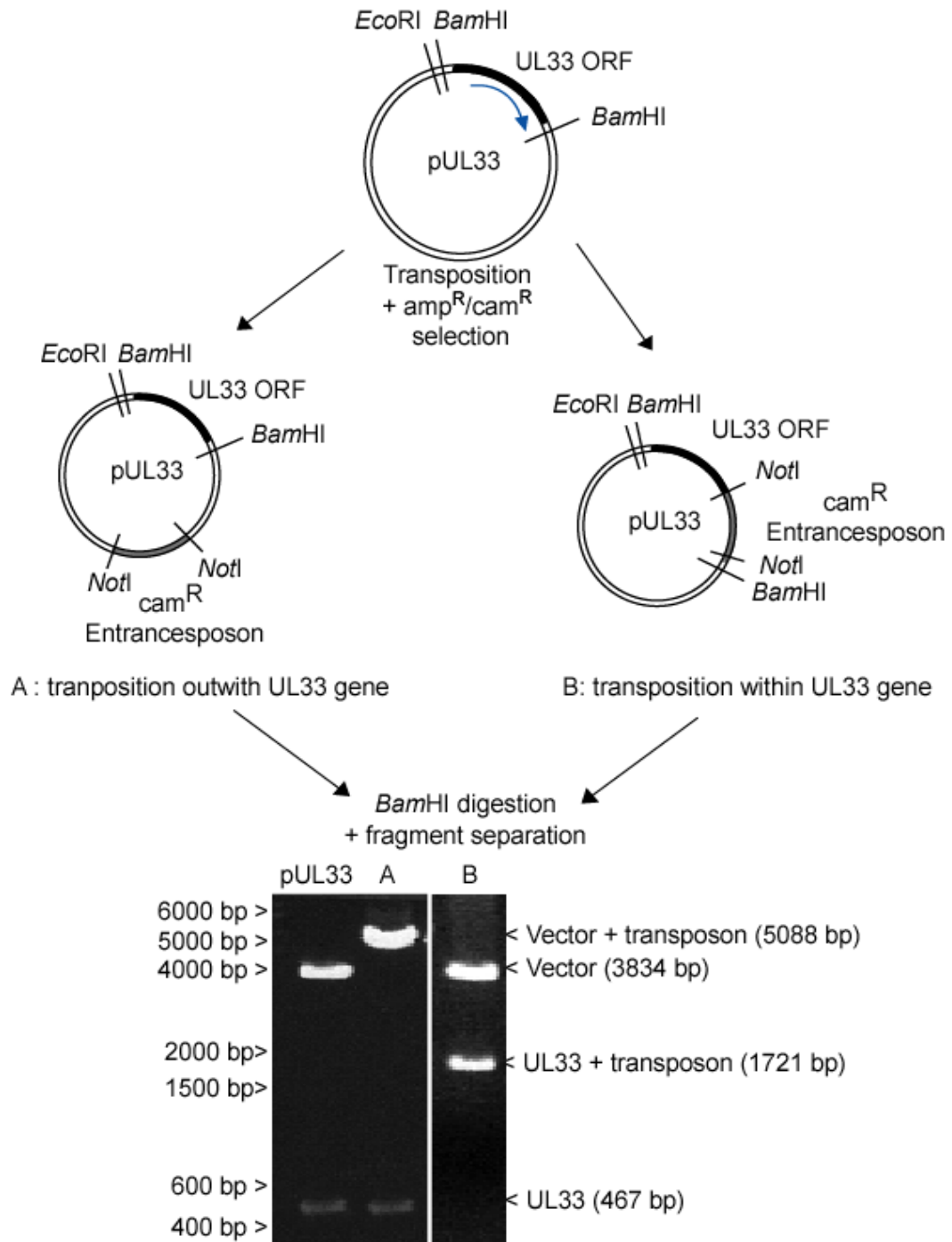


Figure 3.3: Screening for insertions within the UL33 gene.

Transposition was carried out as detailed and DNA isolated from colonies under selection for *amp^R* and *cam^R*. Digestion with *BamHI* allowed the resolution of two populations of plasmids. Population A, containing the transposon within the vector sequence, is indicated by the release of 5088 bp and 467 bp fragments. Digest of population B releases fragments 3834 bp and 1721 bp in length, denoting the presence of the transposon within the UL33 gene. A representative 0.8% agarose gel is shown. The positions of molecular weight markers are shown at the left hand side.

Figure 3.3: Screening for insertions within the UL33 gene

Identification of the approximate site of insertion was achieved by digestion with *EcoRI*, which cuts near the 5' end of the UL33 gene, and *NotI*, which cuts within the 15 bp inserted sequence. **Figure 3.4** shows the resultant EtBr-stained agarose gel of plasmids digested with *NotI* and *EcoRI*. As expected, pUL33 is linearised. All other plasmids liberated fragments between 200-600 bp, consistent with transposition within the UL33 fragment. Increasing size of the smaller fragment indicates increasing distance of the transposition event from the *EcoRI* site in pUL33.

3.2.2 Sequencing of UL33 insertional mutants

To determine the precise position of insertion, aliquots of DNA from each of the 23 clones were sequenced using the 'CMV' primer (section 2.1.11). Analysis of the resulting sequences confirmed that, other than the 15 bp inserted through transposition, all of the mutants were identical to the UL33 gene of pUL33. The positions and nucleotide sequences of the 15 bp insertions within the UL33 gene are noted in **Figure 3.5**. For clarity, the target site duplication is indicated at the 3' end of the 15bp insert. Several clones were indistinguishable by DNA sequencing and contained insertions after nucleotide 138 (marked by an *). A single representative clone of these mutants, clone 8 (subsequently re-named in51), was used in subsequent experiments. Altogether, sixteen distinct mutants with 15 bp insertions in the UL33 gene were chosen for analysis.

To establish the amino acid sequence of each UL33 mutant, the nucleotide sequences were inputted into the ExPASy Translate program (section 2.1.14). Resultant sequences were aligned with the wt UL33 amino acid sequence using the ClustalX multiple alignment program, and the precise sequence and position of insertions determined with respect to the wt UL33 protein (**Figure 3.6**).

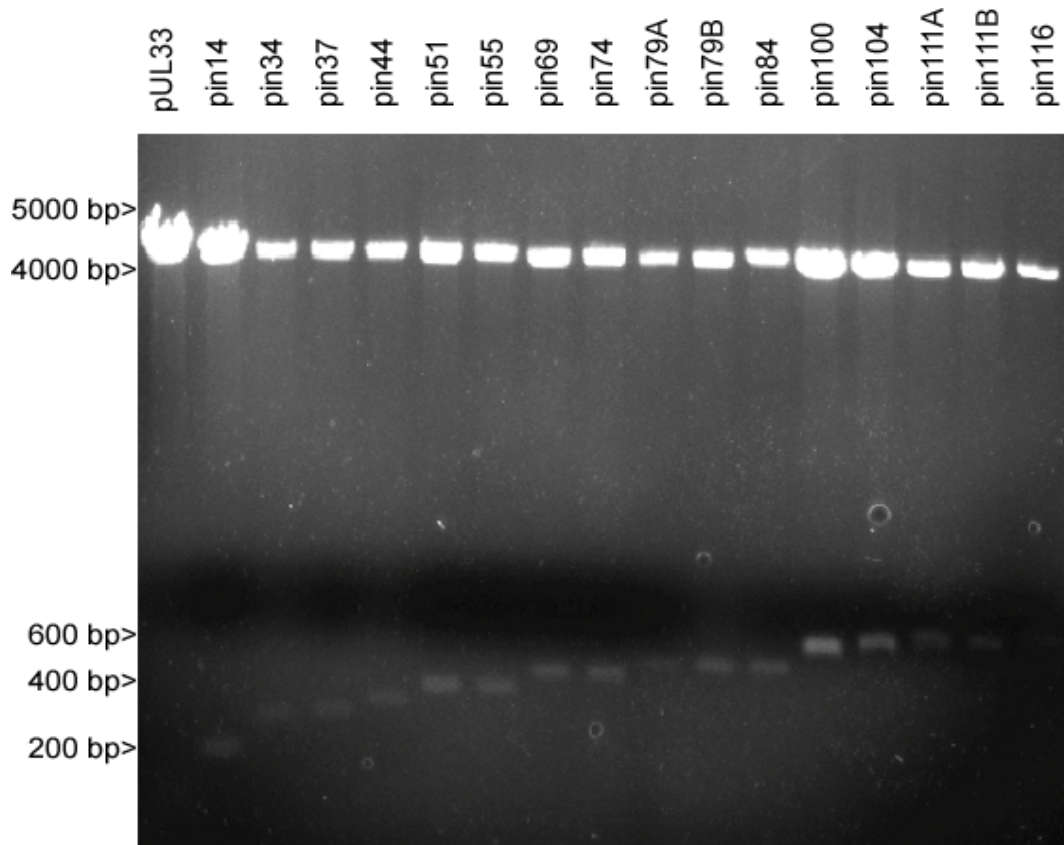


Figure 3.4: Mapping positions of insertion within UL33 by restriction digest

Approximately 1 μg of indicated plasmid DNA was digested with the restriction endonucleases *EcoRI* and *NotI*. Fragments were separated on a 1% agarose gel. Liberation of a fragment <600 bp is indicative of successful transposition, with increasing size of the liberated fragment denoting that the unique *NotI* site lies further towards the 3' end of the UL33 gene. Positions of size markers are indicated.

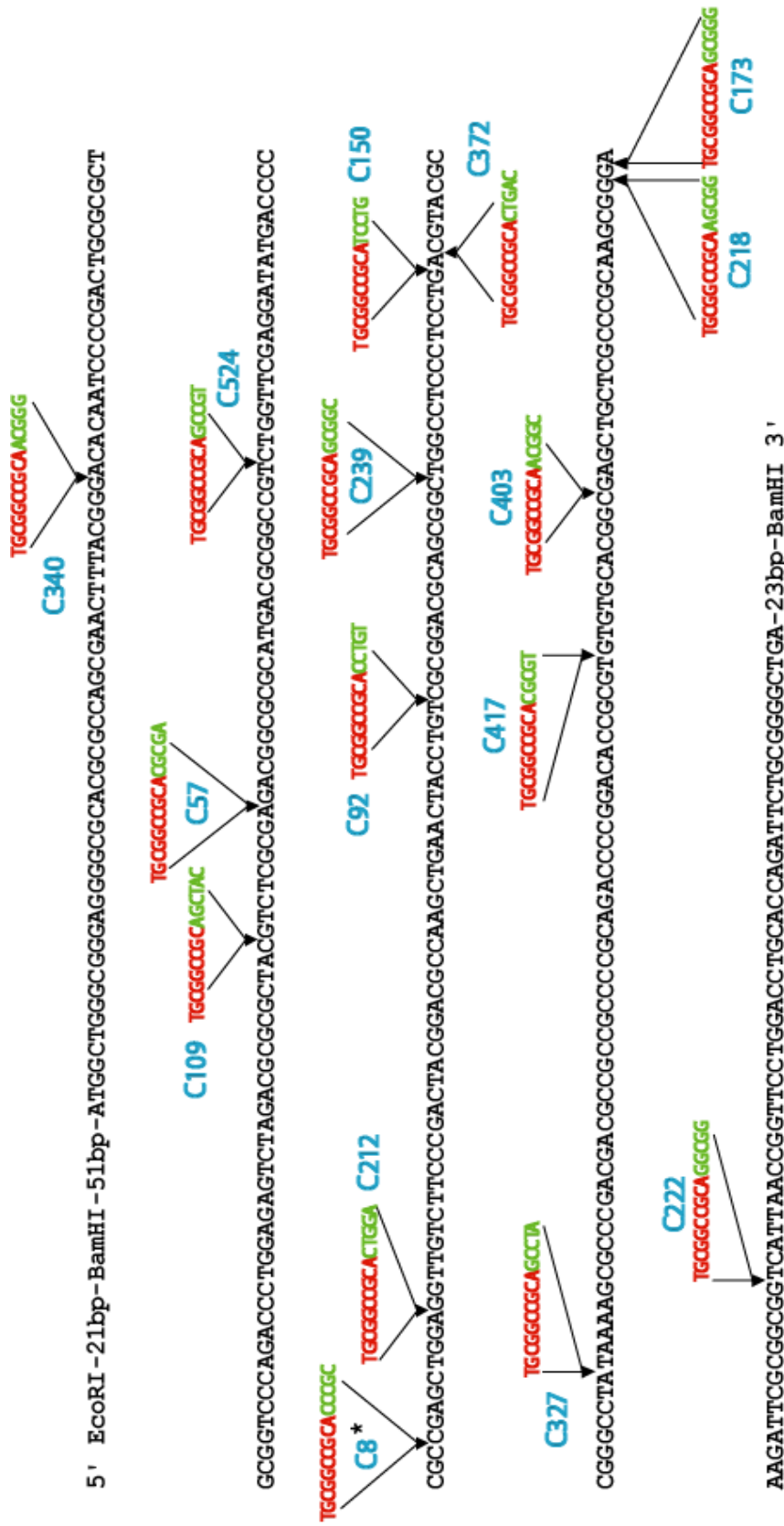


Figure 3.5: Position and sequence of 15 bp insertions within the UL33 gene.

Nucleotide sequences of mutated plasmids were determined by DNA sequencing and aligned with ClustalX. Mutants are indicated by clone number, and the position at which clonally identical insertions were observed is denoted by an *. For clarity, the 5 bp target site duplication (indicated in green) is shown at the 3' end of each insertion. The positions of flanking *Bam*HI and *Eco*RI sites are shown.

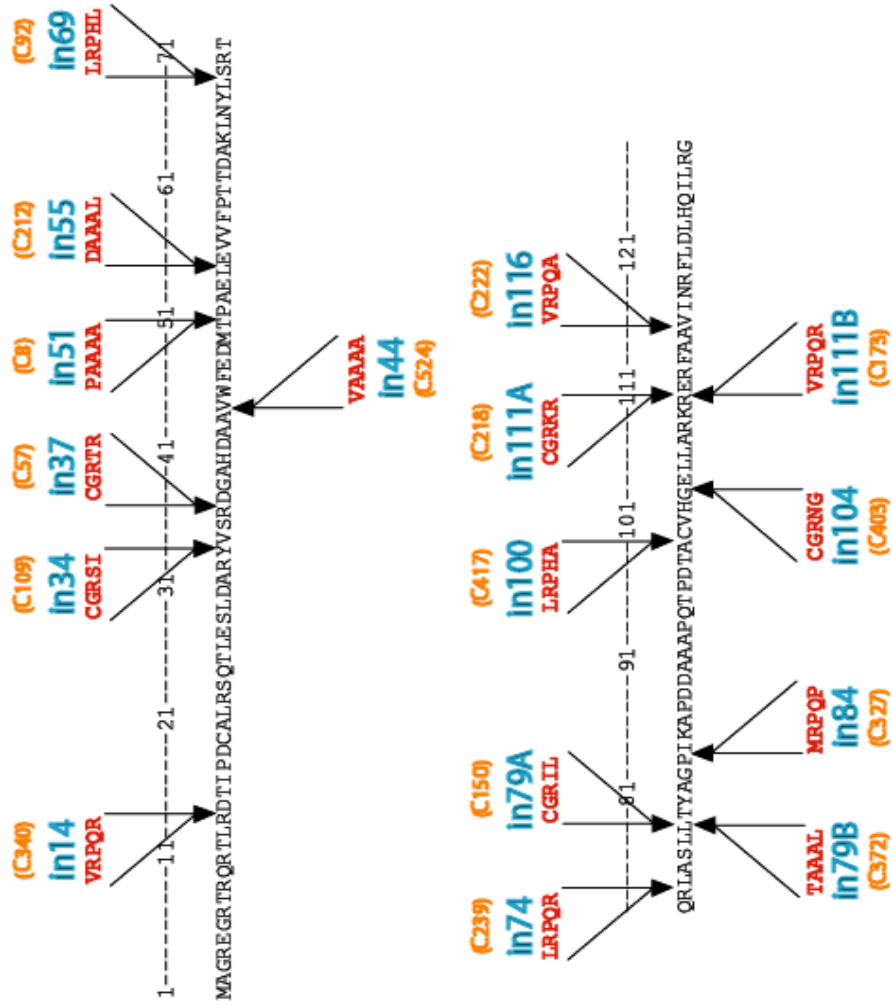


Figure 3.6: Position and sequence of 5 aa insertions in the UL33 protein.

Amino acid sequences of the sixteen insertional mutants were determined from their nucleotide sequences by the Translate program. Positions and sequences of the 5 aa inserts are shown relative to the wild-type protein sequence. Mutants are named according to the last unaltered amino acid before insertion (blue), and the clone number indicated in brackets. Mutants encoding insertions at different positions within the same codon are denoted A and B respectively.

The clones were designated according to the last unaltered amino acid before the insertion, and will be referred to as such for the remainder of the work. Two pairs of mutants (in79A/B and in111A/B) contained insertions at different positions within the same codon, and differed only in the identity of the inserted amino acids.

3.2.3 Expression and localisation of mutated UL33 proteins

Although DNA sequencing indicated the mutated plasmids all encoded full-length UL33 polypeptides containing 5 aa inserts, it was unknown whether any of the insertions would have deleterious effects on the stability of UL33, or on recognition by antibody R148. Protein expression from the mutated plasmids was therefore examined.

Plasmids encoding either mutated or wild type UL33 proteins, or an empty vector control, were transfected into BHK monolayers by the calcium phosphate method (section 2.2.7.1), and the cells DMSO boosted after 4 hours. At 20 h post-transfection, cell extracts were lysed by boiling in the presence of SDS, and resultant proteins were separated by SDS-PAGE on 15% polyacrylamide gels. Separated proteins were transferred onto a PVDF membrane and immunoblotted using the UL33-specific rabbit polyclonal antibody R148 (section 2.1.12). The membrane was exposed to HRP-coupled protein-A and proteins detected using an ECL substrate system (**Figure 3.7**, panel A). To confirm that equal amounts of protein were loaded, duplicate membranes were probed with an anti-actin antibody (section 2.1.12), which was detected using protein-A-HRP together with the ECL system described above (panel B).

The results indicate that wt UL33 migrated with an apparent molecular mass of approximately 19 kDa, higher than the predicted M_r of 14.4 kDa, but in agreement with earlier studies (Reynolds *et al.*, 2000). No UL33 protein was observed in pCMV10-

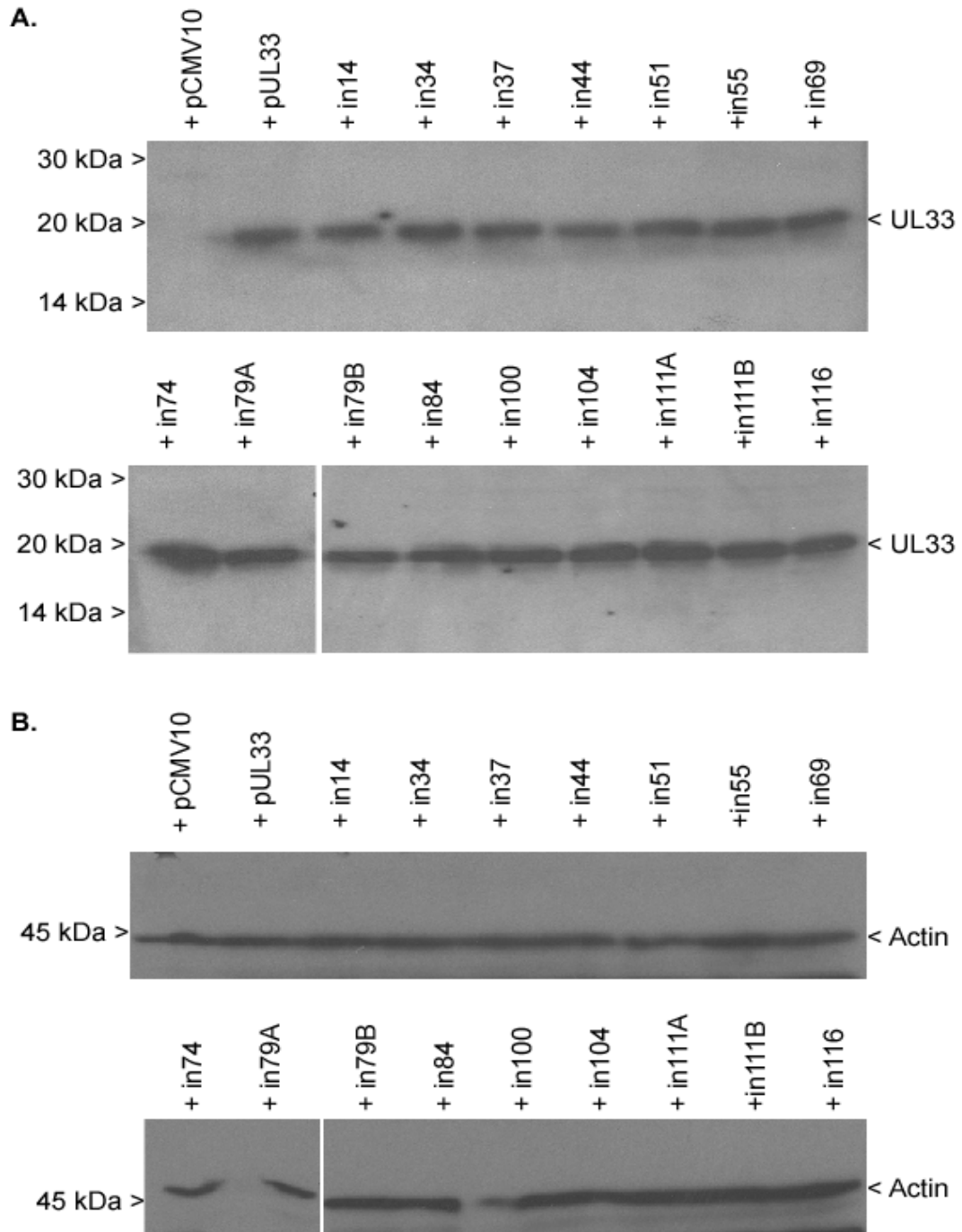


Figure 3.7: Analysis of mutated polypeptide expression in transfected cells

BHK cells were transfected with the indicated plasmids and proteins were separated on 15% polyacrylamide gels and transferred onto PVDF membranes. Membranes were reacted with a UL33-specific antibody (R148), together with protein-A-HRP. Bound protein was detected using an ECL substrate system (**A**). Duplicate membranes were incubated with an anti-actin antibody and protein-A-HRP, and processed using the ECL system (**B**).

transfected cells, confirming that R148 detects a UL33-specific product. All of the mutated UL33 plasmids expressed polypeptides which were recognised by R148, and which exhibited similar mobility to the wt protein. The actin controls (panel B) confirmed that similar amounts of protein were loaded in each instance. Thus, none of the insertions had a significant effect on the size or stability of UL33, or its recognition by R148.

Indirect immunofluorescence assays were used to investigate the intracellular localisation of both wild type and mutated UL33 proteins. 0.5 µg of pUL33 or an empty vector control (pCMV10) were transfected into BHK cells by the Lipofectamine method (section 2.2.7.2). Sixteen hours after transfection, the cells were fixed and permeabilised with paraformaldehyde and NP40 as described (section 2.2.14). After incubation with the R148 antibody for one hour, the cells were washed with PBSF and bound antibody detected using a FITC-conjugated goat anti-rabbit IgG antibody. The coverslips were examined using a Zeiss LSM 510 confocal microscope in conjunction with a laser with excitation lines at 488 nm, corresponding to the excitation wavelength of the FITC fluorophore. Images were exported and compiled in Adobe Photoshop. The results are shown in **Figure 3.8**.

No fluorescence was observed in cells transfected with pCMV10 (panel A). In contrast, cells transfected with pUL33 exhibited bright fluorescence in both the nucleus and cytoplasm (panel B), although UL33 was present predominantly in the nucleus. Furthermore, UL33 was excluded from the nucleolus of transfected cells. A population of cells (~10% of transfected cells) exhibited a distinctive localisation pattern with UL33 mainly present in the cytoplasm (panels C and D). These data confirmed the suitability of R148 for the study of UL33 localisation in transfected cells.

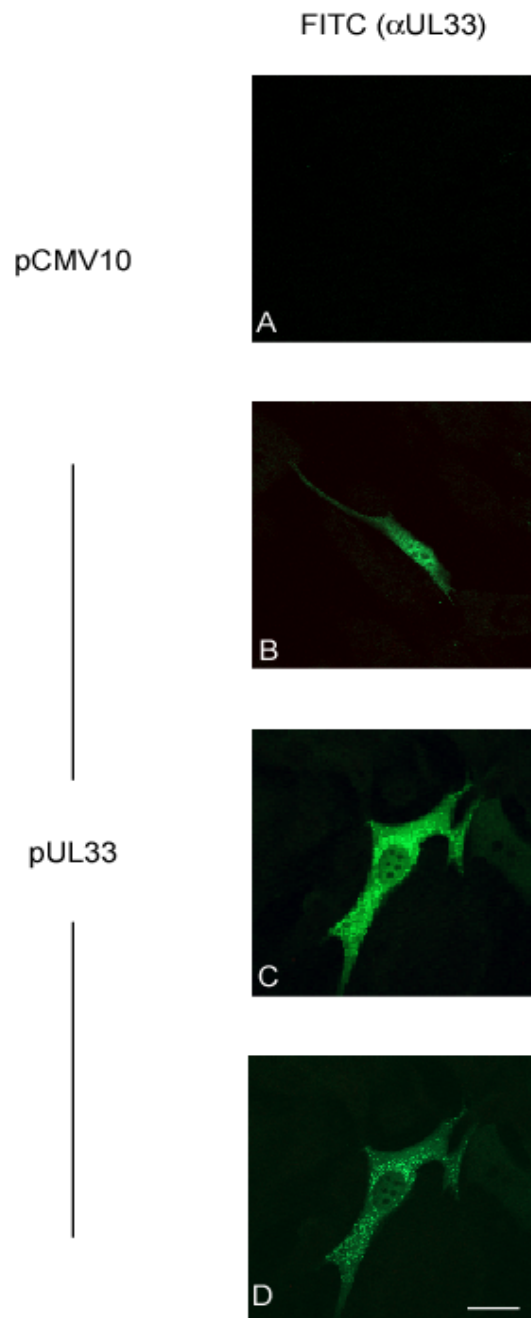


Figure 3.8: Localisation of the UL33 protein in transfected cells.

BHK cells were transfected with the indicated plasmids by lipofection. Twenty hours post-transfection, cells were fixed and permeabilised with paraformaldehyde and NP40, and probed with R148. Coverslips were incubated with a FITC-coupled anti-rabbit antibody, and examined by confocal microscopy. Panels C and D show a cell representative of a sub-population of cells over-expressing UL33. The settings for panel D were altered to avoid saturation. Scale bar = 20 μ m

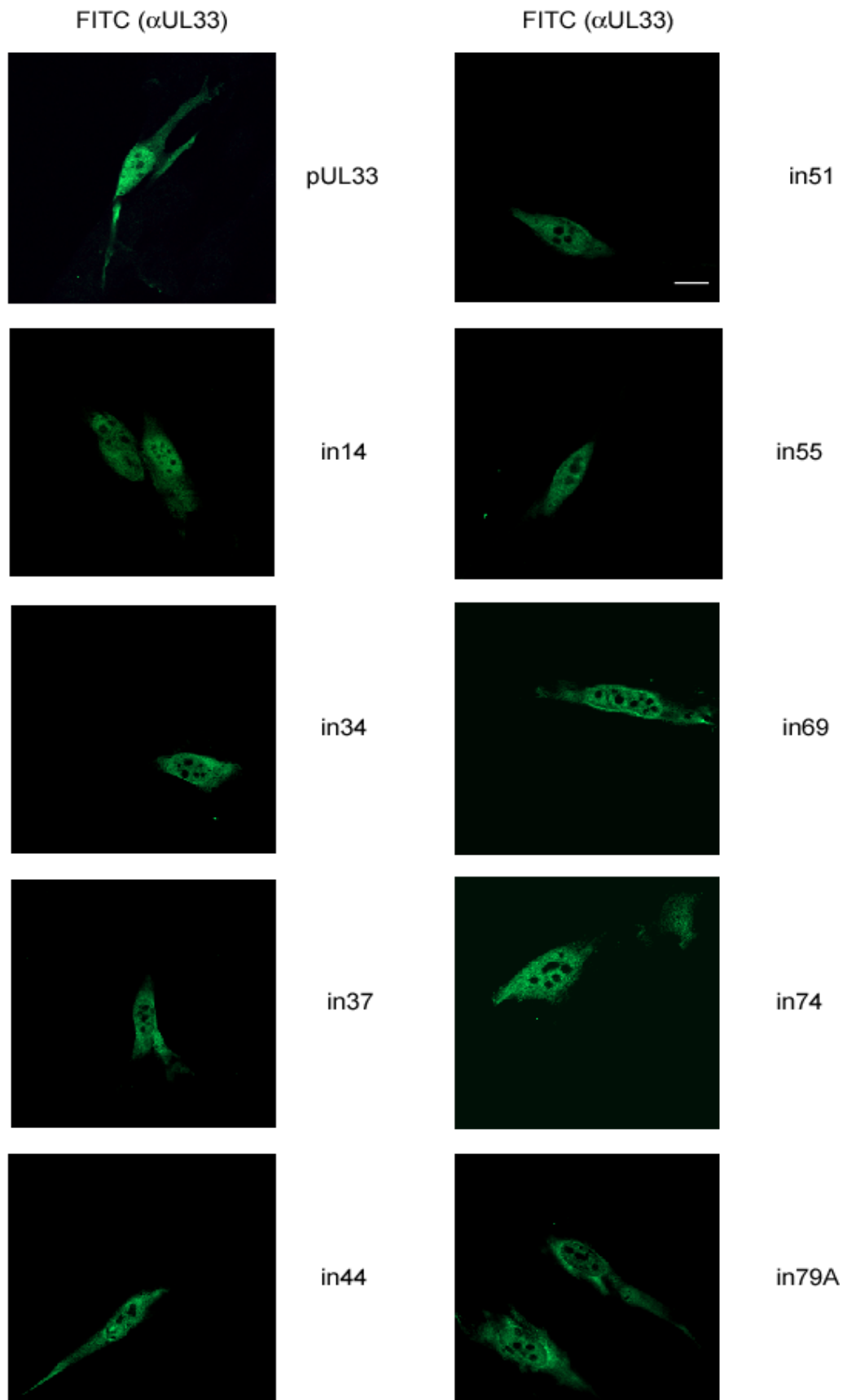
A similar experiment was performed to examine the localisation of the mutated UL33 proteins. Cells were transfected with plasmids expressing wt and mutated UL33 and processed as described above. The results are shown in **Figure 3.9**. As before, cells transfected with pCMV10 did not exhibit fluorescence above background levels (data not shown). As observed above, wt UL33 localised throughout the cell, but was mainly concentrated in the nucleus. In cells transfected with plasmids expressing UL33 insertional mutants, no significant changes in cellular localisation were observed compared with wt UL33. Similar expression levels were observed for each of the mutants, although, as seen with wt UL33, a proportion of cells exhibited a distinct localisation pattern with UL33 being predominantly present in punctuate cytoplasmic foci (not shown). These data suggest that insertions in the UL33 ORF have little effect on localisation of the mutated polypeptides in the absence of other viral proteins.

Section 3.3 Ability of UL33 insertional mutants to complement the growth of UL33 mutant viruses

To analyse the ability of insertional mutants to complement growth of viruses lacking functional versions of UL33, a transient complementation assay was utilised. The assay assesses complementation of mutant virus growth by proteins supplied *in trans*, usually under the control of a constitutively active promoter, under conditions non-permissive for input virus replication. Progeny virus yield is subsequently determined by titration under permissive conditions. Low pH treatment following initial infection (Rosenthal *et al.*, 1984) was used to inactivate the infectivity of particles that had not penetrated the cells, thereby reducing the background titres due to residual inoculum.

3.3.1 Complementation yield analysis using *ts1233*

To analyse the ability of mutants to complement growth of *ts1233*, BHK cells were



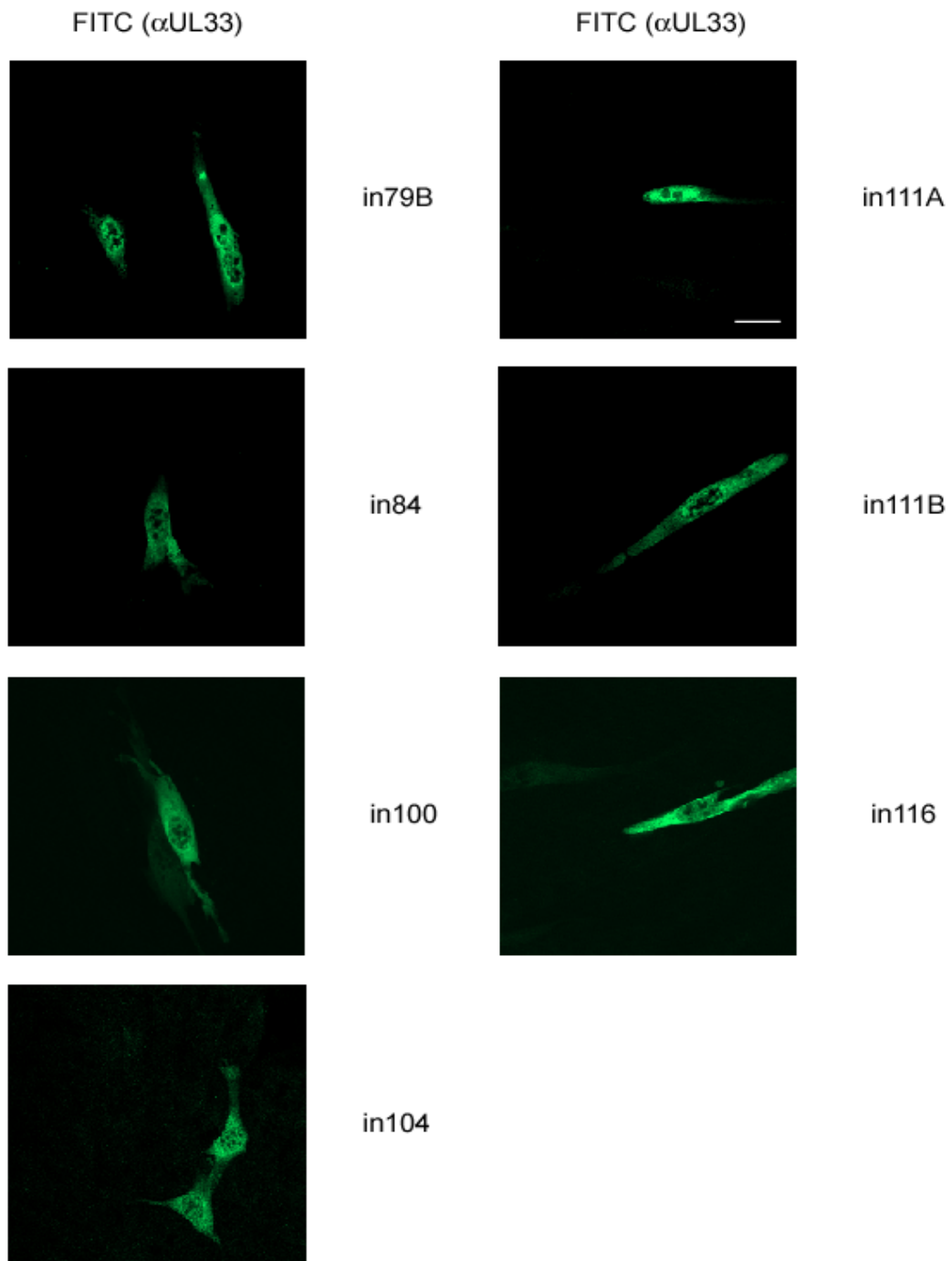


Figure 3.9: The cellular localisation of mutated UL33 proteins in transfected cells.

BHK cells were transfected with the indicated plasmids expressing insertional mutants of UL33 and processed as described in the legend to Figure 3.8. Scale bar = 20µm.

transfected with plasmids expressing mutated or wt UL33 proteins by the calcium phosphate procedure, and DMSO boosted after 4 hours. Six hours post-transfection, cells were infected with 5 p.f.u./cell of *ts1233* and incubated at the NPT of 39.2 °C. One hour after virus addition residual virus was neutralised with an acid-glycine wash (section 2.2.10). Eighteen hours post-infection (h.p.i) progeny virus was harvested and titrated on BHK cells at the PT of 32 °C. After four days, the cells were stained, plaques counted, and viral titres calculated. **Figure 3.10** shows progeny virus titres obtained for each mutant expressed as a percentage of the titre obtained with pUL33.

pUL33 effectively complemented growth of *ts1233*, achieving titres between 1.8×10^5 and 4.5×10^5 p.f.u./ml. The yield from untransfected cells or cells receiving the vector pCMV10 was between 5% and 14% of that obtained with pUL33. This may represent the presence of *ts+* revertants in the stock, leak of the *ts* virus or residual inoculum. Five of the sixteen mutants, containing insertions at positions 34, 37, 44, 79 and 100, complemented *ts1233* growth to titres reaching 50-80% of those achieved using pUL33. Furthermore, one mutant, in84, resulted in a significantly higher average titre (>130%). With the exception of in79B, the remaining mutants did not support growth of *ts1233* above background levels. The yields from cells receiving in79B were approximately 20% of pUL33 levels, suggesting that this mutant may complement growth to a low extent.

To confirm that similar amounts of UL33 were expressed in each instance, duplicate monolayers, transfected and infected as described, were analysed by western blotting using antibody R148 in conjunction with an actin loading control (**Figure 3.11**). Similar amounts of UL33 were detectable with transfection of each of the plasmids expressing wt or mutated UL33 proteins. UL33 was detected in lower amounts in cells infected

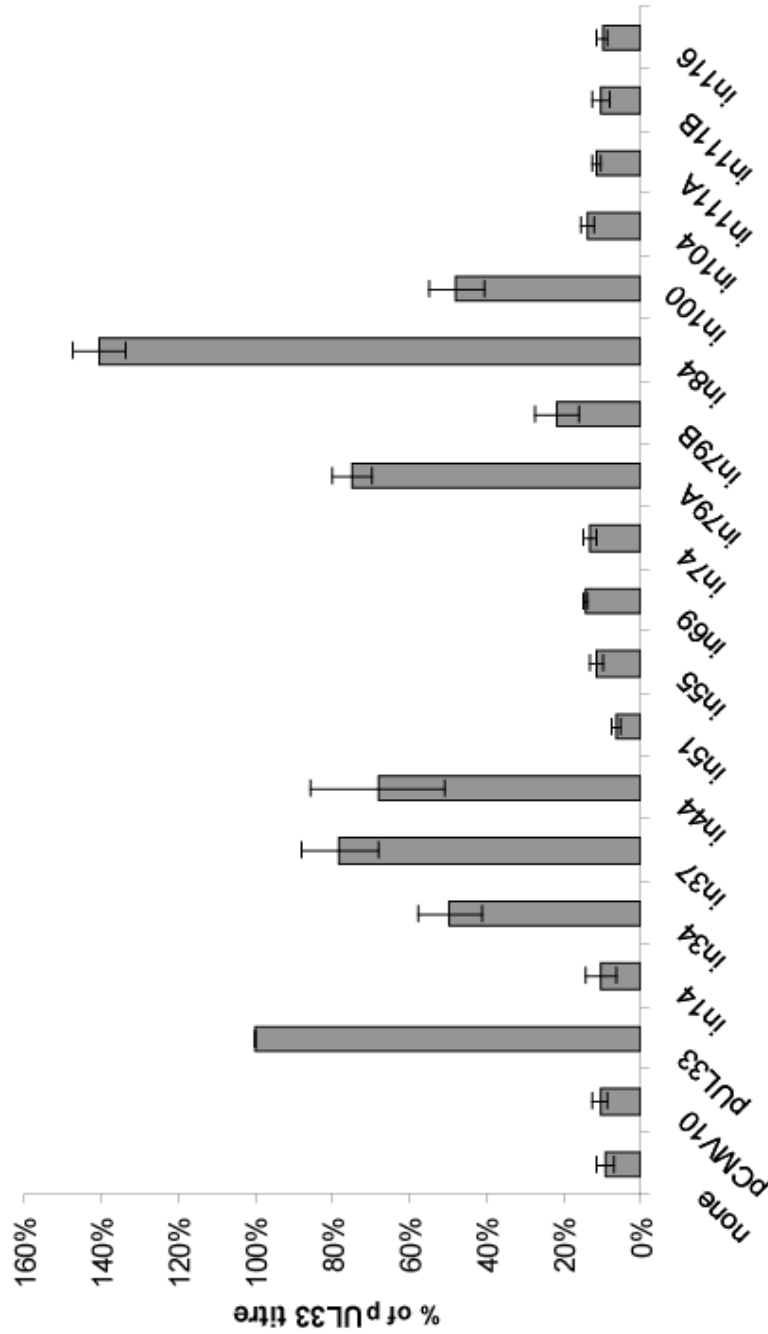


Figure 3.10: Ability of mutants to complement Δ UL33 growth

BHK cells were transfected with the indicated plasmid, and super-infected with Δ UL33. After virus neutralisation, cells were incubated at the NPT of 39.2 °C for 18 h. Progeny virus was harvested, and titres determined on BHK cells at the PT of 32 °C. Average titres from three independent experiments are displayed as percentages of titres obtained with pUL33. Error bars represent standard deviation within the triplicates.

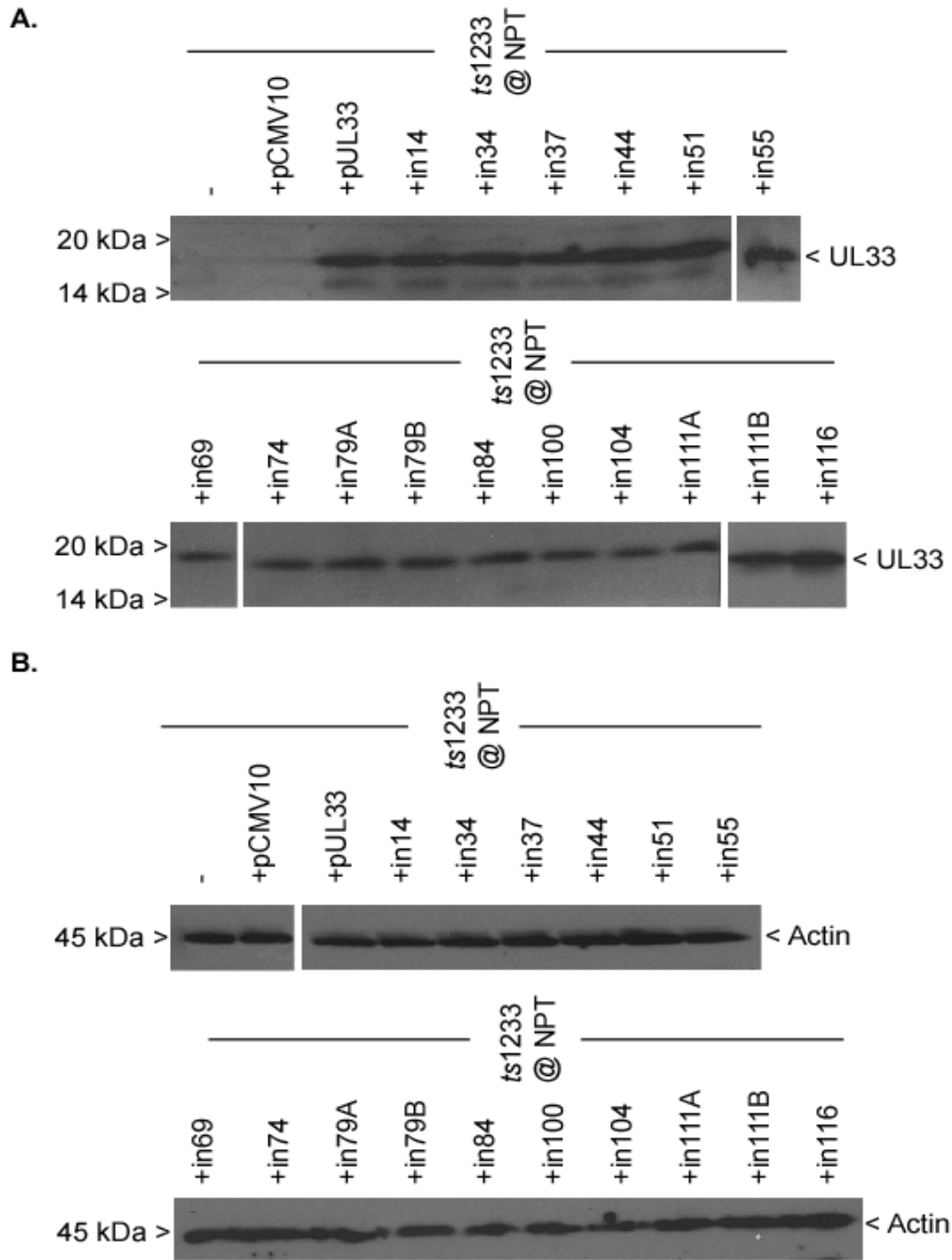


Figure 3.11: Western analysis of UL33 expression in the *ts1233* complementation assay

BHK monolayers were transfected and super-infected as indicated in the legend to Figure 3.10. Cell lysates were prepared and samples separated by SDS-PAGE on 15% polyacrylamide gels. Proteins were transferred to PVDF membrane and UL33 polypeptides detected using the R148 antibody and protein-A-HRP (panel A). To ensure equal amounts of lysate were loaded, duplicate membranes were incubated with an anti-actin antibody and protein-A-HRP (B).

with *ts1233* alone, or those receiving *ts1233* in conjunction with pCMV10. The actin control indicated that comparable amounts of protein were loaded in each case.

The data indicate the importance of several regions of UL33 in supporting growth of *ts1233* at the NPT, namely at position 14 and between amino acids 51-74 and 104-116. The nature of the inserted amino acids at position 79 (in79A and in79B) seemed to affect the functionality of the mutated proteins.

3.3.2 Complementation yield analysis using *dUL33*

The ability of mutants to complement the growth of the null mutant *dUL33* was similarly analysed. In this case the infected BHK cells were incubated at 37 °C, progeny virus was harvested and titrated on the complementing 20A cell line.

Figure 3.12 shows the yields achieved expressed as a percentage of the titre obtained after transfection of pUL33. Western blot analysis confirmed that wt and mutated UL33 proteins were expressed at similar levels, and that comparable amounts of protein were examined (**Figure 3.13**). In agreement with previous studies UL33 was not detectable in cells infected with *dUL33* alone (Reynolds *et al.*, 2000), nor in superinfected cells that had been transfected with pCMV10.

With pUL33, titres between 2.76×10^6 and 4.5×10^6 p.f.u./ml were obtained. The yields from untransfected cells or cells receiving pCMV10 were between 3% and 5% of those observed with pUL33. Seven of the sixteen mutants, containing insertions at amino acids 34, 37, 44, 79 (in79A and in79B), 84 and 100 complemented growth to between 50% and 80% of the titres obtained with wild type UL33. In contrast to the results obtained using *ts1233*, in84 did not give higher yields than pUL33, and in79B was as effective as in79A at complementing mutant virus growth. The remaining nine mutants

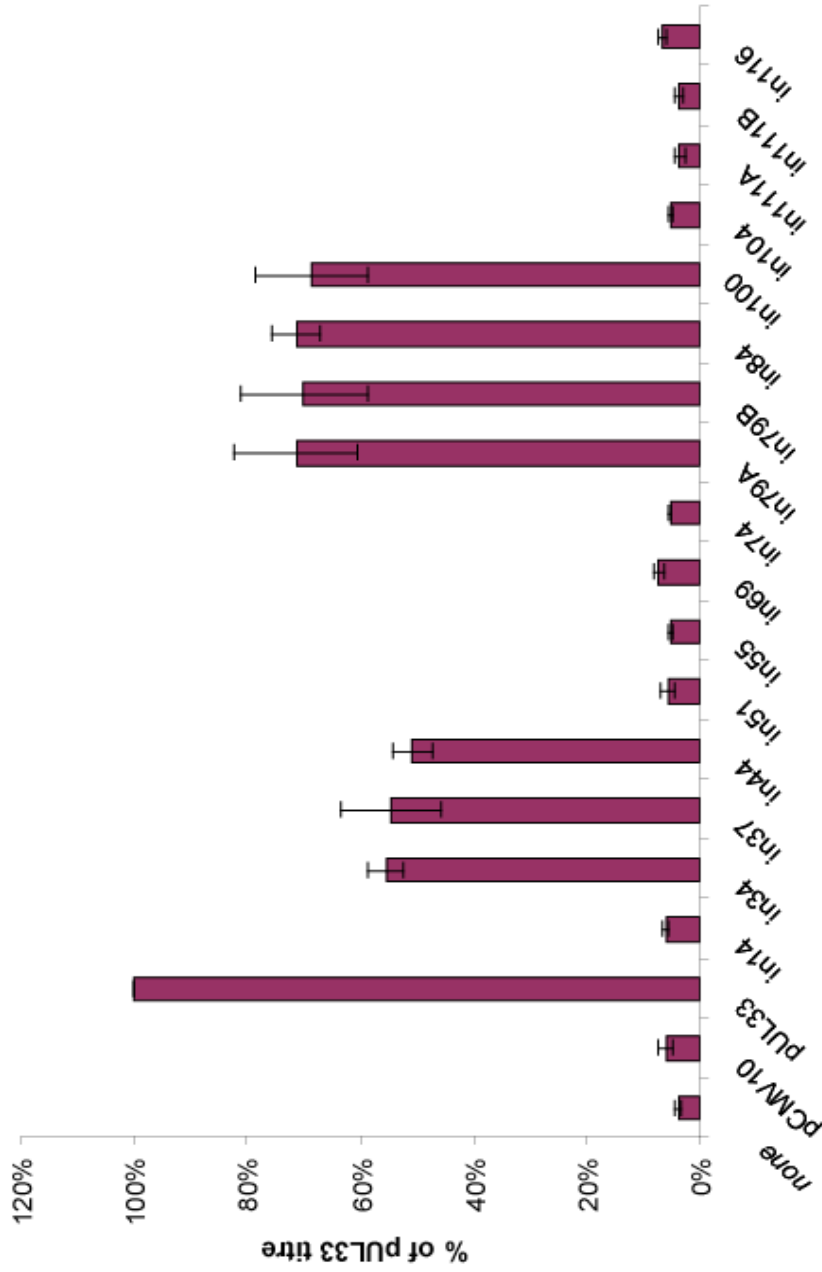


Figure 3.12: Ability of mutants to complement *Δ*UL33 growth.

BHK cells were transfected with the indicated plasmid, and super-infected with *Δ*UL33. After virus neutralisation, cells were incubated at 37 °C for eighteen hours. Progeny virus was harvested, and titres determined on 20A cells at 37 °C. Average titres from three independent experiments are displayed, and expressed as percentage of wt plasmid titres. Error bars represent standard deviation within the triplicates.

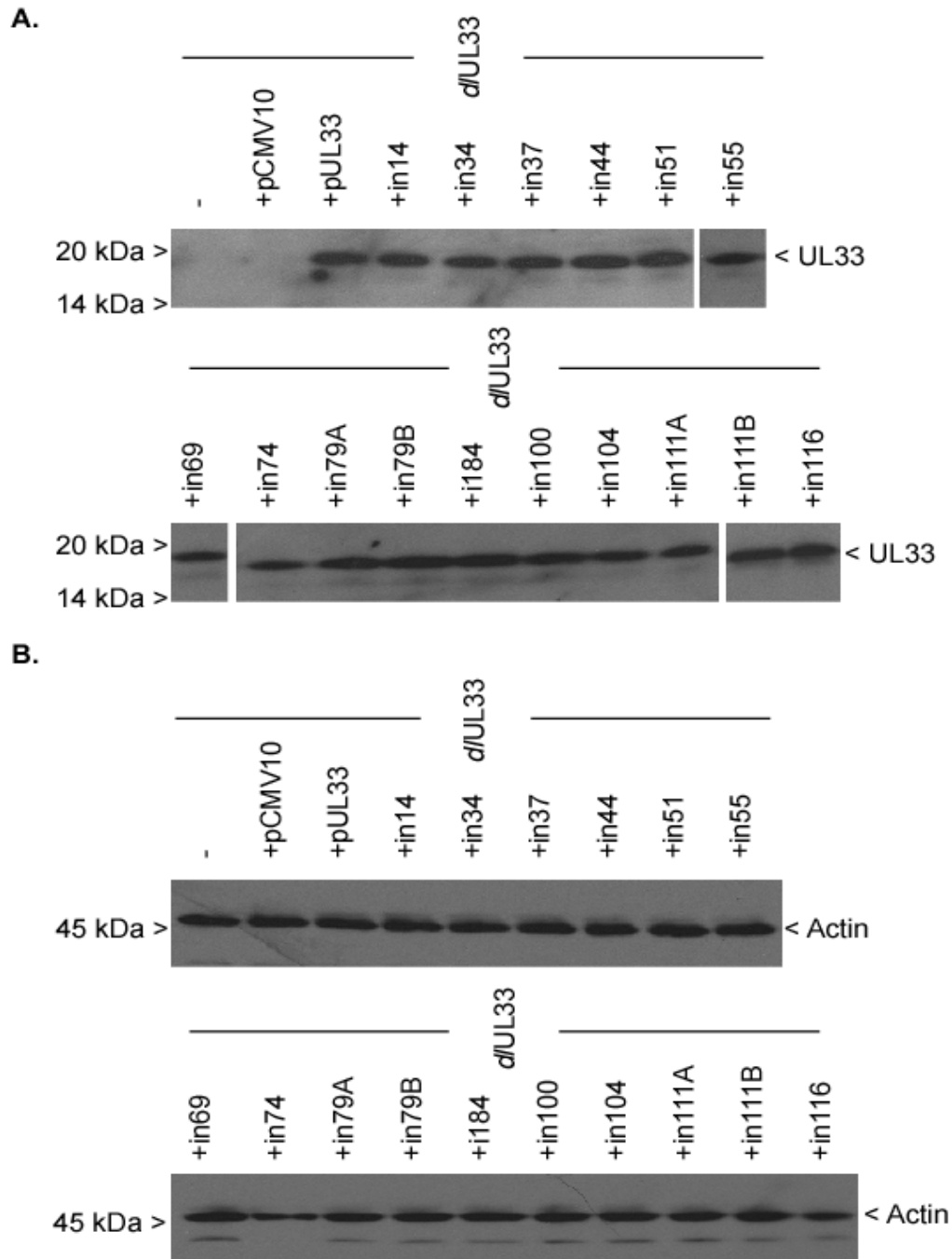


Figure 3.13: Western analysis of UL33 expression in the *dUL33* complementation assay

BHK monolayers were transfected and super-infected as indicated in the legend to Figure 3.12. Cell lysates were prepared and samples separated by SDS-PAGE on 15% polyacrylamide gels. Proteins were transferred to a PVDF membrane and UL33 polypeptides detected using the R148 antibody and protein-A-HRP (**A**). To ensure equal amounts of lysate were loaded, duplicate membranes were incubated with an anti-actin antibody and protein-A-HRP (**B**).

were unable to complement virus replication. Overall, the pattern of complementation was very similar to that seen with *ts1233*, confirming that the regions surrounding position 14, and between amino acids 51-74 and 104-116, are important for viral growth.

Section 3.4 Ability of UL33 insertion mutants to support amplicon packaging

HSV-1 amplicons, bacterial plasmids containing a functional origin of replication and packaging signals, have provided convenient tools for analysing the replication and packaging of HSV-1 DNA (Stow *et al.*, 1983; Spaete & Frenkel, 1985). Previous studies have demonstrated that amplicons bearing the minimal packaging sequence Uc-DR1-Ub, together with the viral lytic origin of replication *ori_s*, are replicated as concatemers and packaged in the presence of wt HSV-1 helper virus (Nasseri & Mocarski, 1988; Hodge & Stow, 2001).

The amplicon assay (**Figure 3.14**) provides a sensitive assay for DNA packaging, since unreplicated input amplicon DNA can be separated by digestion with *DpnI*, enabling essentially zero background signals. In contrast, a proportion of infecting viral genomes invariably fail to be uncoated, and give rise to a background signal of DNaseI-resistant DNA even in the absence of *de novo* packaging.

The following experiments investigate the ability of the sixteen UL33 mutants to complement the packaging defects exhibited by *ts1233* and *dUL33* in the transient amplicon packaging assay.

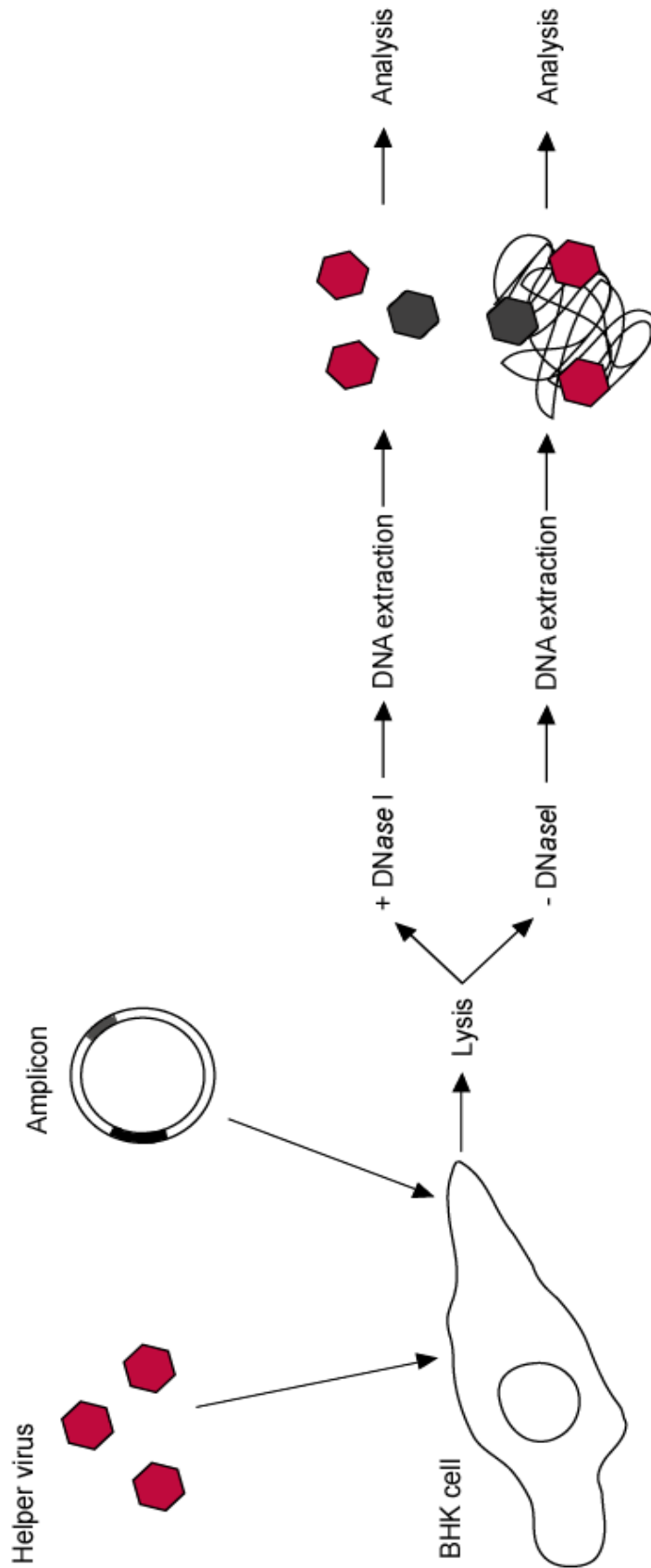


Figure 3.14: The amplicon packaging assay

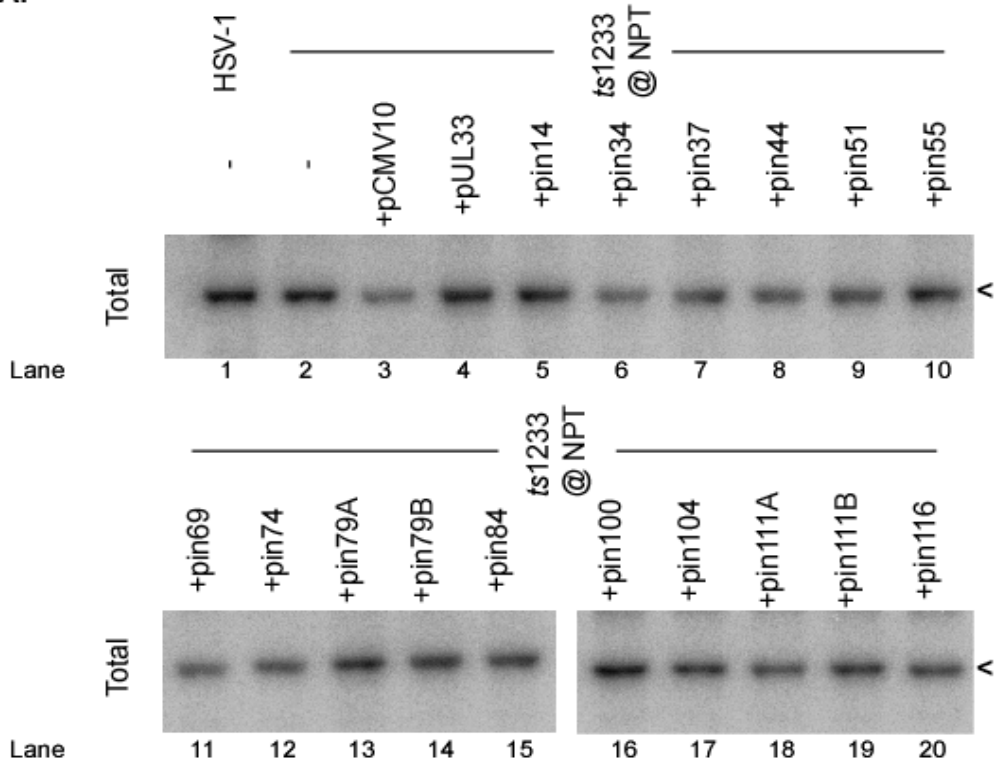
The amplicon packaging assay utilises a plasmid, termed an amplicon, containing minimum signals for viral DNA replication (*ori_v*) and packaging (*Uc-DR1-Ub*). Amplicon DNA is transfected into cells permissive for HSV-1 replication, and the cells super-infected with HSV-1. This provides helper functions required for replication and encapsidation of the amplicon, which is packaged as a concatamer (grey virions). After sixteen hours, cells are harvested and divided into two samples. One sample is lysed in the absence of DNaseI, allowing isolation of both packaged and unpackaged DNA. Lysis of the second sample in the presence of DNaseI removes cellular and un-encapsidated viral DNA. DNA is prepared from the two samples and analysed by Southern blotting.

3.4.1 Amplicon packaging using *ts1233* helper virus

To assay the ability of mutants to support amplicon DNA packaging, monolayers of BHK cells were transfected with 1 µg of plasmids expressing wt or mutated UL33 together with 1 µg of the amplicon pSA1 by the calcium phosphate method. Cells were DMSO boosted four hours post-transfection. To provide other functions necessary for viral DNA replication and packaging, cells were super-infected six hours post-transfection with 5 p.f.u./cell of either HSV-1 or *ts1233*, and shifted to the NPT of 39.2 °C. At 18 h.p.i. DNase-resistant and total DNA were prepared as described (sections 2.2.8.2 and 2.2.8.3), and samples were digested with *EcoRI* and *DpnI*. DNA fragments were separated by agarose gel electrophoresis and Southern blotted. The membrane was probed with ³²P-labelled pAT153 to detect the amplicon and a representative phosphorimage is shown in **Figure 3.15**. Quantification of data from three independent experiments is presented in **Table 3.1**.

Neither replication nor packaging of amplicons was observed in mock-infected cells (not shown). *ts1233* is defective in DNA packaging but DNA replication occurs to wt levels (Al-Kobaisi *et al.*, 1991). Unsurprisingly, therefore, similar levels of replicated pSA1 were detected following infection with either *ts1233* or wt HSV-1 (lanes 1 and 2). DNA replication was not significantly affected in cells transfected with pCMV10 or any of the UL33-expressing plasmids (lanes 3-20). Replicated pSA1 was packaged in cells infected with wt HSV-1 (lane 21), but not with *ts1233* (lane 22), consistent with the known phenotype of this mutant. In the presence of pUL33 (lane 24), but not pCMV10 (lane 23), packaged DNA was detected in *ts1233*-infected cells, demonstrating that wt UL33 expressed from pUL33 can support DNA packaging.

A.



B.

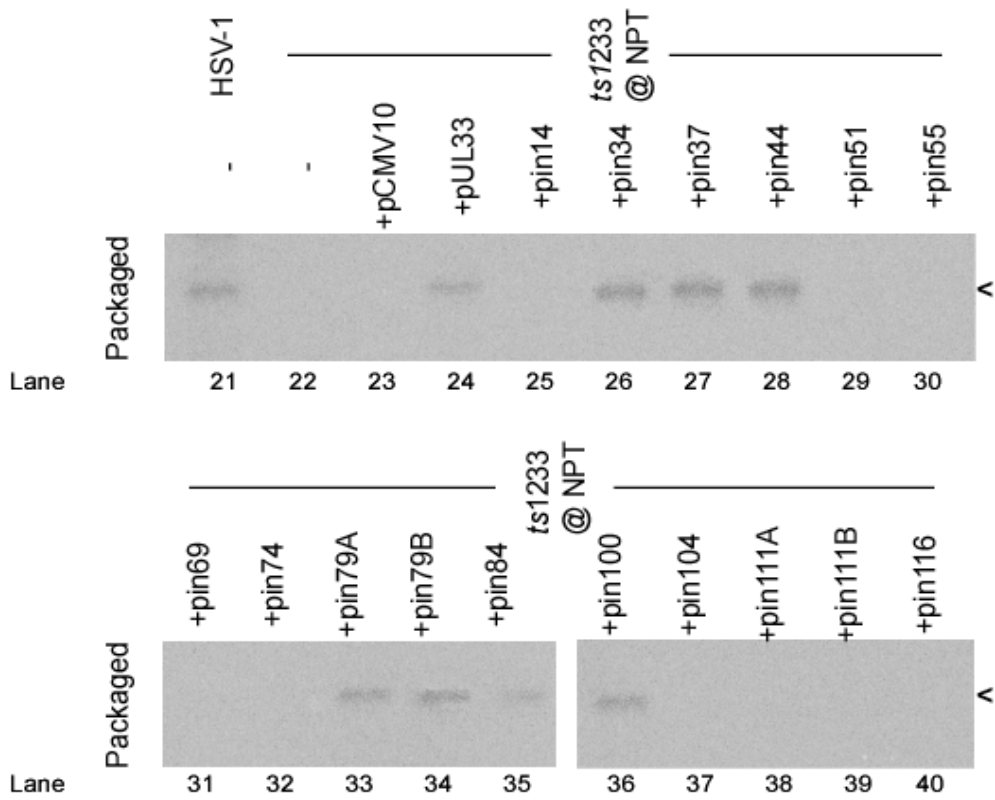


Figure 3.15: Ability of mutants to package amplicon DNA in the presence of *ts1233*.

BHK cells were transfected with the denoted plasmid, together with pSA1. After DMSO boosting, cells were superinfected with wt HSV-1 or *ts1233* as indicated. Sixteen h.p.i., cells were harvested, and total (panel **A**) or packaged DNA (**B**) prepared. After digestion with *EcoRI* and *DpnI*, fragments were separated by agarose gel electrophoresis. pSA1 was detected by hybridisation to ³²P-labelled pAT153, and the position of linear molecules denoted by a <.

Plasmid	Experiment 1 % packaged relative to HSV-1	Experiment 2 % packaged relative to HSV-1	Experiment 3 % packaged relative to HSV-1	Mean packaged DNA (relative to HSV-1) (%)
-	13.61	2.01	0.49	5.37
pCMV10	8.90	5.70	0.80	5.13
pUL33	62.37	59.87	44.13	55.46
pin14	15.51	12.55	13.66	13.91
pin34	51.93	44.93	92.15	63.00
pin37	41.41	63.11	64.22	56.25
pin44	77.04	32.66	81.72	63.81
pin51	4.61	6.21	1.58	4.13
pin55	4.89	1.20	4.04	3.37
pin69	11.04	6.26	16.65	11.32
pin74	14.70	9.75	22.18	15.54
pin79A	54.01	24.88	93.20	57.36
pin79B	32.80	34.78	143.70	70.42
pin84	69.61	56.76	182.32	102.90
pin100	88.34	34.56	193.46	105.45
pin104	4.61	1.50	36.04	17.05
pin111A	10.72	4.21	28.85	14.49
pin111B	13.46	10.48	37.01	20.32
pin116	16.87	6.82	26.25	16.65

Table 3.1: Quantification of amplicon packaging in the presence of *ts1233*

Phosphorimages from three independent experiments were quantified using Quantity One software (section 2.1.14). Bands were quantified according to counts within each band, and expressed as total counts/mm² (not shown). The percentage of packaged DNA in each instance was calculated by dividing the counts in the DNase-resistant band by those in the total DNA band, and expressed as a % of values achieved in cells transfected with pSA1 alone and superinfected with wt HSV-1.

Seven of the sixteen mutants examined supported DNA packaging. Insertions at amino acids 34, 37, 44, 79, 84 and 100 did not affect the ability of UL33 to support amplicon packaging (lanes 26-28 and 33-36). However, insertions at amino acids 14, 51, 55, 69, 74, 104, 111 and 116 rendered UL33 unable to support amplicon DNA encapsidation (lanes 25, 29-32 and 37-40).

Western blot analysis was performed on duplicate monolayers as previously described for the yield complementation assay, and confirmed that similar levels of UL33 were expressed in each case (data not shown).

Comparison of these data with the results of the complementation yield assay for *ts1233* (Figure 3.10) shows a complete correlation between the ability to package DNA and generate viable progeny. However, it should be noted that *in79B*, which complemented viral growth poorly, supported amplicon packaging as efficiently as pUL33.

3.4.2 Packaging of *ts1233* genomes in the presence of mutated UL33 proteins

One of the drawbacks of the amplicon assay is that a range of differently sized molecules containing between one (4.4 kbp) and approximately 34 (150 kbp) copies of the amplicon are packaged into capsids. This represents an obvious difference from the way in which the viral genome is itself packaged.

To determine whether packaging of the helper virus genome was affected in the same way as the amplicon, the membrane from Figure 3.15B was stripped and re-probed with ³²P-labelled pGX153, which contains the *Bam*HI P fragment of HSV-1 inserted

into pAT153, to allow the simultaneous detection of viral and amplicon DNA. The resulting phosphorimage is shown in **Figure 3.16**. As DNA samples were cleaved with *EcoRI* and *DpnI* before Southern analysis, probing with pGX153 should detect three bands corresponding to the HSV-1 *EcoRI* N (2.4 kbp), G and F fragments (16.1 and 16.2 kbp respectively; migrate as one band), and the amplicon (4.3 kbp) (Porter & Stow, 2004a).

Figure 3.16 demonstrates that there is absolute correlation between the ability to support packaging of the amplicon and helper virus genomes. This confirms that the amplicon assay represents a valid approach to analyse the role of UL33 in packaging the viral genome.

3.4.3 Amplicon packaging using *dUL33*

To scrutinise the ability of UL33 mutants to package DNA in the presence of the *dUL33* helper virus, further amplicon packaging assays were undertaken in which transfected monolayers were super-infected with 5 p.f.u./cell of *dUL33* or wt HSV-1 and incubated at 37°C. Samples were analysed and a representative phosphorimage is shown in **Figure 3.17**. Quantification of data from three independent experiments is shown in **Table 3.2**. Western blot analysis performed on duplicate monolayers confirmed that similar levels of UL33 were expressed in each instance (data not shown).

When grown on non-complementing cells, *dUL33* exhibits a defect in DNA packaging but not replication of viral DNA (Patel *et al.*, 1996). Consistent with this phenotype, amplicon DNA was efficiently packaged by HSV-1 (lane 21), but not by *dUL33* (lane 22), despite being replicated effectively by both viruses (lanes 1 and 2). Supply of UL33

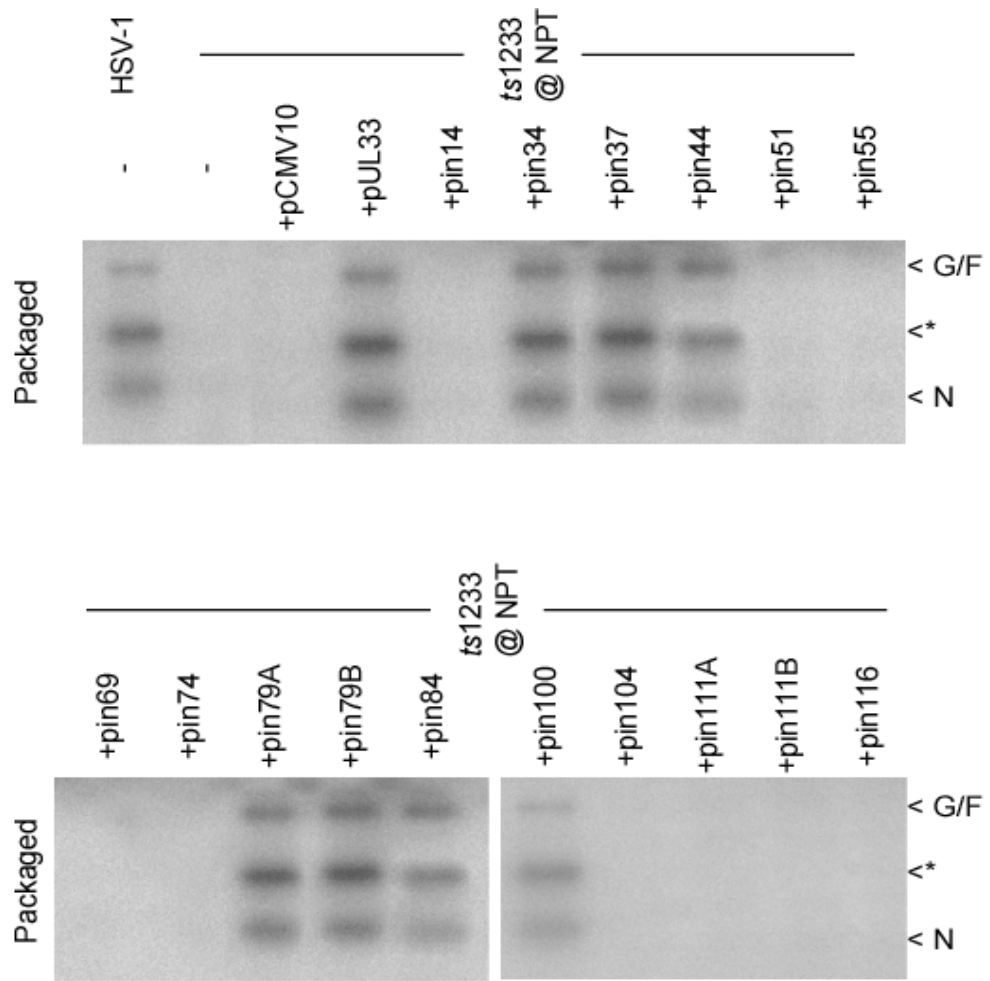
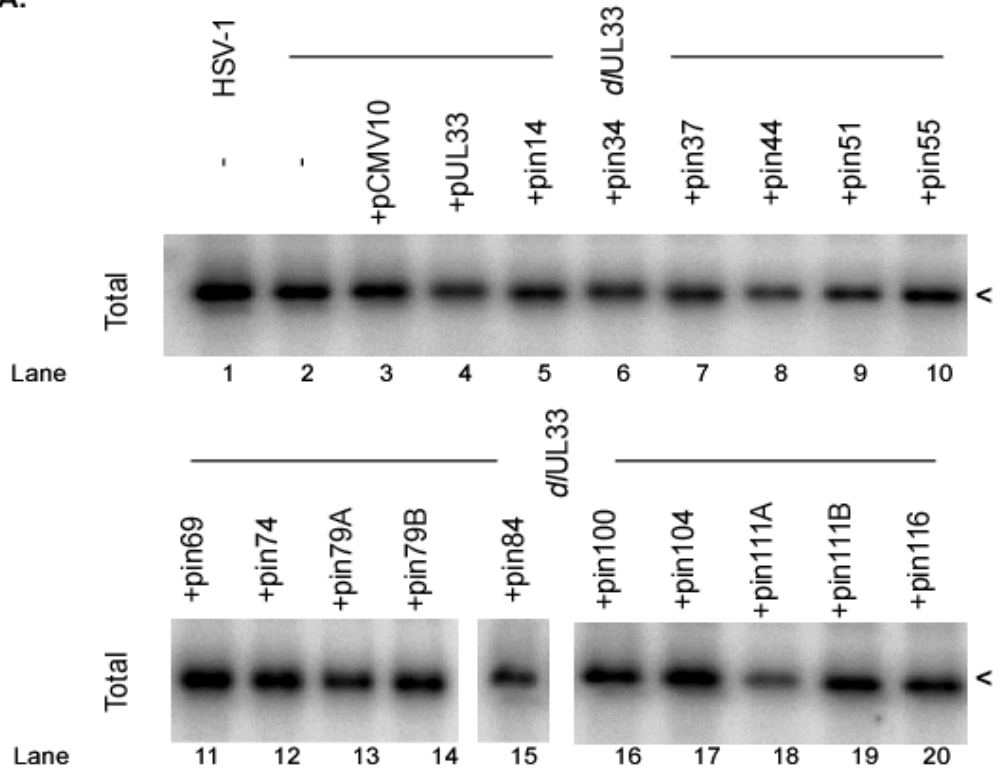


Figure 3.16: Ability of UL33 mutants to package *ts1233* genomes

The membrane from Figure 3.15B was stripped and re-probed with ^{32}P -labelled pGX153. Fragments arising from packaged amplicon are signified with a <*. The position of the HSV-1 *Eco*RI fragments G/F and N are indicated.

A.



B.

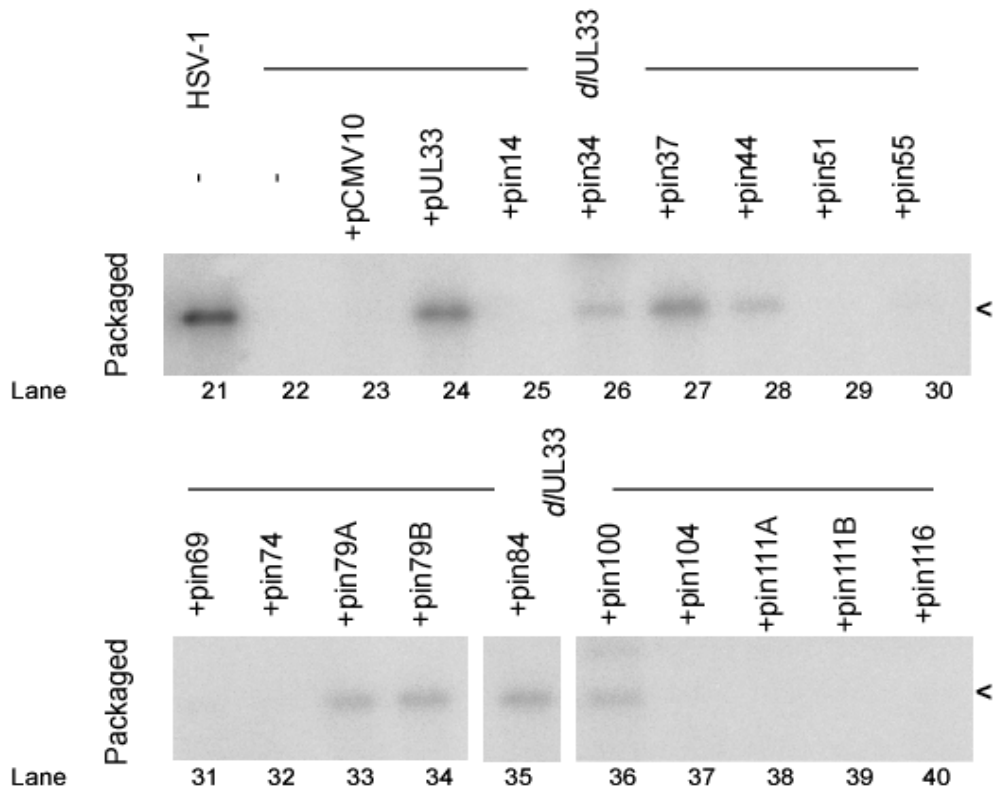


Figure 3.17: Ability of mutants to package amplicon DNA in the presence of *ΔUL33*

BHK cells were transfected with the denoted plasmid together with pSA1. After DMSO boosting, cells were superinfected with wt HSV-1 or *ΔUL33* as indicated. Sixteen h.p.i., cells were harvested, and total (panel **A**) or packaged DNA (**B**) prepared. After digestion with *EcoRI* and *DpnI*, fragments were separated by agarose gel electrophoresis. pSA1 was detected by hybridisation to ³²P-labelled pAT153, and the position of linear molecules denoted by a <.

Plasmid	<u>Experiment 1</u> <u>% packaged</u> <u>relative to HSV-1</u>	<u>Experiment 2</u> <u>% packaged</u> <u>relative to HSV-1</u>	<u>Experiment 3</u> <u>% packaged</u> <u>relative to HSV-1</u>	<u>Mean packaged</u> <u>DNA (relative to</u> <u>HSV-1) (%)</u>
-	3.84	8.18	14.93	8.98
pCMV10	4.88	8.74	16.00	9.87
pUL33	63.12	62.55	61.62	62.43
pin14	2.86	11.67	12.28	8.93
pin34	11.84	84.60	74.88	57.10
pin37	35.38	84.46	57.30	59.05
pin44	13.92	94.71	45.82	51.48
pin51	0.21	9.78	7.95	5.98
pin55	2.31	1.10	15.18	6.20
pin69	3.44	1.17	34.56	13.06
pin74	3.62	0.28	18.47	7.46
pin79A	14.23	53.72	67.03	44.99
pin79B	13.49	70.40	55.70	46.53
pin84	25.55	199.35	52.98	92.63
pin100	10.48	189.00	96.77	98.75
pin104	1.81	3.41	13.87	6.36
pin111A	2.74	0.98	4.18	2.63
pin111B	0.06	4.32	14.92	6.44
pin116	1.72	6.56	15.08	7.78

Table 3.2: Quantification of amplicon packaging in the presence of *dUL33*

Phosphorimages from three independent experiments were quantified according to the legend for Table 3.1, and packaged DNA is displayed as a % of that encapsidated by HSV-1.

in trans complemented the *Δ*UL33 packaging defect (lane 24). Complete correlation was observed between the results shown in Figure 3.17 and the ability of mutants to support DNA packaging in *ts1233* infected cells. Furthermore, absolute correspondence was apparent between the ability of the mutants to complement *Δ*UL33 viral growth (Figure 3.12) and support DNA packaging.

3.4.4 Packaging of *Δ*UL33 genomes by UL33 mutants

To examine the ability of the UL33 mutants to support packaging of *Δ*UL33 genomes, the membrane from Figure 3.17B was stripped and re-probed with ³²P-labelled pGX153. The resultant phosphorimage is shown in **Figure 3.18**. In agreement with the results obtained using *ts1233*, absolute correlation was observed between the ability of mutants to support packaging of pSA1 and helper virus genomes.

3.4.5 Ability of mutants to inhibit wt HSV-1 packaging

Previous results indicated that several UL33 mutants were unable to both package DNA and to complement growth of viruses lacking functional UL33. It is possible that one or more of these non-functional mutants might be dominant-negative inhibitors of the DNA packaging process. To examine this possibility, experiments were performed using a modified transient amplicon packaging assay in which helper functions were provided in all cases by wt HSV-1.

BHK cells were transfected with 1 μg of plasmids encoding non-functional UL33 mutants together with 1 μg of pSA1, and DMSO boosted as previously described. Helper functions were provided by super-infection with 5 p.f.u./cell of HSV-1. At sixteen h.p.i., total and packaged DNA was prepared as described (section 2.2.8). Aliquots of DNA were digested, separated by agarose gel electrophoresis and Southern blotted. Membranes were probed with ³²P-labelled pAT153, and a

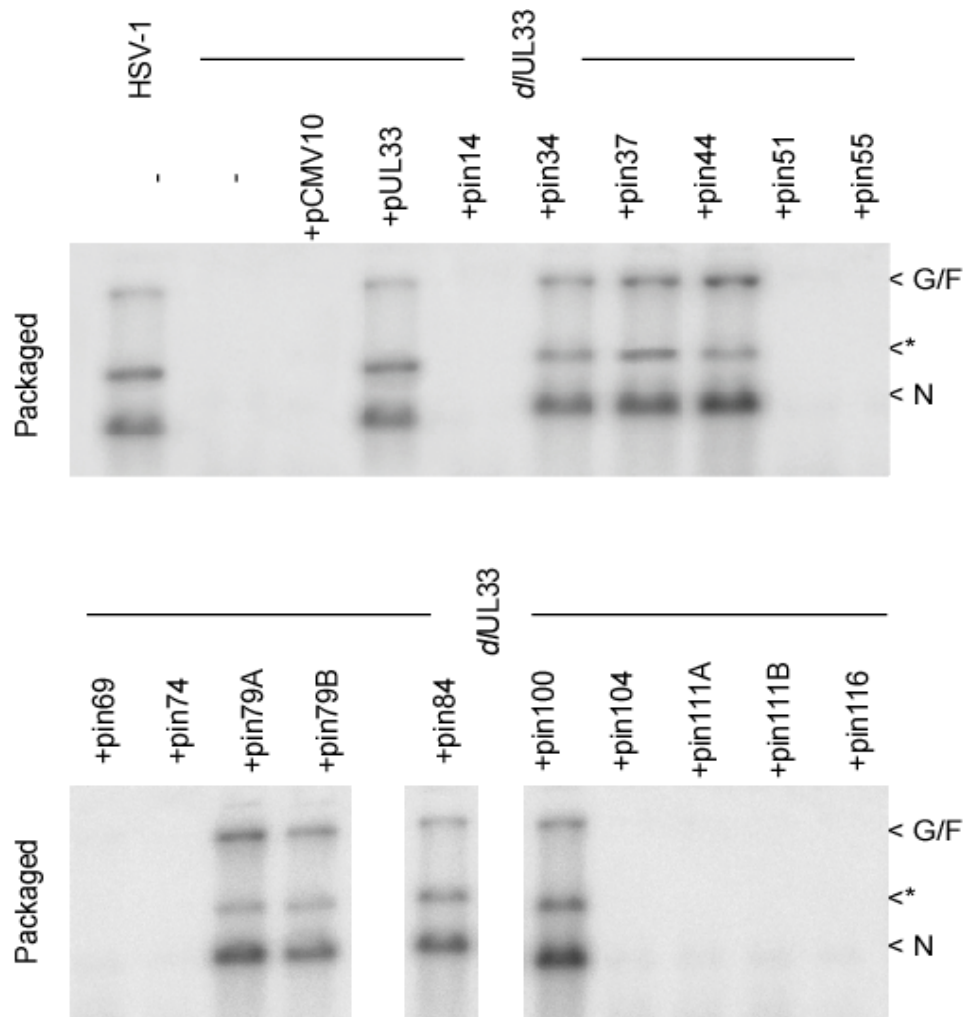


Figure 3.18: Ability of UL33 mutants to package *d*UL33 genomes.

The membrane from Figure 3.17B was stripped and re-probed with ³²P-labelled pGX153. Fragments arising from packaged amplicon are signified with a <*. The position of the HSV-1 *Eco*RI fragments G/F and N are indicated.

representative phosphorimage is shown in **Figure 3.19**. Quantification of data representing three independent experiments is presented in **Table 3.3**.

As expected, similar levels of pSA1 replication were observed in all instances, with the exception of in111A (lane 9). Examination of the EtBr-stained gel revealed that this anomaly was due to inefficient recovery of total DNA rather than decreased plasmid replication. In agreement with previous results, amplicon packaging was observed in cells infected with wt HSV-1 (lane 12). Moreover, in cells receiving both wt helper virus and pUL33, no decrease in packaging was observed, indicating that supply of additional UL33 *in trans* has no inhibitory affect on DNA packaging (lane 13). In three independent experiments, no reproducible inhibition of HSV-1 DNA packaging was observed by any of the mutants examined. This indicates that none of the mutants that are unable to support DNA packaging is a strong dominant inhibitor of DNA packaging.

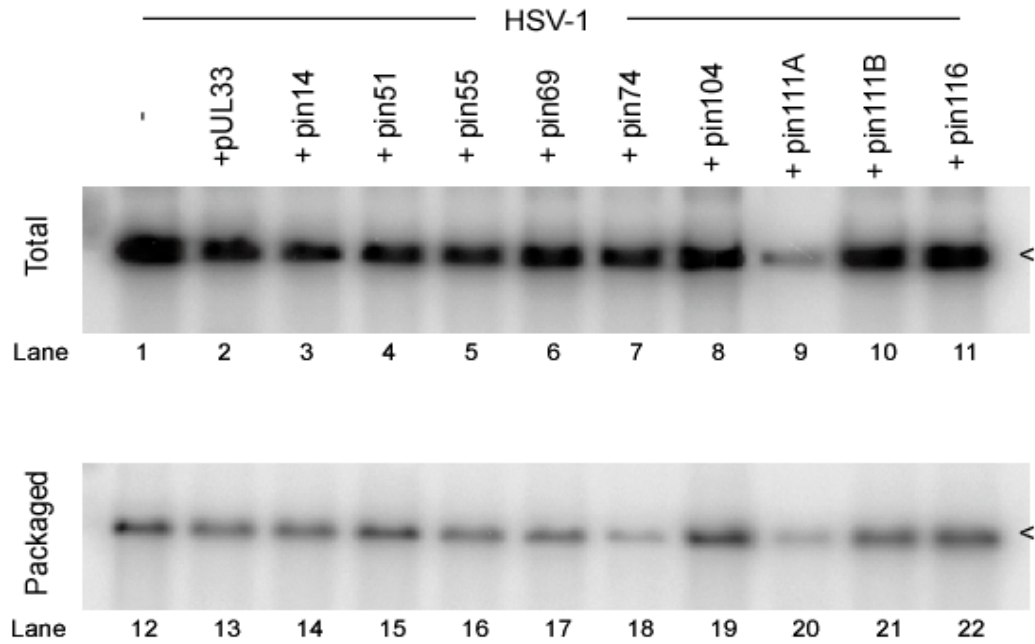


Figure 3.19: Ability of mutants to act as dominant negative DNA packaging inhibitors.

BHK cells were transfected with the indicated plasmids together with pSA1, and superinfected with wt HSV-1. Sixteen h.p.i. total and encapsidated DNA were harvested and aliquots digested with *Eco*RI and *Dpn*I. After agarose gel electrophoresis, fragments were detected with 32 P-labelled pAT153. The position of pSA1 monomers is denoted by an <. The reduced levels of replicated amplicon observed in cells transfected with in111A were not seen in other independent experiments. Data shown is from experiment 3 denoted in Table 3.3.

Plasmid	Experiment 1 % packaged DNA (relative to HSV-1)	Experiment 2 % packaged DNA (relative to HSV-1)	Experiment 3 % packaged DNA (relative to HSV-1)	Mean packaged DNA (relative to HSV-1) (%)
-	100	100	100	100
pUL33	103.18	156.38	94.53	118.03
pin14	134.87	217.43	120.91	157.74
pin51	167.51	242.08	144.54	184.71
pin55	255.69	244.65	99.16	199.83
pin69	163.39	272.42	76.86	170.83
pin74	116.51	209.22	35.92	120.55
pin104	161.68	143.84	148.28	151.27
pin111A	115.34	234.22	129.18	159.58
pin111B	197.90	184.42	113.39	165.24
pin116	150.57	233.78	130.34	171.56

Table 3.3: Quantification of dominant-negative packaging assays

Phosphorimages from three independent experiments were quantified according to the legend for Table 3.1, and packaged DNA expressed as a percentage of that packaged by HSV-1 in the absence of any UL33-expressing plasmid.

Section 3.5 Discussion

3.5.1 Isolation and initial characterisation of mutants

Sixteen insertion mutants of UL33 were isolated using the Mutation Generation System. Initial analysis confirmed that all mutated plasmids expressed stable polypeptides that exhibited similar nuclear and cytoplasmic localisation compared to wt UL33 in transient expression assays. It is well established that macromolecules (and complexes thereof) of <50 kDa can diffuse freely into and out of the nucleus via nuclear pores (reviewed by Talcott & Moore, 1999). Localisation of UL33 in both the nucleus and cytoplasm is consistent with the protein being able to diffuse freely through nuclear pores, and with the absence of nuclear localisation and export signals from its sequence (bioinformatics analysis; not shown). This in turn suggests that the protein is not assembled into oligomers with molecular weight greater than approximately 50 kDa when expressed alone. Interestingly, both wild type and mutated UL33 polypeptides were consistently restricted from the nucleoli of transfected cells.

However, it was noted that in a small number of cells, both wt and mutated UL33 localised in punctuate foci in the cytoplasm (Figure 3.8, panels C+D). It is well documented that misfolded proteins can form protein aggregates (reviewed in Stirling *et al.*, 2003) and that it is possible that UL33 misfolding is responsible for the generation of cytoplasmic aggregates observed in these cells.

3.5.2 Ability of mutants to support DNA packaging and complement virus growth

Importantly, no correlation was apparent between the nature of the inserted amino acids and the ability of mutants to support DNA packaging or complement viral

growth. With the partial exception of in79B, absolute correlation was observed between the ability of mutants to support growth of viruses lacking functional UL33 genes and their ability to direct packaging of both amplicon and viral DNA. This suggests that the only essential function of UL33 is in the initiation of the cleavage packaging process. Were UL33 required at a later stage of the viral life cycle (e.g. the latter stages of DNA packaging or post-packaging virion maturation) it might be expected that some of the mutants would support DNA packaging but fail to complement growth of *ts1233* or *dlUL33*. Mutant in79B complemented growth of *ts1233* less efficiently than growth of *dlUL33*, but supported DNA packaging in the presence of both viruses. The reason for the poor complementation of *ts1233* growth is presently unclear, but could indicate that a combination of the in79B protein with the thermolabile UL33 polypeptide inhibits a late stage during viral replication.

Although none of the mutant proteins unable to support DNA packaging exhibited dominant inhibitory activity, this property has been documented for mutated versions of HSV-1 DNA replication proteins (Stow *et al.*, 1993; Chen & Knipe, 1996; Barnard *et al.*, 1997). Recently, it was also demonstrated that deletion of a NLS from the packaging protein UL15 created a dominant mutant able to inhibit HSV-1 replication (Yang *et al.*, 2007).

Several regions of UL33 were identified which, when disrupted, prohibited complementation of both mutant growth and DNA packaging. Perturbation of regions surrounding amino acid 14, and between residues 51-74 and 104-116, abrogated UL33 function. Alignment of 34 herpesvirus UL33 homologues from the Refseq database, representing the α , β , and γ *herpesviridae* subfamilies, revealed two regions displaying a high degree of sequence conservation (not shown). Error! Reference source not found.

shows the position of

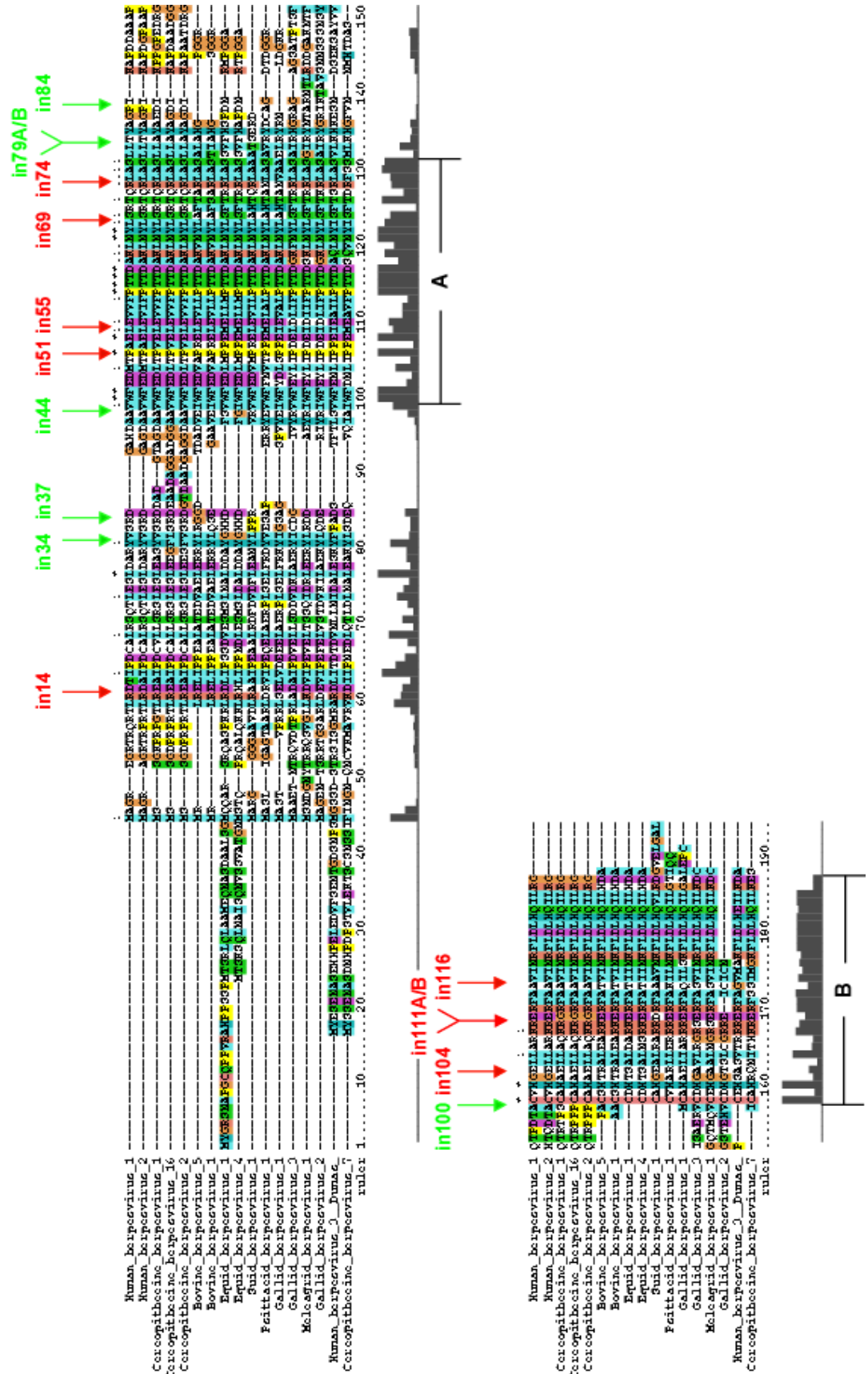


Figure 3.20: The position of UL33 insertional mutants relative to amino acids conserved amongst the *alphaherpesvirinae*.

Amino acid sequences of the indicated *alphaherpesvirinae* UL33 proteins were obtained from the Refseq database, and aligned using ClustalX. Relative sequence conservation is illustrated by grey bars, and absolutely conserved amino acids marked with a *. Regions conserved within all herpesvirus UL33 sequences are denoted A and B. Positions of insertion mutants are indicated by arrows, with green and red arrows denoting functional and non-functional mutants respectively.

Refseq accession numbers: HHV-1: NC_001806; HHV-2: NC_001798;
Cercopithicine HV-1: NC_004812; Cercopithicine HV-16: NC_007653;
Cercopithicine HV-2: NC_006560; Bovine HV-1: NC_001847;
Bovine HV-5: NC_005261; Equid HV-1: NC_001491; Equid HV-4: NC_001844;
Suid HV-1: NC_006151; Psittacid HV-1: NC_005264; Gallid HV-1: NC_006623;
Gallid HV-2: NC_002229; Gallid HV-3: NC_002577; HHV-3: NC_001348;
Meleagrid HV-1: NC_002641; Cercopithicine HV-7: collated with Cercopithicine
HV-9 as NC_002686.

the sixteen insertional mutants in relation to regions of high sequence conservation amongst the 17 *alphaherpesvirinae* UL33 sequences. A correlation between mutant functionality and sequence conservation surrounding the position of insertion was evident. Mutants unable to support DNA packaging and complement *d*/UL33 or *ts*1233 growth generally contained 5 aa inserts in regions of high sequence conservation. For example, insertion of 5 aa adjacent to Pro⁵², which is absolutely conserved amongst all herpesvirus homologues of UL33, renders in51 unable to direct DNA packaging. Similarly, the non-functional mutant in69 encodes an insertion of five residues between Leu⁶⁹ and Ser⁷⁰, which are highly conserved among herpesvirus UL33 homologues. In contrast, mutants retaining the ability to support DNA packaging generally contained 5 aa insertions in areas of low sequence conservation, e.g. in44 and in84. Nevertheless, insertion of 5 aa within the poorly conserved N-terminus of UL33 abolished the ability of in14 to support DNA packaging. Interestingly, *ts*1233 contains a single amino acid substitution in this region (Ile-Asp at position 17) that prevents DNA packaging at the NPT. This indicates that there are sequences in the relatively poorly conserved N-terminus of UL33 that are vital for DNA packaging.

When the positions of mutations were compared to the predicted UL33 secondary structure (**Figure 3.20**), it was evident that non-functional mutants all contained insertions within areas predicted to form helices. In contrast, the functional mutants were generally outside predicted helices, although two (in79A/B) were located near the end of a helix. The PSIPRED program (section 2.1.14) was chosen to predict secondary structure on the basis of its high CASP3 score, indicative of a high accuracy of prediction (Jones, 1999; McGuffin *et al.*, 2000). However, the program Jpred also predicted a similar secondary structure for the wt UL33 protein (not shown).

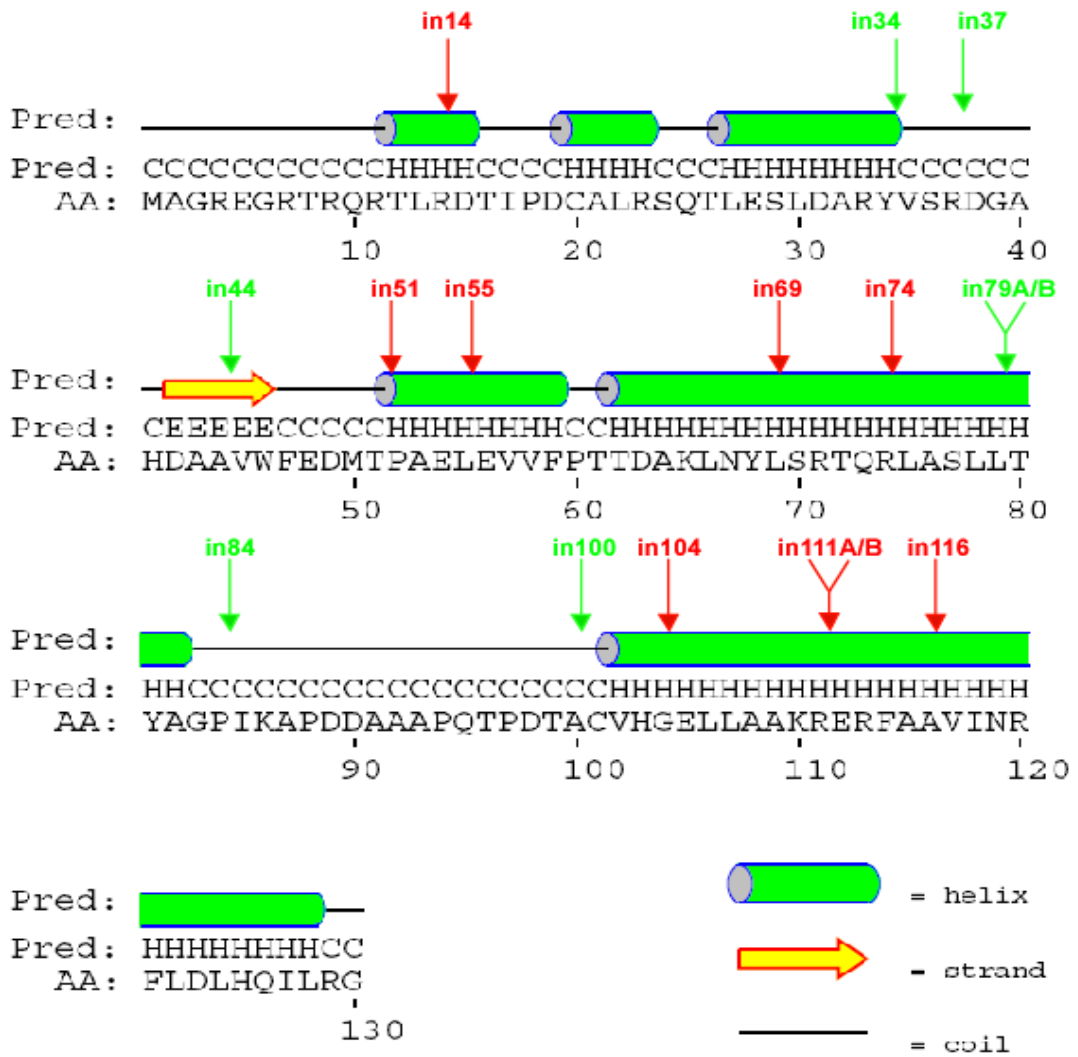


Figure 3.21: The position of 5 aa inserts relative to the predicted secondary structure of UL33.

The secondary structure of wt UL33 was predicted using the PSIPRED program. The position of the sixteen insertion mutants is indicated, with functional and non-functional mutants denoted by green and red arrows respectively.

Several explanations for the inability of a subset of mutants to direct DNA packaging can be envisaged: (i) the insertions in UL33 may render mutated proteins unable to interact with cellular or viral partners, through either global or local changes in protein folding; (ii) mutations may hinder interactions of UL33 or the terminase complex with HSV-1 DNA; (iii) whilst mutations may have no effect on protein-protein or protein-DNA interactions, they may render UL33 unable to fulfil an enzymatic function critical for packaging; (iv) mutated UL33 polypeptides may be unable to correctly target to sites of DNA packaging. Experiments described in the following chapters were designed to investigate some of these possibilities.

Chapter 4: Interaction of wt and mutated UL33 proteins with the terminase components UL15 and UL28

Section 4.1 Introduction

UL33 was first identified as a probable component of the viral terminase complex in 2002, alongside the UL15 and UL28 proteins (Beard *et al.*, 2002). In co-immunoprecipitation assays, all three proteins interacted with one another. However, recent studies of mutant viruses lacking the individual terminase subunits suggested that, whilst UL33 interacts directly with UL28, interaction between UL33 and UL15 is indirect and mediated through a common interaction with UL28 (Jacobson *et al.*, 2006).

Previous experiments (described in chapter 3) demonstrated that several insertion mutants of UL33 were unable to support DNA packaging or mutant virus growth, although the expression and localisation of these proteins when expressed alone resembled that of wt UL33. One explanation is that the insertions rendered the mutated proteins unable to interact with viral protein partners. The experiments described in this chapter therefore examined the interaction of wt and mutated UL33 proteins with UL15 and UL28.

Section 4.2 Interaction of wt and mutated UL33 proteins with UL15

Although UL33 has been identified as a component of the HSV-1 terminase complex, it remains controversial whether UL33 interacts with UL15 directly (Beard *et al.*, 2002; Jacobson *et al.*, 2006). Initial experiments were therefore undertaken to examine whether wt UL15 and UL33 proteins interacted in the absence of UL28. Subsequently,

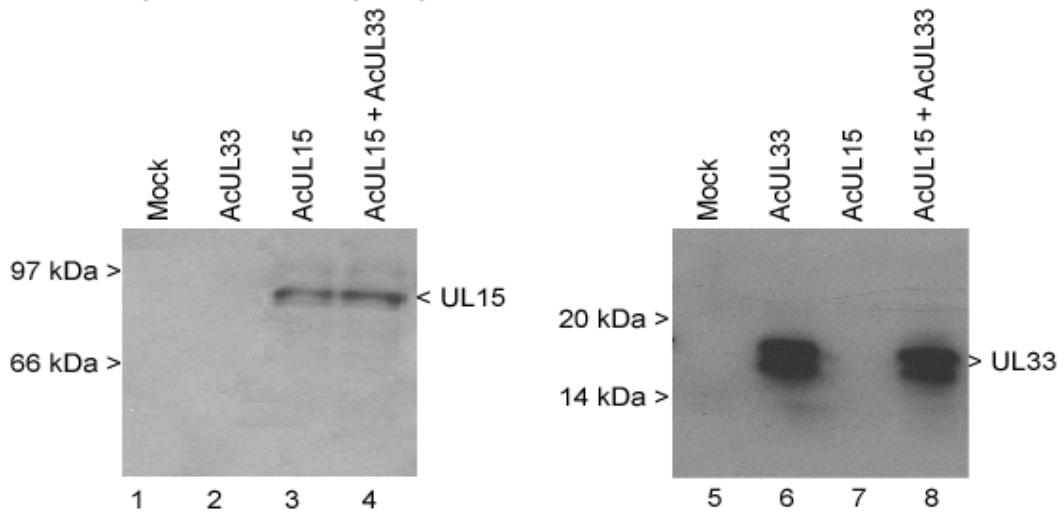
the studies were extended to examine the ability of mutated UL33 proteins to interact with UL15.

4.2.1 UL15 and UL33 interact in recombinant baculovirus-infected cells

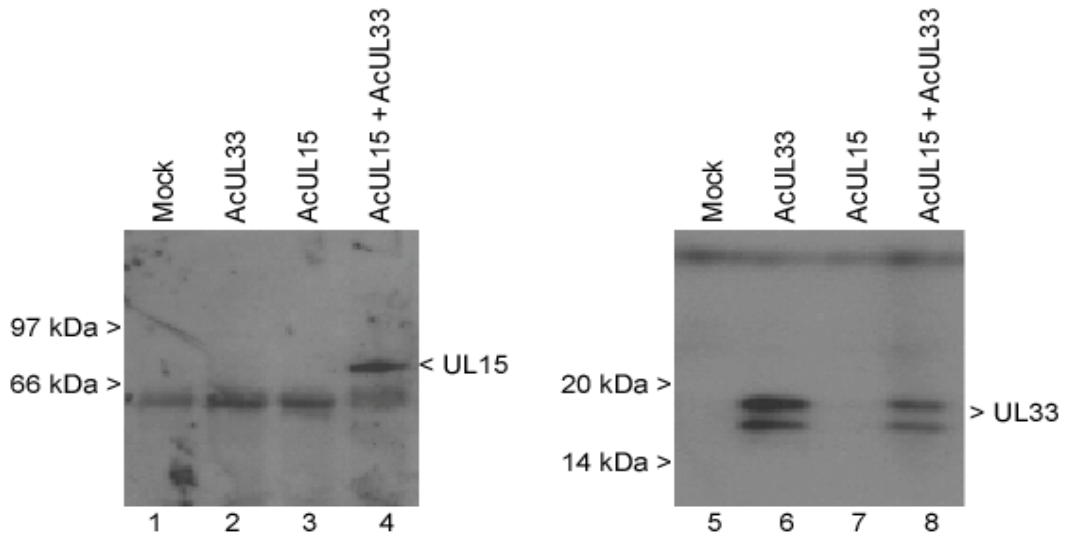
The interaction between UL15 and UL33 was first examined by co-immunoprecipitation of proteins expressed in insect cells by recombinant AcMNPVs under the control of the polyhedrin promoter. Monolayers of *Sf21* cells (approximately 2×10^6 cells) were infected with 5 p.f.u./cell of baculoviruses expressing either UL15 (AcUL15) or UL33 (AcUL33), or both viruses together. Forty-eight hours post-infection cells were harvested and lysed, and insoluble proteins removed by centrifugation (section 2.2.11). Soluble extracts were pre-cleared with a non-specific antibody and protein-A-sepharose, and then incubated with rabbit antibodies specific to UL15 or UL33 (R605 and R148 respectively). Immune complexes were collected by overnight incubation with protein-A-sepharose, followed by centrifugation and extensive washing. The proteins were separated by SDS-PAGE on 8% or 15% gels, transferred to PVDF membranes, and probed with R605 or R148, respectively. Bound antibody was detected using protein-A-HRP and ECL as before, and the results are shown in **Figure 4.1**.

UL15 was not detected in mock-infected cells, nor in cells infected with AcUL33 alone, but was expressed at similar levels in cells receiving AcUL15 alone or in combination with AcUL33 (panel A; lanes 3 and 4). Similarly, UL33 was detected in cells receiving AcUL33 both in the presence and absence of UL15, but not in mock-infected cells nor cells infected solely with AcUL15 (panel A; lanes 5 to 8). This confirmed the suitability of both R148 and R605 for detecting these proteins following expression in insect cells.

A. Extract prior to immunoprecipitation



B. Immunoprecipitation with R148



C. Immunoprecipitation with R605

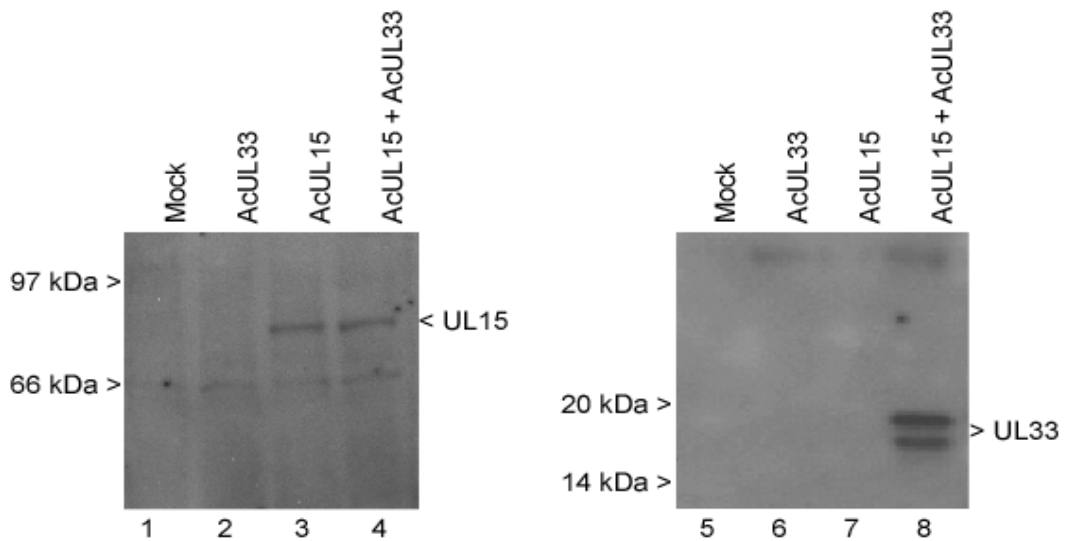


Figure 4.1: Co-immunoprecipitation of UL15 and UL33 from recombinant baculovirus-infected cells.

Sf21 cells were mock-infected or infected with the indicated recombinant baculoviruses. Forty-eight hours post infection, cells were lysed and soluble extracts prepared.

A. Samples of extract prior to immunoprecipitation were separated by SDS-PAGE on 8% (left-hand panel) or 15% (right-hand panel) polyacrylamide gels, proteins transferred to PVDF membranes, and detected with R605 (left-hand panel) or R148 (right-hand panel) respectively.

B. After preclearing with a non-specific rabbit antibody, samples of extract were incubated with R148, the immune complexes precipitated with protein-A sepharose, and the protein species resolved and detected as in A.

C. After preclearing with a non-specific rabbit antibody, samples of extract were incubated with R605 and the immune complexes isolated and analysed as in A.

UL33 was efficiently precipitated from cells infected with AcUL33 by its cognate antibody (panel B; lanes 5-8). Furthermore, UL15 was co-immunoprecipitated from lysates of cells expressing both UL15 and UL33 by R148 (panel B; lane 4), and its precipitation was dependent on the presence of UL33 (panel B; lane 3). Reciprocal precipitations using R605 demonstrated that UL15 was precipitated specifically from AcUL15-infected cells (panel C; lanes 1-4), and that UL33 was specifically co-precipitated from cells receiving AcUL15 and AcUL33 (panel C; lanes 6-8).

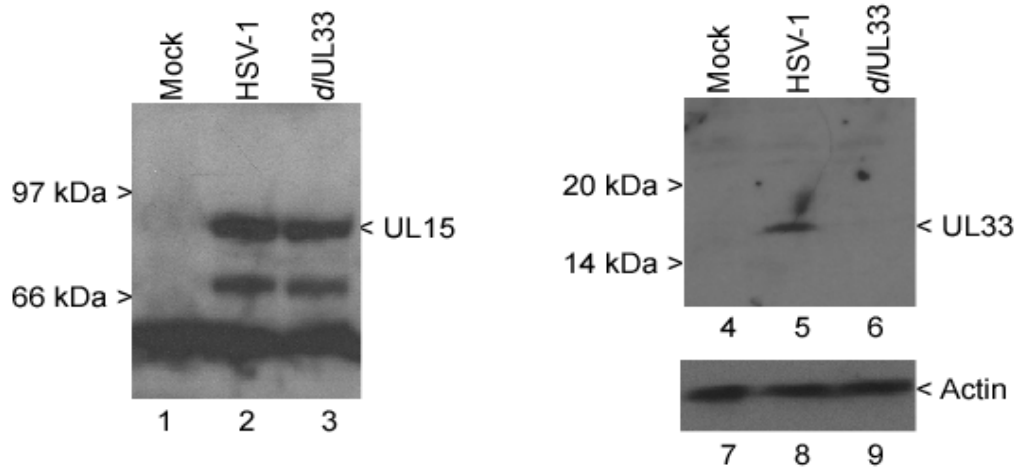
Together, these data support the conclusion that UL15 and UL33 can interact specifically in the absence of other HSV-1 proteins, in agreement with the original findings of Beard and colleagues (2002), but in contrast to later reports (Jacobson *et al.*, 2006).

4.2.2 UL15 and UL33 interact in HSV-1 infected cells

The above experiment indicates that UL33 and UL15 interact when over-expressed under the control of the AcMNPV PH promoter. To extend these findings immunoprecipitation analysis was carried out on HSV-1-infected cells. Approximately 2×10^7 BHK cells were mock-infected, or infected with 5 p.f.u./cell of either HSV-1 or *Δ*UL33. Twenty hours post infection cells were harvested and soluble lysates were prepared and precleared, before being incubated with R148 (section 2.2.11). Immune complexes were collected after overnight incubation with protein-G-sepharose and extensive washing. Western blot analysis of lysates and immune complexes was performed as described for Figure 4.1. The resultant immunoblots are shown in **Figure 4.2**.

In agreement with previous results (Section 3.3), UL33 was undetectable in mock-

A. Extract prior to immunoprecipitation



B. Immunoprecipitation with R148

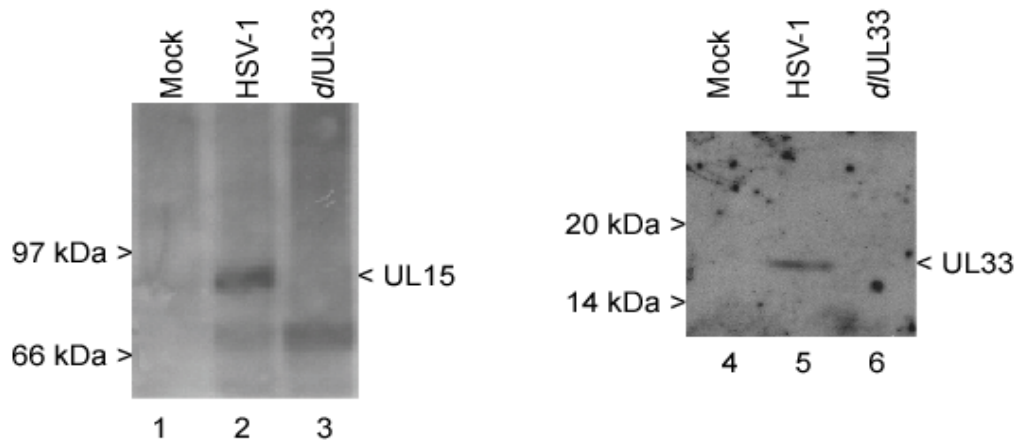


Figure 4.2: Co-immunoprecipitation of UL15 and UL33 from HSV-1-infected cells.

BHK cells were mock-infected or infected with HSV-1 or *d/UL33*. Twenty hours post infection, cells were lysed and soluble extracts prepared.

A. Samples of extract prior to immunoprecipitation were separated by SDS-PAGE on 8% (left-hand panel) or 15% (right-hand panel) polyacrylamide gels, proteins transferred to PVDF membranes, and detected with anti-actin antibody (lanes 7-9), R148 (lanes 4-6) or R605 (lanes 1-3) in conjunction with protein A-HRP.

B. Samples of soluble extract were precleared with a non-specific rabbit antibody and incubated with R148. The immune complexes were precipitated with protein-A sepharose, and the protein species resolved and detected with R605 (lanes 1-3) and R148 (lanes 4-6).

infected cells or in cells infected with the *Δ*UL33 virus, but was detectable in HSV-1-infected cells (panel A; lanes 4-6). UL15 was detected in both HSV-1- and *Δ*UL33-infected cells but not in mock-infected cells, indicating that a lack of UL33 did not affect UL15 expression (panel A; lanes 1-3). Equal amounts of lysate were loaded in all instances (panel A; lanes 7-9). As expected, UL33 was efficiently precipitated by R148 from HSV-1-infected cells, but not from cells infected by *Δ*UL33 (panel B; lanes 4-6). UL15 was co-precipitated with UL33 from HSV-1-infected cells, but not from *Δ*UL33-infected cells, indicating that precipitation of UL15 by R148 requires UL33 (panel B; lanes 1-3).

These data lend further support to the proposal that UL33 and UL15 interact, although the possibility that other cellular or viral factors mediate this interaction cannot be excluded.

4.2.3 Immunofluorescence assay for the interaction of wt UL33 with UL15pp65

To further analyse the ability of UL33 to interact with UL15 in the absence of other HSV-1 proteins, an immunofluorescence assay was utilised. BHK cells were transfected with 1 µg of either pJM19 (expressing a pp65-tagged version of UL15 under the control of the HCMV MIEP; Abbotts *et al.*, 2000) or pUL33, or both plasmids together. The cells were fixed and permeabilised as before (section 3.2.3), and incubated with R148 and a mouse anti-pp65 antibody (section 2.1.12). Bound antibodies were detected using FITC-conjugated anti-rabbit and Cy5-conjugated anti-mouse secondary antibodies. This allowed simultaneous detection of the two proteins within co-transfected cells. The coverslips were examined by confocal microscopy using lasers with excitation lines at 488 nm and 633 nm, corresponding to the

excitation wavelengths of the FITC and Cy5 fluors respectively. The same settings were maintained throughout, with the two channels scanned separately. Images were captured and processed as before, and representative results of two independent experiments are shown in **Figure 4.3**.

In agreement with previous reports (Abbotts *et al.*, 2000; White *et al.*, 2003), pp65-tagged UL15 was localised to the nucleus of transfected cells, but was excluded from nucleoli (panels A-C). In addition, in cells transfected with pJM19 alone, no FITC-specific fluorescence was observed (panel B). As before, in cells receiving pUL33 only, UL33 alone was localised throughout the cell, but excluded from the nucleoli (panel E). No Cy5-specific fluorescence was observed in these cells (panel D). In approximately 20% of cells expressing UL33 alone, UL33 was restricted to the nucleus. In cells receiving pJM19 and pUL33, both proteins were restricted to the nucleus in about 80% of cases (panels G and H), and merging of the channels revealed extensive co-localisation (panel and I). In the remainder of cells expressing both proteins, a small proportion of UL33 was also present in the cytoplasm (data not shown). In agreement with the immunoprecipitation studies, these data further demonstrate that UL15 and UL33 interact in the absence of UL28.

4.2.4 Ability of mutated UL33 proteins to interact with UL15-pp65

To determine whether any of the mutants were compromised in their ability to interact with UL15, a similar experiment was performed. In this case, BHK cells were transfected with plasmids expressing wt or mutated UL33 proteins, together with pJM19. Resultant images of a subset of the mutants are shown in **Figure 4.4**. These are representative of the phenotype exhibited by all of the mutants in this assay.

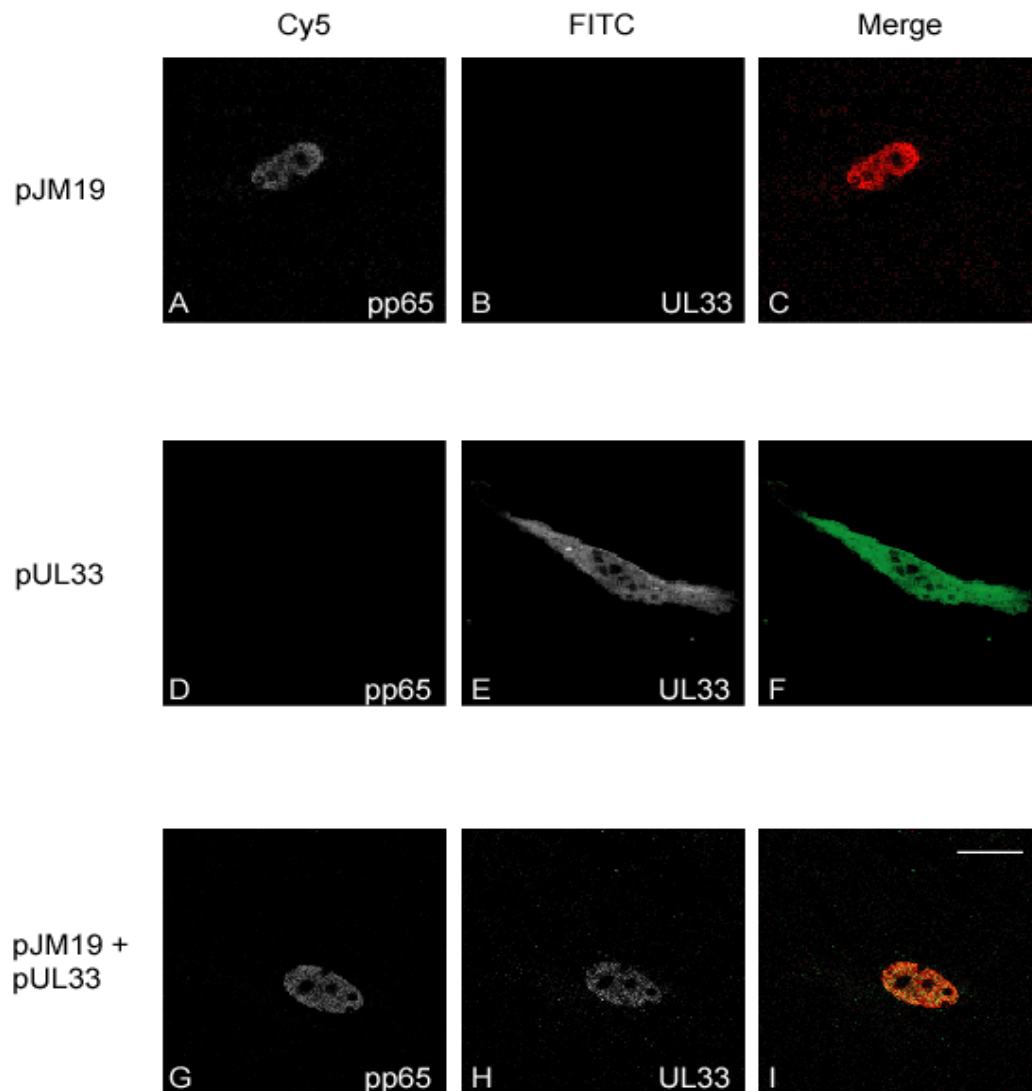


Figure 4.3: Co-localisation of UL15-pp65 and UL33 in transfected cells.

BHK cells were transfected with the indicated plasmids by lipofection. Twenty hours post-transfection, cells were fixed and permeabilised with paraformaldehyde and NP40, and probed with a mouse anti-pp65 antibody and R148. Coverslips were incubated with a Cy5-coupled anti-mouse antibody, and a FITC-coupled anti-rabbit antibody, and processed for confocal microscopy. Identical settings were maintained throughout, with the separate channels shown in grey and a merged image in colour. Scale bar = 20 μ m.

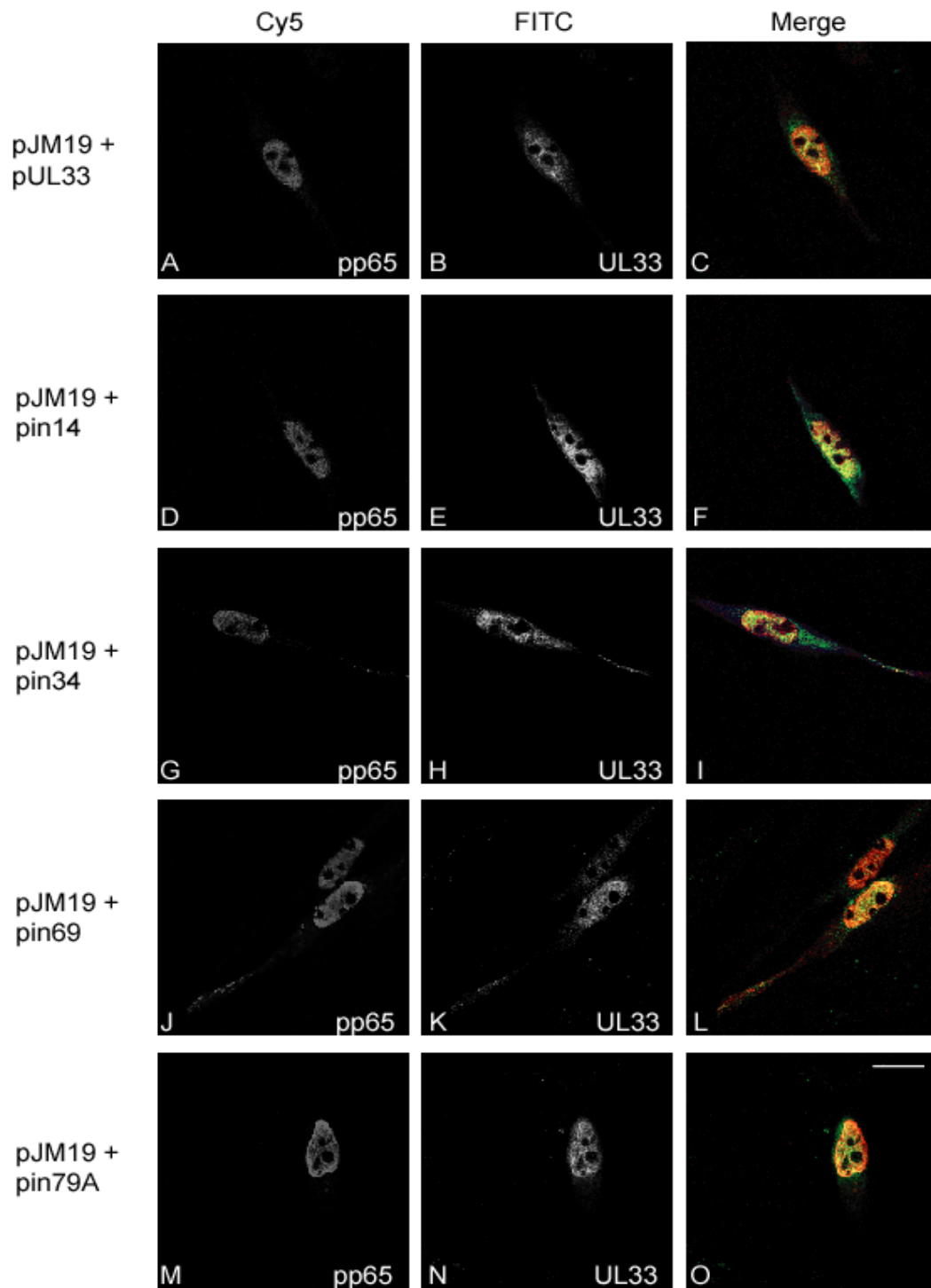


Figure 4.4: Subcellular localisation of UL15-pp65 and mutated UL33 proteins in transfected cells.

BHK cells were transfected with the indicated plasmids by lipofection. Cells were treated as described in the legend to Figure 4.3. Identical settings were maintained throughout, with the separate channels shown in grey and a merged image in colour. The subset of images shown are representative of all the mutants analysed. Scale bar = 20 μ m.

As before, UL15-pp65 alone was restricted to the nucleus of transfected cells (data not shown). Similarly, wt UL33 exhibited both cytoplasmic and nuclear localisation in the absence of UL15 (not shown), but co-localised with UL15-pp65 in the nucleus when the proteins were co-expressed (panels A-C). Each of the 16 mutants displayed a similar phenotype, with UL15 and UL33 co-localising within the nucleus of co-transfected cells (represented by in14, in34, in69 and in79A in panels D-F, G-I, J-L and M-O respectively). As observed with wt UL33, the proportion of cells with mutated UL33 protein restricted to nuclei was increased by the co-expression of UL16-pp65 (20% when expressed alone compared to 80% in the presence of UL15-pp65), although some UL33 was detected in the cytoplasm of a small proportion of cells (represented by in14 and in34 in panels D-F and G-I).

These data suggest that none of the 16 insertions in the UL33 ORF perturb the interaction of the mutated proteins with UL15. A failure of these two proteins to interact therefore cannot account for the inability of any of the mutants to support DNA packaging.

Section 4.3 Interaction of wt and mutated UL33 proteins with UL28

An interaction between UL28 and UL33 was first demonstrated by Beard and co-workers (2002). Recently, studies have suggested that amino acids 604-736 of UL28 are important in mediating this interaction, and that UL28 protects UL33 from proteasomal degradation (Jacobson *et al.*, 2006). To analyse the ability of wt and mutated UL33 proteins to interact with UL28, similar approaches to those detailed in Section 4.2 were used.

4.3.1 UL28 and UL33 interact in recombinant baculovirus-infected cells

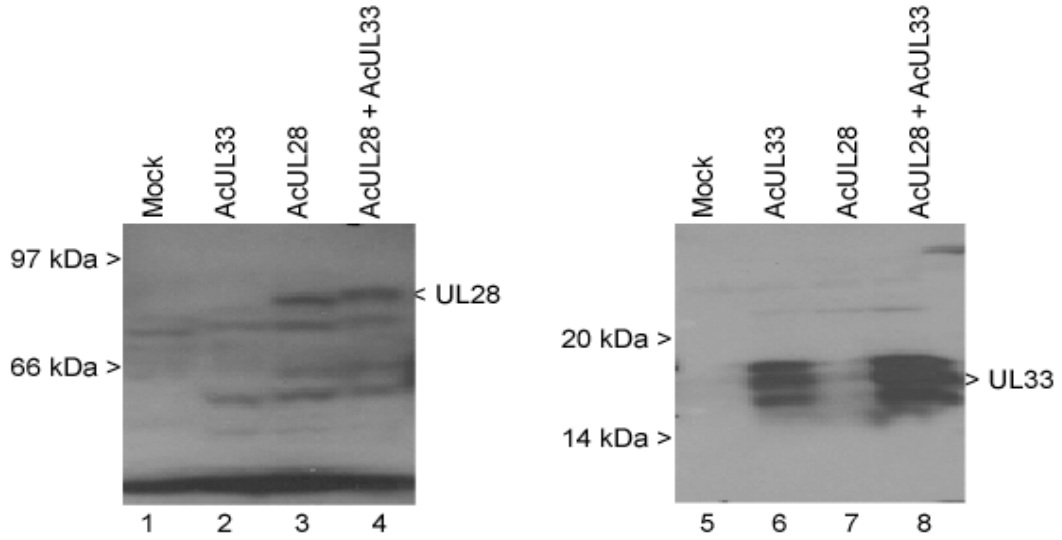
The ability of UL28 and UL33 to interact independently of other HSV-1 proteins was examined using recombinant baculoviruses. Monolayers of *Sf21* cells were infected with 5 p.f.u./cell of either AcUL33 or a recombinant baculovirus expressing UL28 (AcUL28; Abbotts *et al.*, 2000), or both viruses together. Infected cells were harvested forty-eight hours post-infection, and clarified lysates prepared. Duplicate aliquots were pre-cleared as before and incubated with either R148 or a rabbit anti-UL28 antibody, R123 (section 2.1.12; Abbotts *et al.*, 2000). Immune complexes, isolated on protein-A-sepharose, were analysed by western blotting. Membranes were probed with R148 or R123 and bound antibody detected as previously described. The results are shown in **Figure 4.5**.

UL28 was detected in extracts of cells receiving AcUL28, but not from mock-infected cells or those receiving AcUL33 alone (lanes 1-4 of panel A). R123 specifically precipitated UL28 from lysates containing UL28 (panel B, lanes 1-4). Moreover, UL33 was specifically co-precipitated by R123 from cells receiving both AcUL28 and AcUL33 (panel B; lanes 5-8). In reciprocal assays, UL33 was detected in cells infected with AcUL33 (panel A; lanes 5-8), and precipitated from extracts of these cells by R148 (panel C; lanes 5-8). UL28 was efficiently co-precipitated by R148, but only in the presence of UL33 (panel C; lanes 1-4). These data support the previous conclusion that UL28 and UL33 interact in the absence of other viral proteins (Beard *et al.*, 2002).

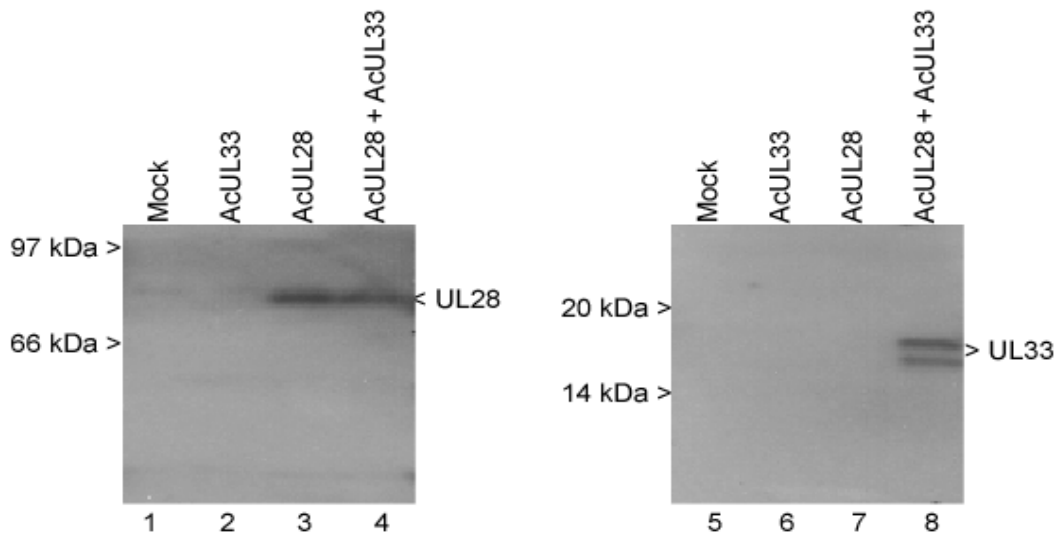
4.3.2 UL28 and UL33 interact in HSV-1-infected cells

The interaction between UL28 and UL33 was also examined in HSV-1-infected cells. An aliquot of clarified lysate described in section 4.2.2 was incubated with R148, and the resulting immune complexes isolated and detected by western blotting using R148

A. Extract prior to immunoprecipitation



B. Immunoprecipitation with R123



C. Immunoprecipitation with R148

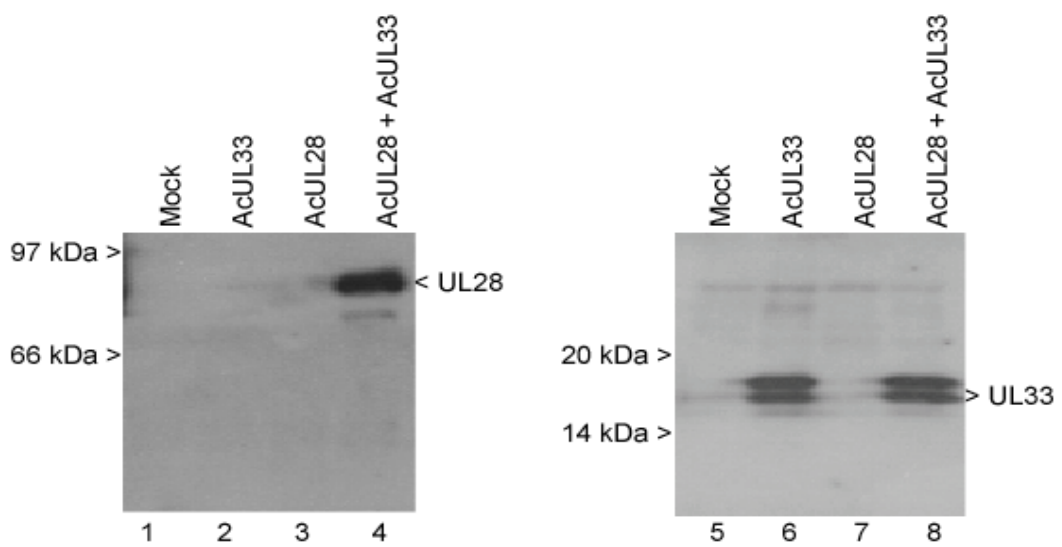


Figure 4.5: Co-immunoprecipitation of UL28 and UL33 from recombinant baculovirus-infected cells.

*Sf*21 cells were mock-infected or infected with the indicated recombinant baculoviruses. Forty-eight hours post infection, cells were lysed and soluble extracts prepared.

A. Samples of extract prior to immunoprecipitation were separated by SDS-PAGE on 8% (left-hand panel) or 15% (right-hand panel) polyacrylamide gels, proteins transferred to PVDF membranes, and probed with R123 (left-hand panel) or R148 (right-hand panel) respectively.

B. After preclearing with a non-specific rabbit antibody, samples of extract were incubated with R123, the immune complexes precipitated with protein-A sepharose, and the protein species resolved and detected as in A.

C. After preclearing with a non-specific rabbit antibody, samples of extract were incubated with R148 and the immune complexes isolated and analysed as in A.

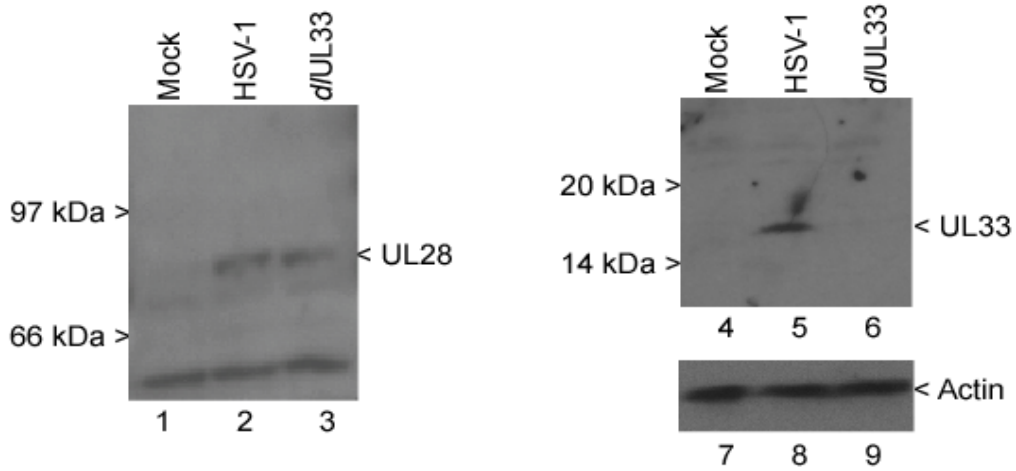
or R123. The results are shown in **Figure 4.6**. Lanes 4-9 of panel A and 4-6 of panel B, showing the UL33 and actin controls, were also presented in Figure 4.2 and discussed in section 4.2.2. Lanes 1-3 of panel A demonstrate that UL28 was absent from mock-infected cells, but detectable in both HSV-1- and *Δ*UL33-infected cells. Moreover, UL28 was co-immunoprecipitated with UL33 from cells infected with HSV-1 by R148, but not from cells receiving *Δ*UL33 (panel B; lanes 1-3). These data confirm previous reports that UL28 and UL33 interact in HSV-1-infected cells (Beard *et al.*, 2002; Jacobson *et al.*, 2006).

4.3.3 Immunofluorescence assay for the interaction of wt UL33 with UL28-cMyc

To examine whether UL28 was able to alter the subcellular localisation of UL33 (or vice versa), BHK cells were transfected with either pUL33 or pUL28-cMyc, or the two plasmids together. pUL28-cMyc encodes a cMyc epitope-tagged version of UL28 under the control of the HCMV MIEP (section 2.1.9; White *et al.*, 2003). The cells were transfected, fixed and permeabilised as before (section 4.2.3), and incubated with R148 and an anti-mouse cMyc-antibody. Bound antibodies were detected using the anti-rabbit FITC and anti-mouse Cy5 conjugates described previously, allowing the simultaneous detection of UL28-cMyc and UL33 in co-transfected cells. Images were captured as before, with the two channels scanned separately, and are shown in **Figure 4.7**.

In the absence of UL33, UL28-cMyc localised to the cytoplasm of transfected cells (panels A and C), in agreement with previous studies (White *et al.*, 2003). No FITC-specific fluorescence was observed in cells receiving pUL28-cMyc alone (panel B). Consistent with previous data, UL33 alone localised throughout cells transfected with

A. Extract prior to immunoprecipitation



B. Immunoprecipitation with R148

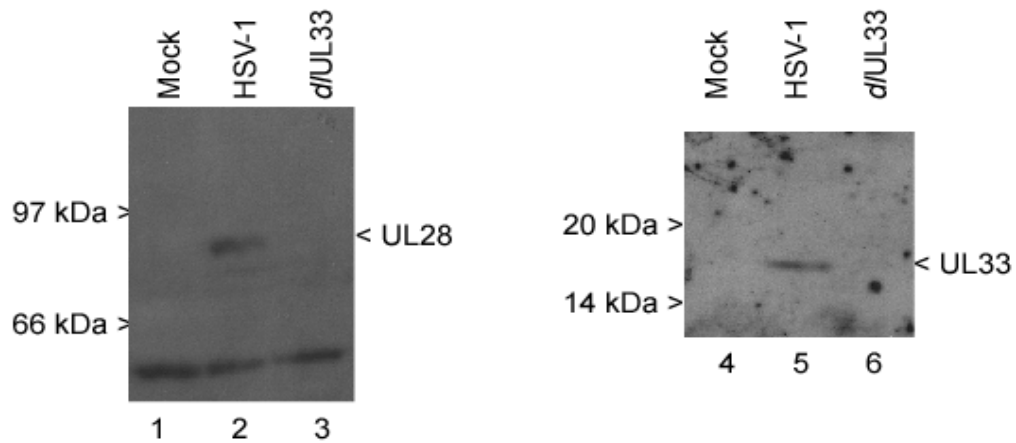


Figure 4.6: Co-immunoprecipitation of UL28 and UL33 from HSV-1 infected cells.

The soluble extracts and immunoprecipitates from mock-infected, HSV-1-infected and *d*UL33-infected BHK cells described in Figure 4.2 were used.

A. Samples of extract prior to immunoprecipitation were separated by SDS-PAGE on an 8% polyacrylamide gel, proteins transferred to a PVDF membrane, and detected with R123 (lanes 1-3). Note that the UL33 and actin controls (lanes 4-6 and 7-9 respectively) are the same as shown in Figure 4.2.

B. Samples of the immune complexes precipitated by R148 (Figure 4.2) were resolved on an 8% polyacrylamide gel, and the protein species resolved and detected with R123 (lanes 1-3). Note that the UL33 control (lanes 4-6) is identical to that shown in Figure 4.2.



pUL33, but was predominantly present in the nuclei (panels E and F). No Cy5-specific signal was observed in this population of cells (panel D). In cells co-expressing UL33 and UL28-cMyc, both proteins were confined to the cytoplasm, where they largely co-localised. This indicates that UL28 alters the localisation of UL33 and suggests that the two proteins interact.

However, an alternative explanation might be that UL28-cMyc non-specifically inhibits the nuclear uptake of proteins, thereby indirectly restricting UL33 to the cytoplasm. Therefore, the effect of UL28-cMyc on the localisation of the HSV-1 origin-binding protein, UL9, which is normally efficiently translocated to the nucleus when expressed alone (Malik *et al.*, 1996), was examined. BHK cells were transfected with either pUL28-cMyc or pE9 (expressing UL9 under the control of the HCMV MIEP; Stow *et al.*, 1993), or both plasmids together. The cells were fixed and permeabilised as previously described, and probed with a mouse anti-UL9 antibody (M13924; Stow *et al.*, 1998) and a rabbit anti-UL28 antibody (R123). Bound antibody was detected with FITC-conjugated anti-rabbit and Cy5-conjugated anti-mouse secondary antibodies. Images were taken and processed as described above, and are shown in **Figure 4.8**.

UL28-cMyc localised solely to the cytoplasm when expressed alone or with UL9 (panels E and H). In contrast, UL9 was present solely in the nucleus both when expressed alone or in conjunction with UL28-cMyc (panels A and G). Therefore, UL28-cMyc does not non-specifically inhibit entry of proteins into the nucleus. The co-localisation observed between UL28-cMyc and UL33 in Figure 4.7 is therefore likely to represent a specific interaction between the two proteins.

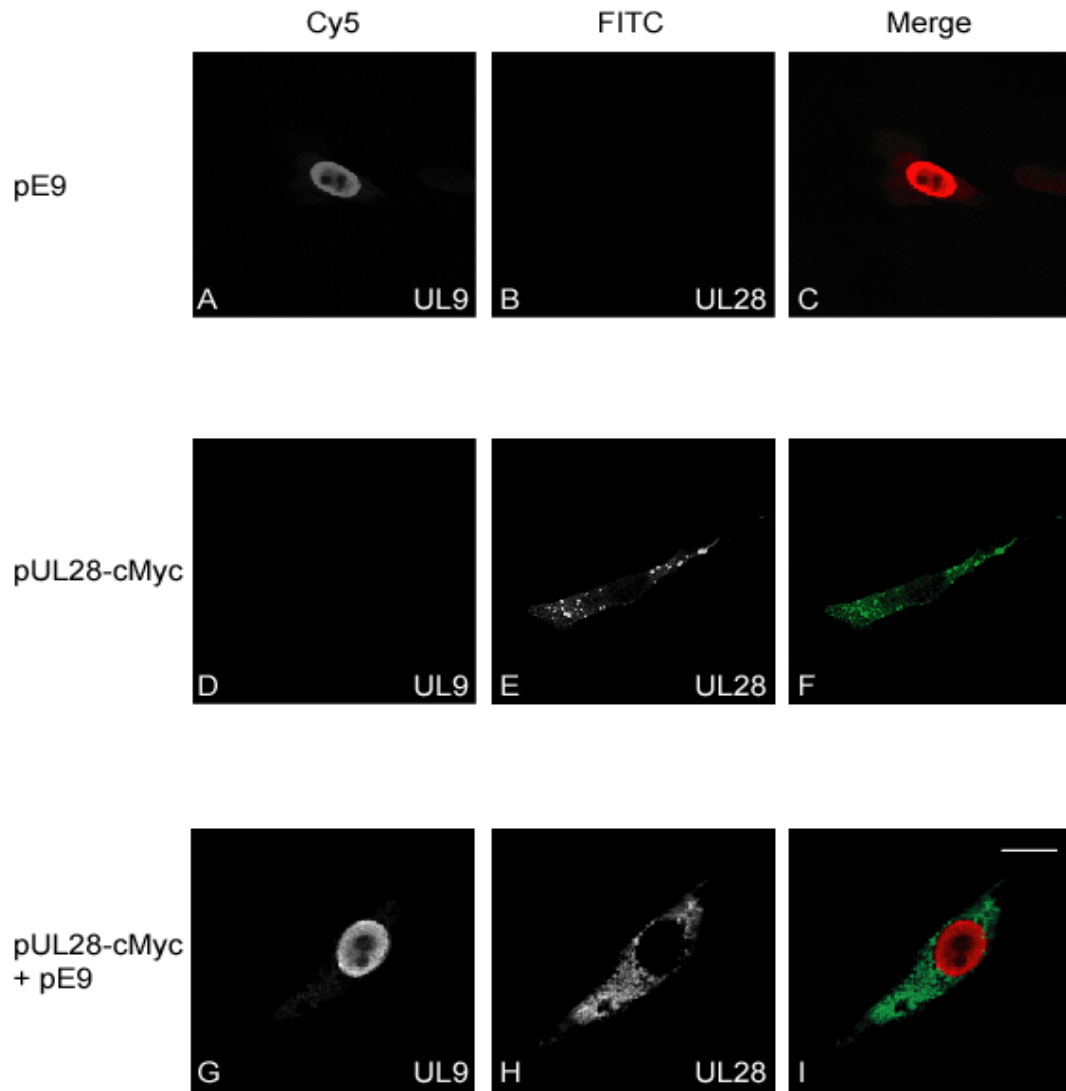


Figure 4.8: Intracellular distribution of UL28-cMyc and UL9 in transfected cells.

BHK cells were transfected with the indicated plasmid(s) by lipofection. Twenty hours post-transfection, cells were fixed and permeabilised as described (Figure 4.3), and probed with rabbit anti-UL28 (R123) and mouse anti-UL9 (M13924) antibodies. Coverslips were incubated with Cy5-coupled anti-mouse and FITC-coupled anti-rabbit antibodies, and processed for confocal microscopy. Identical settings were maintained throughout, with individual channels shown in grey and a merged image in colour. Scale bar = 20µm

4.3.4 Ability of mutated UL33 proteins to interact with UL28-cMyc

To examine the ability of UL33 insertion mutants to interact with UL28-cMyc, a similar experiment was performed. In this case, cells were transfected with plasmids expressing wild type or mutated UL33 proteins together with pUL28-cMyc. The cells were fixed, permeabilised and processed as before, and images captured as previously described. Confocal microscopy revealed that the mutants displayed two distinct phenotypes, summarised in **Table 4.1**. A subset of images representative of these phenotypes is shown in **Figure 4.9**.

Controls with UL28-cMyc or wt UL33 alone were in agreement with previous experiments i.e. UL28-cMyc exhibited a cytoplasmic distribution, whereas UL33 was localised throughout the cells (data not shown). When co-expressed, the proteins again co-localised within the cytoplasm (panels A-C). The majority of the UL33 mutants exhibited a phenotype similar to wt UL33 (represented by in14 and in79A shown in panels D-F and M-O respectively). However, four of the mutants, in34, in37, in69 and in84, displayed a distinctive phenotype in which UL28-cMyc was localised in the cytoplasm, but UL33 was mainly within the nucleus of co-transfected cells (represented by in34 and in69 in panels G-I and J-L). Notably, UL28-cMyc was unable to restrict UL33 to the cytoplasm and relatively little colocalisation was apparent in the merged images, indicating that the interaction between these proteins had been perturbed.

These data therefore suggested that insertions at amino acids 34, 36, 69 and 83 disrupted the ability of UL33 to bind UL28. Surprisingly, three of the four mutants



Mutant	Ability to support DNA packaging and viral growth	Ability to co-localise with UL28-cMyc
UL33	+	+
in14	-	+
in34*	+	-
in37*	+	-
in44	+	+
in51	-	+
in55	-	+
in69	-	-
in74	-	+
in79A	+	+
in79B	+	+
in84*	+	-
in100	+	+
in104	-	+
in111A	-	+
in111B	-	+
in116	-	+

Table 4.1: Ability of UL33 mutants to interact with UL28-cMyc in an immunofluorescence assay. The ability of mutants to co-localise with UL28-cMyc is displayed, together with their ability to support DNA packaging and mutant virus growth. Mutants unable to co-localise with UL28-cMyc are indicated in bold, with those able to support DNA packaging denoted by an *.

unable to interact with UL28 in this assay were fully able to support DNA packaging and growth of mutant viruses lacking UL33, suggesting that interaction between UL28 and UL33 may not be necessary for DNA packaging to occur (Table 4.1).

Furthermore, several mutants retaining the ability to co-localise with UL28 were unable to support DNA packaging.

4.3.5 Creation of recombinant baculoviruses expressing mutated UL33 proteins

To examine further the ability of UL33 insertion mutants to interact with UL28, recombinant baculoviruses were generated expressing individual mutated UL33 proteins under the control of the AcMNPV polyhedrin promoter. The recombinant viruses were created using the Invitrogen Bac-to-Bac system (section 2.2.6) (**Figure 4.10**). Briefly, this system allows insertion of the gene of interest into a mini-*att*Tn7 site within a cloned AcMNPV genome (Bacmid), via Tn7-mediated transposition. After transposition has been confirmed, transfection of recombinant Bacmid DNA into insect cells generates recombinant baculovirus progeny bearing the foreign gene.

To introduce the mutated UL33 genes into the transfer plasmid pFastBac1, UL33-containing fragments were liberated from mutated plasmids by digestion with *Bam*HI as previously described (section 3.2.1). Concurrently, pFastBac1 was digested with *Bam*HI, linearised DNA was purified and dephosphorylated with CIP. Ligation of the UL33-containing *Bam*HI fragment into pFastBac1 gave rise to colonies containing plasmids with the gene of interest under the control of the AcMNPV polyhedrin promoter, between the two arms of the Tn7 transposon. The presence and orientation of the UL33 fragment was confirmed by digestion of plasmid DNA with *Xba*I (results not shown).

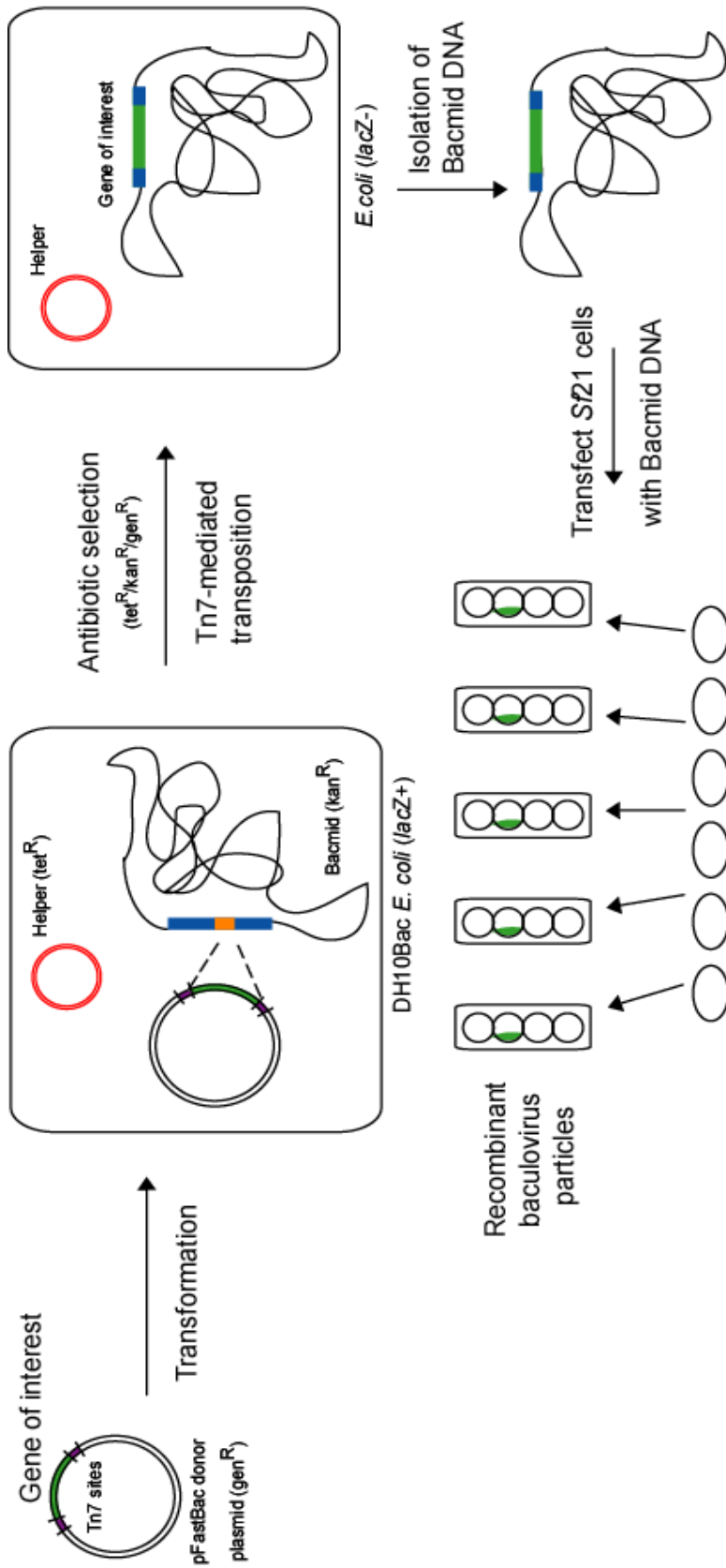


Figure 4.10: Principles of the Bac-to-Bac Baculovirus Expression system.

The gene of interest (green) is first cloned into a pFastbac transfer vector, downstream of the AcMNPV polyhedrin promoter. The expression cassette is flanked by the left and right arms of Tn7 (purple). DH10Bac *E. coli* contain the AcMNPV genome cloned as a bacterial artificial chromosome (Bacmid) encoding the *lacZ* gene (blue), into which the Tn7 attachment site (orange) has been inserted. A helper plasmid (red) provides the Tn7 transposition function *in trans*. Transformation of the donor plasmid into DH10Bac cells allows transposition of the gene of interest into the *lacZ* gene of the Bacmid. Colonies displaying gen^R, tet^R, kan^R, and exhibiting a lacZ- phenotype in the presence of X-gal are identified, and the recombinant Bacmid DNA isolated. Transfection of this DNA into insect cells results in the production of recombinant baculovirus particles expressing the gene of interest under the control of the polyhedrin promoter.

To facilitate recombination of the mutated genes into Bacmids, the pFastbac derivatives were transformed into electrocompetent DH10Bac *E. coli*. The transformants were selected for kan^R, gen^R and tet^R to confirm the presence of the Bacmid, pFastBac1 and helper plasmids respectively. As transposition of the gene of interest into the mini-*attTn7* site of the Bacmid disrupts expression of β -galactosidase from the *lacZ* gene, transformants were also screened for their inability to express functional β -galactosidase on media containing X-gal. To verify the phenotype of the recombinant Bacmids, two rounds of screening were used. The resultant Bacmid DNA was isolated using a modified alkaline lysis procedure (section 2.2.6.1).

PCR analysis confirmed the presence of mutated UL33 genes within the recombinant Bacmids (not shown). PCR products of 2600 bp, indicating successful transposition of the UL33 gene into the mini-*attTn7* site, were obtained for all of the recombinant Bacmids using the flanking M13 (-40) forward and reverse primers. To generate recombinant baculoviruses, Bacmid DNA was transfected into monolayers of *Sf21* cells by lipofection (section 2.2.6.2). After the onset of cell lysis (approximately 72 hours post-transfection) progeny virus was collected and subsequently amplified to generate high titre stocks. The recombinant baculoviruses were designated Acin13 to Acin117 in accordance with the mutated UL33 protein expressed.

4.3.6 Ability of mutated UL33 proteins to interact with UL28 in insect cells

To extend the findings of the previous fluorescence studies (section 4.3.4), the ability of mutated proteins to interact with UL28 was analysed in baculovirus-infected insect cells. *Sf21* monolayers were infected with 5 p.f.u./cell of baculoviruses expressing wild type or mutated UL33 proteins, together with 5 p.f.u./cell AcUL28. Forty-eight hours

post-infection, clarified lysates were prepared, precleared, and incubated with R148. Immune complexes were collected after overnight incubation with protein-A-sepharose as before. The isolated proteins were analysed by western blotting (**Figure 4.11**). Due to time constraints, only one experiment was performed.

In all cases except mock-infected cells or those receiving AcUL28 alone, UL33 proteins were precipitated effectively by R148 (lanes 3-20). Only a single protein species was precipitated by R148 from cells expressing mutated UL33 proteins (lanes 5-20), in contrast to the doublet precipitated from cells expressing wt UL33 (lanes 3 and 4). The single species co-migrated with the smaller of the two protein species expressed by AcUL33. It is possible that wt UL33 may be subject to post-translational modifications not undergone by the mutated proteins, although this seems unlikely. It is also conceivable that AcUL33 contains a mixture of two viruses, one containing an insertion in the UL33 gene, which gives rise to the larger UL33 polypeptide observed. A third possibility is that the UL33 gene of AcUL33 might encode alternative transcriptional termination sites, preventing efficient termination of transcription.

Furthermore, in every instance in which UL28 and wt or mutated UL33 were co-expressed, both proteins were co-precipitated by R148 (lanes 4-20 & 24-40). These preliminary results suggest that none of the insertion mutants are impaired in their ability to interact with UL28, in contrast to the results obtained in immunofluorescence assays.

Section 4.4 Characterisation of UL33 internal deletion mutants

As previously described, immunofluorescence studies suggested that insertions at

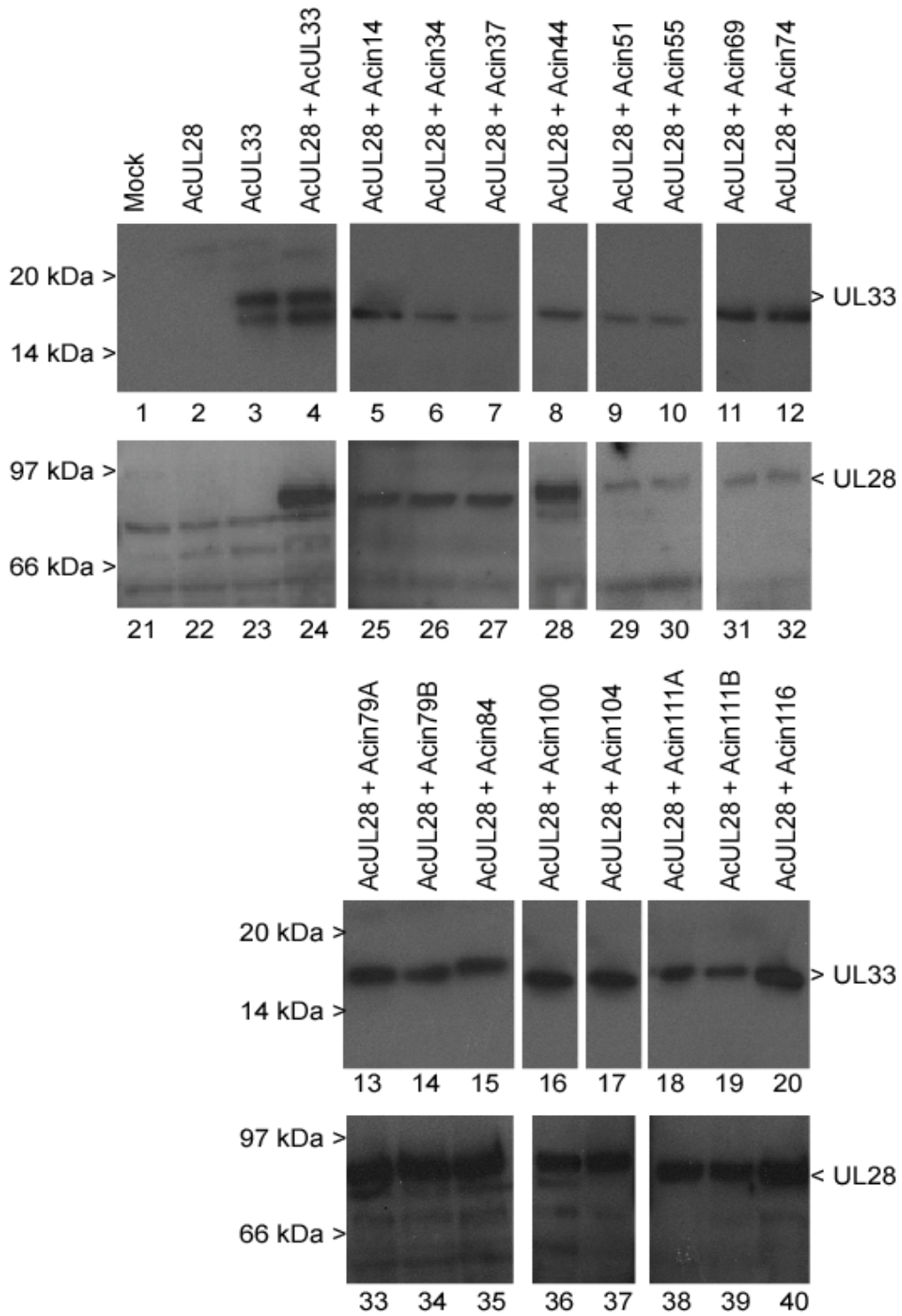


Fig 4.11: Interaction of mutated UL33 proteins with UL28 in recombinant baculovirus-infected cells

*Sf*21 cells were infected with the indicated baculoviruses, and soluble extracts prepared. Lysates were incubated with R148, and immune complexes collected and analysed by western blotting. Membranes were probed with R148 and R123, and the positions of UL28 and UL33 are indicated.

positions 34, 36, 68 and 83 rendered UL33 unable to interact with UL28-cMyc.

Although this conflicted with data from co-immunoprecipitation studies, two further mutants were created to further investigate the role of these regions in UL28 binding.

In plasmid p Δ 1 amino acids Val³⁵, Ser³⁶ and Arg³⁷ of UL33 are replaced by the sequence CGRTR. This plasmid was constructed by ligating the N-terminal *Eco*RI plus *No*I fragment of pin34 and the C-terminal *Hind*III plus *No*I fragment of pin37 into *Eco*RI-*Hind*III cleaved pCMV10.

Plasmid p Δ 2 was similarly created by joining the N-terminal *No*I/*Eco*RI fragment from pin84 to the C-terminal *No*I/*Hind*III fragment of pin100. In this plasmid amino acids 85-100 of UL33 are replaced by the sequence MRPHA. The identities of the plasmids were confirmed by DNA sequencing and the resulting changes to the UL33 protein are shown in **Figure 4.12**.

4.4.1 Ability of Δ 1 and Δ 2 to support DNA packaging and mutant virus growth

The ability of Δ 1 and Δ 2 to support DNA packaging was examined using an amplicon packaging assay (section 3.4.3). BHK cells were transfected with pSA1, together with either pCMV10 or plasmids expressing wt or mutated UL33 proteins. The cells were super-infected with 5 p.f.u./cell of either HSV-1 or *d*UL33. After eighteen hours, total and packaged DNA was prepared as previously described and analysed by agarose gel electrophoresis and Southern blotting. Replicated and packaged pSA1 was detected by hybridisation to ³²P-labelled pAT153, and the resultant phosphorimage is shown in panel A of **Figure 4.13**.

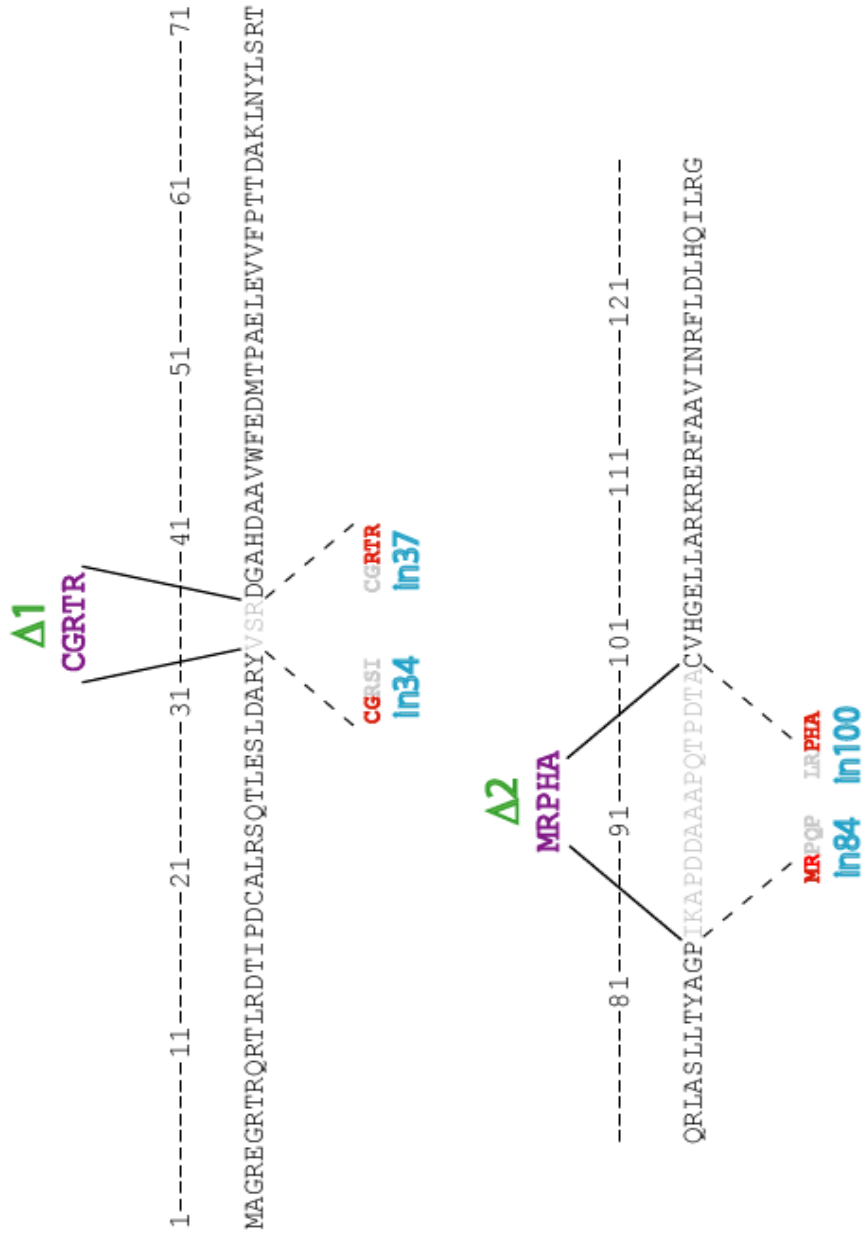


Fig 4.12: Sequences of proteins encoded by pΔ1 and pΔ2

The creation of pΔ1 and pΔ2 is detailed in the text. Inserted amino acids are denoted in purple, and originate from amino acids encoded by in34 and in37 (pΔ1) and in84 and in100 (pΔ2) [indicated in red]. Deleted amino acids are indicated in grey. It should be noted that in34, in37, in84 and in100 are able to support mutant virus growth and DNA packaging.

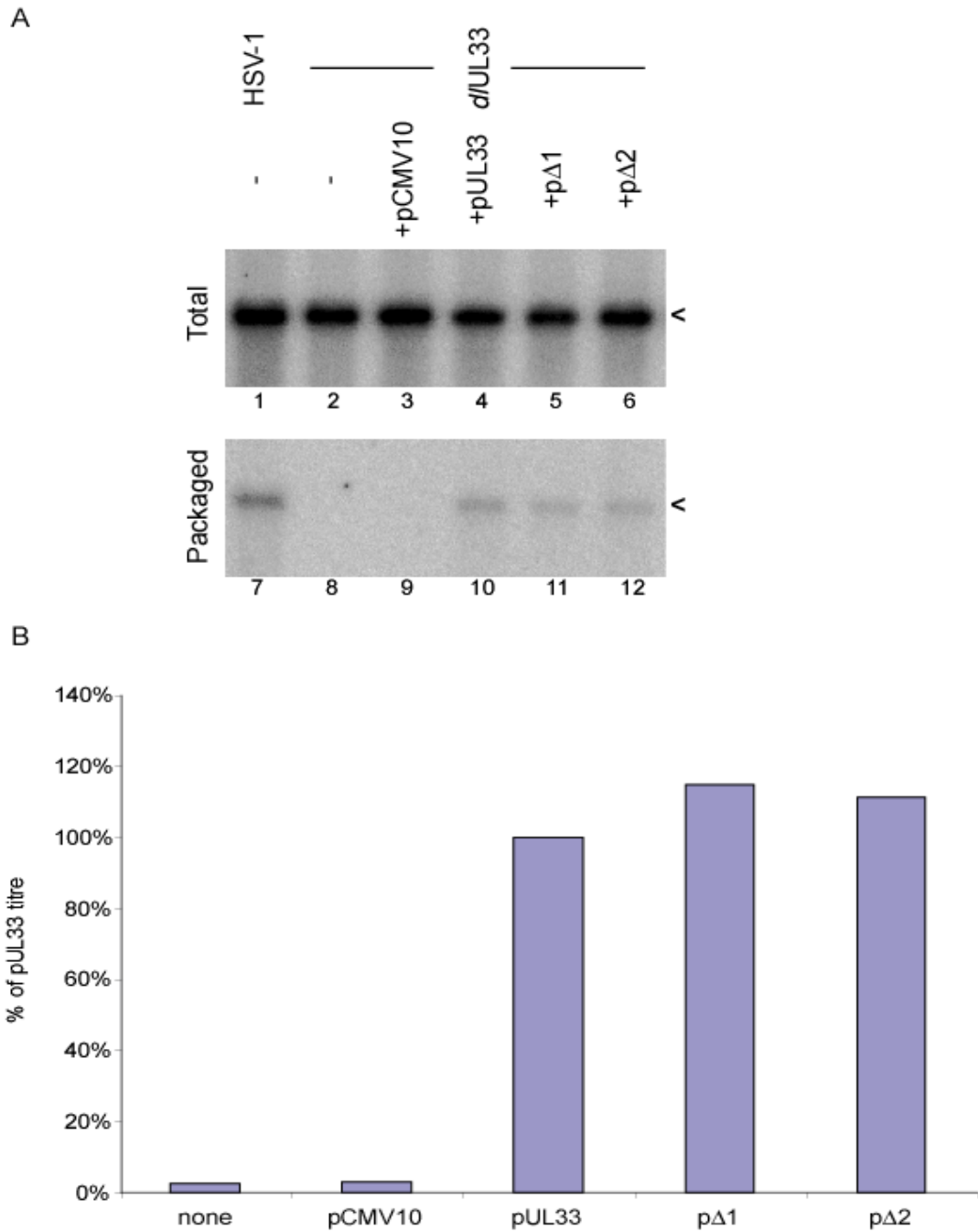


Fig. 4.13: Ability of UL33 internal deletion mutants to support DNA packaging and *d*UL33 growth

A. BHK cells were transfected with the indicated plasmids together with pSA1, and super-infected with either HSV-1 or *d*UL33 as described in the legend to Fig 3.17. Total and packaged DNA were prepared and analysed as previously described. The position of linear pSA1 molecules is denoted by "<". **B.** Cells were transfected and super-infected as above. Progeny virus was harvested and titrated on 20A cells (see Fig 3.12 for details). Titres are expressed as a percentage of that obtained with pUL33.

pSA1 was replicated to a similar degree in all instances (lanes 1-6 of panel A), and was efficiently packaged by HSV-1 (lane 7). In agreement with previous data, *d*UL33 was unable to package DNA (lane 8). This defect was not restored by the supply of empty vector *in trans* (lane 9). In contrast, pUL33, p Δ 1 and p Δ 2 supported amplicon packaging to similar extents (lanes 10-12).

Simultaneously, the ability of Δ 1 and Δ 2 to support mutant virus growth was assessed using a complementation yield assay (section 3.3.2). The cells were transfected and super-infected as outlined above. One hour after super-infection, residual virus was neutralised as described previously, and cells incubated at 37 °C. After eighteen hours, progeny virus was harvested and titrated on 20A cells. Panel B of **Figure 4.13** shows the yields obtained expressed as a percentage of the titre obtained with pUL33, and indicated that both Δ 1 and Δ 2 could also complement growth of *d*UL33.

UL33 expression in replicate plates was analysed by western blotting (**Figure 4.14**). As expected, UL33 was detected in cells infected with HSV-1, but not *d*UL33 in the presence or absence of pCMV10 (lanes 1-3). Both p Δ 1 and p Δ 2 expressed polypeptides that were recognised by R148, although the mobility of the Δ 2 protein was increased relative to wt UL33 (lanes 4-6). This change in mobility is consistent with the p Δ 2 product being approximately 8% shorter than wt UL33.

4.4.2 Immunofluorescence assay for the interaction of Δ 1 and Δ 2 with UL15-pp65

To examine the ability of the UL33 proteins to interact with UL15, BHK cells were transfected with pUL33, p Δ 1 or p Δ 2 in the presence or absence of pJM19. The cells

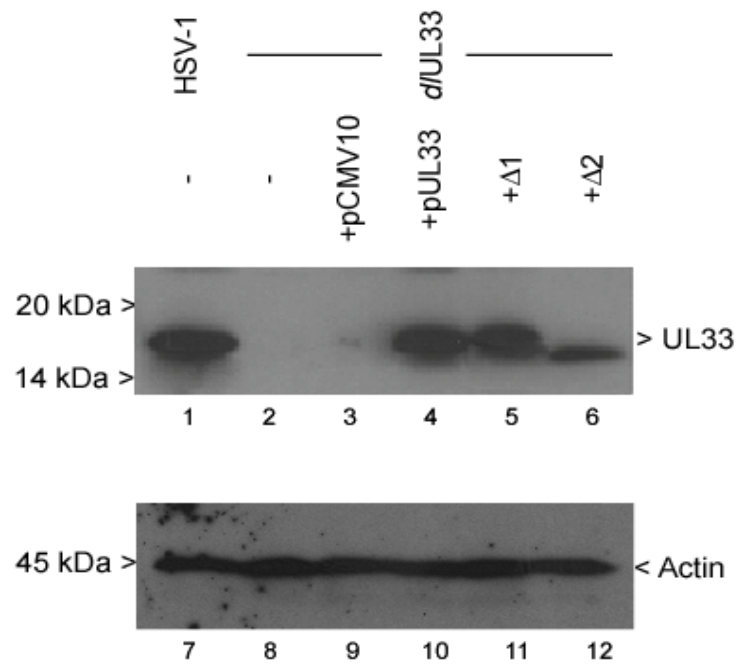


Fig. 4.14: Expression of UL33 internal deletion mutants

Cells were transfected with the indicated plasmids, and super-infected as described in the legend to Figure 4.13. Twenty hours post-transfection, cell lysates were prepared and the proteins analysed by western blotting. Membranes were incubated with R148 and anti-actin antibodies, and bound antibody detected using protein-A-HRP and ECL as previously described (Figure 3.7).

were fixed, permeabilised and processed as described previously (section 4.2.3), and the resultant images are shown in **Figure 4.15**.

UL33 expressed alone from p Δ 1 and p Δ 2 showed a similar localisation to wt UL33 (panels A-C and D-F respectively). Similarly, UL15-pp65 alone was localised in the nucleus as observed before (not shown). UL33 and UL15-pp65 were again co-localised within the nuclei of co-transfected cells (panels G-I). Δ 1 exhibited a similar phenotype to wt UL33, and co-localised with UL15-pp65 in the nucleus (panels J-L). However, Δ 2 behaved differently, with both UL15-pp65 and UL33 being restricted to, and co-localised within, the cytoplasm of co-transfected cells (panels M-O). These data suggested that deletion of a portion of UL33 did not affect interaction with UL15-pp65, but inhibited nuclear import of the resulting complex.

To exclude the possibility that the Δ 2 protein non-specifically inhibited the nuclear import of proteins, the effects of Δ 1 and Δ 2 on UL9 localisation were examined. BHK cells were transfected with p Δ 1 or p Δ 2 and pE9, and fixed or permeabilised as before. The coverslips were incubated with R148 and M13924, and bound antibody detected using anti-rabbit FITC and anti-mouse Cy5 conjugates. Confocal microscopy was carried out as described in section 4.2.3, and the resultant images can be seen in **Figure 4.16**.

In cells co-expressing UL9 and either Δ 1 or Δ 2, UL33 was localised throughout the transfected cells (panels B and E), and UL9 was confined the nucleus (panels A, C, D and F). These data therefore indicate that Δ 2 does not inhibit nuclear import of UL9, and suggest that the observed cytoplasmic co-localisation of Δ 2 and UL15-pp65 is due

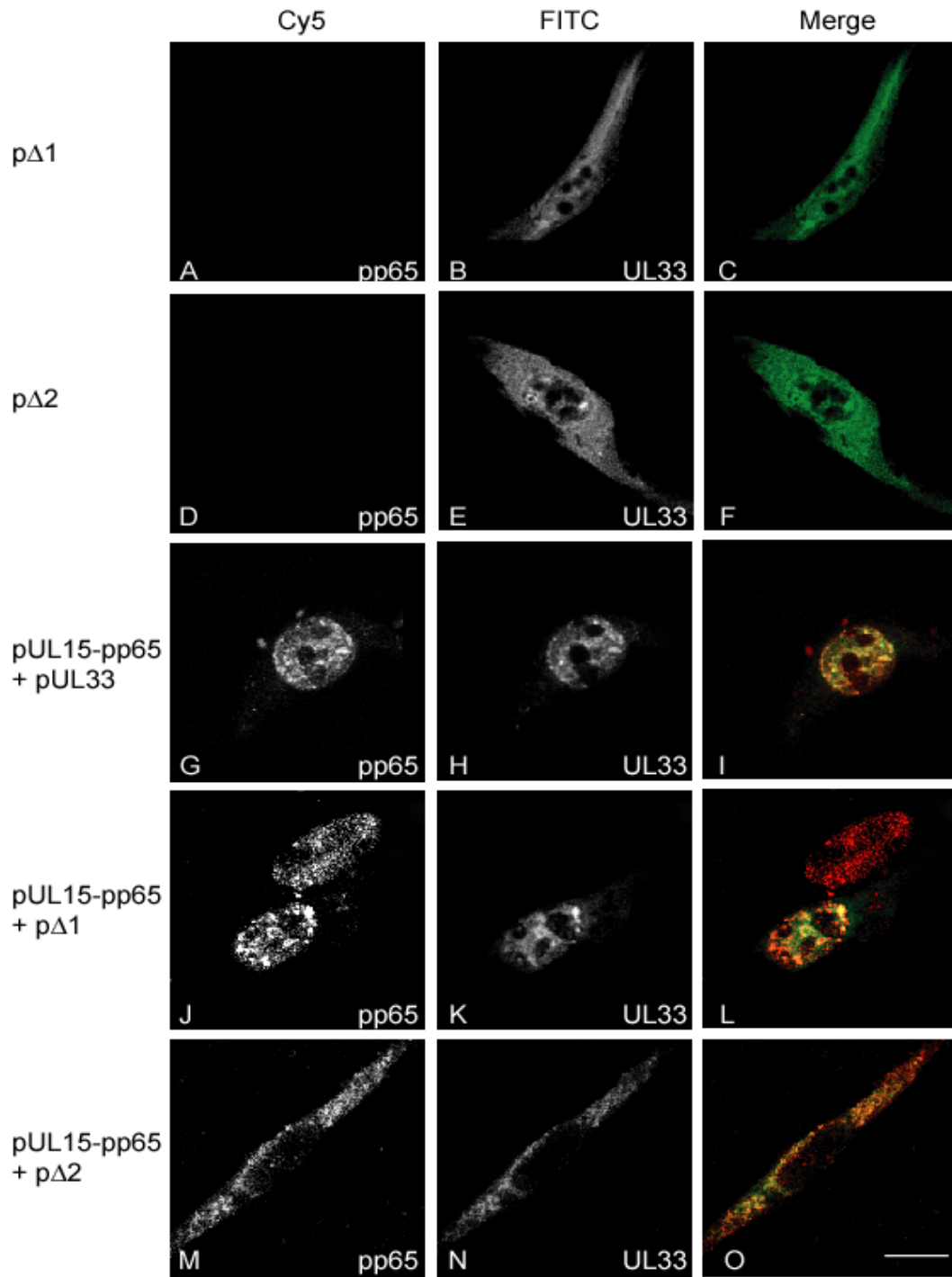


Figure 4.15: Ability of UL33 internal deletion mutants to interact with UL15-pp65.

BHK cells were transfected with the indicated plasmids by lipofection. Twenty hours post-transfection, cells were fixed, permeabilised and analysed by confocal microscopy as previously described (Figure 4.3). Identical settings were maintained throughout, with individual channels shown in grey and a merged image in colour. Scale bar = 20µm.

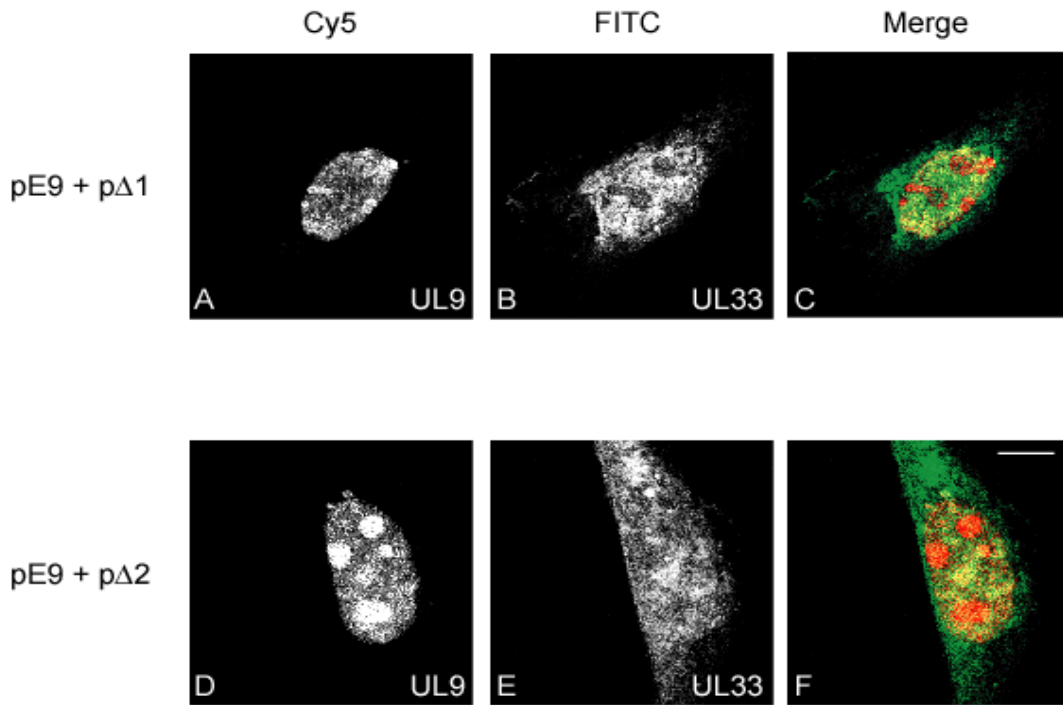


Figure 4.16: Subcellular distribution of internal UL33 deletion mutants and UL9 in transfected cells.

BHK cells were transfected with the indicated plasmids by lipofection. Twenty hours post-transfection, cells were fixed and permeabilised as described (Figure 4.8) and probed with R148 and M13924. Coverslips were incubated with Cy5-coupled anti-mouse and FITC-coupled anti-rabbit antibodies, and processed for confocal microscopy. Identical settings were maintained throughout, with individual channels shown in grey and a merged image in colour. Scale bar = 10 μ m.

to a specific interaction.

4.4.3 Immunofluorescence assay for the interaction of $\Delta 1$ and $\Delta 2$ with UL28-cMyc

In similar experiments, $\Delta 1$ and $\Delta 2$ were screened for their ability to interact with UL28-cMyc. BHK cells were transfected with pUL28-cMyc, together with pUL33, p $\Delta 1$ or p $\Delta 2$. The cells were fixed and permeabilised as before, and processed exactly as described in section 4.3.3. Settings were maintained throughout, and representative images are shown in **Figure 4.17**.

As observed previously, UL28-cMyc and UL33 co-localised in the cytoplasm of co-transfected cells, and UL33 was absent from the nucleus (panels A-C). A similar phenotype was observed in cells expressing $\Delta 2$ and UL28-cMyc, with the proteins co-localising in the cytoplasm (panels G-I). In contrast, in cells co-expressing UL28-cMyc and $\Delta 1$, UL33 was present throughout the cell (panel E), whilst UL28-cMyc was found exclusively in the cytoplasm (panels D and F). This suggests that UL28-cMyc is unable to confine $\Delta 1$ to the cytoplasm, and that $\Delta 1$ is altered in its ability to interact with UL28-cMyc.

Together with previous results (Figure 4.9), these data indicate that perturbation of the region surrounding residues 34-37 affects the ability of UL33 to interact with UL28. However, replacement of the region spanning residues 84-100 with five amino acids did not affect the ability of UL33 to interact with UL28, even though in84 was affected.

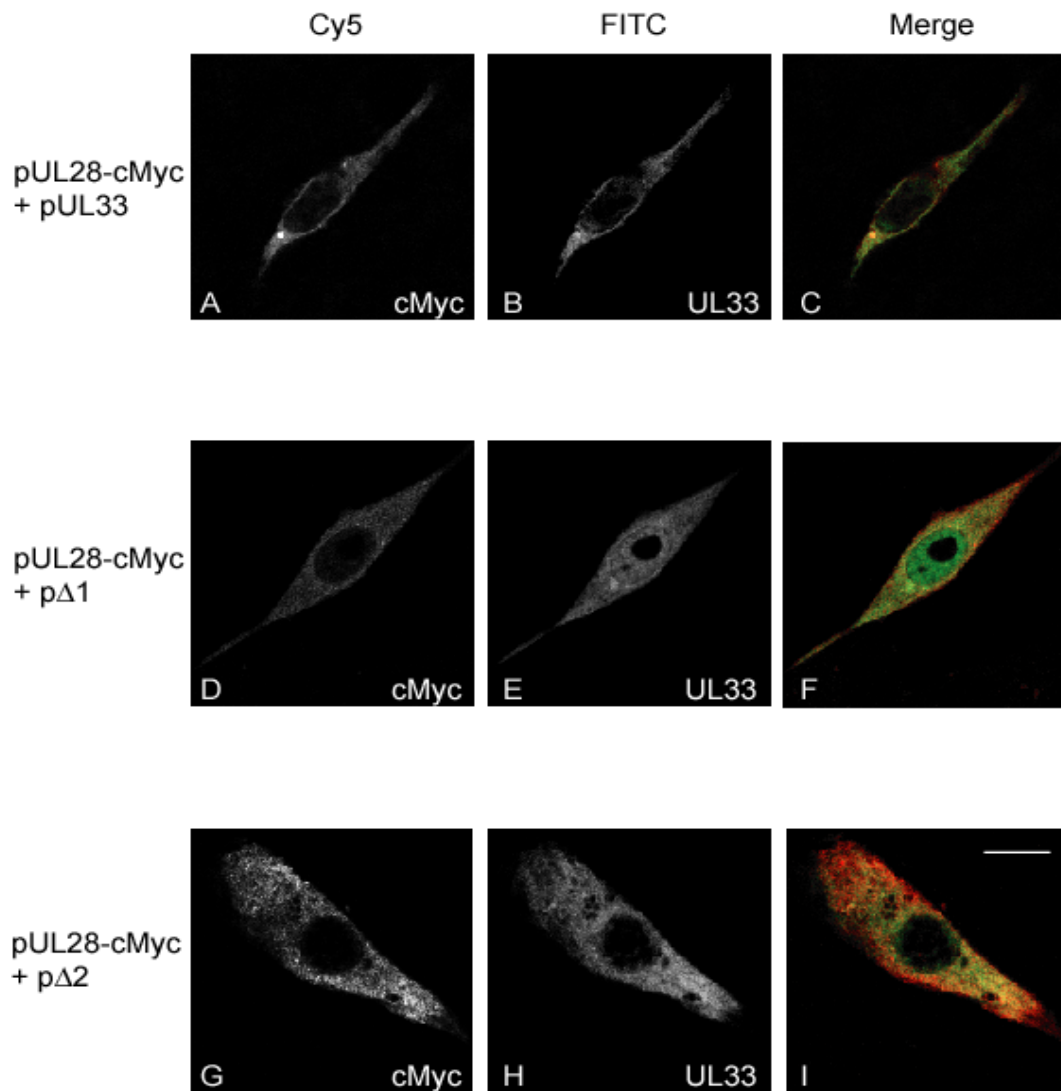


Figure 4.17: Ability of UL33 internal deletion mutants to interact with UL28-cMyc.

BHK cells were transfected with the indicated plasmids by lipofection. Twenty hours post-transfection, cells were fixed, permeabilised and analysed by confocal microscopy as previously described (Figure 4.7). Identical settings were maintained throughout, with individual channels shown in grey and a merged image in colour. Scale bar = 20 μ m.

4.4.4 Localisation of the UL15-UL28-UL33 complex in transfected cells

Although immunofluorescence data suggested that $\Delta 1$ was defective in its ability to interact with UL28-cMyc, whilst $\Delta 2$ was impaired in its ability to be transported to the nucleus in complex with UL15-pp65, both mutants supported DNA packaging.

Therefore, the ability of $\Delta 1$ and $\Delta 2$ to localise to the nucleus in the presence of UL15 and UL28 was analysed by immunofluorescence. BHK cells were transfected with pJM19 and pUL28-cMyc in combination with either pUL33, p $\Delta 1$ or p $\Delta 2$. The cells were fixed and permeabilised as before, and treated with R148 together with either anti-pp65 or anti-cMyc antibodies. Bound antibodies were detected with FITC and Cy5 conjugates, and images captured by confocal microscopy. The same settings were maintained for each antibody combination, and resultant images are shown in **Figure 4.18**.

When UL15-pp65, UL28-cMyc and UL33 were co-expressed, all localised to the nucleus, where they co-localised extensively (panels A-C, G-I and M-O show the localisation of UL15-pp65 and UL33; panels D-F, J-L and P-R show the localisation of UL28-cMyc and UL33). When $\Delta 1$ or $\Delta 2$ were expressed with UL15 and UL28, both exhibited a similar localisation to wt UL33 i.e. all three proteins co-localised in the nucleus (panels G-I and M-O show the localisation of $\Delta 1$ or $\Delta 2$ together with UL15-pp65; panels J-L and P-R show that of $\Delta 1$ or $\Delta 2$ in conjunction with UL28-cMyc).

Thus, both $\Delta 1$ and $\Delta 2$ formed a complex with both UL28-cMyc and UL15-pp65 in the nuclei of transfected cells.

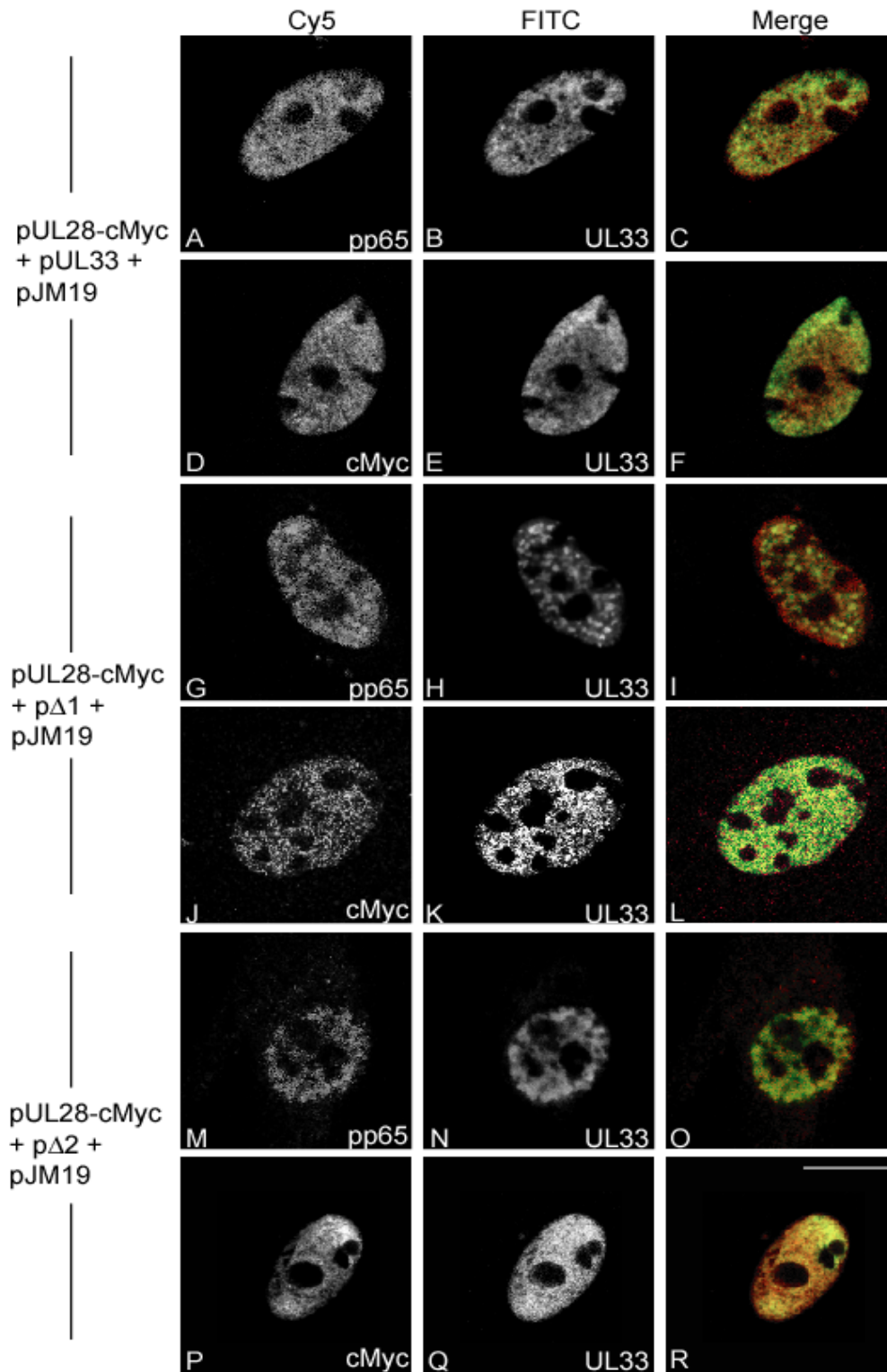


Figure 4.18: Localisation of the UL15-UL28-UL33 complexes in transfected cells

BHK cells were transfected with the indicated plasmids by lipofection. Twenty hours post-transfection, cells were fixed, permeabilised and analysed by confocal microscopy as previously described (Figures 4.3 and 4.7). Identical settings were maintained throughout, with individual channels shown in grey and a merged image in colour. Scale bar = 20µm.

Section 4.5 Discussion

4.5.1 Interaction between UL15 and UL33

Data from both immunofluorescence and immunoprecipitation studies supported the original report that UL15 and UL33 interact in the absence of UL28 (Beard *et al.*, 2002). However, this result conflicts with more recent studies suggesting that UL15 interacts with UL33 only in the presence of UL28 (Yang and Baines, 2006; Jacobson *et al.*, 2006). The observed nuclear localisation of the UL15-pp65-UL33 complex agrees with findings that UL15 contains a nuclear localisation signal required for transport of both UL28 and UL33 into the nucleus (Yu & Weller, 1998a; Koslowski *et al.*, 1999; Abbotts *et al.*, 2000; Yang *et al.*, 2007).

Yang and Baines (2006) suggested that the interaction between UL15 and UL33 observed by Beard *et al.* (2002) was due to over-expression of the two proteins. My immunofluorescence and immunoprecipitation data cannot exclude this possibility, as both approaches involve proteins expressed under the control of strong promoters (the HCMV MIEP and the AcMNPV polyhedrin promoter respectively). The observed co-precipitation of UL15 and UL33 from HSV-1-infected cells (Figure 4.6) confirms the findings of Yang and Baines (2006) but could be mediated through another protein such as UL28. Later immunofluorescence experiments using an HSV-1 UL28 null mutant (section 6.4.1) nevertheless provide evidence for the formation of a nuclear UL15-UL33 complex, and suggest that the observations made both by myself (this section) and Beard *et al.* (2002) may be indicative of a genuine interaction between these proteins.

Immunofluorescence analysis of the UL33 insertion mutants suggested that, although a

subset of these mutants was unable to support DNA packaging, all sixteen mutated proteins could interact with UL15-pp65. Replacement of Val³⁵, Ser³⁶ and Arg³⁷ with Cys-Gly-Arg-Thr-Arg, or substitution of residues 84-100 with Met-Arg-Pro-His-Ala (in $\Delta 1$ and $\Delta 2$ respectively), did not affect the ability of UL33 to support DNA packaging and *d*UL33 growth. Furthermore, neither $\Delta 1$ nor $\Delta 2$ was impaired in its ability to co-localise with UL15-pp65. The observed cytoplasmic co-localisation of $\Delta 2$ and UL15-pp65 suggested that, whilst these two proteins interact, the lesion in $\Delta 2$ precludes import of the complex into the nucleus. However, in the absence of UL15-pp65, $\Delta 2$ exhibited a similar localisation to wt UL33 (not shown), indicating that $\Delta 2$ does not form cytoplasmic aggregates when expressed alone. The cytoplasmic retention of UL15 by $\Delta 2$ is surprising given the ability of the $\Delta 2$ protein to complement *d*UL33 growth and DNA packaging. However in cells co-expressing UL15-pp65, UL28-cMyc and $\Delta 2$, all three proteins did co-localise within the nucleus. This suggests that retention of the UL15-pp65- $\Delta 2$ complex within the cytoplasm may be due to masking of the UL15 NLS, which can be overcome by the addition of UL28-cMyc.

The results with the UL33 mutants indicate that none of the mutations alone is sufficient to abolish the UL15-UL33 interaction and suggest that (i) UL33 may interact with UL15 via more than one region or (ii) the region required for interaction is relatively short (10-15 aa). It will be important to confirm the results of the experiments with the UL33 mutants using other approaches, for example immunoprecipitation assays with the recombinant baculoviruses described in section 4.3.5. Whether nucleic acid is involved in mediating the UL15-UL33 interaction also remains to be explored.

4.5.2 Interaction between UL28 and UL33

My immunofluorescence and immunoprecipitation data provide evidence for an interaction between the wild type UL28 and UL33 proteins, in agreement with previous findings (Beard *et al.*, 2002; Jacobson *et al.*, 2006). The cytoplasmic co-localisation of transiently expressed UL28-cMyc and UL33 is also consistent with the proposal that UL15 (specifically a nuclear localisation signal within UL15) is required for import of UL28 and UL33 into the nucleus (Yu & Weller, 1998a; Koslowski *et al.*, 1999; Abbotts *et al.*, 2000; Yang *et al.*, 2007).

Immunofluorescence experiments suggested that four UL33 insertion mutants (in34, in37, in69 and in84) were impaired in their ability to interact with UL28, implicating these regions as being important for binding. This finding also lends further support to the proposal that UL15 and UL33 interact in the absence of UL28. Were UL33 dependent upon UL28 to interact with UL15, it would be expected that mutants unable to interact with UL28-cMyc would not be able to be incorporated into a functional UL15-UL28-UL33 complex. However, three of the mutants (in34, in37 and in84) supported UL33 mutant virus growth and DNA packaging, suggesting that UL33 may also be able to be recruited into a functional complex via an interaction with UL15.

In contrast, immunoprecipitation analysis of mutated UL33 proteins expressed under the control of the AcMNPV polyhedrin promoter demonstrated that all 16 insertion mutants retained their ability to interact with UL28. This suggested that, in this assay, the mutations introduced were insufficient to perturb the UL28-UL33 interaction.

Several explanations for the disparity between these assays can be envisaged. Firstly,

the presence of a cMyc epitope may affect the ability of UL28 to interact with certain UL33 mutants. Secondly, it is also possible that baculovirus-expressed UL28 and UL33 proteins may associate whilst being incubated for prolonged periods on ice, giving rise to false-positive interactions by immunoprecipitation. Thirdly, the temperature at which the mutated proteins were expressed may be important for their interaction with UL28. It is conceivable that an insertion in UL33 might preclude correct protein folding at 37 °C (the temperature at which transfected BHK cells were incubated), but that folding at 28 °C (the temperature at which baculovirus-infected *Sf*21 cells were incubated) was unaffected. It will be important to confirm these results by carrying out immunofluorescence in *Sf*21 cells, or by using mammalian expression systems to carry out immunoprecipitation experiments at 37 °C.

Replacement of Val³⁵, Ser³⁶ and Arg³⁷ of UL33 with CGRTR (Δ 1) abrogated cytoplasmic retention of UL33 by UL28-cMyc, as previously observed with in34 and in37, further implicating this region in the UL28-UL33 interaction. This result is surprising given the ability of the Δ 1 protein to complement *d*UL33 growth and DNA packaging. However, Δ 1 was able to co-localise with both UL15 and UL28 in triply transfected cells (Figure 4.18). Alignment of UL33 gene homologues revealed that the substituted regions in Δ 1 exhibited poor sequence conservation, consistent with Δ 1 supporting viral growth and DNA packaging (**Figure 4.19**). The failure of Δ 1 to interact with UL28-cMyc could be due to the net insertion of two amino acids, or to the specific loss of residues 35, 36 and 37. Nevertheless, perturbation of the UL28-UL33 interaction with this mutant is apparently overcome in the context of HSV-1 infection by virtue of its ability to interact with UL15.

Substitution of amino acids Ile⁸⁵ to Ala¹⁰⁰ of UL33 with MRPHA ($\Delta 2$) did not affect the ability of $\Delta 2$ to support DNA packaging and *d*UL33 growth. This is consistent with the poor sequence conservation exhibited by this dispensable region (Figure 4.19). However, although in84 was unable to co-localise with UL28-cMyc, $\Delta 2$ was unaffected in this regard. The reason for this discrepancy is unclear, but may reflect the nature of the inserted amino acids (MRPQP for in84; MRPHA for $\Delta 2$).

In summary, analysis of the ability of the mutated UL33 proteins to interact with UL15 and UL28 failed to explain why a subset of mutants could not package DNA. Eight of the nine mutants that were unable to package DNA (in14, in51, in55, in74, in 104, in111A, in111B and in116) appeared completely unaltered in their ability to interact with UL15 and UL28. The ninth mutant unable to package DNA, in69, was unable to co-localise with UL28-cMyc in immunofluorescence assays. This might explain the inability of in69 to support DNA packaging, but it should be noted that other mutants exhibiting this phenotype (in34, in37 and in84) complemented *d*UL33 growth and packaging. Experiments described in chapter 5 were therefore designed to investigate whether UL33 might interact with other HSV-1 DNA packaging proteins, and if so, whether perturbation of such interactions could account for the behaviour of the UL33 mutants.

Chapter 5: Interaction of wt and mutated UL33 with other packaging proteins

Section 5.1 Introduction

The preceding immunoprecipitation and immunofluorescence experiments (Chapter 4:) demonstrated that the ability of mutated UL33 proteins to interact with the terminase proteins UL15 and UL28 did not correlate with their ability to support mutant virus growth or DNA packaging. It is conceivable, however, that interactions of wt UL33 with other viral or cellular partners may be vital for successful DNA packaging. Although several protein-protein interactions involving UL33 homologues have been reported in other herpesviruses (notably HSV-2, VZV and KSHV; Yamauchi *et al.*, 2001; Yamauchi *et al.*, 2002; Uetz *et al.*, 2006), there have been no reports of interactions between homologues of HSV-1 UL33 and the HSV-1 DNA packaging proteins UL6, UL25 and UL32. Uetz *et al.* (2006) identified an interaction between the VZV homologues of HSV-1 UL33 and UL17 by yeast-2-hybrid screening, although this interaction was not observed in similar studies on the homologous EBV proteins (Calderwood *et al.*, 2007).

The initial aims of the work presented in this chapter were therefore to determine whether wild-type UL33 was able to interact with UL6, UL17, UL25 and UL32. During the course of these experiments, novel interactions with UL6 and UL25 were observed. Subsequently, the ability of mutated UL33 proteins to interact with these proteins was examined.

Section 5.2 Interactions of UL33 with UL6 and UL6in269

Interactions have previously been demonstrated between the UL15 and UL28 terminase components, and the HSV-1 portal protein UL6 (White *et al.*, 2003; Yang *et al.*, 2007).

However, despite UL33 being a probable component of the putative terminase complex, it is unknown whether it interacts with UL6. Experiments were therefore carried out to determine whether UL6 and UL33 interacted.

5.2.1 Co-immunoprecipitation of UL6 and UL33 from HSV-1 infected cells

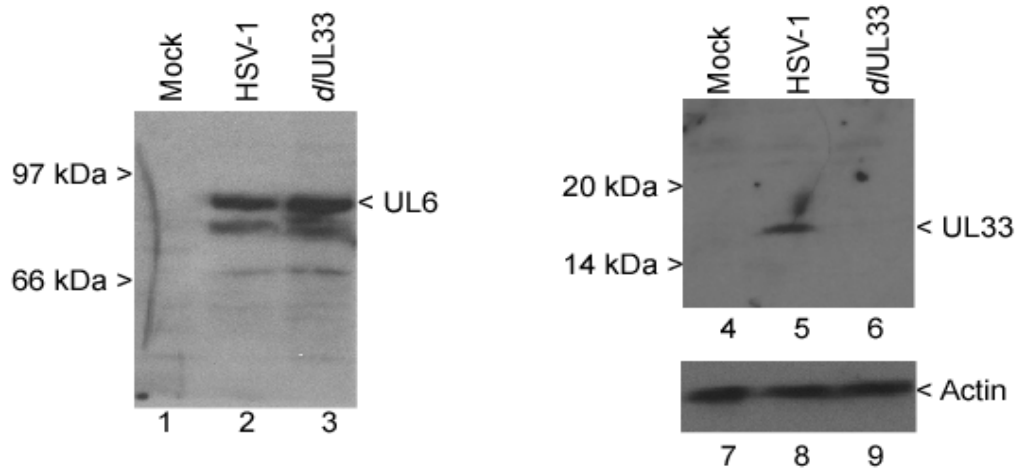
To examine whether UL33 and UL6 interacted in HSV-1-infected cells, immunoprecipitation analysis was carried out on the HSV-1 and Δ UL33-infected cell lysates detailed in section 4.2.2. Lysates were immunoprecipitated with R148, the immune complexes collected and proteins resolved by western blotting with either R148 or a rabbit anti-UL6 antibody R992 (2.1.12). The results are shown in **Figure 5.1**. Lanes 4-9 of panel A and 4-6 of panel B, showing the UL33 and actin controls, were presented in Figure 4.2 and discussed in section 4.2.2.

UL6 was detected in HSV-1 and Δ UL33-infected cell lysates, but was absent from mock-infected cells (panel A; lanes 1-3). Both UL6 and UL33 were co-precipitated by R148 from HSV-1-infected cells, but not from Δ UL33-infected cells (panel B; lanes 1-3 and lanes 4-6 respectively), indicating that the co-precipitation of UL6 by R148 required UL33. These data suggest that UL6 forms part of a complex that contains UL33.

5.2.2 Co-immunoprecipitation of UL6 and UL33 from recombinant baculovirus-infected insect cells

Although data suggested that UL6 and UL33 interacted, it was unclear whether this interaction was dependent upon the presence of UL15 and UL28. It was conceivable that R148 precipitated a complex of UL15-UL28-UL33-UL6 from HSV-1 infected cells, rather than just the UL33-UL6 moieties, and that UL6 and UL33 interacted via UL28 and/or UL15.

A. Extract prior to immunoprecipitation



B. Immunoprecipitation with R148

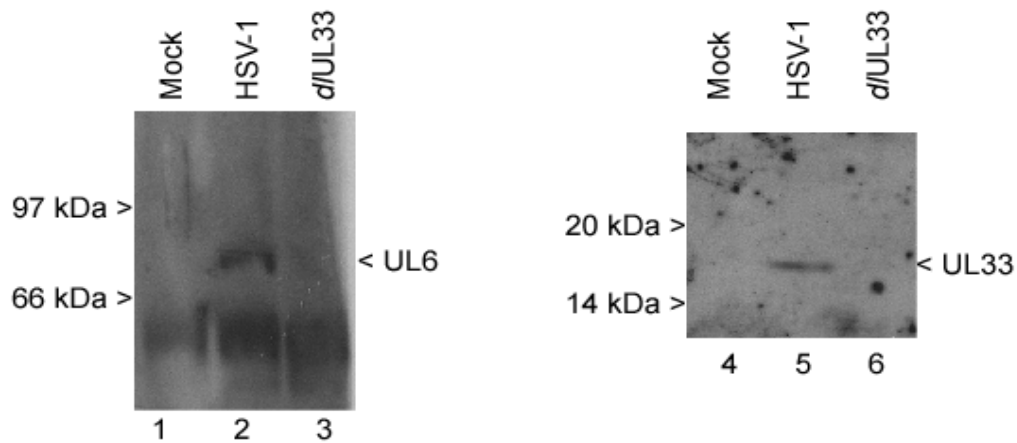


Figure 5.1: Co-immunoprecipitation of UL6 and UL33 from HSV-1-infected cells.

The soluble extracts and immunoprecipitates from mock-infected, HSV-1-infected and *d*UL33-infected BHK cells described in Figure 4.2 were used.

A. Samples of extract prior to immunoprecipitation were separated by SDS-PAGE on an 8% polyacrylamide gel, proteins transferred to a PVDF membrane, and detected with R992 (lanes 1-3), R148 (lanes 4-6) or anti-actin antibody (lanes 7-9). Note that the controls (lanes 4-9) are the same as shown in Figure 4.2.

B. Samples of the immune complexes precipitated by R148 (Figure 4.2) were resolved on an 8% polyacrylamide gel, and the protein species detected with R992 (lanes 1-3), or R148 (lanes 4-6). Note that the UL33 control (lanes 4-6) is that shown in Figure 4.2.

To examine whether UL6 and UL33 interacted in the absence of the other terminase proteins, immunoprecipitation analysis was carried out on UL6 and UL33 expressed by recombinant baculoviruses under the control of the AcMNPV polyhedrin promoter. Sf21 monolayers were infected with 5 p.f.u./cell of recombinant baculoviruses expressing either UL33 (AcUL33) or UL6 (AcUL6), or both viruses together. Cell lysates were prepared, precleared and precipitated with either R148 or R992. Immune complexes were collected and analysed by western blotting, and the results are shown in **Figure 5.2**.

UL33 was precipitated by the UL33 antibody R148 from cells infected with AcUL33 alone or in conjunction with AcUL6, but not from mock-infected cells or those receiving AcUL6 alone (panel A; lanes 5-8). UL6 was precipitated by R148 from cells receiving AcUL33 and AcUL6, but not from cells receiving AcUL6 alone, indicating that co-precipitation of UL6 and UL33 by R148 required UL33 (panel A; lanes 1-4). In reciprocal experiments, the anti-UL6 antibody R992 precipitated UL6 from cells receiving AcUL6 in both the presence and absence of AcUL33 (panel B; lanes 1-4). Furthermore, R992 co-precipitated UL33 from cells receiving both AcUL6 and AcUL33 (panel B; lanes 5-8). Together, these data confirmed the earlier result (Figure 5.1) suggesting that UL6 and UL33 interacted, and provided the first demonstration of an interaction in the absence of other HSV-1 proteins, notably UL15 and UL28.

5.2.3 Co-localisation of wt UL6 and UL33-HIS₆ in transfected cells

To further analyse the ability of UL33 and UL6 to interact in the absence of other HSV-1 proteins, the subcellular localisation of UL6 was examined in the presence of a His₆-tagged version of UL33. Previous studies revealed that this protein was able to support amplicon DNA packaging as efficiently as wild-type UL33 (G. Reid, unpublished results). BHK cells were transfected with pAS30 and pUL33-His₆ (encoding UL33-His₆), either

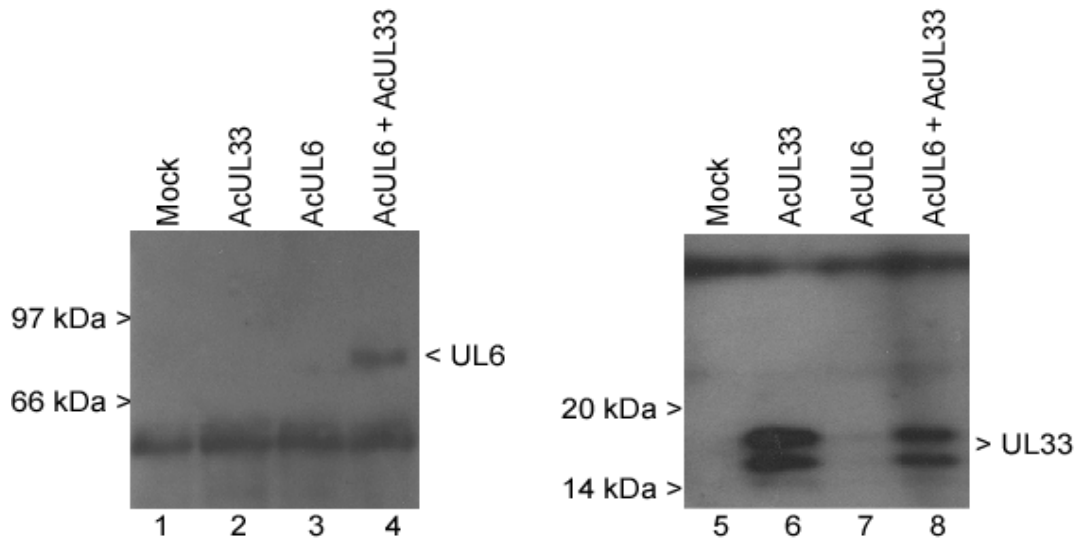
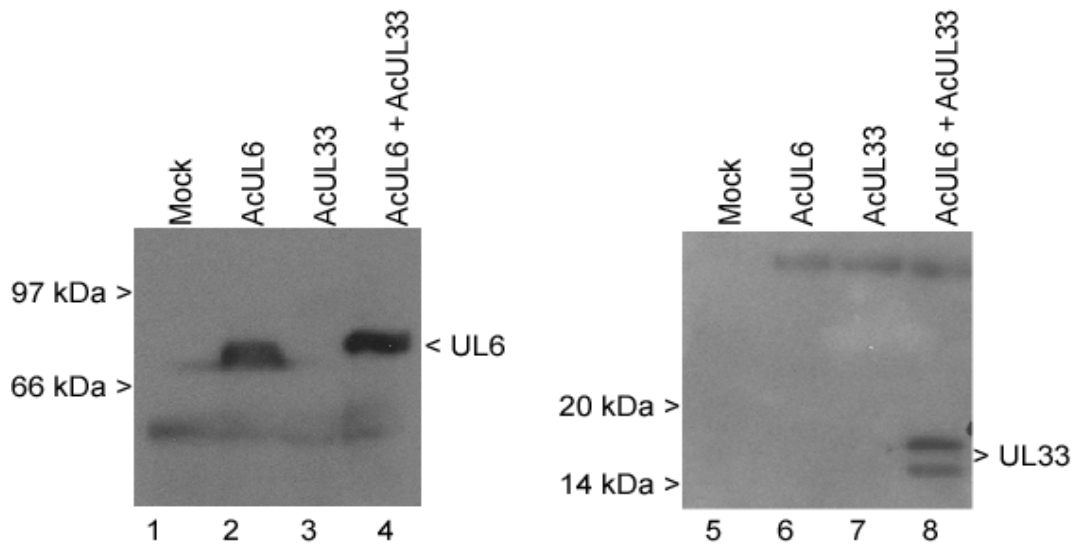
A. Immunoprecipitation with R148**B. Immunoprecipitation with R992**

Figure 5.2: Co-immunoprecipitation of UL6 and UL33 from recombinant baculovirus-infected cells.

*Sf*21 cells were mock-infected or infected with the indicated recombinant baculoviruses. Forty-eight hours post infection, cells were lysed and duplicate soluble extracts prepared. **A.** After preclearing with a non-specific rabbit antibody, soluble extracts were incubated with R148, the immune complexes precipitated with protein-A sepharose, and the protein species separated by SDS-PAGE on 8% (left-hand panel) or 15% (right-hand panel) polyacrylamide gels. Proteins were detected by western blotting using R148 (right-hand panel) or R992 (left-hand panel).

B. Precleared soluble extracts were incubated with R992 and the immune complexes isolated and analysed as in A. The apparent discrepancy between the mobility of the protein species in lanes 2 and 4 is due to the polyacrylamide gel warping prior to transfer.

alone or in combination. pAS30 expresses the HSV-1 UL6 gene under the control of the HCMV MIEP (Patel *et al.*, 1996). Fixed and permeabilised monolayers were incubated with R992 and mouse anti-HIS₆ antibodies (section 2.1.12), and processed for confocal microscopy. Representative images are shown in **Figure 5.3**.

In contrast to the localisation of wild-type UL33, UL33-His₆ localised solely to the cytoplasm of transfected cells (panels D and F). UL6 was present solely in the nuclei of cells transfected with pAS30 (panels A-C), consistent with previous studies (Patel *et al.*, 1996; White *et al.*, 2003). No non-specific fluorescence was apparent with either antibody. In cells co-expressing both proteins, UL6 and UL33-His₆ localised to the cytoplasm (panels G and H respectively), and merging of the channels revealed extensive co-localisation (panel I). These data therefore agree with the previous conclusion that UL6 and UL33 interact specifically and in the absence of other HSV-1 proteins.

5.2.4 Immunofluorescence assay for the interaction of wt UL33 with UL6

Similar experiments were carried out to analyse whether wild type UL33 and UL6 colocalised in the absence of other HSV-1 proteins. BHK cells were transfected with either pAS30 or pUL33, or both plasmids together. Monolayers were reacted with R148 and a mouse anti-UL6 antibody (M175; section 2.1.12), cells were processed for confocal microscopy, and representative images shown in **Figure 5.4**.

UL6 again localised to the nuclei of transfected cells (panels A and C). No FITC-specific fluorescence was observed in cells transfected with pAS30 (panel B). As observed before, UL33 was localised throughout transfected cells (panels E-F). In cells co-expressing UL6 and UL33, both proteins localised within the nucleus, and revealed extensive co-localisation (panels G-L). In the majority of cells (approximately 95%) expressing both

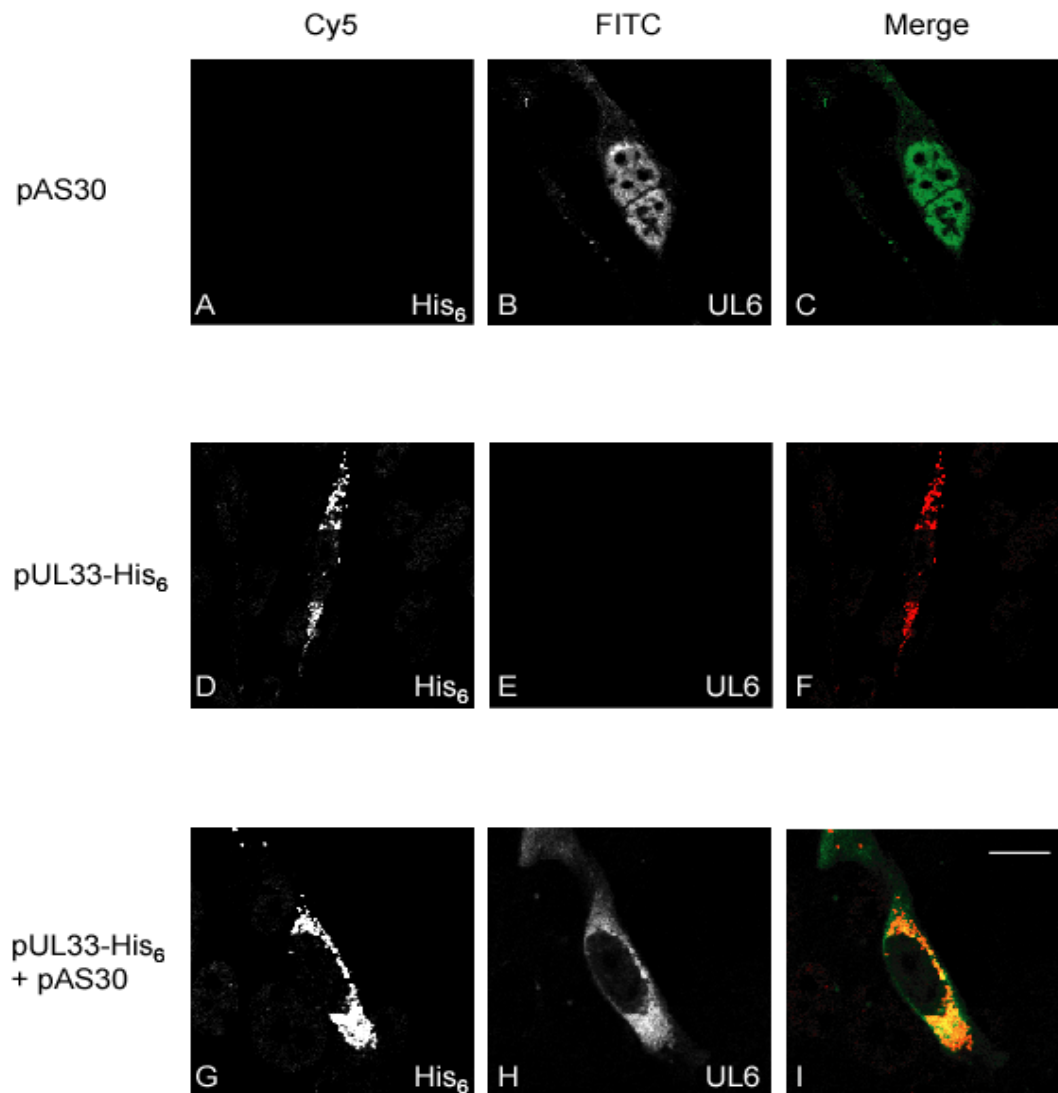


Figure 5.3: Co-localisation of UL6 and UL33-His₆ in transfected cells.

BHK cells were transfected with the indicated plasmids by lipofection. Twenty hours post-transfection, cells were fixed and permeabilised with paraformaldehyde and NP40, and probed with a mouse anti-His₆ antibody and R992. Coverslips were incubated with Cy5-coupled anti-mouse and FITC-coupled antibodies, and processed for confocal microscopy. Identical settings were maintained throughout, with the separate channels shown in grey and a merged image in colour. Scale bar = 20µm.

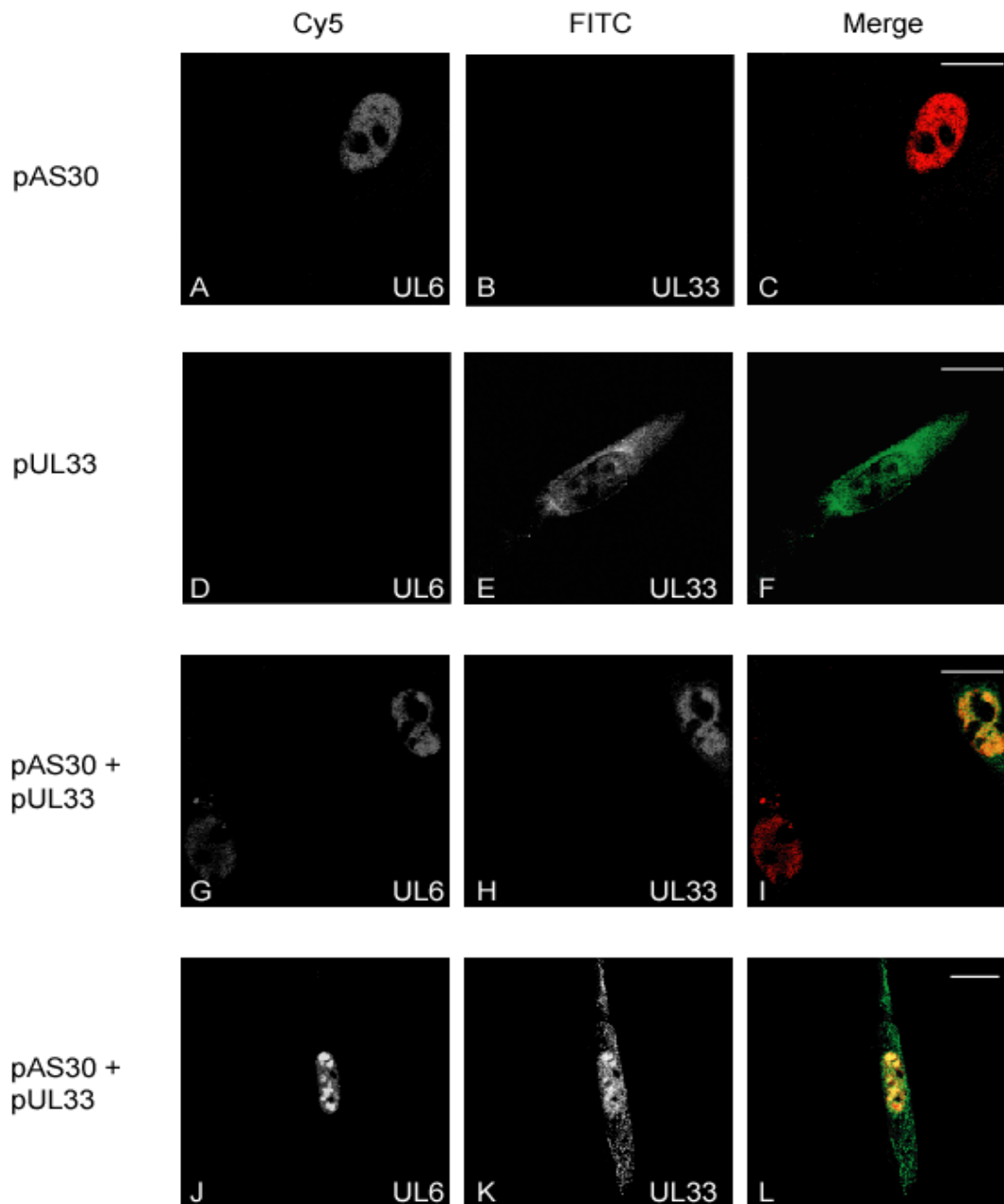


Figure 5.4: Co-localisation of UL6 and UL33 in transfected cells.

BHK cells were transfected with the indicated plasmids by lipofection. Twenty hours post-transfection, cells were fixed and permeabilised as described (Figure 5.3), and probed with a mouse anti-UL6 antibody (M175) and R148. Coverslips were incubated with Cy5-coupled anti-mouse and FITC-coupled anti-rabbit antibodies, and processed for confocal microscopy. Identical settings were maintained throughout, with individual channels shown in grey and a merged image in colour. Scale bars = 20 μ m.

proteins, UL33 was restricted solely to the nucleus (panels H and I). This figure is significantly greater than the percentage of cells showing exclusive nuclear localisation when UL33 is expressed alone (section 3.2.3). However, in a small proportion of cells (5% of the population co-expressing both proteins), UL33 was present in both nucleus and cytoplasm, although predominantly in the nucleus, where it co-localised with UL6 (represented by panels K-L). Both proteins were consistently absent from nucleoli. In combination, these data support the proposal that UL6 and UL33 interact in the absence of other HSV-1 proteins.

5.2.5 Ability of mutated UL33 proteins to interact with wt UL6

The ability of mutated UL33 proteins to interact with UL6 was analysed in similar experiments. In this instance, BHK cells were transfected with plasmids expressing wild type or mutated UL33 proteins, together with pAS30. Images of a subset of the mutants are shown in **Figure 5.5**, and are representative of the phenotype exhibited by all 16 mutants in this assay.

The localisation of UL33 and UL6 when expressed alone was identical to that observed previously (data not shown). When co-expressed, both proteins again co-localised within the nuclei of cells (panels A-C). All of the mutants examined exhibited a similar phenotype to wt UL33 in which the UL33 protein was predominantly nuclear, where it co-localised extensively with UL6 (represented by in14, in37, in69 and in100 in panels D-O). It should be noted that, in a small proportion of the cells co-expressing mutated UL33 and UL6, that some UL33 was apparent in the cytoplasm (typified by in14 and in37 in panels E and H respectively). The proportion of cells in which UL33 was restricted to the nucleus was increased in all instances in the presence of UL6.

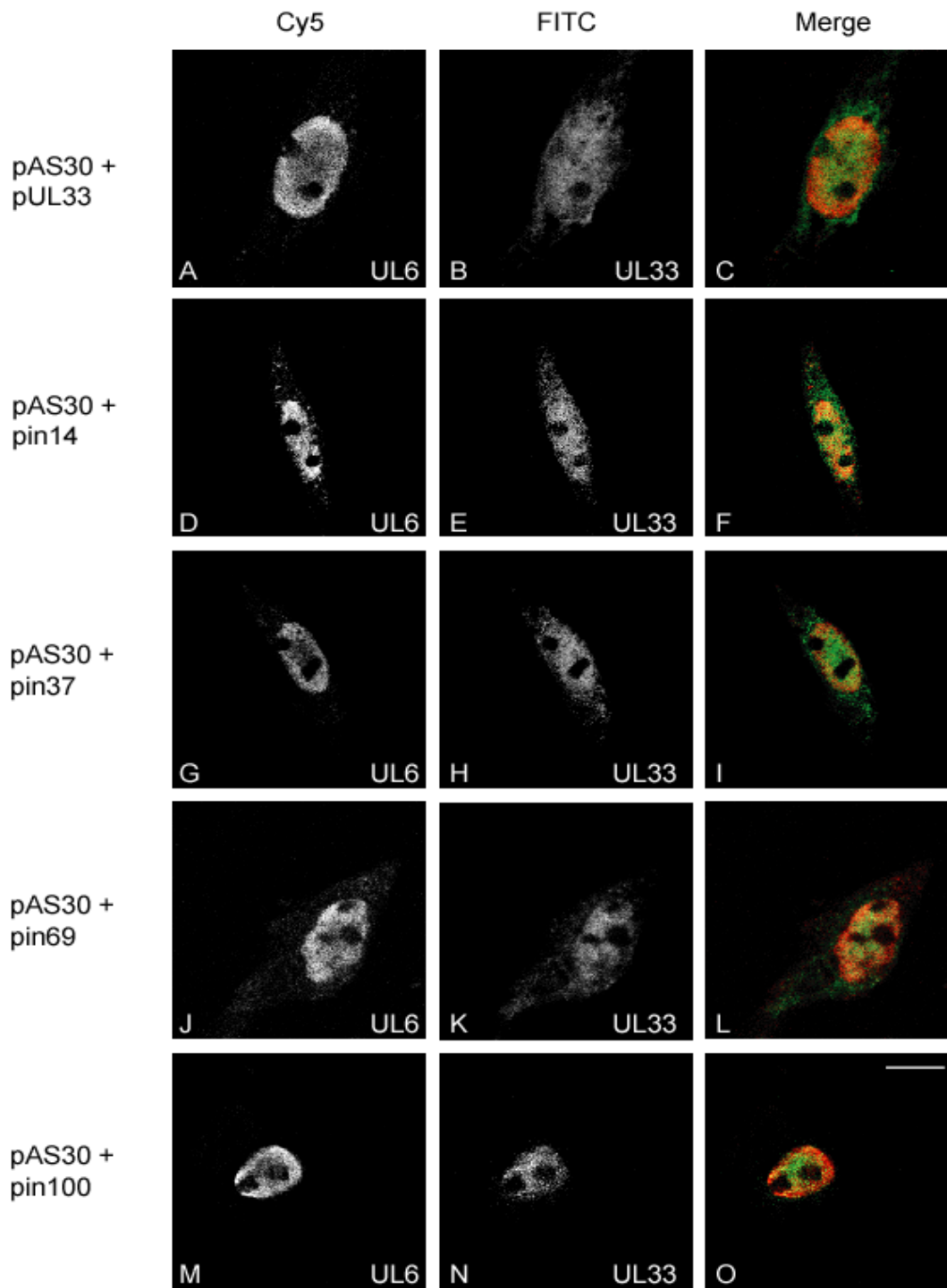


Figure 5.5: Co-localisation of UL6 and mutated UL33 proteins in transfected cells.

BHK cells were transfected with the indicated plasmids by lipofection, and processed as described in the legend to Figure 5.4. Coverslips were analysed by confocal microscopy, with identical settings maintained throughout. Images are representative of all of the mutants examined. Individual channels are shown in grey and a merged image in colour. Scale bar = 20 μ m.

Together, these data suggested that none of the mutated UL33 proteins was compromised in its ability to interact with UL6. Therefore, the inability of several mutants to support DNA packaging could not be explained in terms of their failure to interact with UL6.

5.2.6 Immunofluorescence assay for the interaction of wt UL33 with UL6in269

Previous studies revealed that insertion of four amino acids between the conserved residues Phe²⁶⁹ and Glu²⁷⁰ of UL6 rendered the resulting protein (UL6in269) unable to support DNA packaging (White *et al.*, 2003). Furthermore, UL6in269 was restricted solely to the cytoplasm of transfected cells, in contrast to the nuclear localisation of wt UL6. To further examine the interaction between UL6 and UL33, the localisation of UL33 was examined in the presence of UL6in269.

BHK cells were transfected with pUL33 or pUL6in269 (encoding UL6in269), or both plasmids together. Fixed and permeabilised cells were incubated with R148 and M175 and processed for confocal microscopy. UL33 and UL6 were detected by excitation of FITC and Cy5 fluors respectively, and representative images are shown in **Figure 5.6**.

UL6in269 was localised solely to the cytoplasm of transfected cells (panels A-C), consistent with the published phenotype (White *et al.*, 2003). The localisation of UL33 was as observed previously (panels D-F). In cells co-expressing both UL6in269 and UL33 both proteins were present exclusively in the cytoplasm (panels G and H) and exhibited extensive co-localisation (panel I). These data demonstrated that UL33 interacted with UL6in269, in agreement with data from immunoprecipitation studies of wt UL6. However, it should be noted that UL6in269 is unable to support DNA

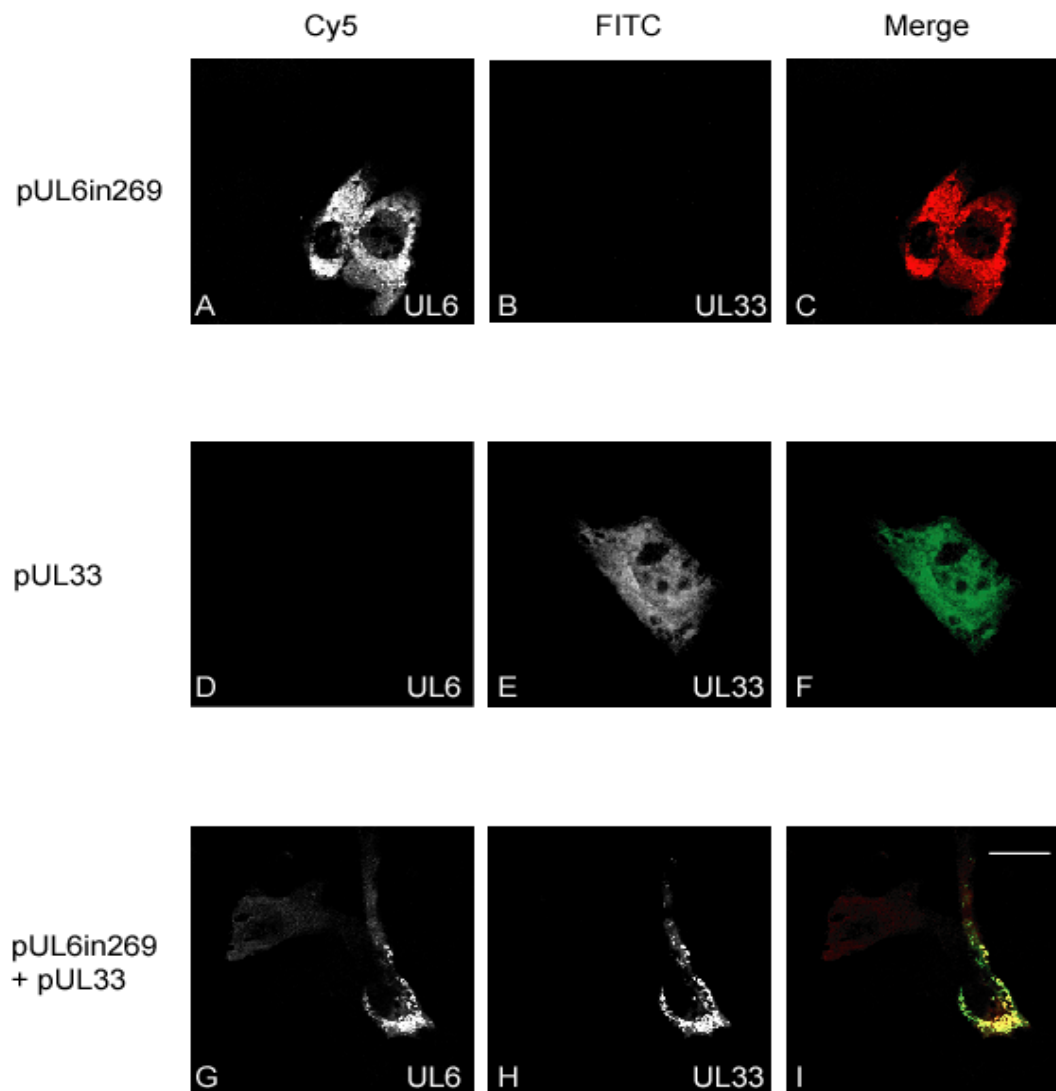


Figure 5.6: Co-localisation of UL6in269 and UL33 in transfected cells.

BHK cells were transfected with the indicated plasmids by lipofection. Cells were treated exactly as described in the legend to Figure 5.4, and analysed by confocal microscopy. Identical settings were maintained throughout, with the separate channels shown in grey and a merged image in colour. Scale bar = 20 μ m.

packaging.

One explanation for the cytoplasmic localisation of UL6in269 and UL33 was that UL6in269 non-specifically inhibits the nuclear uptake of proteins. To examine this possibility, the localisation of HSV-1 UL9 was examined in the presence of UL6in269. To this end, BHK cells were transfected with pUL6in269, pE9, or both plasmids together. Coverslips were incubated with R992 and the UL9 antibody M13924, and processed as described before (section 4.3.1). **Figure 5.7** is representative of the images obtained.

The subcellular localisations of UL6in269 and UL9 when expressed alone (panels A-C and D-F respectively) were identical to those observed previously. The localisation of UL6in269 and UL9 was unaltered when both proteins were co-expressed, with UL9 localised to the nucleus and UL6in269 restricted solely to the cytoplasm (panels G-I). Thus, UL6in269 did not inhibit the nuclear uptake of UL9, and the cytoplasmic co-localisation observed in cells expressing UL33 and UL6in269 was therefore considered to represent a specific interaction.

5.2.7 Ability of mutated UL33 proteins to interact with UL6in269

To analyse the ability of mutated UL33 proteins to co-localise with UL6in269, similar experiments were performed. In this case, cells were transfected with plasmids expressing wt or mutated UL33 proteins together with pUL6in269. A subset of the resulting images is shown in **Figure 5.8**, and is representative of all of the mutants analysed.

As before, wt UL33 was excluded from the nucleus in the presence of UL6in269 and the two proteins extensively co-localised within the cytoplasm (panels A-C). A similar

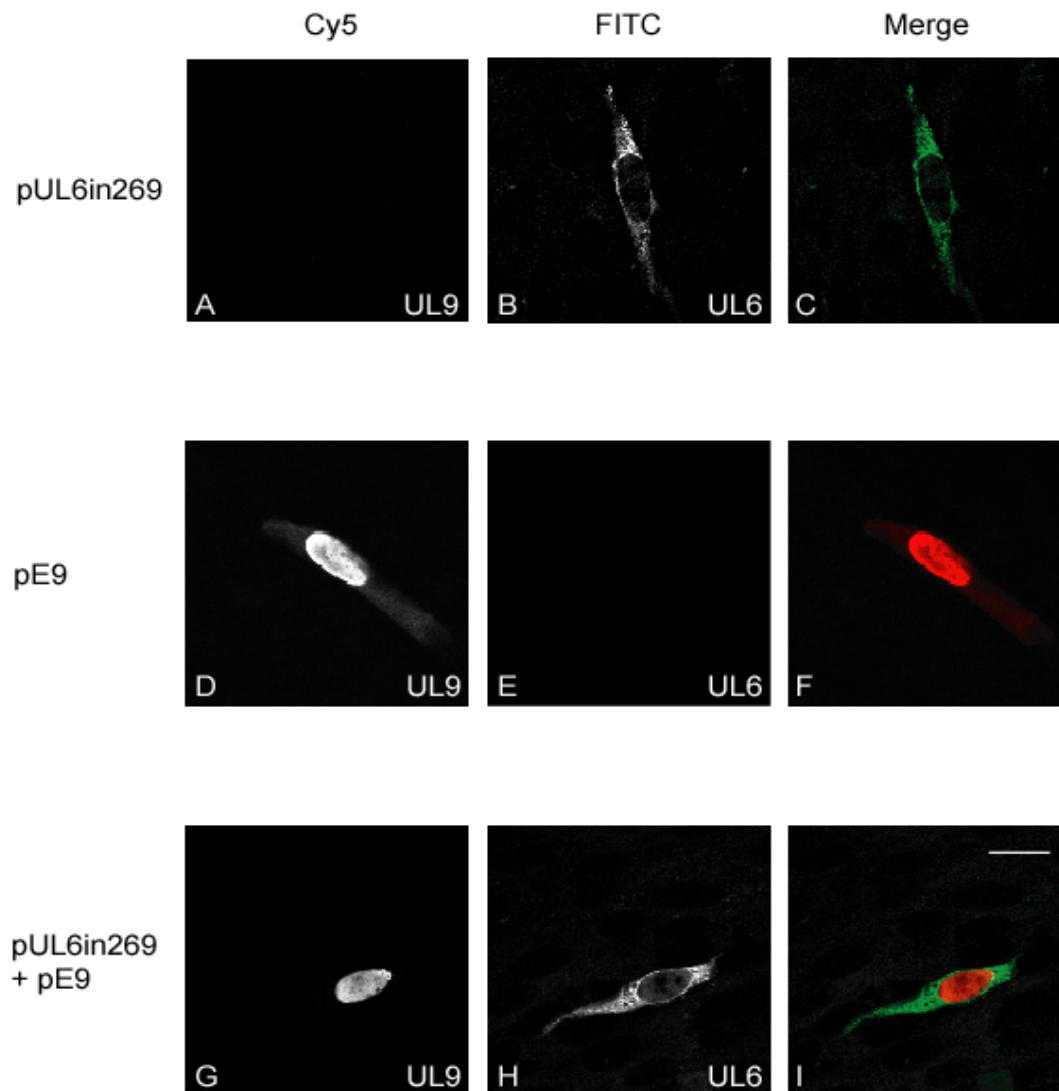


Figure 5.7: Intracellular localisation of UL6in269 and UL9 in transfected cells.

BHK cells were transfected with the indicated plasmids by lipofection. Twenty hours post-transfection, cells were fixed and permeabilised with PFA and NP40, and probed with a mouse anti-UL9 antibody (M13924) and R992. Coverslips were incubated with Cy5-coupled anti-mouse and FITC-coupled anti-rabbit antibodies, and processed for confocal microscopy. Identical settings were maintained throughout, with the separate channels shown in grey and a merged image in colour. Scale bar = 20 μ m.

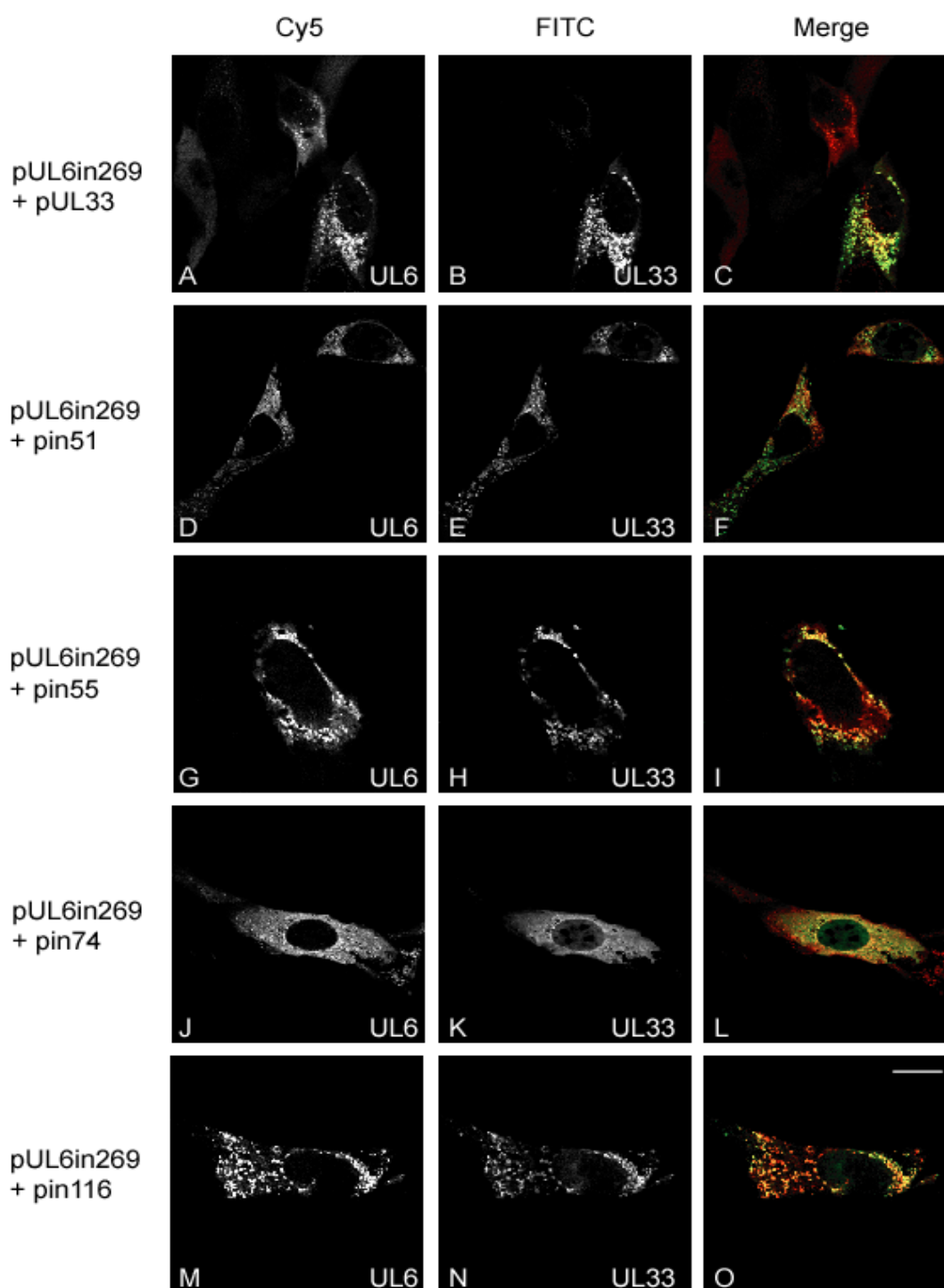


Figure 5.8: Co-localisation of UL6in269 and mutated UL33 proteins in transfected cells.

BHK cells were transfected with the indicated plasmids by lipofection. Cells were treated exactly as described in the legend to Figure 5.4, and analysed by confocal microscopy. Images are representative of all of the mutants examined. Identical settings were maintained throughout, with individual channels shown in grey and a merged image in colour. Scale bar = 20 μ m.

phenotype was exhibited by all of the 16 mutants examined (represented by in51, in55, in74 and in116 in panels D-O). These data, together with the results from co-localisation studies with wt UL6, suggested that all the mutants retain the ability to interact with UL6.

Section 5.3 Interaction of UL33 with UL17

Similar approaches were employed to examine potential interactions between the HSV-1 UL33 and UL17 proteins.

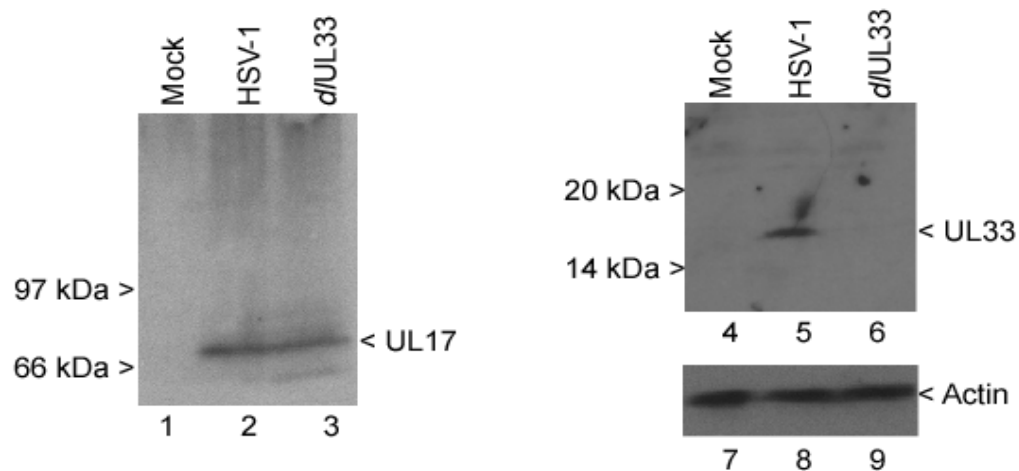
5.3.1 Immunoprecipitation analysis of UL17 and UL33 from HSV-1 infected cells

Firstly, immunoprecipitation analysis was performed on the HSV-1-infected cell lysates described in section 4.2.2. Isolated immune complexes precipitated by R148 were resolved by western blotting and membranes probed with R148 or a rabbit anti-UL17 antibody, R1218 (section 2.1.12). The resultant immunoblots are shown in **Figure 5.9**. Lanes 4-9 of panel A and 4-6 of panel B, showing the UL33 and actin controls, were also presented in Figure 4.2 and discussed in section 4.2.2. Although UL17 was readily detectable by R1218 in virally infected cell lysates (panel A; lanes 1-3), it was absent from immune complexes precipitated by R148 (panel B; lanes 1-3). Thus UL17 is not co-precipitated with UL33 by R148, suggesting that UL17 does not interact with UL33 in HSV-1-infected cells.

5.3.2 Immunoprecipitation analysis of UL17 and UL33 from recombinant baculovirus-infected insect cells

The ability of UL17 and UL33 to interact was next examined by immunoprecipitation of recombinant baculovirus-expressed proteins. Monolayers of *Sf*21 cells were infected with 5 p.f.u./cell of AcUL33 or a recombinant baculovirus expressing UL17 (AcUL17), or both viruses together. Proteins were precipitated by R148 or R1218, and the resulting

A. Extract prior to immunoprecipitation



B. Immunoprecipitation with R148

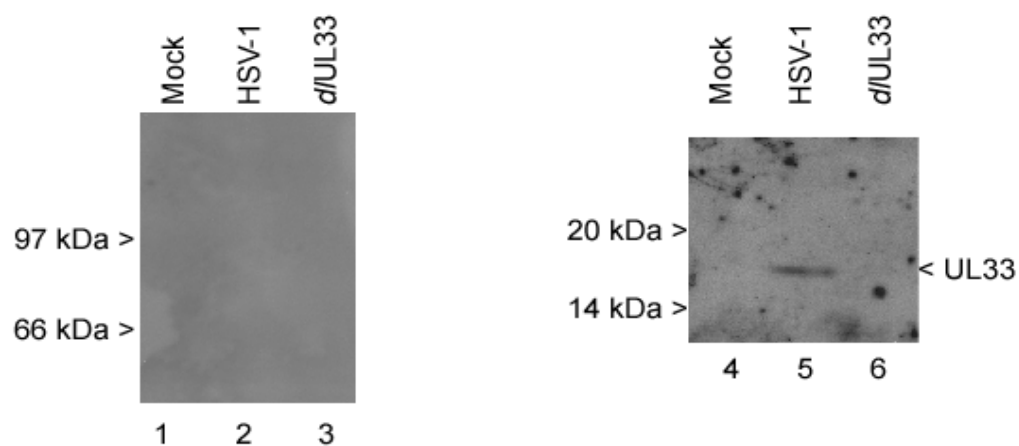


Figure 5.9: Immunoprecipitation of UL17 and UL33 from HSV-1-infected cells.

The soluble extracts and immunoprecipitates from mock-infected, HSV-1-infected and *d/UL33*-infected BHK cells described in Figure 4.2 were used.

A. Samples of extract prior to immunoprecipitation were separated by SDS-PAGE on an 8% polyacrylamide gel, proteins transferred to a PVDF membrane, and detected with R1218 (lanes 1-3), R148 (lanes 4-6) or anti-actin antibody (lanes 7-9). Note that the controls (lanes 4-9) are the same as shown in Figure 4.2.

B. Samples of the immune complexes precipitated by R148 (Figure 4.2) were resolved on an 8% polyacrylamide gel, and the protein species detected with R1218 (lanes 1-3), or R148 (lanes 4-6). Note that the UL33 control (lanes 4-6) is that shown in Figure 4.2.

immune complexes analysed by western blotting (**Figure 5.10**).

Both UL17 and UL33 were precipitated by their cognate antibodies (panels B; lanes 1-4 and A; 5-8 respectively). However, no UL17 was detected in immune complexes precipitated with R148, despite the presence of UL17 in cell extracts (panel A; lanes 1-4). Consistent with these findings, no UL33 was detectable in complexes precipitated by R1218 (panel B; lanes 5-8). Together, these data further support the conclusion that UL17 and UL33 do not interact.

5.3.3 Sub-cellular localisation of UL17 and UL33 in transfected cells

Finally, the localisation of UL17 was examined in conjunction with UL33 in co-transfected cells. BHK monolayers were transfected with pUL33, pMH19 (which encodes the HSV-1 UL17 gene under the control of the HCMV MIEP), or both plasmids together. Coverslips were incubated with R148 and a mouse anti-UL17 antibody (M203; section 2.1.12), processed for confocal microscopy, and the resultant images are shown in **Figure 5.11**.

The localisation of UL33 when expressed alone was as observed previously (panels A-C). UL17 was localised predominantly in the nuclei of cells, with a small amount of protein in the cytoplasm (panels D and F). No FITC-specific signal was observed in cells transfected with pMH19 alone (panel E). The co-expression of both proteins did not alter the sub-cellular localisation of either UL17 (panel G) or UL33 (panel H). This is consistent with data from the immunoprecipitation experiments suggesting that UL17 and UL33 do not interact.

Section 5.4 Interaction of UL33 with UL25

Although an interaction has previously been reported between HSV-1 UL25 and the *a*

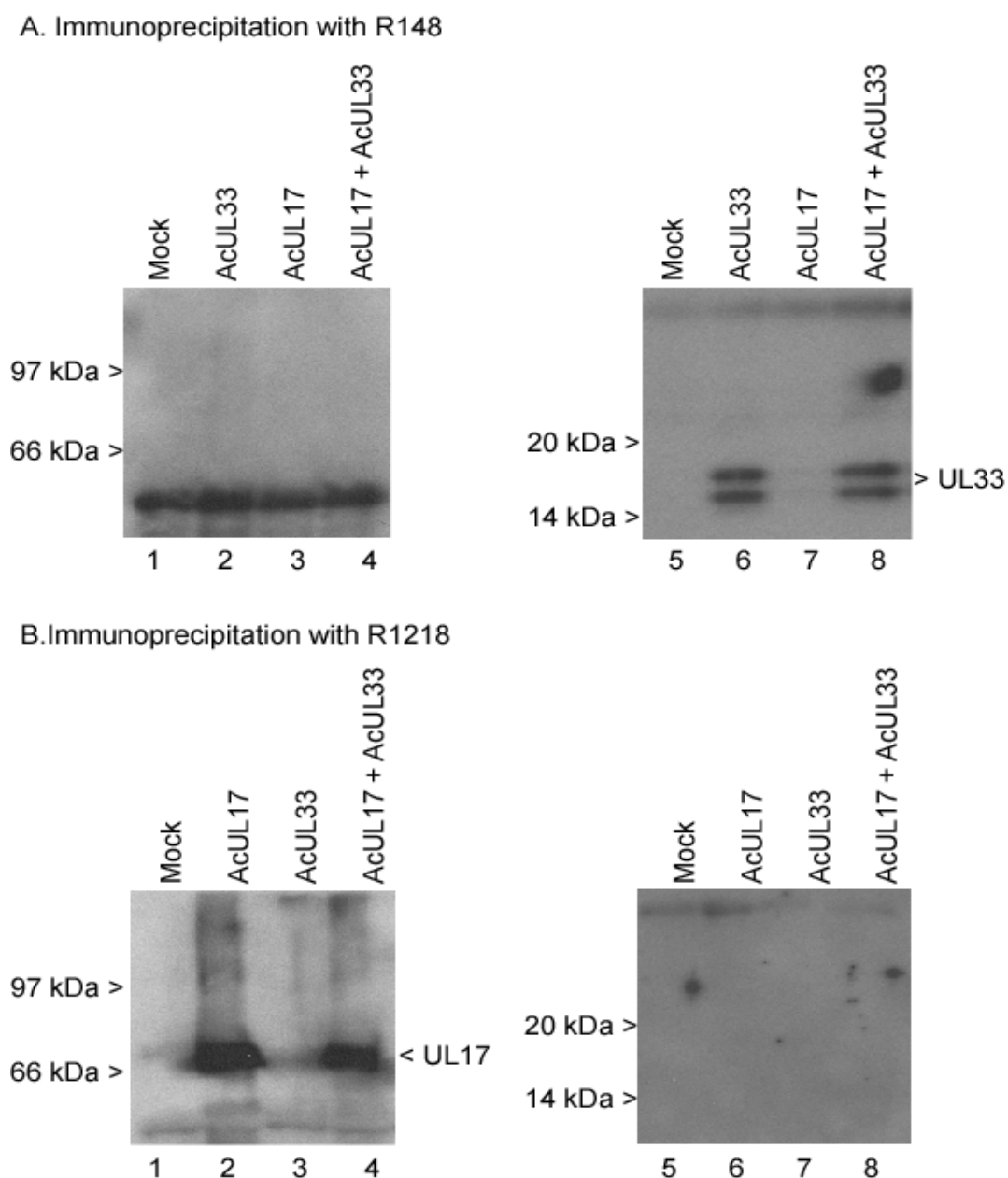


Figure 5.10: Immunoprecipitation of UL17 and UL33 from recombinant baculovirus-infected cells.

Sf21 cells were mock-infected or infected with the indicated recombinant baculoviruses. Forty-eight hours post infection, cells were lysed and duplicate soluble extracts prepared.

A. After preclearing with a non-specific rabbit antibody, soluble extracts were incubated with R148, the immune complexes precipitated with protein-A sepharose, and the protein species separated by SDS-PAGE on 8% (left-hand panel) or 15% (right-hand panel) polyacrylamide gels. Proteins were detected by western blotting using R148 (right-hand panel) or R1218 (left-hand panel).

B. Precleared soluble extracts were incubated with R1218 and the immune complexes isolated and analysed as in A.

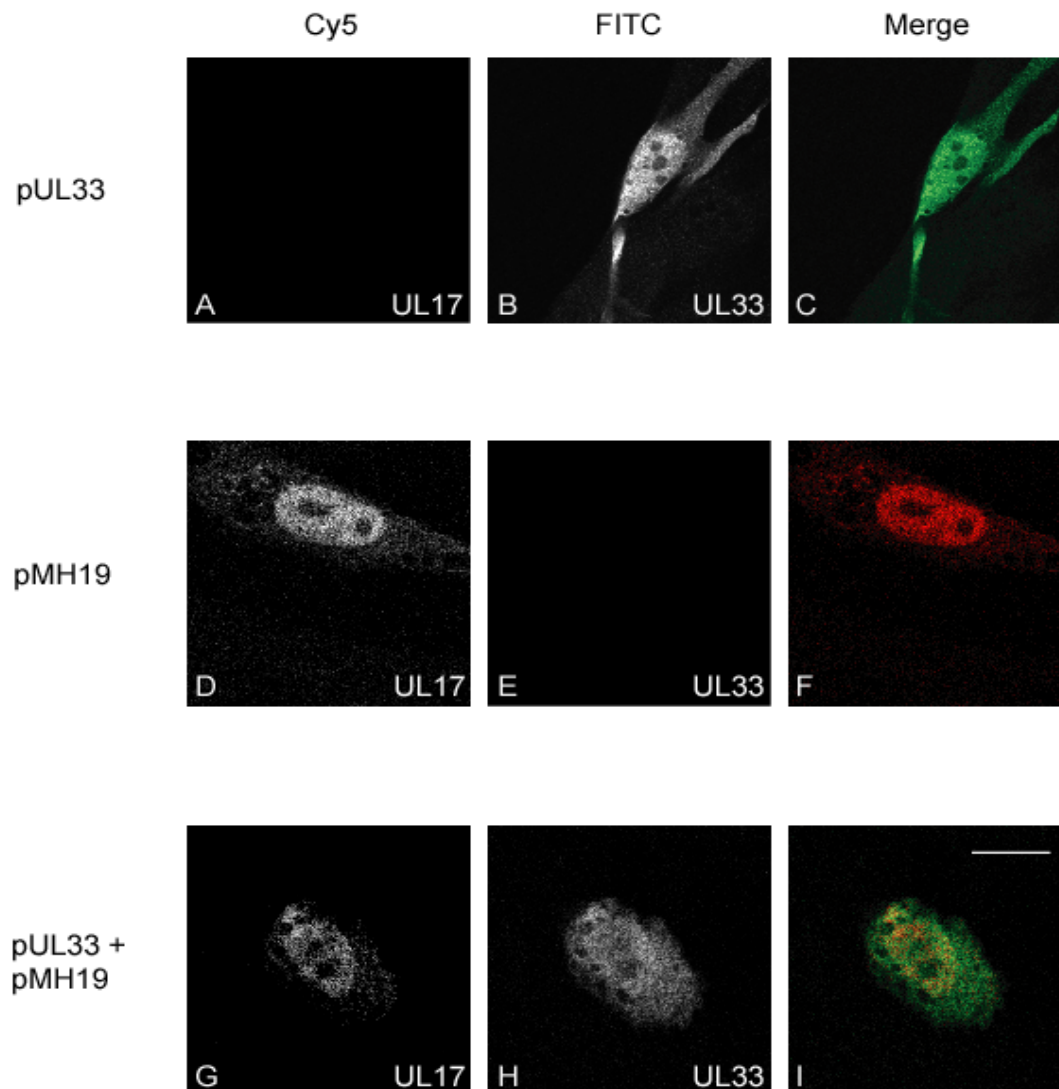


Figure 5.11: Intracellular localisation of UL17 and UL33 in transfected cells.

BHK cells were transfected with the indicated plasmids by lipofection. Twenty hours post-transfection, cells were fixed and permeabilised and probed with a mouse anti-UL17 antibody (M203) and R148. Coverslips were incubated with Cy5-coupled anti-mouse and FITC-coupled anti-rabbit antibodies, and analysed by confocal microscopy, with identical settings maintained throughout. The separate channels are shown in grey and a merged image in colour. Scale bar = 20 μ m.

sequence (Ogasawara *et al.*, 2001), it is not known whether UL25 interacts with the terminase components. The next series of experiments therefore examined whether UL25 and UL33 interacted.

5.4.1 Co-immunoprecipitation of UL25 and UL33 from HSV-1 infected cells

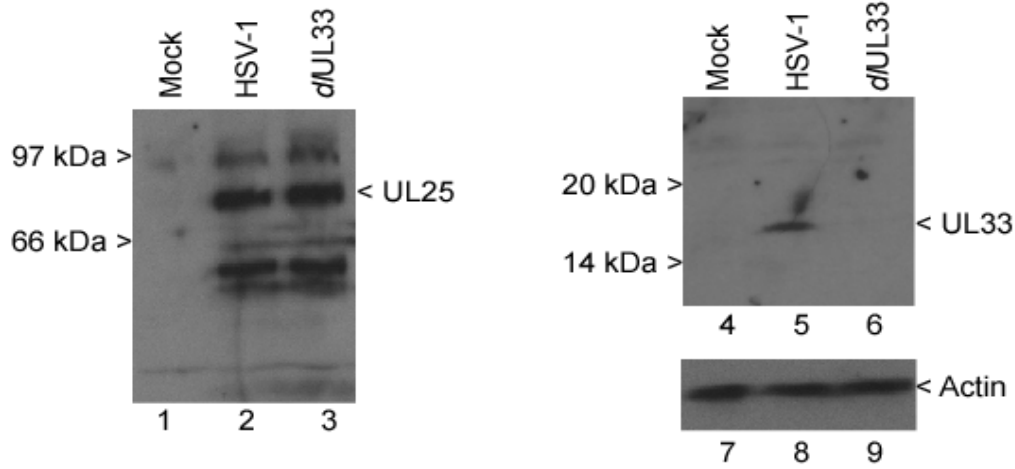
The virally-infected cell lysates described previously (4.2.2) were analysed by immunoprecipitation to ascertain whether UL25 was precipitated with UL33. Immune complexes precipitated by R148 were resolved by western blotting and the membranes probed with either R148 or a rabbit anti-UL25 antibody, R335. The resulting immunoblots are shown in **Figure 5.12**. Lanes 4-9 of panel A and 4-6 of panel B, showing the UL33 and actin controls, were discussed in section 4.2.2 and also presented in Figure 4.2.

UL25 was efficiently detected by R335 in the lysates of cells infected with HSV-1 and *d*UL33, but not from mock-infected cells (panel A; lanes 1-3). Moreover, R148 co-precipitated UL33 and UL25 from HSV-1-infected cells (panel B; lanes 2 and 5). Neither UL33 nor UL25 was precipitated from *d*UL33-infected or mock-infected cells (panel B; lanes 1, 3, 4 and 6). These data suggested that UL25 was present in complexes containing UL33 and precipitated by R148.

5.4.2 Co-immunoprecipitation of UL25 and UL33 in recombinant baculovirus-infected insect cells

To examine whether UL25 and UL33 interacted in the absence of other HSV-1 proteins, immunoprecipitation analysis was carried out on insect cells infected with AcUL33 and AcUL25 (expressing UL25 under the control of the AcMNPV polyhedrin promoter) alone, or in combination. Infected cell lysates were incubated with either R148 or R335, and immune complexes analysed by western blotting (**Figure 5.13**). R148 precipitated

A. Extract prior to immunoprecipitation



B. Immunoprecipitation with R148

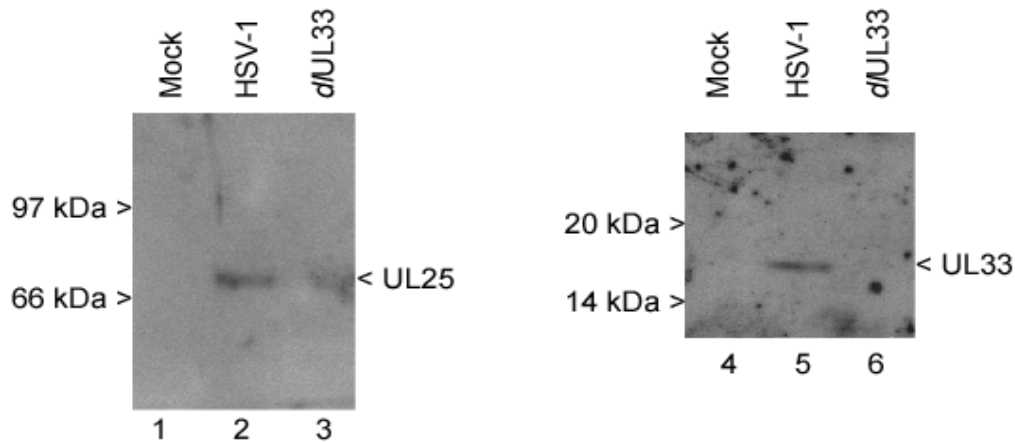


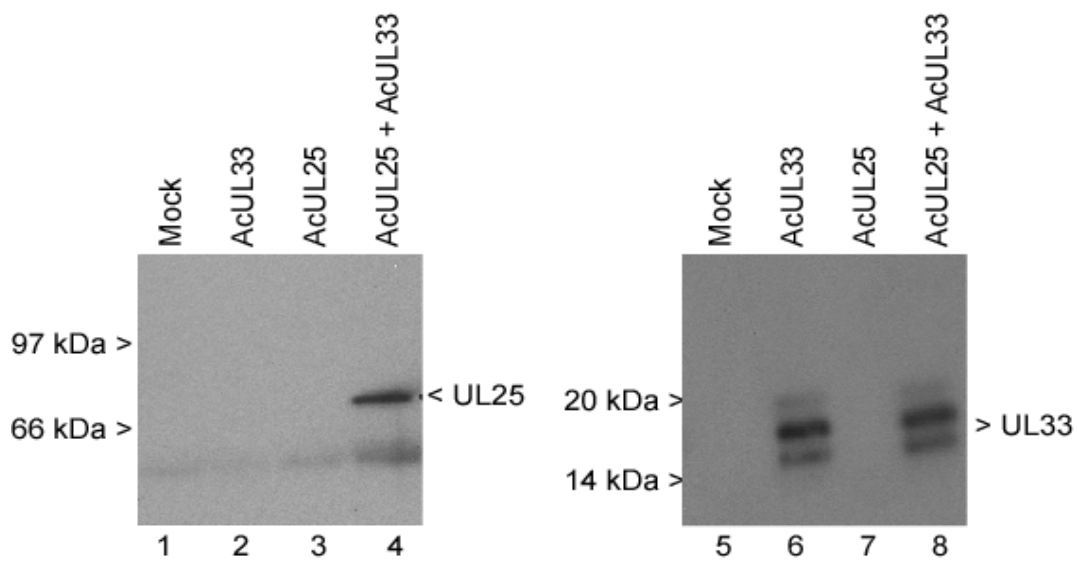
Figure 5.12: Co-immunoprecipitation of UL25 and UL33 from HSV-1-infected cells.

The soluble extracts and immunoprecipitates from mock-infected, HSV-1-infected and Δ UL33-infected BHK cells described in Figure 4.2 were used.

A. Samples of extract prior to immunoprecipitation were separated by SDS-PAGE on an 8% polyacrylamide gel, proteins transferred to a PVDF membrane, and detected with R335 (lanes 1-3), R148 (lanes 4-6) or anti-actin antibody (lanes 7-9). Note that the controls (lanes 4-9) are the same as shown in Figure 4.2.

B. Samples of the immune complexes precipitated by R148 (Figure 4.2) were resolved on an 8% polyacrylamide gel, and the protein species detected with R335 (lanes 1-3) or R148 (lanes 4-6). Note that the UL33 control (lanes 4-6) is that shown in Figure 4.2.

A. Immunoprecipitation with R148



B. Immunoprecipitation with R335

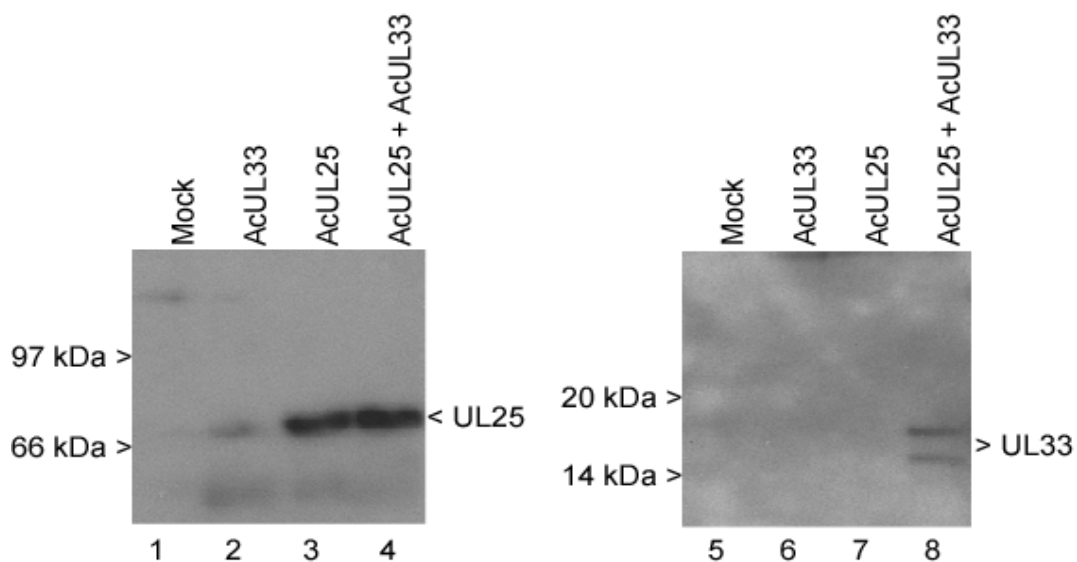


Figure 5.13: Co-immunoprecipitation of UL25 and UL33 from recombinant baculovirus-infected cells.

*Sf*21 cells were mock-infected or infected with the indicated recombinant baculoviruses. Forty-eight hours post infection, cells were lysed and duplicate soluble extracts prepared. **A.** After preclearing with a non-specific rabbit antibody, soluble extracts were incubated with R148, the immune complexes precipitated with protein-A sepharose, and the protein species separated by SDS-PAGE on 8% (left-hand panel) or 15% (right-hand panel) polyacrylamide gels. Proteins were detected by western blotting using R148 (right-hand panel) or R335 (left-hand panel). **B.** Precleared soluble extracts were incubated with R335 and the immune complexes isolated and analysed as in A.

both UL25 and UL33 from cells co-expressing the two proteins (panel A). In addition, R335 was able to co-precipitate UL25 and UL33 from cells receiving both AcUL25 and AcUL33 (panel B). Thus, these results extend the previous finding (Figure 5.12), and indicate that UL25 and UL33 interact in the absence of other viral proteins.

5.4.3 Co-localisation of UL25 and UL33 in transfected cells

To further investigate the ability of UL25 and UL33 to interact in the absence of other HSV-1 proteins, an immunofluorescence assay was used. In this instance BHK cells were transfected with pUL33 or a plasmid expressing UL25 (pIM96), or both plasmids together. Fixed, permeabilised monolayers were incubated with R148 and a mouse anti-UL25 antibody (M166; section 2.1.12), and processed for confocal microscopy.

Representative images are shown in **Figure 5.14**.

Consistent with previous observations, UL33 localised throughout transfected cells, but was present predominantly within the nucleus (panels A-C). UL25 was localised solely to the cytoplasm of expressing cells (panels D and F), and no FITC-specific signal was observed from such cells (panel E). When co-expressed, both proteins were present in the cytoplasm (panels G and H), where they exhibited partial co-localisation (panel I). The restriction of UL33 to the cytoplasm of these cells, and the observed co-localisation, further supports the conclusion that UL25 and UL33 are able to interact.

As with UL28-cMyc and UL6in269, it was conceivable that UL25 may inhibit the nuclear import of proteins when over-expressed. Therefore the localisation of HSV-1 UL9 was examined in the presence of UL25. BHK cells were transfected with pIM96, pE9, or both plasmids together. Proteins were detected using R335 and M13924 in conjunction with the FITC and Cy5 conjugates previously described. Resulting images are shown in

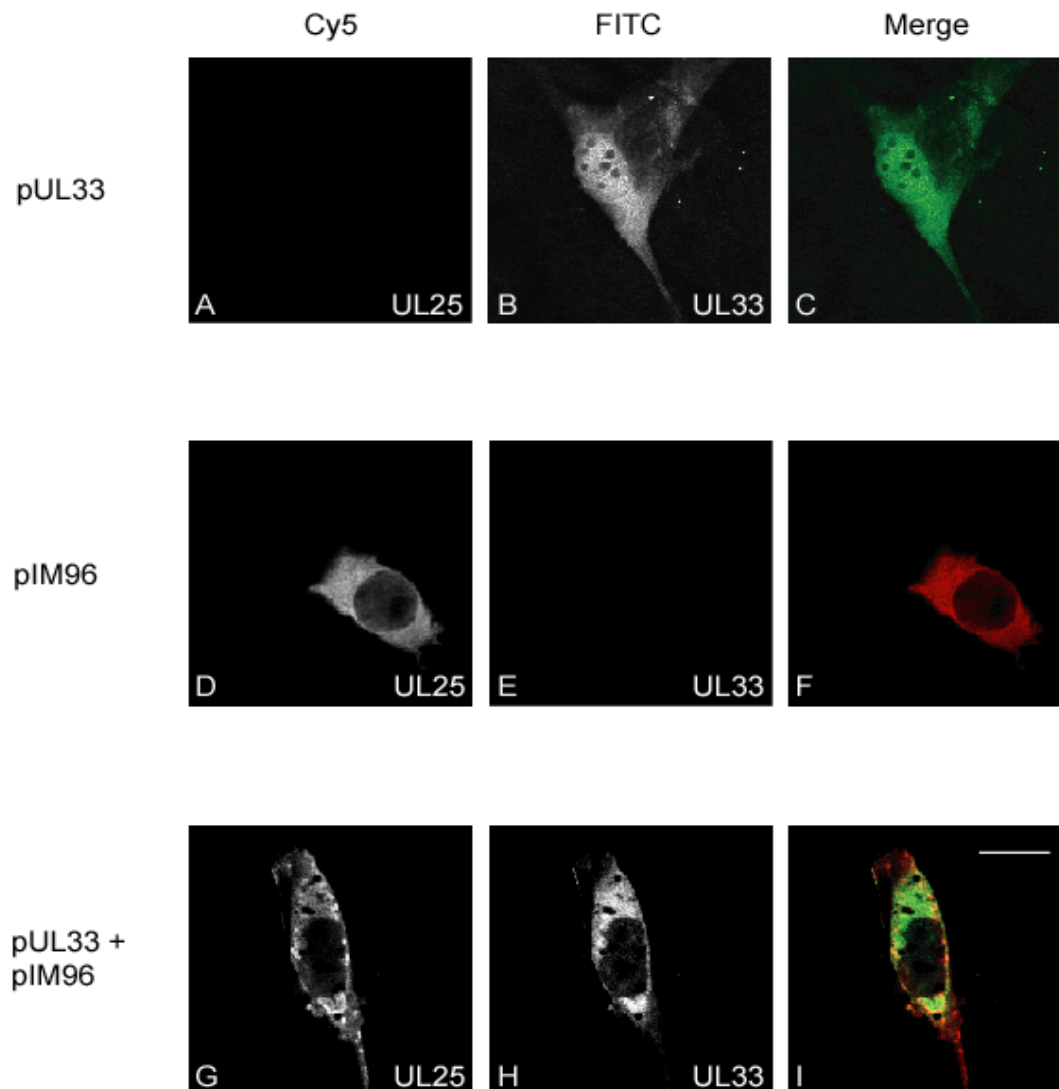


Figure 5.14: Co-localisation of UL25 and UL33 in transfected cells.

BHK cells were transfected with the indicated plasmids by lipofection. Twenty hours post-transfection, cells were fixed and permeabilised with paraformaldehyde and NP40, and probed with a mouse anti-UL25 antibody (M166) and R148. Coverslips were incubated with Cy5-coupled anti-mouse and FITC-coupled anti-rabbit antibodies, and processed for confocal microscopy. Identical settings were maintained throughout, with the separate channels shown in grey and a merged image in colour. Scale bar = 20µm.

Figure 5.15.

When individually expressed, both UL25 and UL9 exhibited the same sub-cellular localisation as previously described, with UL9 localising to the nuclei and UL25 solely within the cytoplasm (panels D-F and A-C respectively). In cells co-expressing both proteins, no change was observed in the localisation of either protein (panels G-I). Thus, the nuclear uptake of proteins was not inhibited by UL25, and the cytoplasmic retention of UL33 by UL25 was therefore considered likely to represent a specific interaction.

5.4.4 Co-localisation of UL25 and mutated UL33 proteins in transfected cells

Similar experiments were performed to analyse the ability of mutated UL33 proteins to interact with UL25. In this case, BHK cells were transfected with plasmids expressing wt or mutated UL33 proteins together with pIM96. Resultant images are shown in **Figure 5.16**, and are representative of the phenotype exhibited by all of the mutants examined. When wt UL33 and UL25 were co-expressed, UL33 was restricted to the cytoplasm as observed previously (panel B), and partially co-localised with UL25 (panels A and C). All of the mutated versions of UL33 exhibited a similar phenotype whereby UL33 localised to the cytoplasm (represented by in14, in37, in100 and in116 in panels D, G, J and M) and co-localised with UL25 (panels F, I, L and O). This therefore suggested that none of the mutated UL33 polypeptides was affected in its ability to co-localise with UL25.

Section 5.5 Interactions of UL33 with UL32

Similar approaches were used to determine whether UL33 was able to interact with the HSV-1 UL32 protein.

5.5.1 Immunoprecipitation of UL32 and UL33 from HSV-1-infected cells

Initially, immunoprecipitation analysis was carried out on the virus-infected cell lysates

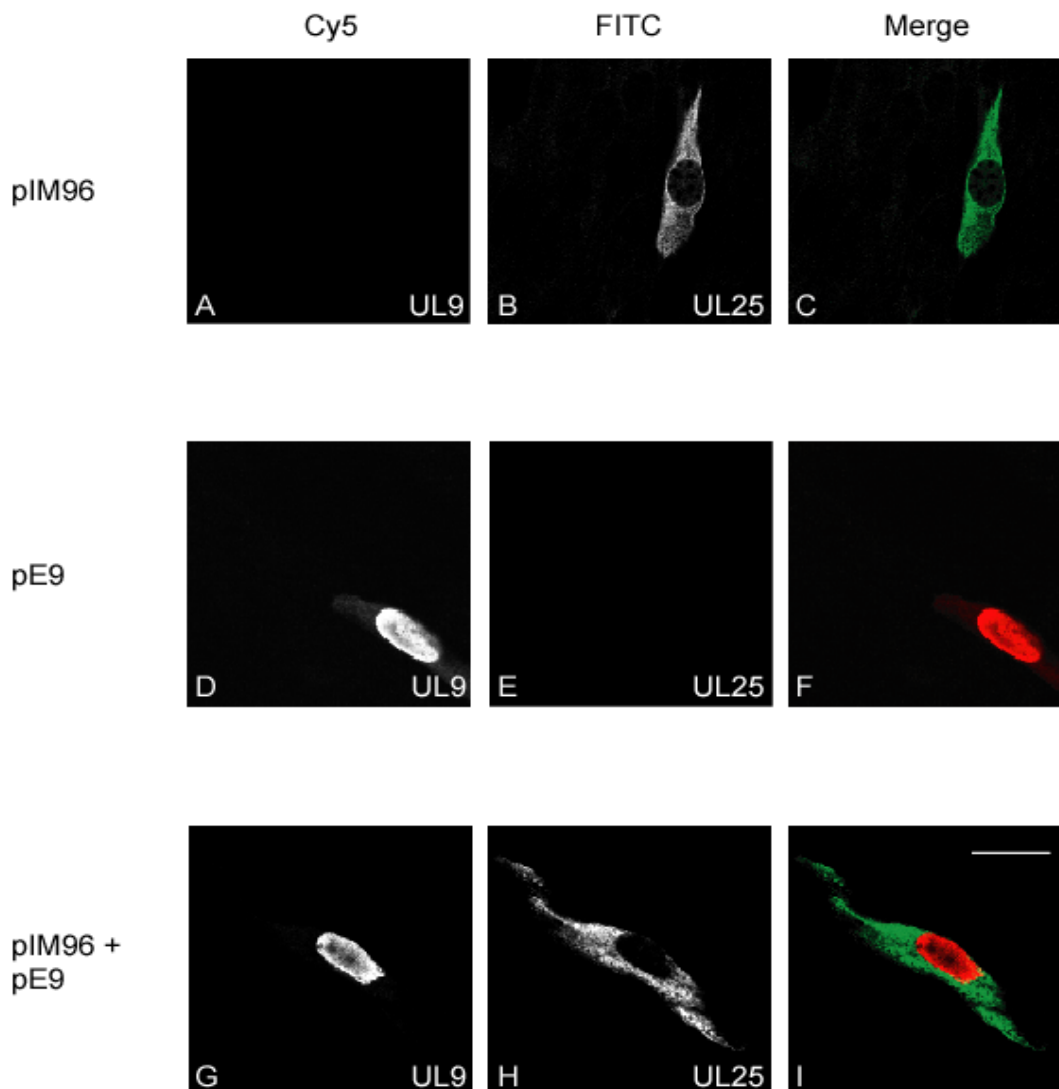


Figure 5.15: Intracellular localisation of UL25 and UL9 in transfected cells.

BHK cells were transfected with the indicated plasmids by lipofection. Twenty hours post-transfection, cells were fixed and permeabilised with paraformaldehyde and NP40, and probed with M13924 and R335. Coverslips were incubated with Cy5-coupled anti-mouse and FITC-coupled anti-rabbit antibodies, and processed for confocal microscopy. Identical settings were maintained throughout, with the separate channels shown in grey and a merged image in colour. Scale bar = 20 μ m.

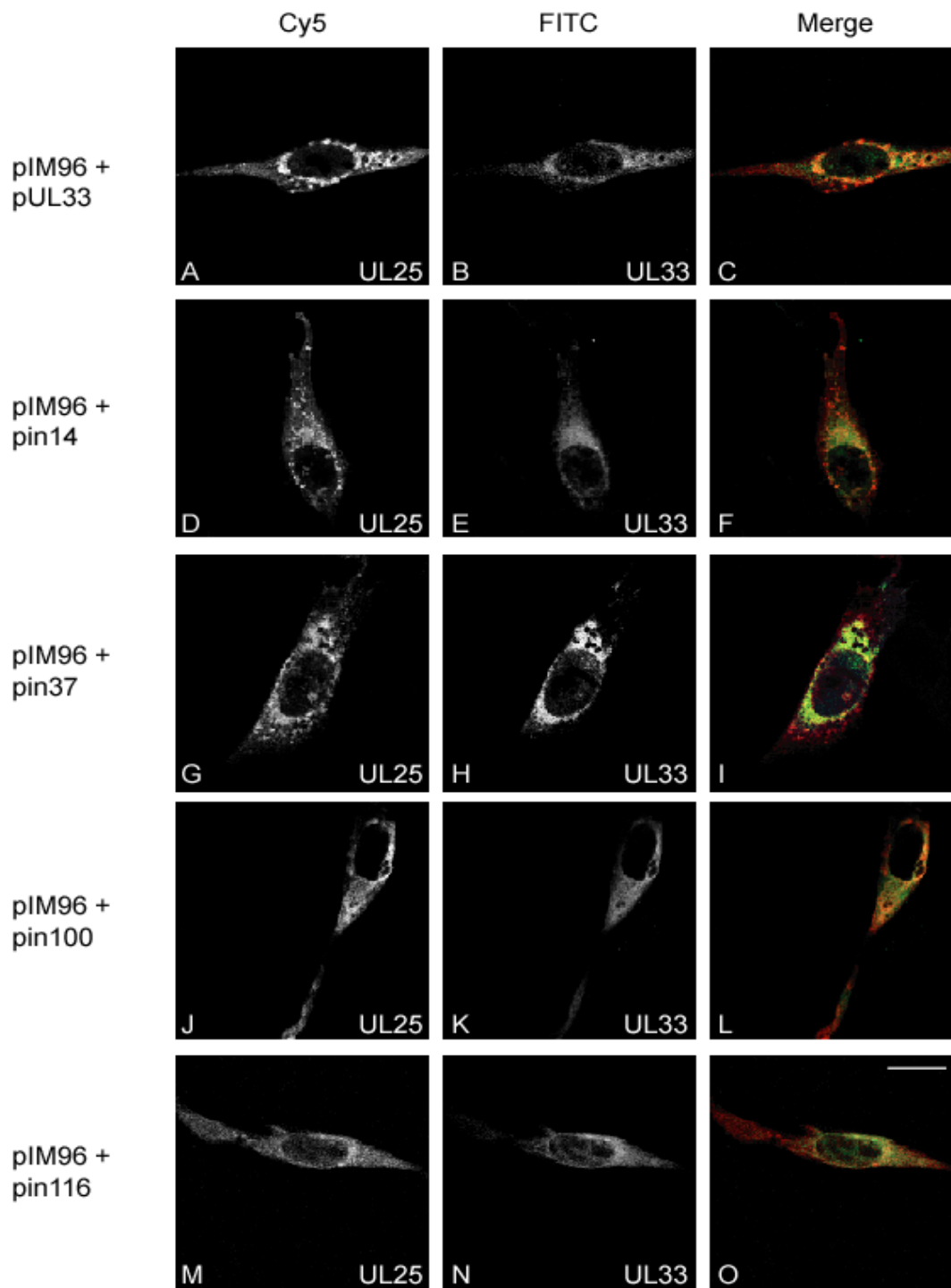


Figure 5.16: Co-localisation of UL25 and mutated UL33 proteins in transfected cells.

BHK cells were transfected with the indicated plasmids by lipofection. Cells were treated as described in the legend to Figure 5.14, and analysed by confocal microscopy. Images are representative of all of the mutants examined. Identical settings were maintained throughout, with individual channels shown in grey and a merged image in colour. Scale bar = 20 μ m.

detailed in section 4.2.2. Protein complexes precipitated by R148 were isolated and analysed by western blotting. Membranes were probed with R148 or a rabbit anti-UL32 antibody, RC12 (section 2.1.12), and the immunoblots are shown in **Figure 5.17**. Lanes 4-9 of panel A and 4-6 of panel B, showing the UL33 and actin controls, were presented in Figure 4.2 and discussed in section 4.2.2. UL32 was detected by RC12 in both HSV-1- and *d*UL33-infected cells (panel A; lanes 1-3). However, no UL32 was detected in immune complexes precipitated by R148 (panel B; lanes 1-3), suggesting that UL33 and UL32 do not interact in HSV-1 infected cells.

5.5.2 Immunoprecipitation of UL32 and UL33 from baculovirus-infected insect cells

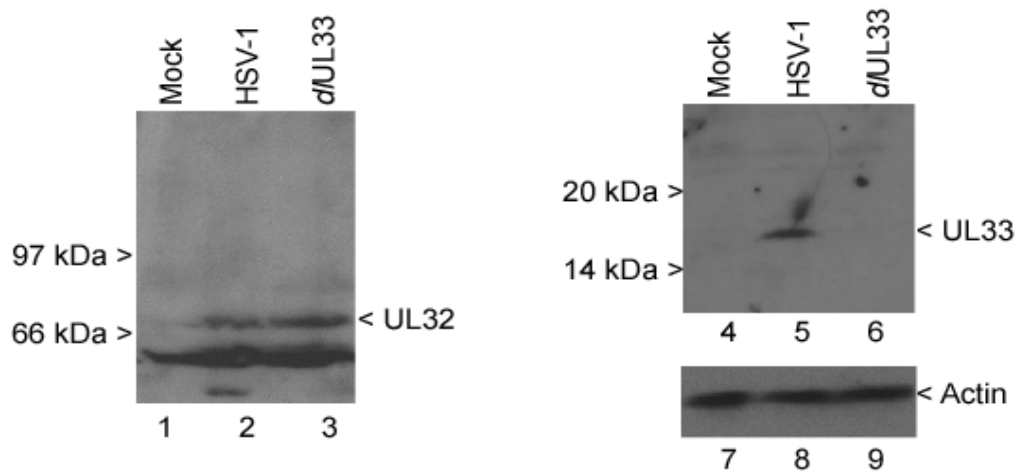
Potential interactions between UL33 and UL32 were also examined by immunoprecipitation of baculovirus-expressed proteins. *Sf*21 monolayers were infected with AcUL33 or AcUL32 (expressing UL32 under the control of the AcMNPV polyhedrin promoter), or both viruses together. Infected cell lysates were incubated with RC12 or R148 and the immune complexes collected and analysed by western blotting. The resulting immunoblots are shown in Error! Reference source not found..

Whilst both UL32 and UL33 were efficiently precipitated by their cognate antibodies (panel A; lanes 5-8 and panel B; lanes 1-4 respectively), no UL32 was apparent in complexes precipitated by R148 (panel A; lanes 1-4). Furthermore, no UL33 was detected in RC12-precipitated complexes (panel B; lanes 5-8). Together, these data support the conclusion that UL32 and UL33 do not interact.

5.5.3 Sub-cellular localisation of UL32 and UL33 in transfected cells

Immunofluorescence experiments were also carried out to examine the sub-cellular localisation of UL33 in conjunction with UL32. BHK cells were transfected as before

A. Extract prior to immunoprecipitation



B. Immunoprecipitation with R148

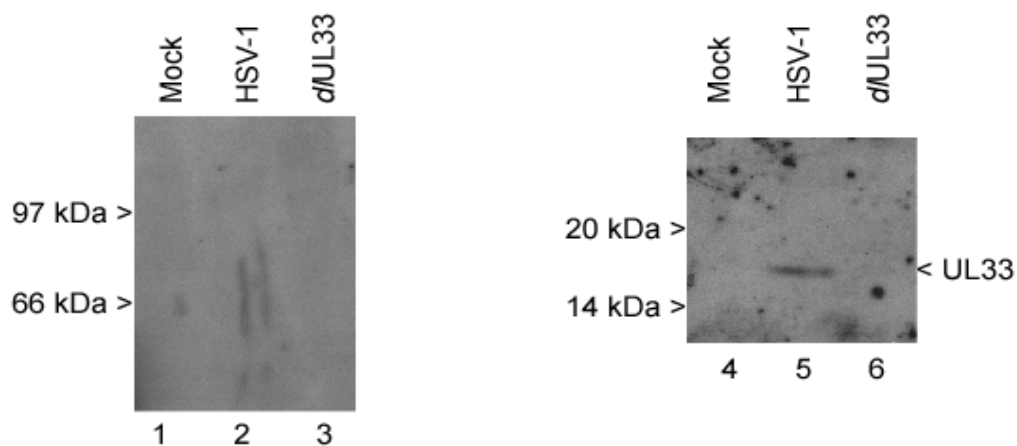


Figure 5.17: Immunoprecipitation of UL32 and UL33 from HSV-1-infected cells.

The soluble extracts and immunoprecipitates from mock-infected, HSV-1-infected and *dUL33*-infected BHK cells described in Figure 4.2 were used.

A. Samples of extract prior to immunoprecipitation were separated by SDS-PAGE on an 8% polyacrylamide gel, proteins transferred to a PVDF membrane, and detected with RC12 (lanes 1-3), R148 (lanes 4-6) or anti-actin antibody (lanes 7-9). Note that the controls (lanes 4-9) are the same as shown in Figure 4.2.

B. Samples of the immune complexes precipitated by R148 (Figure 4.2) were resolved on an 8% polyacrylamide gel, and the protein species detected with RC12 (lanes 1-3) or R148 (lanes 4-6). Note that the UL33 control (lanes 4-6) is that shown in Figure 4.2.

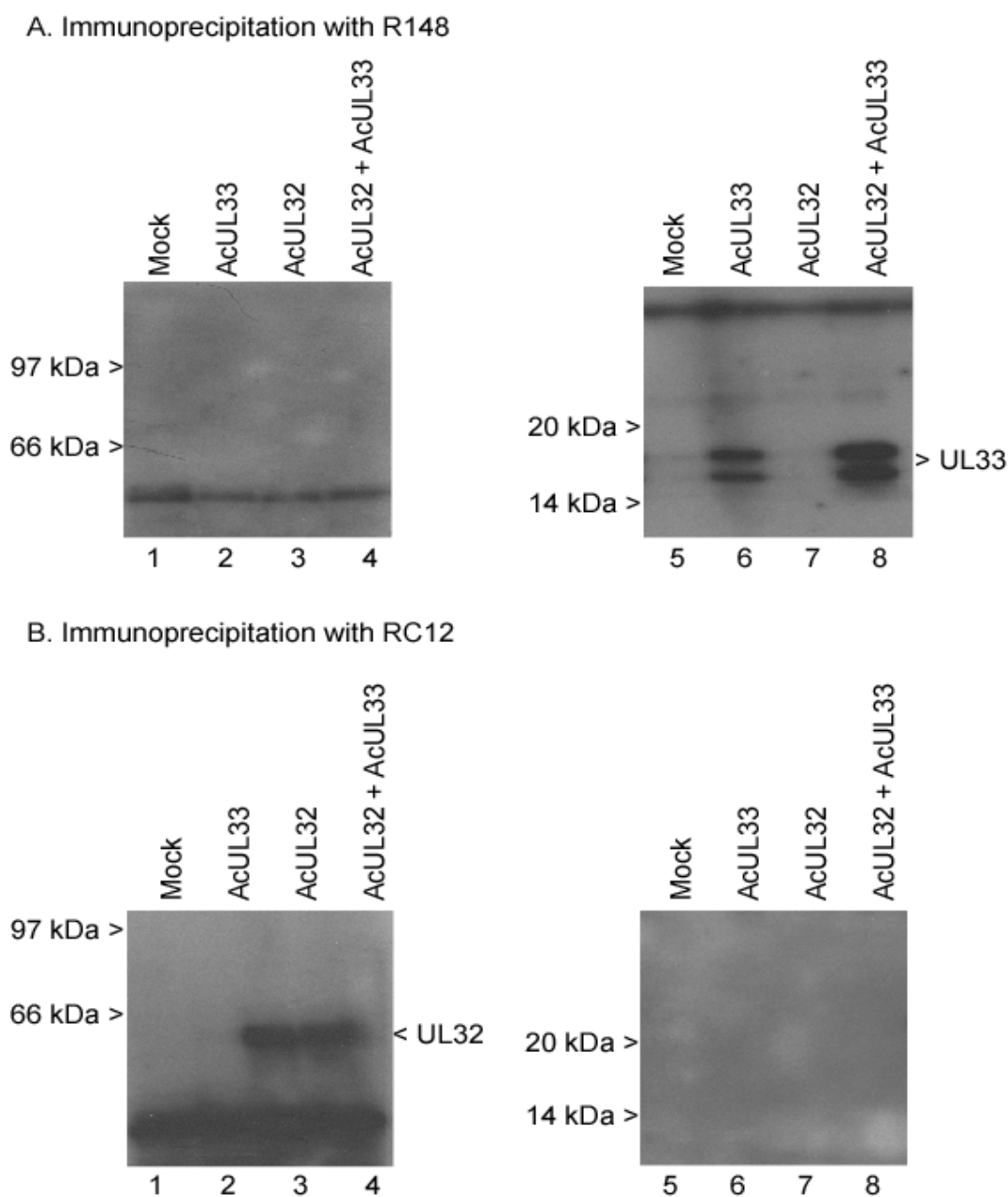


Figure 5.18: Immunoprecipitation of UL32 and UL33 from recombinant baculovirus-infected cells.

Sf21 cells were mock-infected or infected with the indicated recombinant baculoviruses. Forty-eight hours post infection, cells were lysed and duplicate soluble extracts prepared. **A.** After preclearing with a non-specific rabbit antibody, soluble extracts were incubated with R148, the immune complexes precipitated with protein-A sepharose, and the protein species separated by SDS-PAGE on 8% (left-hand panel) or 15% (right-hand panel) polyacrylamide gels. Proteins were detected by western blotting using R148 (right-hand panel) or RC12 (left-hand panel). **B.** Precleared soluble extracts were incubated with RC12 and the immune complexes isolated and analysed as in A.

with pUL33 or pUL32 (encoding UL32 under the HCMV MIEP), either individually or together. Fixed and permeabilised cells were incubated with RC12 and a mouse anti-UL33 antibody, M51(4) (section 2.1.12). The FITC and Cy5 conjugates described previously were used to simultaneously detect UL32 and UL33 respectively. Resultant images obtained by confocal microscopy are shown in **Figure 5.19**.

As observed previously using R148, UL33 localised throughout transfected cells and no background signal was apparent in the FITC channel (panels D-F). UL32 was localised solely to the cytoplasm of transfected cells (panels A and C), consistent with the predominantly cytoplasmic localisation of UL32 described previously (Chang *et al.*, 1996; Lamberti & Weller, 1998). In cells transfected with pUL32 and pUL33, the localisation of both proteins was unchanged (panels G-I) i.e. UL32 in the cytoplasm and UL33 throughout the cell. Thus, unlike UL28-cMyc, UL25 and UL6in269, UL32 was unable to retain wt UL33 in the cytoplasm when over-expressed. These data therefore confirm that UL32 and UL33 are unable to interact.

Section 5.6 Discussion

5.6.1 UL33 interacts with UL6

Immunoprecipitation and immunofluorescence experiments demonstrated a novel interaction between UL33 and the HSV-1 portal protein UL6. The anti-UL33 antibody R148 was able to co-precipitate UL6 and UL33 from HSV-1-infected cells, and from insect cells mixedly infected with baculoviruses expressing UL6 and UL33. It was evident that this interaction required neither UL15 nor UL28, suggesting that UL33 and UL6 interact directly. Thus, including previous observations for UL15 and UL28 (White *et al.*, 2003), UL6 is able to interact separately with all three subunits of the putative terminase.

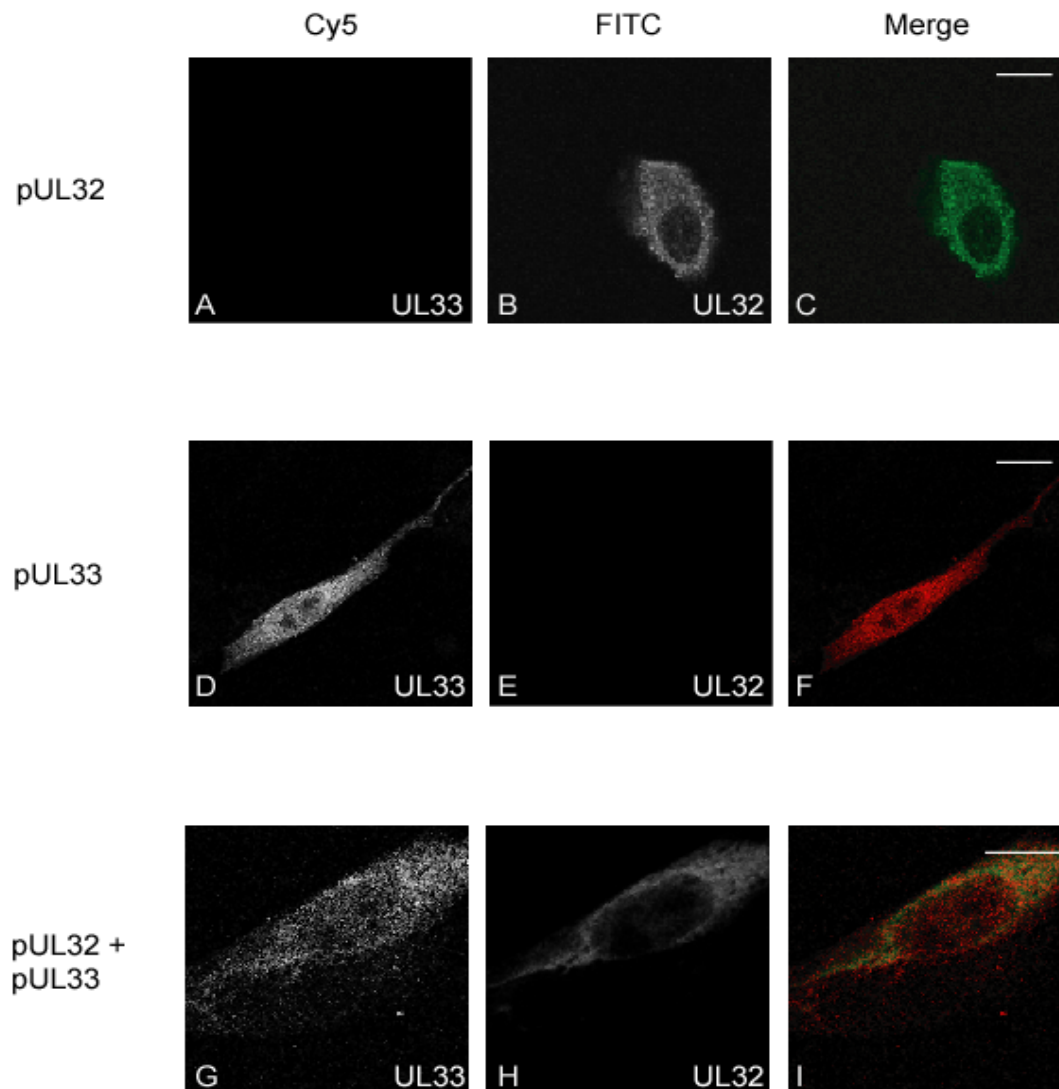


Figure 5.19: Intracellular localisation of UL32 and UL33 in transfected cells.

BHK cells were transfected with the indicated plasmids by lipofection. Twenty hours post-transfection, cells were fixed and permeabilised with paraformaldehyde and NP40, and probed with a mouse anti-UL33 antibody (M51(4)) and RC12. Coverslips were incubated with Cy5-coupled anti-mouse and FITC-coupled anti-rabbit antibodies, and processed for confocal microscopy. Identical settings were maintained throughout, with the separate channels shown in grey and a merged image in colour. Scale bars = 20 μ m.

Wild type UL6 and UL33 proteins co-localised in the nucleus of transfected cells.

Although it is unclear whether the two proteins initially interact in the nucleus or the cytoplasm, it was evident that UL33 is retained in the nucleus when co-expressed with UL6. In a small proportion of cells, some UL33 was evident in the cytoplasm (e.g. panel L of Figure 5.4). This may represent a population of cells in which more UL33 was expressed relative to UL6. Thus, UL6 might become 'saturated' with UL33, and excess UL33 would be able to spread throughout the cell.

Immunofluorescence studies demonstrated that the cytoplasmic mutant UL6in269 retained UL33 within the cytoplasm of transfected cells, strengthening the conclusion that UL6 and UL33 interact. Similarly, UL33-His₆, which is more cytoplasmic than wt UL33 when expressed alone, restricted UL6 to the cytoplasm, consistent with an interaction between the two proteins. The reason why UL33-His₆ is more cytoplasmic than its wt counterpart is unknown, but may reflect a change in the size, charge or folding of the tagged protein that precludes nuclear import. Since UL33-His₆ is capable of supporting DNA packaging, both itself and UL6 are presumably capable of nuclear uptake in the context of a viral infection.

Immunofluorescence experiments demonstrated that all of the UL33 insertional mutants interacted with both wt UL6 and UL6in269. Further experiments demonstrated that both $\Delta 1$ and $\Delta 2$ were retained in the cytoplasm by UL6in269 (data not shown). No correlation was therefore observed between the ability of mutants to support DNA packaging and their ability to interact with UL6, and it remains unclear whether interaction between UL6 and UL33 is necessary for DNA packaging. The ability of all the mutants to bind to UL6 meant it was also not possible to identify any specific regions

of UL33 required for the interaction. Immunoprecipitation experiments with the baculovirus-expressed mutated UL33 proteins detailed in section 4.3.3 could provide further information in support of this conclusion. The possible role of the UL6-UL33 interaction is discussed in Chapter 7:

5.6.2 UL33 interacts with UL25

Immunoprecipitation and immunofluorescence results demonstrated that UL33 was able to interact with the HSV-1 DNA packaging protein UL25, both in the presence and absence of the other HSV-1 packaging proteins. The UL33 antibody R148 co-precipitated UL25 from HSV-1-infected BHK cells, and from *Sf*21 cells infected with AcUL25 and AcUL33. UL25 also restricted UL33 to the cytoplasm of co-transfected BHK cells in a specific manner, although the proteins did not precisely co-localise (Figure 5.14). These data provide the first evidence of an interaction between UL33 and UL25.

Immunofluorescence analysis of UL33 insertion mutants suggested that all 16 mutants interacted with UL25, as all were restricted to the cytoplasm when expressed with UL25. In similar experiments, both $\Delta 1$ and $\Delta 2$ were also able to interact with UL25 (data not shown). No correlation was therefore evident between the ability of mutants to interact with UL25, and their ability to support DNA packaging and mutant virus growth. As before, it would be useful to confirm these findings in co-immunoprecipitation experiments.

Cryo-electron microscopy studies of HSV-1 A- and C-capsids led to the suggestion that UL17 and UL25 form a C-capsid specific heterodimer (CCSC) spanning two triplexes on

the outer capsid surface (Cardone *et al.*, 2007). As shown in **Figure 5.20**, fitting of the N-terminally-truncated UL25 crystal structure (Bowman *et al.*, 2006) into the CCSC led to the suggestion that UL25 occupies a position within the CCSC distal to the nearest penton (Cardone *et al.*, 2007). It can be envisaged that if UL25 also occupies a similar position near the portal vertex, then the proximity of UL6 and UL25 may permit UL33 to interact with both proteins simultaneously. It is feasible that this could act to stabilise the interaction between the terminase and the capsid, or enhance the activity of terminase during the latter stages of encapsidation, as proposed by Stow (2001). Given that UL25 is present in greater amounts in C-capsids than B-capsids or procapsids (Sheaffer *et al.*, 2001), and seems to function during the latter stages of packaging (McNab *et al.*, 1998; Hodge & Stow, 2001), it is also possible that UL33 may play a role in its recruitment to capsids late during packaging. The observed interaction may also reflect the ability of free (i.e. non-terminase associated) UL33 to bind UL25.

It should be noted that the over-expression of UL6, UL25 and UL33 may contribute to some of the results obtained. Data from the immunoprecipitation of baculovirus-expressed proteins, and the examination of transfected cells by confocal microscopy, cannot exclude this possibility, as both involve proteins expressed under the control of strong promoters. The observed precipitation of UL6 and UL25 by R148 from HSV-1 infected cells (Figure 5.1 and Figure 5.12) supports the proposal that the two proteins interact with UL33, although these could be indirect interactions mediated by other proteins. However, it is unlikely that whole capsids were precipitated by R148, as both the capsid-associated UL17 protein and the major capsid protein VP5 were absent from the immune complexes (Figure 5.9 and data not shown). At present, a possible role for nucleic acid in mediating these interactions has not been excluded, although neither UL6 nor UL33 has been reported to exhibit any nucleic acid binding activity. Moreover, the

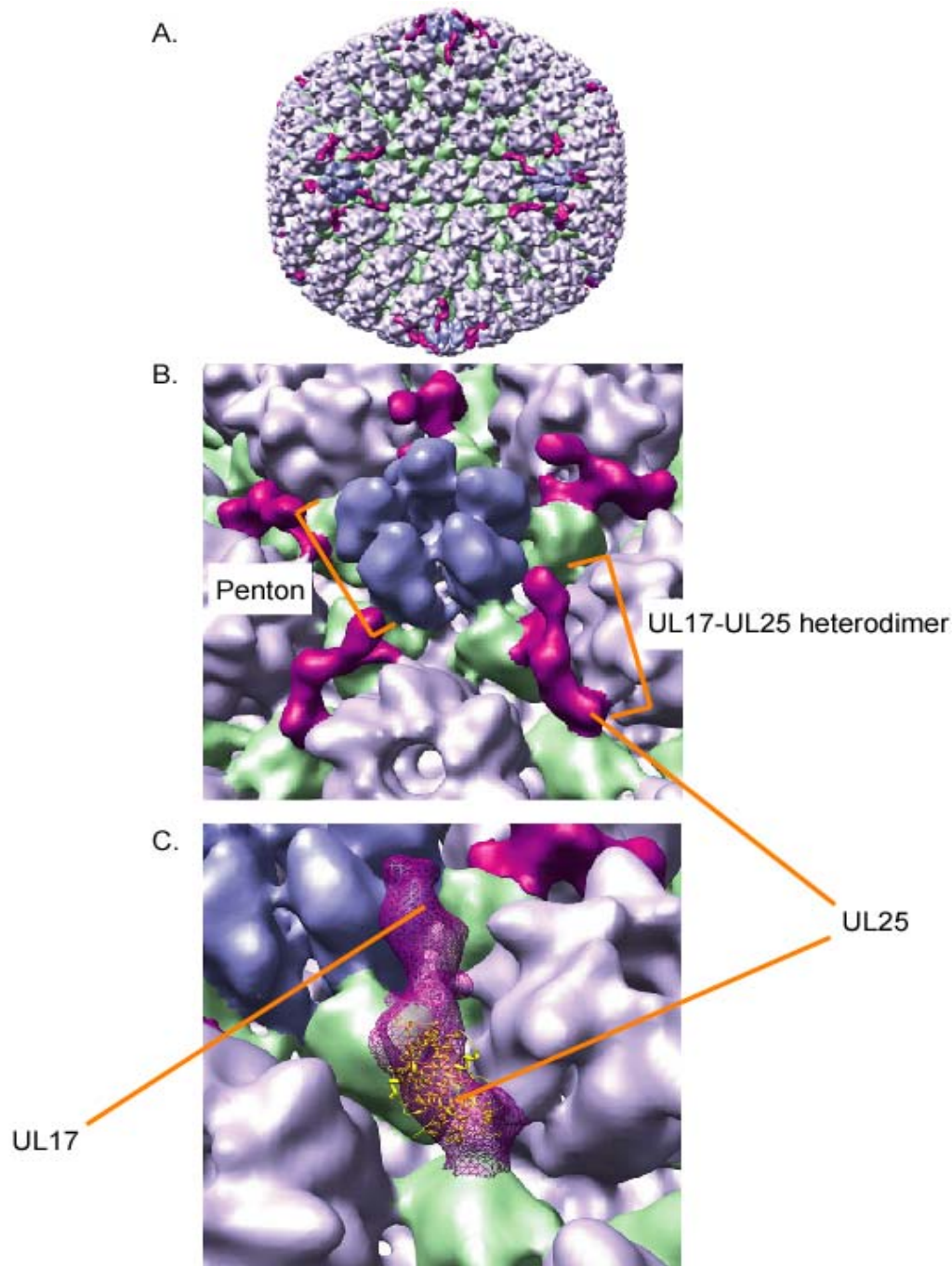


Figure 5.20: The location of the proposed UL17-UL25 heterodimer on C-capsids (from Trus *et al.*, 2007)

A. Surface rendering of a cryo-electron microscopy reconstruction of an HSV-1 C-capsid. Pentons are shown in blue, hexons in purple and the triplex proteins in green. The C-capsid specific component (CCSC) is in magenta.

B. shows a close-up view of the region surrounding a penton, with the penton and CCSC labelled. UL25 is thought to be distal to the penton.

C. Optimal forced fit of the UL25 crystal structure (yellow; Bowman *et al.*, 2005) into the CCSC.

reported UL25 DNA binding activity (Ogasawara *et al.*, 2001) was not confirmed in gel shift assays (N. Stow, unpublished results).

5.6.3 UL33 interacts with neither UL17 nor UL32

Results from immunoprecipitation studies suggested that wt UL33 does not detectably interact with either UL17 or UL32 in either HSV-1 infected cells or insect cells infected with recombinant baculoviruses. Since reciprocal immunoprecipitations were performed, and polyclonal antibodies used, it is unlikely that masking of epitopes was responsible for the observed absence of co-precipitation. The unaltered immunofluorescence patterns in co-transfected cells expressing UL17 plus UL33, or UL32 plus UL33, are also consistent with UL33 not interacting with either UL17 or UL32.

Global yeast-2-hybrid screens of the proteins encoded by three human herpesviruses (KHSV, VZV and EBV) have identified several interactions involving proteins homologous to HSV-1 UL33 (summarised in **Table 5.1**). The VZV homologue of UL33 interacted with itself and 35 other viral proteins, whilst the homologous KSHV protein interacted with itself and 10 other viral polypeptides (Uetz *et al.*, 2006). No interactions were detected involving the EBV UL33 homologue, BFRF1A (Calderwood *et al.*, 2007). The absence of interaction between UL33 and UL17 in my studies (Figure 5.9-Figure 5.11) conflicts with the findings of Uetz *et al.* (2006), who demonstrated that the VZV homologues of these proteins interacted in a yeast-2-hybrid screen. However, similar experiments did not reveal an interaction between the EBV homologues of these proteins, in agreement with my data (Calderwood *et al.*, 2007).

In summary, the results presented in this chapter demonstrate two novel interactions; between UL33 and UL6, and between UL33 and UL25. However, none of the UL33

mutants was defective in either interaction. It was therefore not possible to identify specific regions of UL33 that might be involved in these interactions, or to provide evidence that these interactions were essential for DNA packaging or virus growth. One possible explanation is that the region(s) of UL33 required for these interactions are quite small (<10 aa), and lie outside any of the insertions. It is also possible that more than one region of UL33 contacts each of these proteins, and that these regions are functionally redundant in the assays used (i.e. binding can still occur if one of these sites is interrupted). Finally, it is conceivable that some of the UL33 mutants might lose their ability to interact with either UL6 or UL25 in the presence of UL15 or UL28, or in the context of viral infection.

VZV Orf 25 (UL33) interacts with: (Uetz <i>et al.</i>, 2006)		KSHV Orf 67A (UL33) interacts with: (Uetz <i>et al.</i>, 2006)	EBV BFRF1A (UL33) interacts with: (Calderwood <i>et al.</i>, 2007)
Orf 1 ‡	Orf 39 (UL20)	Orf 9 (UL30)	No interactions identified
Orf 2 ‡	Orf 41 (UL18)	Orf 23 (UL21)	
Orf 3 (UL55)	Orf 42 (UL15)	Orf 29b (UL15)	
Orf 8 (UL50)	Orf 43 (UL17)	Orf 31 ‡	
Orf 9a (UL49a)	Orf 44 (UL16)	Orf 34 ‡	
Orf 12 (UL46)	Orf 49 (UL11)	Orf 59 (UL42)	
Orf 15 (UL43)	Orf 50 (UL10)	Orf 60 (UL40)	
Orf 18 (UL40)	Orf 51 (UL9)	Orf 63 (UL37)	
Orf 19 (UL39)	Orf 52 (UL8)	Orf 67.5 (UL33)	
Orf 24 (UL34)	Orf 53 (UL5)	Orf 69 (UL31)	
Orf 25 (UL33)	Orf 56 (UL4)	Orf 75 ‡	
Orf 27 (UL31)	Orf 57 ‡		
Orf 30 (UL28)	Orf 59 (UL2)		
Orf 32 ‡	Orf 64 (US10)		
Orf 33 (UL26)	Orf 65 (US9)		
Orf 33.5 (UL26.5)	Orf 67 (US7)		
Orf 36 (UL23)	Orf 68 (US8)		
Orf 38 (UL21)	S/L (UL56)		

Table 5.1: A summary of previously identified protein-protein interactions

involving UL33 homologues from EBV, KSHV and VZV. Interactions involving the UL33 homologues of KSHV and VZV (Uetz *et al.*, 2006) and of VZV (Calderwood *et al.*, 2007), identified by Y2H screening, are summarised above. The names of the homologous genes of HSV-1 are given in brackets where appropriate. ‡ indicates that the interacting partner has no known

Chapter 6: The localisation of terminase proteins to viral replication compartments

Section 6.1 Introduction

During HSV-1 infection, viral genomes, together with viral and cellular proteins, form discrete nuclear complexes known as replication compartments (RCs) that are the sites of viral DNA synthesis (see section 1.2.7). Due to its close association with viral replication forks, the ssDNA-binding protein ICP8, involved in DNA replication, has seen widespread use as a marker for RCs (Quinlan *et al.*, 1984). In addition, capsid assembly and DNA packaging is thought to occur in RCs, as both capsid components and DNA packaging proteins co-localise with ICP8 in infected cells (de Bruyn Kops *et al.*, 1998; Lamberti & Weller, 1998; Taus *et al.*, 1998; Yu & Weller, 1998a).

Several studies have previously examined the localisation of the HSV-1 terminase proteins during infection. UL15 has been observed to co-localise with ICP8 at both early (6 h.p.i) and late (18 h.p.i) times during infection (Ward *et al.*, 1996; Yu & Weller, 1998a). UL33 has similarly been shown to co-localise with ICP8 at late time points (18 h.p.i.) during infection (Reynolds *et al.*, 2000). Although UL28 has not been directly demonstrated to localise to RCs during HSV-1 infection, it does co-localise with UL15 in the nuclei of both transfected cells and HSV-1 infected cells at late times (Abbotts *et al.*, 2000; Yang *et al.*, 2007)

Section 6.2 Visualisation of the terminase proteins in infected cells

Initial immunofluorescence experiments aimed to establish the location of the putative

terminase proteins, and, since DNA packaging is detectable as early as 6 h.p.i. (Lamberti & Weller, 1998), to extend previous observations to these early times after infection.

6.2.1 Visualisation of UL15, UL28 and UL33 in infected cells

To study the localisation of the terminase proteins early after infection, coverslips of BHK cells were mock-infected or infected with 1 p.f.u./cell of HSV-1, and incubated for six hours at 37 °C. After fixation and permeabilisation, cells were incubated in PBS containing 10% human serum for 30 min. To visualise RCs and terminase components simultaneously, cells were incubated with anti-UL15 (R605), anti-UL28 (R123) or anti-UL33 (R148) antibody in conjunction with the mouse anti-ICP8 antibody M7381. Bound antibody was detected using FITC and Cy5 conjugates, and cellular DNA was detected using propidium iodide. Coverslips were examined by confocal microscopy using lasers with excitation lines at 488nm, 633nm and 543nm, corresponding to the excitation wavelength of the FITC, Cy5 and propidium iodide fluors respectively. Representative images are shown in **Figure 6.1**.

As expected, no ICP8-specific signal was observed in mock-infected cells (panels A, G and M), and neither UL15 (panel B), nor UL28 (panel H) nor UL33 (panel N) were evident in these cells. In contrast, in cells receiving HSV-1 discrete nuclear foci of ICP8 were evident, suggesting replication compartments had formed (panels D, J and P). Foci of UL15 (panel E), UL28 (panel K) and UL33 (panel Q) were all detected in HSV-1 infected nuclei, and in each instance co-localised with ICP8 (panels F, L and R respectively).

These results demonstrate that UL15, UL28 and UL33 are all able to localise to RCs

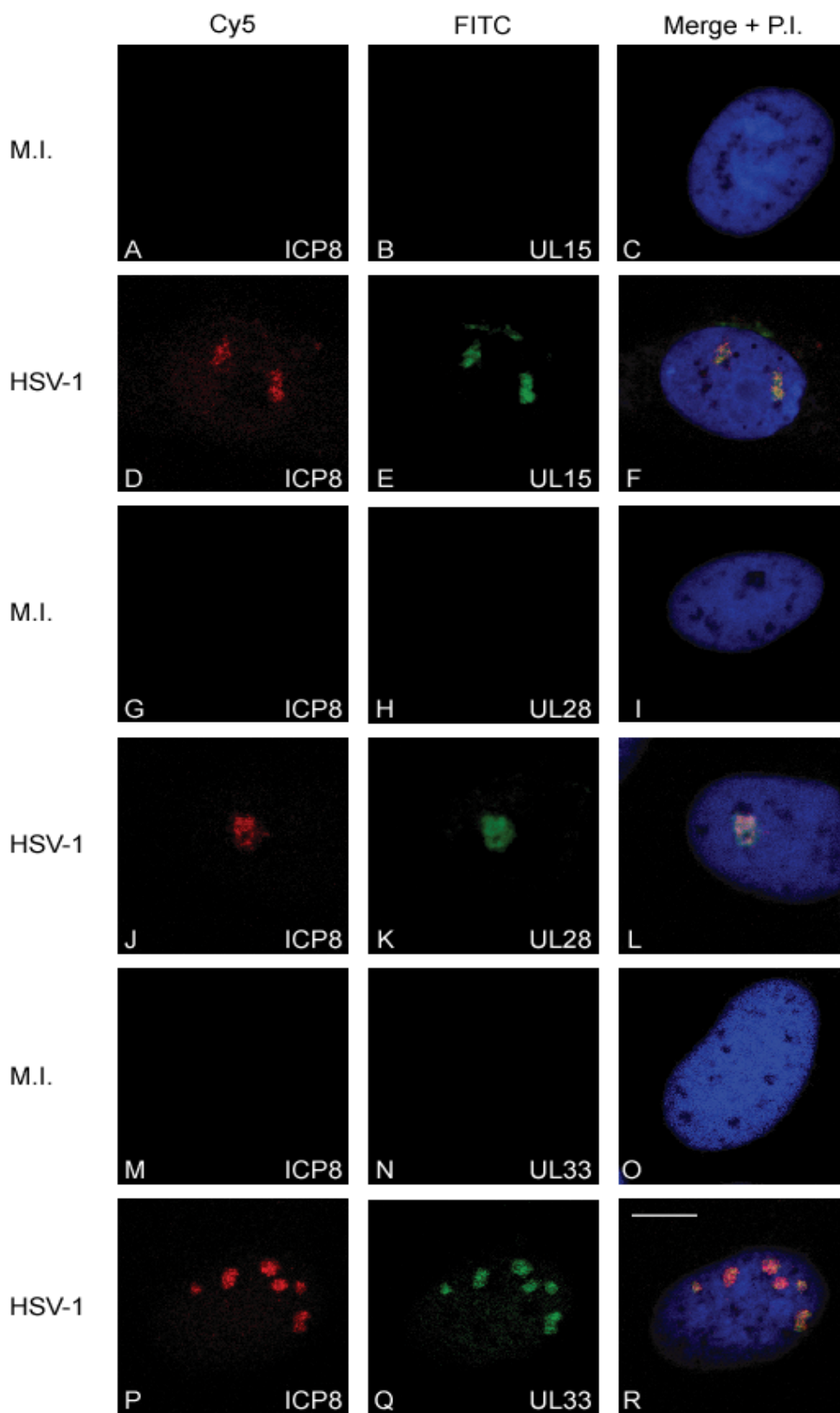


Figure 6.1: Visualisation of the terminase components in HSV-1-infected cells

BHK cells were mock-infected or infected with HSV-1. Six h.p.i. cells were fixed and permeabilised, and incubated with either anti-UL15 (panels A-F), anti-UL28 (panels G-L) or anti-UL33 (panels M-R) antibodies (R605, R123 and R148 respectively) together with an anti-ICP8 antibody (M7381). Coverslips were processed for confocal microscopy, and incubated in propidium iodide prior to mounting. Identical settings were maintained for each antibody combination, with the FITC and Cy5 channels shown separately together with a merged image of all three channels. Scale bar = 10 μ m

early during infection. In addition, the data provide the first direct demonstration that UL28 co-localises with ICP8 during HSV-1 infection, and further support the hypothesis that DNA packaging occurs within RCs, close to sites of viral DNA synthesis.

Section 6.3 Ability of wt and mutated UL33 proteins to localise to RCs

Results presented in chapter 4 and 5 suggested that the inability of several UL33 mutants (in14, in51, in55, in74, in104, in111A, in111B and in116) to support DNA packaging could not be explained by a failure to interact with the UL6, UL15, UL25 and UL28 proteins: thus the basis for these impairments remained unclear. Another possible explanation for their failure to support DNA encapsidation might be a defect in localisation to RCs. Therefore the ability of transiently expressed wt and mutated UL33 polypeptides to localise to viral RCs in *dUL33* infected cells was examined.

6.3.1 Localisation of transiently transfected UL33 in *dUL33*-infected cells

Initially, the ability of transiently expressed wt UL33 to localise to RCs was examined. Coverslips of BHK cells were either mock transfected or transfected with 0.5 µg of pUL33 by lipofection. Six h.p.t. cells were infected with 1 p.f.u./cell of either HSV-1 or *dUL33* respectively, and incubated for a further 6 h at 37 °C. Fixed and permeabilised coverslips were incubated with R148 and M7381, and examined by confocal microscopy. Representative images are shown in **Figure 6.2**.

In agreement with previous experiments, UL33 was detected in discrete foci in HSV-1-infected nuclei (panel B) where it co-localised with ICP8 (panel C). As expected, UL33 was not detectable in cells infected with *dUL33* (panel E), despite the formation of

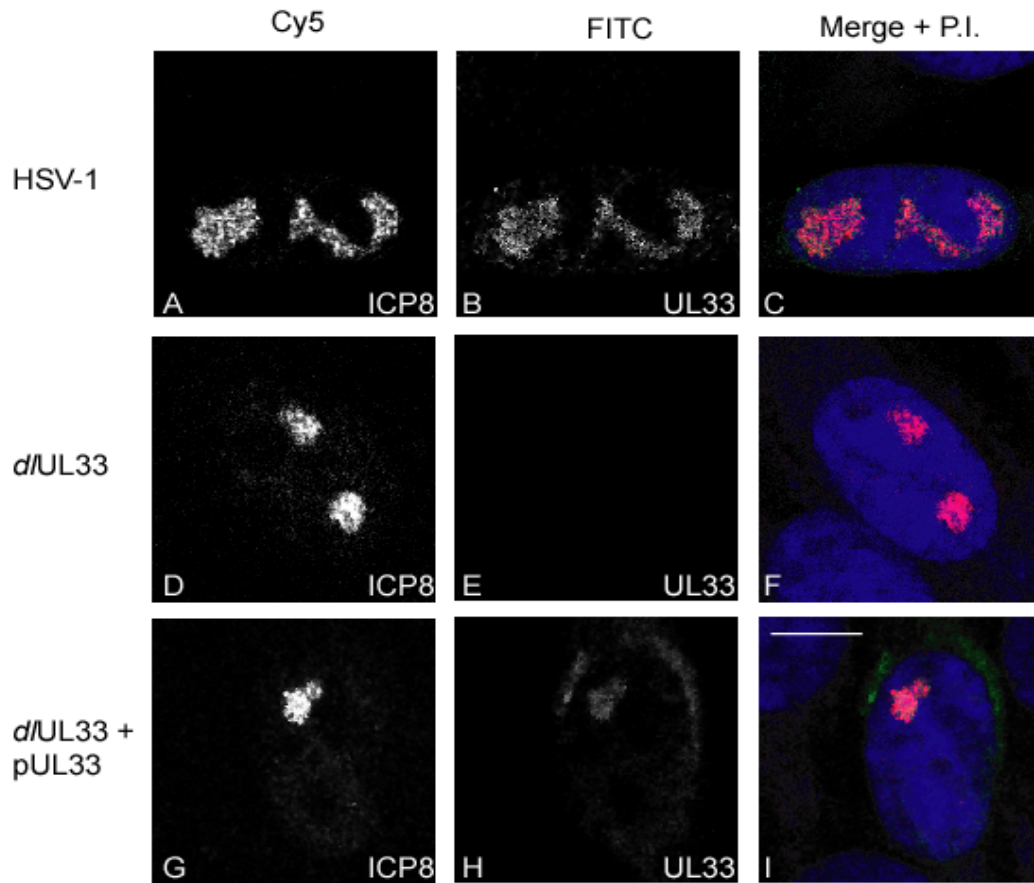


Figure 6.2: Localisation of transiently expressed UL33 in *dUL33*-infected cells

BHK cells were mock-transfected or transfected with 0.5 μg pUL33. Six h.p.t. cells were infected with 1 p.f.u./cell of either *dUL33* or HSV-1. Six h.p.i. cells were fixed and permeabilised, and incubated with anti-UL33 (R148) and anti-ICP8 (M7381) antibodies. Coverslips were processed for confocal microscopy, and incubated in propidium iodide prior to mounting. Identical settings were maintained throughout, with the FITC and Cy5 channels shown separately in grey together with a merged image of all three channels in colour. Scale bar = 10 μm

nuclear ICP8 foci (panels D and F). In cells transfected with pUL33 and infected with Δ UL33, UL33 was detectable in discrete nuclear foci (panel H), which co-localised with ICP8 (panels G and I). These data confirm that the signal observed in HSV-1 infected cells (Figure 6.1) was due to reactivity of R148 with UL33, and not due to overlap from the Cy5 (ICP8) channel. Furthermore, wt UL33 supplied *in trans* was able to localise to viral replication compartments formed in Δ UL33-infected cells.

6.3.2 Ability of mutated UL33 proteins to localise to RCs

Similar experiments were performed to analyse the ability of mutated UL33 proteins to localise to replication compartments. In this case, BHK cells were transfected with 0.5 μ g of plasmids expressing either wt or mutated UL33 proteins, and subsequently infected with Δ UL33. Resultant images of cells expressing a subset of the mutants are shown in **Figure 6.3**, and are representative of the phenotype exhibited by all of the mutants in this assay.

Consistent with Figure 6.2, UL33 was undetectable in Δ UL33-infected cells, despite the formation of RCs (data not shown). Wild-type UL33 expressed by pUL33 was again observed in nuclear foci, and co-localised extensively with ICP8 (panels A-C). A similar phenotype was observed in cells individually expressing the sixteen UL33 insertion mutants (represented by in14, in44, in100 and in104 in panels D-F, G-I, J-L and M-O respectively). Together, these data indicate that none of the UL33 mutants is compromised in its ability to localise to sites of DNA packaging. Thus, the ability of mutants to localise to viral replication centres does not correlate with their capability to support DNA packaging.

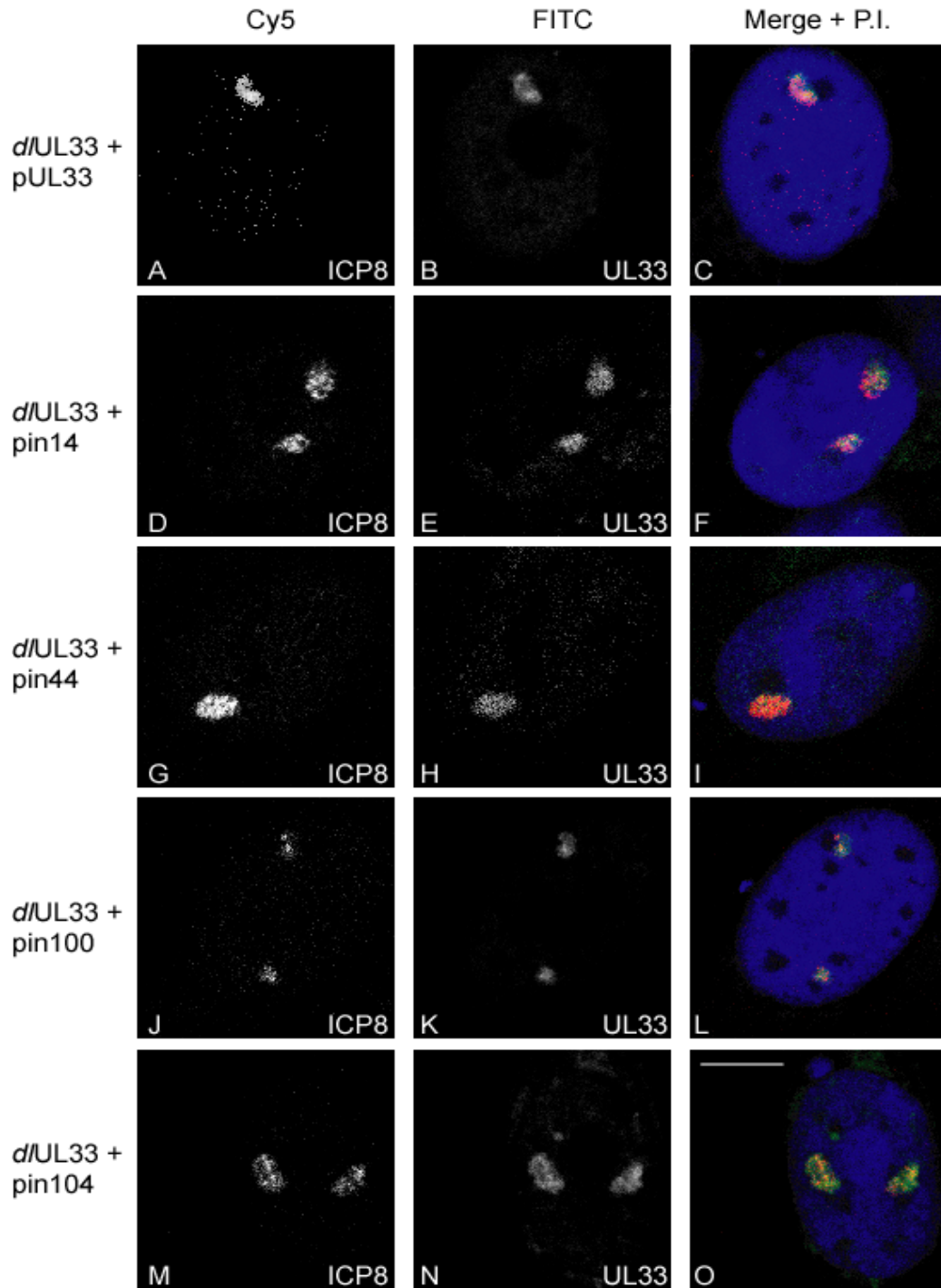


Figure 6.3: Localisation of mutated UL33 proteins in *dUL33*-infected cells

BHK cells were transfected with the indicated plasmid by lipofection. Six h.p.t. cells were infected with 1 p.f.u./cell of *dUL33*. Six h.p.i. cells were fixed and permeabilised, and incubated with anti-UL33 (R148) and anti-ICP8 (M7381) antibodies. Coverslips were processed for confocal microscopy, and incubated in propidium iodide prior to mounting. Identical settings were maintained throughout. Images are representative of all the mutants analysed, with the FITC and Cy5 channels shown separately in grey, and a merged image of all three channels in colour. Scale bar = 10µm

Section 6.4 The role of UL15, UL28 and UL33 in localising the terminase components to replication compartments

Figure 6.1 demonstrated that the putative terminase components UL15, UL28 and UL33 were previously shown to localise to viral replication compartments in HSV-1 infected cells. To determine whether a specific component of the terminase complex was responsible for this localisation, immunofluorescence studies were performed on cells infected with null mutant viruses with lesions in the UL15 (S648 virus; Baines *et al.*, 1997), UL28 (gCB virus; Tengelsen *et al.*, 1993) and UL33 genes (*Δ*UL33 virus; Cunningham & Davison, 1993).

The gCB mutant contains a 1,881 bp deletion that removes the region coding for amino acids 78-706 of UL28, and is defective in DNA packaging and viral growth unless grown on complementing C1 cells (Tengelsen *et al.*, 1993). A similar phenotype is observed when the S648 virus, which contains a stop codon in exon I of the UL15 gene, is grown on non-complementing cells. This defect can be reversed when S648 is grown on complementing clone 17 cells, which express the UL15 gene under the control of its own promoter (Baines *et al.*, 1997).

6.4.1 Localisation of putative terminase components in cells infected with viruses lacking functional copies of UL15, UL28 and UL33

Coverslips of BHK cells were infected with 1 p.f.u./cell of either S648, gCB or *Δ*UL33, and fixed and permeabilised at 6 h.p.i. Coverslips were incubated with antibodies specific to UL15 (R605), UL28 (R123) or UL33 (R148) together with the anti-ICP8 antibody M7381. Cells were analysed by confocal microscopy, and resultant images are shown in **Figure 6.4**.

In each instance, ICP8 foci were visible, suggesting replication compartment formation (panels A, D, G, J, M, P, S, V and Y). In cells infected with gCB, UL28 was not detected (panel N). Nevertheless, both UL15 (panel E) and UL33 (panel W) were detectable in gCB-infected nuclei, and co-localised with ICP8 in each case (panels F and X respectively). In *Δ*UL33-infected cells, no UL33 was detected (panel Z), in agreement with previous observations (Section 3.3). However, both UL15 (panel H) and UL28 (panel Q) were localised to discrete nuclear foci in such cells, where they co-localised with ICP8 (panels I and R respectively).

In cells infected with the UL15 mutant, S648, and probed with the UL15 antibody, no nuclear fluorescence was observed but very weak staining was discernable at the edge of the nucleus (panel B). Similar staining in this region of the cell was also visible in wt HSV-1 infected cells (Figure 6.1, panel E). It is possible that this staining represents the shorter protein, UL15.5, encoded in the same frame as UL15 by the second exon of the UL15 gene, but lacking the nuclear localization signal of UL15 which resides in exon I (Baines *et al.*, 1997; Yu & Weller, 1998a; Yang *et al.*, 2007). The lesion in S648 prevents expression of UL15 but not UL15.5 (Baines *et al.*, 1997). Since antiserum R605 was raised against a C-terminal fragment of UL15, reactivity with UL15.5 would be expected. UL15.5 is non-essential for virus replication and it is unable to compensate functionally for a lack of UL15 (Yu & Weller, 1998a).

In contrast to cells infected with gCB and *Δ*UL33, neither UL28 nor UL33 were detectable in S648-infected cells (panels K and T respectively). Together, these data suggest that neither UL28 nor UL33 are important for localising the remaining

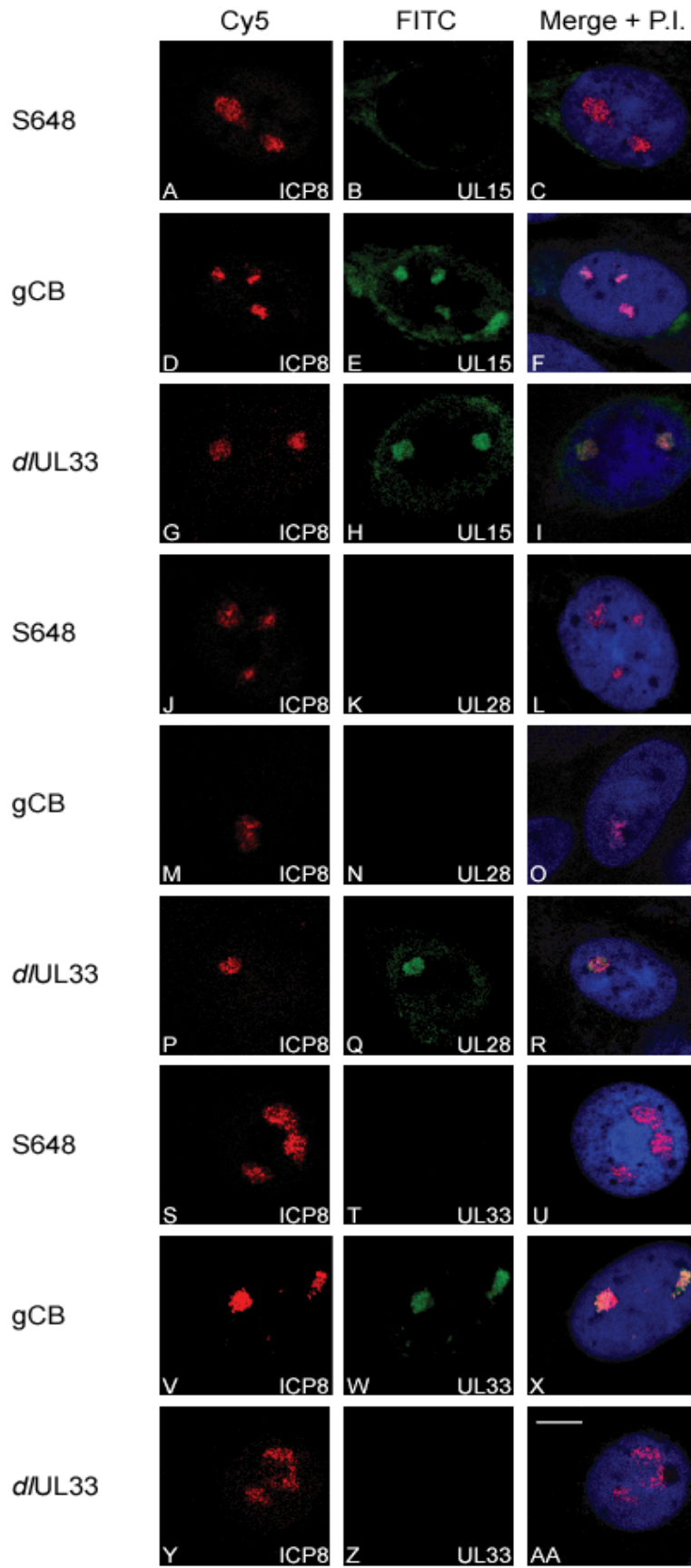


Figure 6.4: Localisation of the terminase components in cells infected with viruses lacking UL15, UL28 or UL33.

BHK cells were infected with 1 p.f.u./cell of the indicated virus. Six h.p.i. cells were fixed and permeabilised, and incubated with either anti-UL15 (panels A-I), anti-UL28 (panels J-R) or anti-UL33 (panels S-AA) antibodies (R605, R123 and R148 respectively) together with an anti-ICP8 antibody (M7381). Coverslips were processed for confocal microscopy, and incubated in propidium iodide prior to mounting. Identical settings were maintained for each antibody combination, with the FITC and Cy5 channels shown separately, together with a merged image of all three channels. Scale bar = 10 μ m

terminase components to replication compartments. However, UL15 seems to be indispensable for targeting UL28 and UL33 to RCs.

6.4.2 Western blot analysis of cells infected with S648, gCB and Δ UL33

In the above experiment, UL28 and UL33 were undetectable by immunofluorescence in cells infected with S648. To analyse the expression of the putative terminase components in mutant virus infected cells, monolayers of BHK cells were mock infected or infected with HSV-1, S648, gCB or Δ UL33. Six h.p.i. cells were harvested, lysates prepared and proteins analysed by western blotting with R605, R123, R148 or an anti-actin antibody. The resultant immunoblots are shown in **Figure 6.5**.

As expected, UL15, UL28 and UL33 were all absent from mock-infected cells (lanes 1, 6, 11 and 16), but were detected in HSV-1-infected cells (lanes 2, 7 and 12 respectively). UL15 was undetectable in S648-infected cells (lane 3), but both UL28 (lane 8) and UL33 (lane 13) were present at similar levels to those observed in HSV-1. Similarly, in gCB-infected cells, no UL28 was detected (lane 9), although the expression of UL15 and UL33 was unaffected compared to HSV-1-infected cells (lanes 4 and 14 respectively). In cells receiving Δ UL33, both UL15 and UL28 were expressed at similar levels to in HSV-1-infected cells (lanes 5 and 10 respectively), but UL33 was undetectable (lane 15). Probing with anti-actin antibody demonstrated that equivalent amounts of lysate were loaded in each instance (lanes 16-20). These data are consistent with the known phenotypes of these viruses, and suggest that the failure to detect UL28 and UL33 by immunofluorescence in S648-infected cells is not due to their degradation in the absence of UL15. Rather, the results suggest that, in S648-infected cells, UL28 and UL33 are probably diffusely localised and thus undetectable by immunofluorescence.

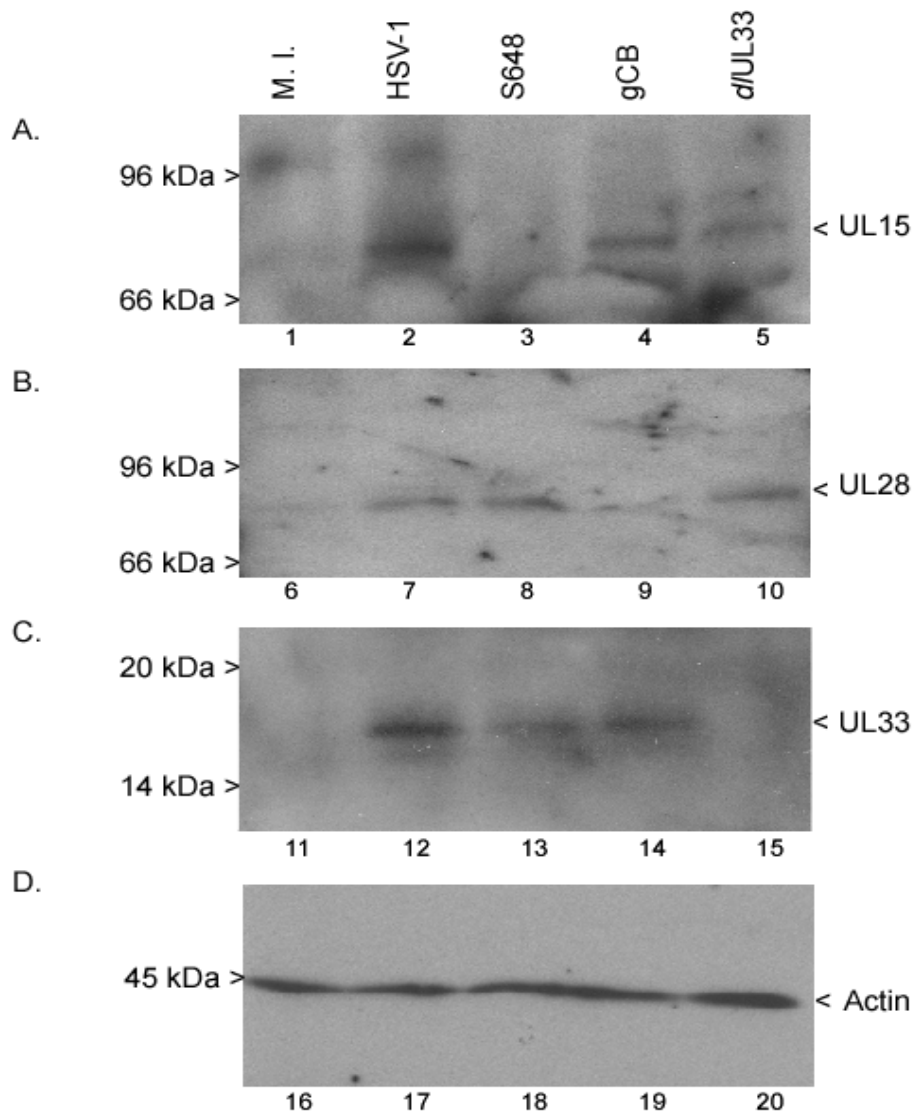


Figure 6.5: Western blot analysis of cells infected with viruses lacking UL15, UL28 or UL33

BHK cells were mock-infected or infected with the indicated virus. Six h.p.i. cells were harvested and lysates prepared. Samples of extract were separated on 8% (panels A+B) or 15% (panels C+D) SDS-PAGE gels and the proteins transferred onto PVDF membranes. Proteins were detected with either R605 (panel A), R123 (panel B), R148 (panel C) or an anti-actin antibody (panel D).

6.4.3 Subcellular location of UL28 and UL33 in the absence of UL15

The previous experiments suggested that, in the absence of UL15, UL28 and UL33 were diffusely localised. However, it was unclear whether these two proteins were capable of nuclear import without UL15. To examine the location of UL28 and UL33, nuclear and cytoplasmic extracts were prepared from HSV-1 or S648 infected cells. Monolayers of BHK cells were mock infected or infected with 1 p.f.u./cell of HSV-1 or S648. Six h.p.i. cells were harvested and cytoplasmic and nuclear fractions prepared by NP40 treatment (section 2.2.12). The fractions were analysed by western blotting and the results are shown in **Figure 6.6**.

Probing with an anti-histone H1 antibody (section 2.1.12) demonstrated that, as expected, this exclusively nuclear protein was only detectable in nuclear fractions (lanes 1-6), and that the extracts were thus suitable to examine the subcellular location of the terminase components. UL15 was detected in both nuclear and cytoplasmic fractions of HSV-1 infected cells, but not in mock-infected or S648-infected cells (lanes 7-12). Both UL28 and UL33 were absent from mock-infected cells (lanes 13-14 and 19-20 respectively) but were present in both nuclear and cytoplasmic fractions of HSV-1 infected cells (lanes 15-16 and 21-22 respectively). Furthermore, in S648-infected cells, the subcellular location of UL28 (lanes 17-18) and UL33 (lanes 23-24) was unaltered; i.e. both proteins were present in both cytoplasm and nucleus. Together, these data suggest that, in the absence of UL15, the remaining terminase components are capable of nuclear import, in agreement with the findings of Yang *et al.* (2007).

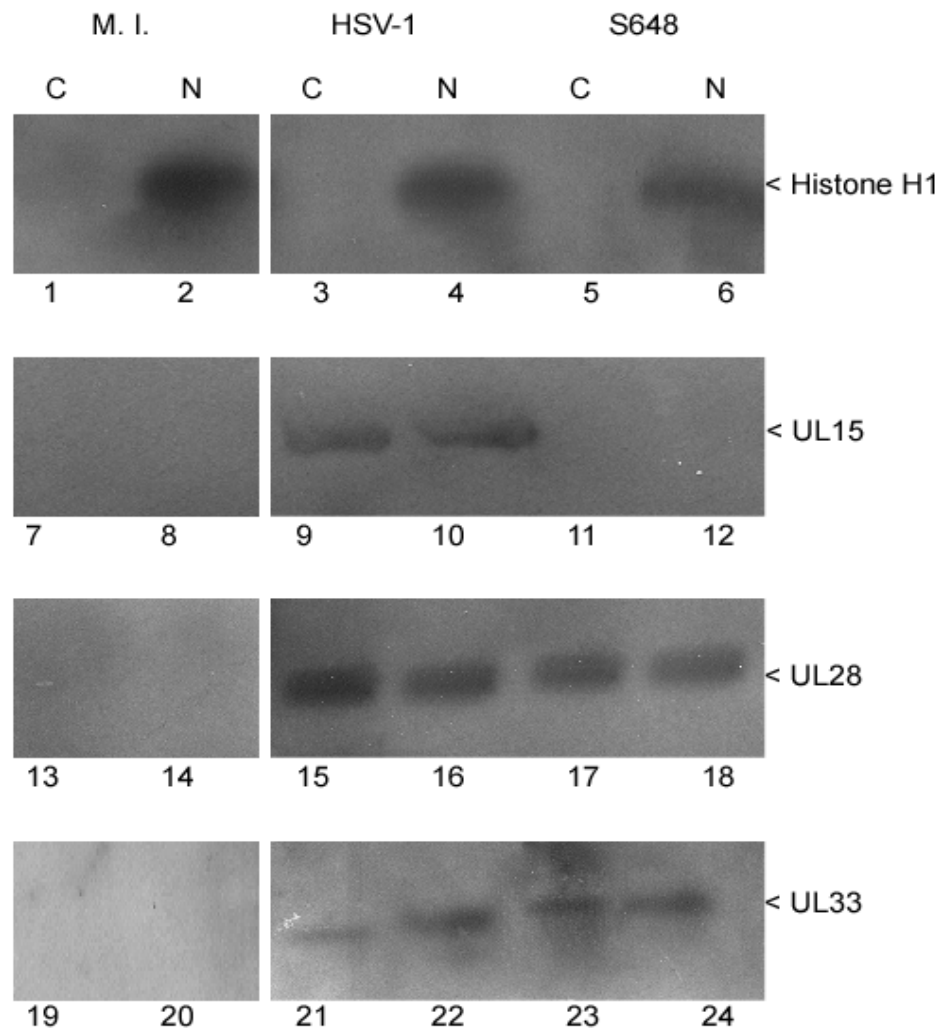


Figure 6.6: The subcellular location of UL28 and UL33 in the absence of UL15.

BHK monolayers were mock infected or infected with 1 p.f.u./cell of HSV-1 or S648. Six h.p.i. cells were harvested, and cytoplasmic (C) or nuclear (N) fractions were prepared. Proteins were separated by SDS-PAGE and detected using antisera reactive to histone H1 (lanes 1-6), UL15 (antibody R605; lanes 7-12), UL28 (antibody R123; lanes 13-18) or UL33 (antibody R148; lanes 19-24).

6.4.4 UL15 supplied *in trans* is sufficient to restore the localisation of UL28 and UL33 to RCs in S648-infected cells

To confirm that UL15 was solely responsible for the inability of UL28 and UL33 to localise to sites of DNA packaging in S648-infected cells, similar immunofluorescence experiments were performed in clone 17 cells. These cells, derived from rabbit skin cells, express UL15 under the control of its own promoter (Baines *et al.*, 1997).

Coverslips of rabbit skin cells or clone 17 cells were mock-infected or infected with 1 p.f.u./cell of either HSV-1 or S648. After fixation and permeabilisation, cells were incubated with R605, R123 or R148 together with M7381. Cells were processed for confocal microscopy, and the resultant images are shown in **Figure 6.7**.

Mock-infected RSC and clone 17 cells exhibited no cross-reactivity with either the terminase protein antibodies, or M7381 (data not shown). The absence of detectable UL15 protein in uninfected clone 17 cells is not surprising since activation of the promoter would only be expected to occur after infection with HSV-1.

Consistent with previous observations in BHK cells, nuclear foci of UL15, UL28 and UL33 were observed in HSV-1-infected RSC cells (panels B, K and T respectively), and co-localised extensively with ICP8 (panels C, L and U respectively). In agreement with the previous observations in BHK cells (Figure 6.4), neither UL15 (panel E) nor UL28 (panel N) nor UL33 (panel W) was detectable in RSC cells receiving S648.

However, clone 17 cells infected with S648 exhibited a phenotype indistinguishable from HSV-1 infected cells in which UL15 (panel H), UL28 (panel Q) and UL33 (panel Z) were visible in nuclear foci, which co-localised with ICP8 in each instance (panels I, R and AA respectively).

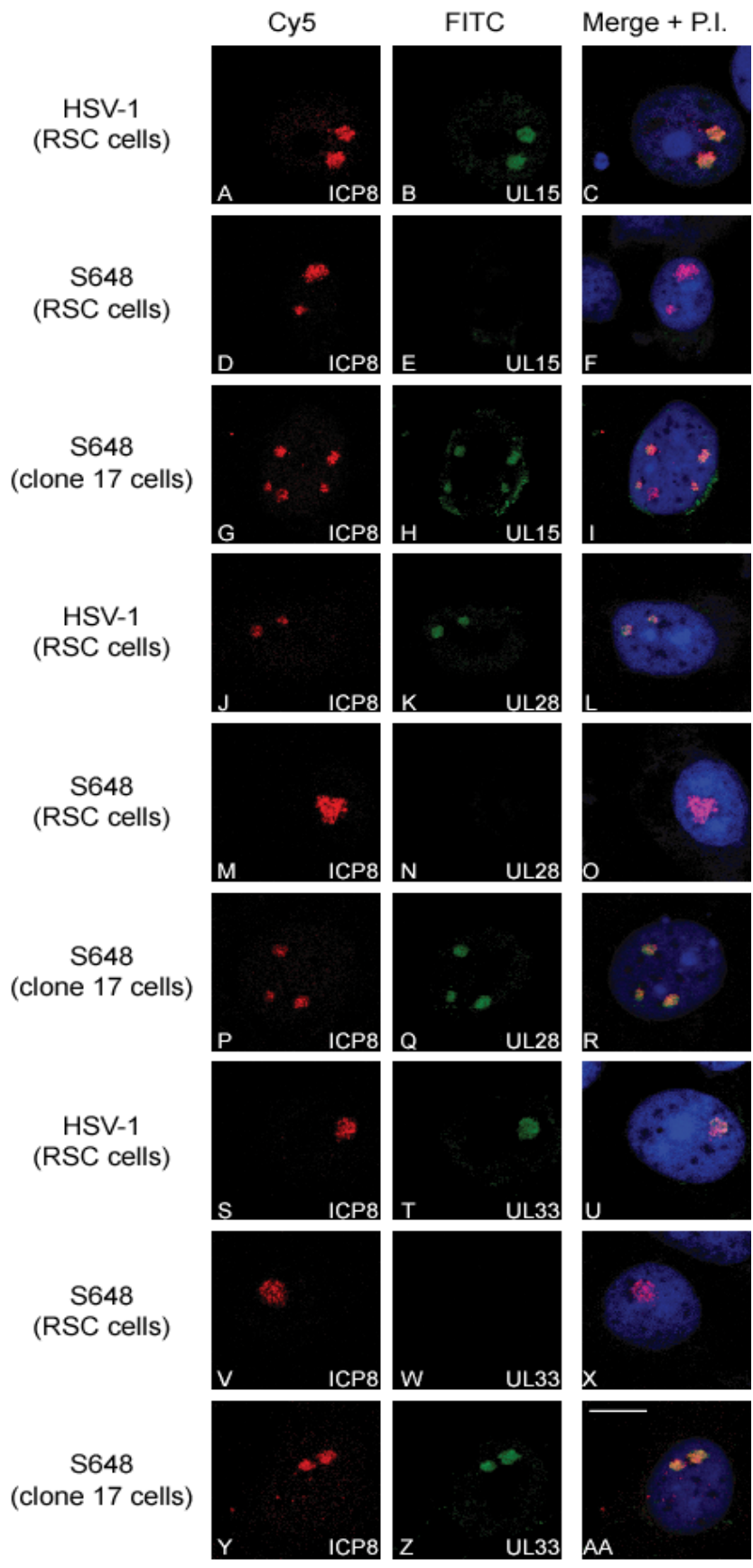


Figure 6.7: Supply of UL15 *in trans* restores the ability of UL28 and UL33 to localise to replication compartments

Rabbit skin cells (RSC) or clone 17 cells were infected with 1 p.f.u./cell of the indicated virus. Six h.p.i., cells were fixed and permeabilised, and incubated with either anti-UL15 (panels A-I), anti-UL28 (panels J-R) or anti-UL33 (panels S-AA) antibodies (R605, R123 and R148 respectively) together with an anti-ICP8 antibody (M7381). Coverslips were processed for confocal microscopy, and incubated in propidium iodide prior to mounting. Identical settings were maintained for each antibody combination, with the FITC and Cy5 channels shown separately, together with a merged image of all three channels. Scale bar = 10µm

Together, these data indicate that UL15 supplied *in trans* restores the ability of the S648-encoded UL28 and UL33 proteins to co-localise with ICP8, and confirms the necessity of UL15 in targeting the terminase subunits UL28 and UL33 to viral replication compartments.

Section 6.5 Localisation of UL6 in HSV-1-infected cells

6.5.1 UL6 localises to RCs early during viral infection

Previous studies demonstrated that the UL6 portal protein co-localised with ICP8 in infected cells, (16 h.p.i.) but was unable to do so in the absence of UL17 (Taus *et al.*, 1998). To extend these findings, the localisation of UL6 was examined at earlier time points during infection. Coverslips of BHK cell were mock infected or infected with either HSV-1 or the UL6-null virus *lacZ*-UL6⁻. This virus contains the *E. coli lacZ* gene inserted into codon 381 of UL6, and is unable to cleave or package DNA unless grown on complementing cells (Patel *et al.*, 1996). Infected cells were fixed and permeabilised at 6 h.p.i., incubated with the anti-UL6 antibody R992 and the anti-ICP8 antibody M7381, and processed for confocal microscopy. Resultant images are shown in **Figure 6.8**.

Neither antibody gave significant background fluorescence (panels A-C) in mock infected cells, but both UL6 and ICP8 were visible as discrete foci in the nuclei of HSV-1-infected cells, where they co-localised extensively (panels D-F respectively). In addition, some cytoplasmic signal was apparent in HSV-1 infected cells incubated with R992 (panel E). This was absent from cells infected with the *lacZ*-UL6⁻ virus, suggesting that the fluorescence was due to the specific reaction of R992 with UL6. This signal might represent either misfolded UL6 that has been ubiquitinated and is

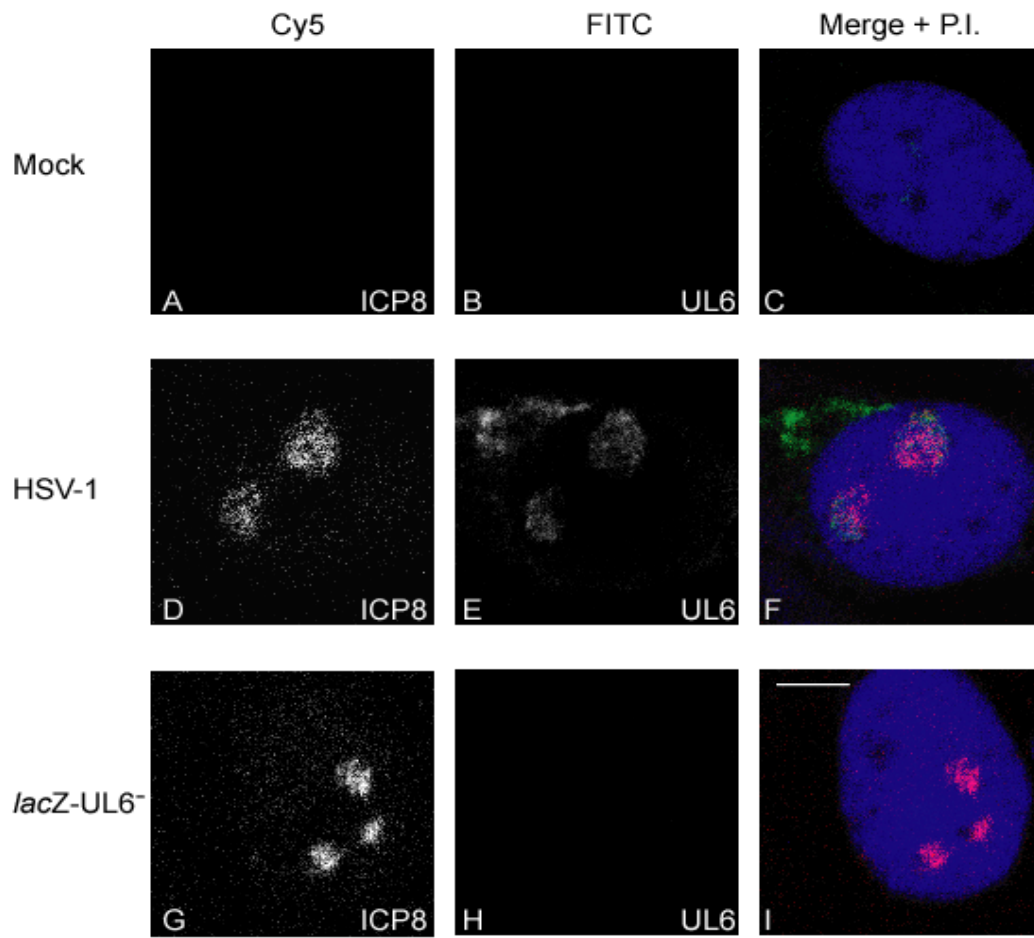


Figure 6.8: UL6 co-localises with ICP8 in HSV-1 infected cells

BHK cells were mock-infected, or infected with 1 p.f.u./cell of HSV-1 or *lacZ*-UL6⁻. Six h.p.i. cells were fixed and permeabilised, and incubated with anti-UL6 (R992) and anti-ICP8 (M7381) antibodies. Coverslips were processed for confocal microscopy, and incubated in propidium iodide prior to mounting. Identical settings were maintained throughout. The FITC and Cy5 channels are shown separately in grey, with a merged image of all three channels in colour. Scale bar = 10 μ m

therefore targeted for proteasomal degradation (Burch & Weller, 2004); a population of UL6 that has yet to be transported into the nucleus; or UL6 incorporated into mature capsids that have left the nucleus. In cells infected with *lacZ*-UL6⁻, ICP8 was present as discrete nuclear foci (panel G) but no UL6 was detected (panel H). These data confirm that the FITC signal observed in HSV-1-infected cells is specifically due to the recognition of UL6 by its cognate antibody, and demonstrate that UL6 localises to RCs early during viral infection.

6.5.2 UL6 is necessary for the localisation of the putative terminase to RCs

To examine whether UL6 is necessary for UL15, UL28 and UL33 to localise to RCs during infection, the localisation of each putative terminase subunit was examined in cells infected with HSV-1 or *lacZ*-UL6⁻. Infected BHK cells were fixed and permeabilised at 6 h.p.i. and treated with UL6, UL15, UL28, or UL33 antibodies together with M7381. Cells were processed for confocal microscopy, and resulting images are shown in **Figure 6.9**.

UL6 and ICP8 were observed in the nuclei of HSV-1-infected cells and extensively colocalised, as observed before (data not shown). Replication compartments were apparent in *lacZ*-UL6⁻ infected cells in each instance, indicated by the formation of ICP8 foci (panels A, D, G and J). As before, no UL6 was detected in these cells (panel B). Furthermore, neither UL15 (panel E) nor UL28 (panel H) nor UL33 (panel K) were detected in *lacZ*-UL6⁻ infected cells. These preliminary results therefore suggest that UL6 is necessary for the localisation of the putative terminase to sites of DNA packaging. However, further experiments are required to confirm these findings, particularly western blot analysis for the expression of terminase components in the

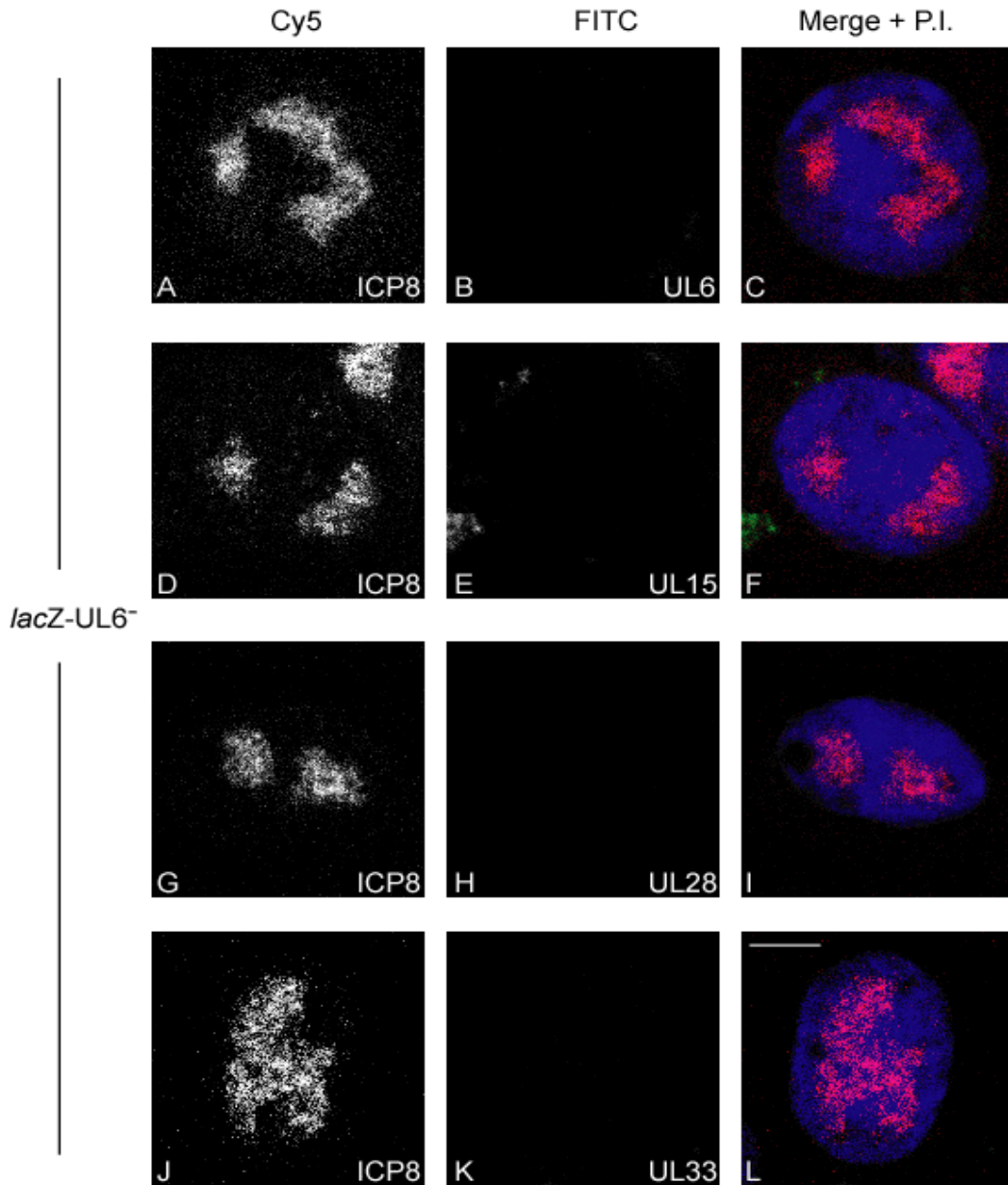


Figure 6.9: UL6 is required for the localisation of terminase components to RCs

BHK cells were infected with 1 p.f.u./cell of *lacZ-UL6⁻*. Six h.p.i. cells were fixed and permeabilised, and incubated with anti-UL6 (R992), anti-UL15 (R605), anti-UL28 (R123) or anti-UL33 (R148) antibodies, together with the anti-ICP8 antibody M7381. Coverslips were processed for confocal microscopy, and incubated with propidium iodide prior to mounting. Identical settings were maintained for each antibody combination. The FITC and Cy5 channels are shown separately in grey, with a merged image of all three channels in colour. Scale bar = 10µm

absence of UL6, and immunofluorescence studies of *lacZ*-UL6⁻ in complementing cells. Moreover, the pattern of some ICP8 foci (represented by panel J) seemed unusual, although the reason for this was unclear.

6.5.3 UL6 localisation to RCs is unaffected by the absence of the putative terminase subunits

Similar experiments were performed to analyse the localisation of UL6 in the absence of UL15, UL28 or UL33. BHK cells were infected with HSV-1, *lacZ*-UL6⁻, S648, gCB or *dUL33*, and proteins detected using R992 and M7381 antibodies. Coverslips were processed for confocal microscopy, and the images are shown in **Figure 6.10**.

As observed previously, UL6 co-localised with ICP8 in HSV-1-infected cells (panels A and C), but was absent from cells infected with *lacZ*-UL6⁻ (panel F). Moreover, UL6 was apparent in virus-infected cells in the absence of UL15 (S648; panel H), UL28 (gCB; panel K) and UL33 (*dUL33*; panel N), and co-localised with ICP8 in each case (panels I, L and O respectively). Therefore, these data suggest that the localisation of UL6 to RCs is independent of the presence of UL15, UL28 and UL33. As before, further experiments are required to confirm these preliminary results.

Section 6.6 Discussion

6.6.1 Localisation of wt UL6, UL15, UL28 and UL33 to RCs

Immunofluorescence experiments demonstrated that the HSV-1 terminase components and portal protein localised to replication compartments at 6 h.p.i., at which time DNA packaging has commenced. These data confirmed previous reports that UL15 is able to localise to RCs (Ward *et al.*, 1996; Yu & Weller, 1998a), and extend the information on the localisation of UL33, which had previously only been examined

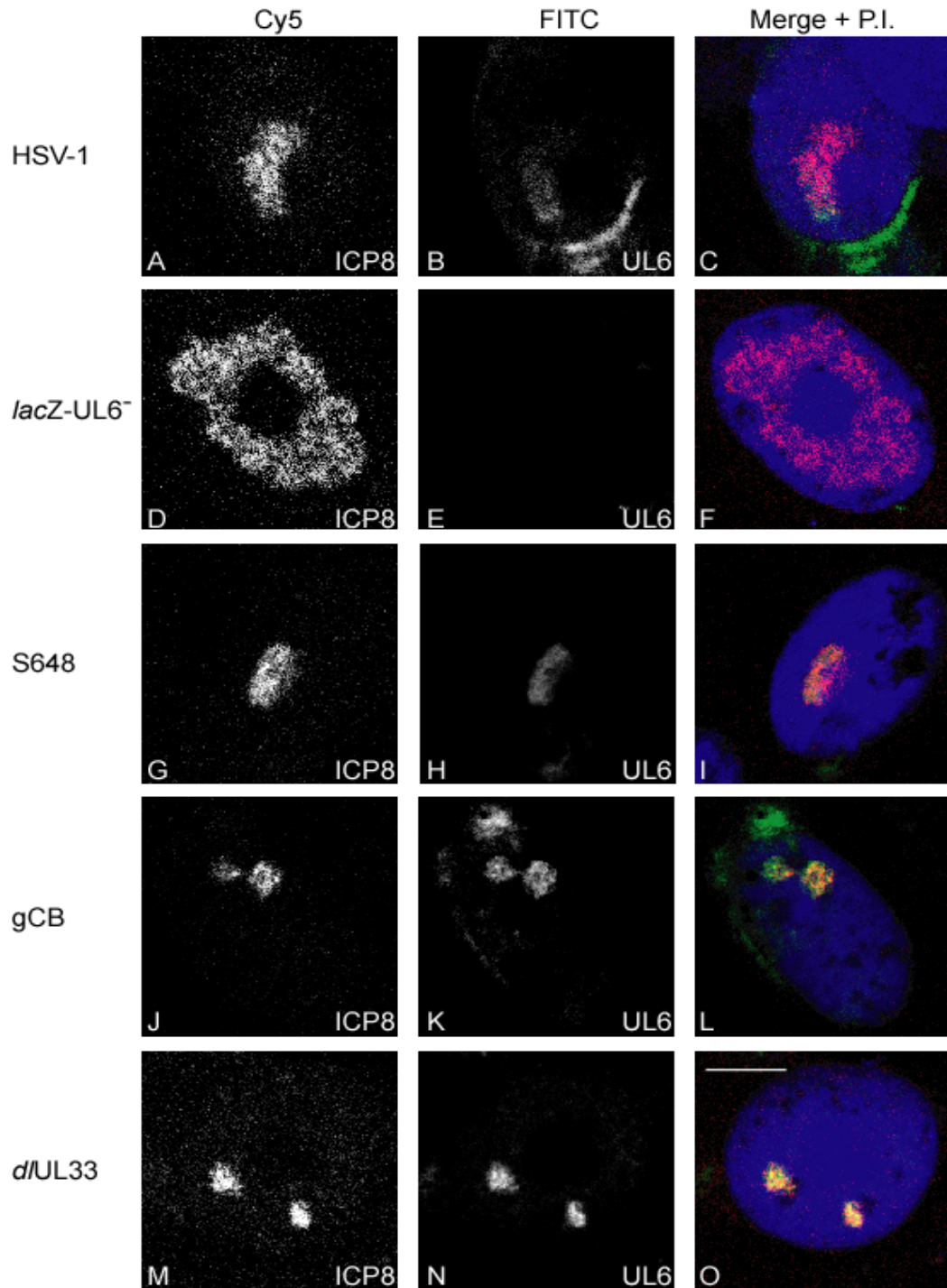


Figure 6.10: Localisation of UL6 to RCs is independent of UL15, UL28 and UL33

BHK cells were infected with 1 p.f.u./cell of the indicated virus. Six h.p.i. cells were fixed and permeabilised, and incubated with the anti-UL6 antibody R992 together with the anti-ICP8 antibody M7381. Coverslips were processed for confocal microscopy, and incubated with propidium iodide prior to mounting. Identical settings were maintained throughout. The FITC and Cy5 channels are shown separately in grey, with a merged image of all three channels in colour. Scale bar = 10µm.

at 18 h.p.i. (Reynolds *et al.*, 2000), to early times after infection. These experiments also provide the first demonstration that HSV-1 UL28 co-localises with ICP8 during viral infection. The homologous HCMV protein, UL56, has similarly been demonstrated to localise to RCs in the presence of replicating DNA (Geisen *et al.*, 2000a). My data also provide evidence that UL6 localises to RCs, in agreement with the findings of previous studies (Taus *et al.*, 1998; Burch & Weller, 2004). Together, the results described above completely support suggestions that DNA packaging occurs within viral RCs (de Bruyn Kops *et al.*, 1998; Lamberti & Weller, 1998; Taus *et al.*, 1998; Yu & Weller, 1998a; Geisen *et al.*, 2000a; Burch & Weller, 2004).

6.6.2 The mechanism of terminase localisation to RCs

In cells infected with gCB or *Δ*UL33, the absence of either UL28 or UL33 did not affect the ability of the remaining terminase components to localise to RCs. The earlier report that UL33 could co-localise with ICP8 in cells infected with a UL15 null mutant (Reynolds *et al.*, 2000) was not confirmed by either my own studies or by Yang *et al.* (2007). The apparent failure of UL28 and UL33 to localise to RCs in cells infected with the UL15-null mutant S648, despite both proteins being expressed in amounts comparable to HSV-1-infected cells, suggests that UL15 is responsible for mediating their localisation to RCs (Figure 6.4, Figure 6.5 & Figure 6.7). In the absence of UL15, it is probable that UL28 and UL33 exhibit a diffuse localisation in both the cytoplasm and nucleus, and are therefore undetectable by immunofluorescence. Cell fractionation studies (Figure 6.6) suggest that both UL28 and UL33 are capable of locating to the nucleus in the absence of UL15, in agreement with similar experiments performed by Yang *et al.* (2007). This result also provides a possible explanation for the presence of UL28 on capsids formed by a UL15-null mutant virus (Yu & Weller, 1998b). However

the nuclear location of UL28 and UL33 is in apparent conflict with previous transfection experiments demonstrating that UL15 is necessary for the nuclear import of UL28 in immunofluorescence assays (Koslowski *et al.*, 1997; Koslowski *et al.*, 1999; Abbotts *et al.*, 2000), and with my data showing that when co-expressed, UL28 and UL33 are both retained in the cytoplasm (section 4.3.3). It is also possible that insoluble cytoplasmic UL28 and UL33 are co-precipitated with nuclei during the cell fractionation procedure used by Yang *et al.* (2007) and myself, and that this accounts for the UL28 and UL33 observed in nuclear fractions (Figure 6.6).

It was recently proposed that UL15, UL28 and UL33 initially formed a complex in the cytoplasm, which is then transported into the nucleus (Yang *et al.*, 2007). Transport of the complex was shown to be dependent upon a nuclear localisation signal within UL15. My data on the localisation of the terminase components are consistent with this model. Notwithstanding the data from fractionation studies, the role of UL15 in the nuclear uptake of the terminase complex is also consistent with previous studies demonstrating nuclear localisation of UL28 and UL15 when expressed together (Koslowski *et al.*, 1997; Koslowski *et al.*, 1999) and also of co-expressed UL15 and UL33 (Chapter 4). Thus UL15 can independently transport UL28 and UL33 into the nucleus and assembly of a complete terminase complex in the cytoplasm is not obligatory for nuclear uptake.

There are several possible mechanisms by which the terminase might be recruited to and/or retained at the sites where the viral genome is replicated. These could involve interactions with other viral or cellular proteins or with viral DNA. Previously, interactions have been described between the VZV UL33 and UL5 homologues (Uetz *et al.*, 2006), and also between the HCMV homologues of UL28 and UL42 (Geisen *et*

al., 2000a). However, no interaction has yet been reported between the HSV-1 terminase components and any DNA replication protein. Another possibility is that interaction of the terminase with the packaging signal might be important. However, as only UL28 has been reported to interact with the packaging signal (Adelman *et al.*, 2001), such a mechanism fails to account for the localisation of UL15 and UL33 to RCs in the absence of UL28. Nevertheless, it remains possible that UL15 or UL33 may possess an as yet uncharacterised DNA binding activity capable of potentiating an interaction with replicated viral genomes.

Previously an interaction of UL15 with the capsid portal protein, UL6, has been described (White *et al.*, 2003; Yang *et al.*, 2007), and it has also been reported that UL15 is unable to associate with maturing capsids in the absence of UL6 (Salmon & Baines, 1998; Sheaffer *et al.*, 2001). An interaction between the terminase and the procapsid portal represents an attractive mechanism by which UL15 might mediate the localisation of the terminase to RCs. In preliminary experiments I demonstrated that a UL6-null mutant did not localise the terminase components to RCs, and that the co-localisation of UL6 and ICP8 was unaffected by the absence of UL15, UL28 or UL33 (Figure 6.9 & Figure 6.10 respectively). These results indicate that UL6 and the terminase employ different mechanisms to localise to RCs. They are also consistent with the observation that UL6 localises to the nucleus of infected cells even when the terminase is confined to the cytoplasm in cells infected with a virus in which the UL15 NLS has been mutated (Yang *et al.*, 2007). My findings thus support the model of Yang *et al.* in which association of the terminase and portal occurs in the nucleus. Future experiments are required to determine whether a stable terminase complex is assembled in cells infected with the UL6-null mutant, and if procapsids lacking UL6 co-localise with RCs. If this is then case it will indicate that a direct interaction between

UL6 and the terminase is required for the accumulation of terminase in RCs, and that this is important in bringing together the capsid, terminase and replicated DNA into a complex to allow cleavage and packaging.

6.6.3 Localisation of mutated UL33 proteins to RCs

Experiments examining the ability of the mutant UL33 proteins to localise to RCs revealed that all sixteen insertion mutants co-localised with ICP8 when transiently expressed in *Δ*UL33-infected cells (Figure 6.3). This is consistent with experiments that demonstrated that each of the mutants retained the ability to interact with UL15 or UL28 when expressed in the absence of other viral proteins (Chapter 4). It therefore seems likely that in each case a trimeric UL15-UL28-UL33 complex can be assembled in the cytoplasm, imported into the nucleus and recruited to RCs. Data presented earlier also suggest that in each case the assembled complex should be capable of interacting with UL6 (Chapter 5).

The reason for the inability of in14, in51, in55, in74, in104, in111A, in111B and in116 to package DNA or support mutant virus growth cannot therefore be explained by their ability to interact with UL6, UL15, UL25 or UL28, or by their ability to traffic to sites of DNA packaging. Several possible explanations for their defectiveness remain: (i) that the terminase complex formed by these mutants is catalytically defective; (ii) that the UL15-UL28-UL33 complexes containing these mutants are unable to bind DNA and thus assemble into a functional pre-packaging complex; (iii) that the functions of UL15 and/or UL28 are defective because UL33 cannot carry out its proposed role of a chaperone to assist their folding; (iv) that these mutants are unable to interact with as yet unidentified cellular or viral proteins necessary for packaging.

Chapter 7: Conclusions

During the course of my studies, sixteen UL33 insertion mutants were isolated and characterised in a variety of assays to determine their ability to support viral growth and DNA packaging, and to interact with other DNA packaging proteins. The results are summarised in **Table 7.1**.

Results presented in chapter 3 revealed that the ability of the mutants to support DNA packaging correlated precisely with their capacity to complement the growth of viruses lacking functional UL33 genes. Combined with previous proposals (Al-Kobaisi *et al.*, 1991; Patel *et al.*, 1996; Reynolds *et al.*, 2000), these data suggest that UL33 functions solely during DNA packaging. Moreover, those mutants able to maintain the packaging of amplicon DNA also fully supported the encapsidation of mutant virus genomes. Thus UL33, unlike UL25 (McNab *et al.*, 1998; Hodge & Stow, 2001), appears to be important for the initiation of DNA packaging, and not solely in the latter stages of encapsidation.

Demonstrations of an interaction between UL33 and UL28 (Section 4.3) were in agreement with the findings of several previous studies (Beard *et al.*, 2002; Jacobson *et al.*, 2006; Yang *et al.*, 2008). In similar experiments, UL33 was also demonstrated to bind UL15 in the absence of UL28 (Section 4.2 and 6.4.1), in accord with initial reports (Beard *et al.*, 2002), but in contrast to the conclusions of more recent publications (Jacobson *et al.*, 2006). Collectively, these data lend further support to a model in which UL33 forms part of the viral terminase complex via direct interactions with each of the

Mutant	Support DNA packaging		Complement mutant virus growth	Interact with UL28		Interact with UL15 with UL6	Interact with UL25	Localise to RCs
				IF	IP			
in14	-	-	-	+	+	+	+	+
in34	+	+	+	+	+	+	+	+
in37	+	+	+	+	+	+	+	+
in44	+	+	+	+	+	+	+	+
in51	-	-	-	+	+	+	+	+
in55	-	-	-	+	+	+	+	+
in69	-	-	-	-	+	+	+	+
in74	-	-	-	+	+	+	+	+
in79A	+	+	+	+	+	+	+	+
in79B	+	+	+	+	+	+	+	+
in84	+	+	+	-	+	+	+	+
in100	+	+	+	+	+	+	+	+
in104	-	-	-	+	+	+	+	+
in111A	-	-	-	+	+	+	+	+
in111B	-	-	-	+	+	+	+	+
in116	-	-	-	+	+	+	+	+
Δ1	+	+	+	-	n.d.	+	+	n.d.
Δ2	+	+	+	+	n.d.	+	+	n.d.

Table 7.1: Summary of the properties of the UL33 insertion and deletion mutants

The table indicates the ability (+) or inability (-) of the mutants to support packaging of DNA, complement virus growth, interact with various protein partners, and localise to replication compartments. n.d. = not determined.

other two terminase components. However, as the UL33-UL15 interaction appears more difficult to demonstrate than the binding of UL28 by UL33 (Jacobson *et al.*, 2006; Yang *et al.*, 2007), it is probably weaker.

The results of immunofluorescence experiments for UL15, and of immunoprecipitation experiments for UL28, suggested that none of the UL33 mutants was defective for interaction with either of the other terminase components. Defects in interactions with these two proteins cannot explain why nine of the mutants did not support DNA packaging. Surprisingly, four mutants appeared perturbed in their interaction with UL28 in immunofluorescence assays, but only one of these, in69, was impaired in DNA packaging. Although the three mutants that support DNA packaging (in34, in37 and in84) may be altered in their interaction with UL28, they can still presumably assemble a functional terminase by interacting with UL15. It therefore seems likely that each mutant (with the possible exception of in69) is capable of forming a trimeric UL15-UL28-UL33 complex, although several mutants are apparently incapable of assembling a functional packaging machinery. Unfortunately the data do not therefore allow the conclusion that UL33 is an obligatory component of the terminase. The possibility remains that it is uncomplexed UL33 that performs an essential role in the packaging process.

Despite the above, the presence of UL33 in the terminase complex is likely to be crucial and several possible roles have previously been proposed: (i) it may ensure that the terminase is correctly folded and assembled; (ii) it may regulate the enzymatic activities of the terminase; (iii) it may have an enzymatic role *per se*; (iv) it may be involved in localising the terminase to sites of DNA packaging (Beard *et al.*, 2002).

The data presented in this thesis is compatible with the first three roles proposed by

Beard and co-workers. However, immunofluorescence studies of *dUL33*-infected cells (section 6.4.1) exclude the possibility that UL33 is important in localising terminase to RCs. Moreover, my data suggest a fifth possible role for UL33, in mediating interactions with other components of the HSV-1 packaging machinery, namely UL6 and UL25.

Bioinformatic analysis (data not shown) failed to reveal any sequence similarity between UL33 and the DNA packaging proteins of either bacteriophage or other DNA viruses excluding herpesviruses. Indeed, BLAST analysis of the UL33 protein sequence retrieved only herpesvirus UL33 gene homologues from the Refseq protein database. Similarly, PATTERN analysis of the UL33 motif F-x₄-P-x₇-P-x₂-D-x₃-N-x₃₃-C-x-H, which is conserved amongst all members of the *alpha*- and *beta*-herpesvirinae (see Figure 3.20 for an alignment of *alphaherpesvirinae* UL33 sequences), failed to retrieve any proteins with known DNA packaging functions outwith the herpesviruses, or proteins encoding ATPase, nuclease, DNA binding or ‘molecular motor’ activities (not shown). It is therefore unclear whether this motif represents a conserved catalytic site within UL33. Furthermore, LOOPP protein-threading analysis of the UL33 amino acid sequence failed to reveal any significant similarity with any proteins whose tertiary structures have been defined. These analyses therefore provided no further information on the possible role of UL33 in encapsidation.

Two novel protein-protein interactions were identified in chapter 5: between UL33 and UL6, and between UL33 and UL25. Given that both UL15 and UL28 interact with UL6 in similar experiments (White *et al.*, 2003), these data indicate that UL6 separately interacts with all three members of the terminase complex. Since DNA packaging is thought to be processive (**Figure 1.5**), it is likely that that interactions

between UL6 and the terminase are transient, perhaps mediated by conformational changes in the portal as packaging nears completion. Analogous changes have been observed in the portal protein of P22 phage (Lander *et al.*, 2006). Data also suggested that UL33 and UL25 interact (Section 5.4). It is conceivable that, as proposed by Stow (2001), UL25 might enhance the activity of the terminase at later stages of packaging, or that UL25 is brought into close proximity to the terminase via interactions with the *a* sequence as the packaging of a genome approaches completion (Ogasawara *et al.*, 2001). Although a population of UL25 has been visualised at sites distal to capsid vertices (Cardone *et al.*, 2007; Figure 5.20), it cannot be excluded that additional UL25 may interact directly with the portal. It is also possible that a population of 'free' UL33, not associated with the terminase, could interact with UL25, implying that UL33 may function at multiple stages during the packaging process. No correlation was apparent between the capability of the insertion mutants to interact with UL6 or UL25 and their ability to support DNA packaging (Table 7.1). Thus, it remains uncertain whether either of these interactions is necessary for DNA encapsidation to occur.

The identification of numerous proteins that interact with UL33 might be interpreted as an indication that it acts as a chaperone protein to ensure the correct folding of a subset of the DNA packaging proteins, as originally suggested by Beard *et al.* (2002). It has previously been demonstrated that a proportion of UL6 is misfolded in infected cells (Burch & Weller, 2004), and it is plausible that UL33 might act to assist the correct folding or assembly of the portal. Presently, no data on the temporal association of UL33 with the terminase, portal and UL25 is available. The data presented may thus be a clue that UL33 performs several distinct roles during encapsidation, by first interacting with the portal during initiation of packaging, and then possibly recruiting UL25 to maturing capsids. The addition of UL25 might then

stabilise capsids, precluding the loss of the DNA, or may assist in terminase function (McNab *et al.*, 1998; Hodge & Stow, 2001; Sheaffer *et al.*, 2001). This model probably requires that UL33 undergo several conformational changes during the packaging process.

One mechanism through which proteins can exhibit such flexibility is by existing in a molten globule state (Romero *et al.*, 2004). Such proteins are compact and contain significant secondary structure (α -helical or β -sheet folds) but with substantial 'disordered' regions, allowing a flexible tertiary structure. This can become fixed through interactions with other protein partners. The HSV-1 capsid protein VP23 has been shown to exist as a molten globule when alone, and this is thought to be necessary for its interaction with VP19C, the other component of triplexes (Kirkidatze *et al.*, 1998). However, bioinformatic analysis of UL33 using the GlobPlot program (Linding *et al.*, 2003) reveals only two small (<10 aa) regions of predicted disordered structure (data not shown), suggesting that its interactions with different partners are unlikely to be facilitated by existing as a molten globule.

A model for the interaction of the terminase with the portal is shown in **Figure 7.1** All six possible pairwise interactions between the 4 proteins have now been described (Abbotts *et al.*, 2000; Beard *et al.*, 2002; White *et al.*, 2003; Jacobson *et al.*, 2006; Yang *et al.*, 2007; my data). This may be important since most models of DNA packaging have to allow for movement of the terminase relative to the portal. A prediction of the model is that terminase might be able to bind to the portal even though one or more of these interactions is abolished. This might therefore explain the

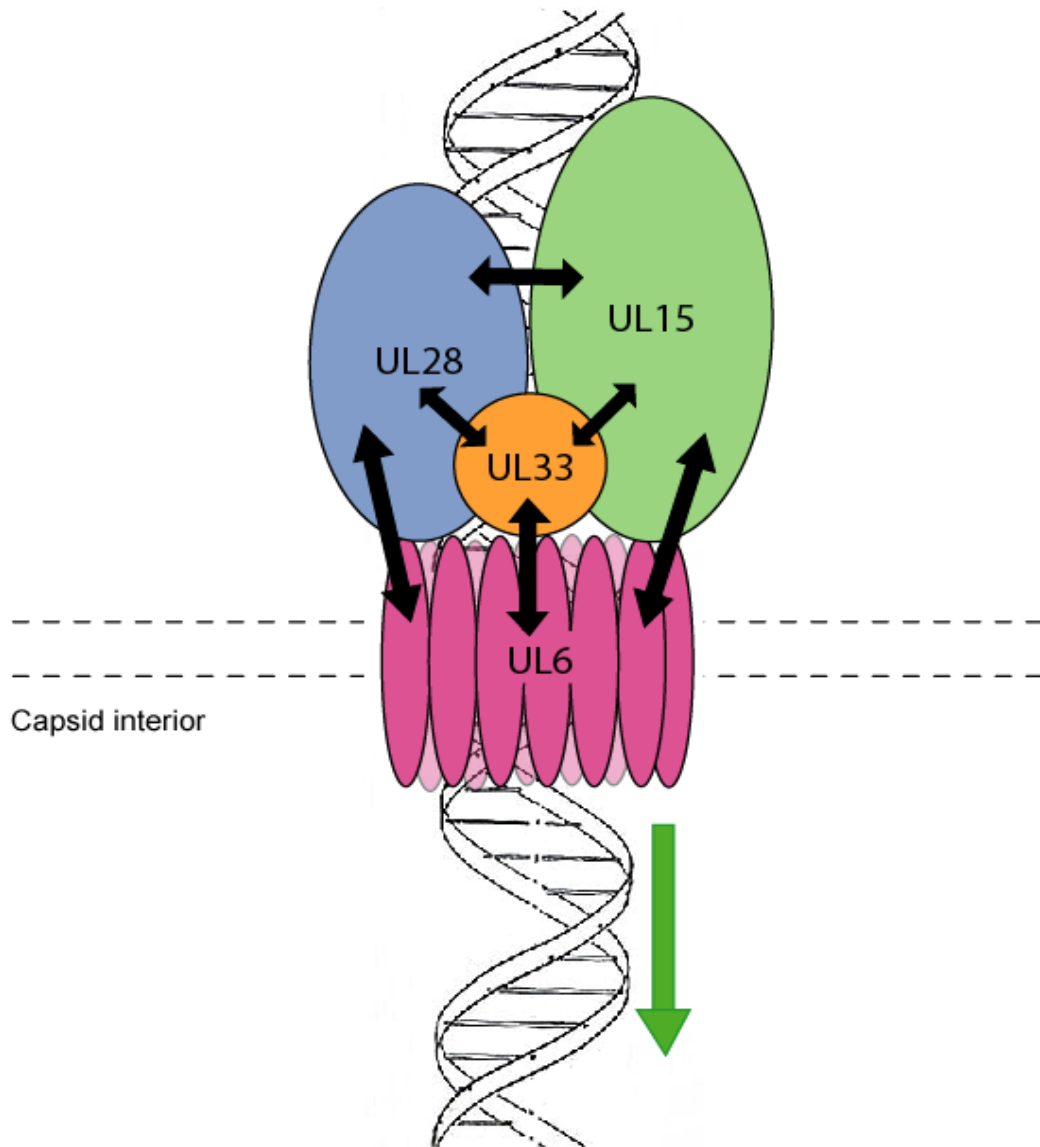


Figure 7.1: A model for terminase assembly on the capsid portal.

During HSV-1 infection, a terminase complex of UL15, UL28 and UL33 assembles at the portal vertex (UL6 dodecamer ring). Interactions (denoted by black arrows) have been demonstrated between: UL15 and UL28 (Abbotts *et al.*, 2000); UL6 and all three of the terminase components (White *et al.*, 2003; Yang *et al.*, 2007; my data); UL28 and UL33 (Beard *et al.*, 2002; Jacobson *et al.*, 2006; my data); UL15 and UL33 (Beard *et al.*, 2002; my data). The precise stoichiometry of the terminase complex is unknown.

ability of several mutants (in34, in37 and in84) mentioned previously to support DNA packaging, despite their apparent inability to interact with UL28 in immunofluorescence assays.

The final results chapter examined the localisation of the terminase to sites of DNA packaging, and demonstrated that UL15 was required for the localisation of UL28 and UL33 to RCs. This extends findings demonstrating that a nuclear localisation signal in UL15 is responsible for terminase complex import (Yang *et al.*, 2007). Together with immunofluorescence studies of co-expressed UL15 and UL28 (Koslowski *et al.*, 1997; Koslowski *et al.*, 1999) and my data demonstrating cytoplasmic localisation of UL28 and UL33 in the absence of UL15 (section 4.3.3), a model can be drawn whereby UL15 is responsible for the nuclear uptake of the terminase complex, which is then recruited to RCs where it is retained via interaction with UL6. Further analysis revealed that all of the UL33 mutants localised to RCs, in accordance with earlier data suggesting that they all interacted with UL15 and UL6 (sections 4.2.4 and 5.2.5 respectively).

In summary, my data suggests that each mutant is capable of forming a trimeric UL15-UL28-UL33 complex, which is imported into the nucleus and directed to sites of DNA packaging by virtue of the presence of UL15. All of the complexes apparently also retain the ability to interact with the portal protein of procapsids. However, the terminases formed by several mutants were unable to support DNA packaging, although the reason for this remains unknown. Several regions of UL33, coincident with predicted alpha-helical regions of the protein, seemed most susceptible to inactivating mutations.

Section 7.1 Future perspectives

Many questions obviously remain to be answered concerning the precise role of the UL33 protein in viral DNA encapsidation, and the reasons why several of my mutants are defective in this activity.

Bioinformatics analysis suggested that UL33 contains motifs modified by the cellular kinases protein kinase C and casein kinase II (not shown). It is presently unknown whether UL33 is phosphorylated during HSV-1 infection, although such modification might account for the discrepancy between the predicted M_r of UL33 and its observed mobility (Reynolds *et al.*, 2000). Therefore, it would be interesting to determine whether UL33 is subjected to phosphorylation, or other post-translational modification, and, if so, what effects this has on UL33's activities or ability to bind protein partners. It is conceivable that such post-translational modification might play a role in altering the conformation of UL33, perhaps acting to release the terminase from the portal once a genome length of DNA has been packaged or to allow UL33 to bind multiple partners.

Adelman *et al.* (2001) suggested that a modified secondary structure of the *a* sequence was important for UL28 recognition. This structure could be formed from a single strand of the DNA. Although this result has not been confirmed, this suggests that exposing a single strand of the packaging signal might be important for its recognition by the terminase. This could possibly be achieved through the activities of several of the enzymes involved in viral DNA synthesis (e.g. UL9 helicase, UL5-UL8-UL52 helicase-primase, ICP8 DNA unwinding activity, UL12 exonuclease activity). It would be interesting to investigate whether the terminase interacted with any of these replication proteins, and whether UL33 played a role. Interestingly, a UL12-null

mutant has previously been shown to package viral DNA with reduced efficiency (Porter & Stow, 2004b).

Performing shotgun mutagenesis procedures and interpreting the results is invariably more complicated for a protein of unknown structure. Crystallographic analysis of the UL33 structure would almost certainly aid the interpretation of the data presented in this thesis, and also suggest mutagenesis strategies to allow specific questions to be posed (e.g. whether specific regions of the surface of UL33 are involved in any of the interactions). Such an analysis would also reveal whether certain regions of the protein are largely disordered, as previously discussed. At present, obtaining sufficient amounts of soluble purified UL33 protein for crystallography (or other biophysical studies) represents a major challenge. However, using a more amenable homologue from another herpesvirus might facilitate structural analysis. It is also noteworthy that UL33 is a relatively small protein and that advances in computer software might eventually enable reliable predictions of tertiary structure.

Ultimately, advancing our knowledge of the functions of UL33 is hampered by the shortage of useful assays. The terminase subunits are largely insoluble when expressed in heterologous systems, and even co-expression of the three subunits has not allowed sufficient amounts of the complex to be purified for biochemical study. If this could be achieved it would be interesting to examine predicted properties such as DNA binding, DNA cleavage and ATP hydrolysis, and to determine whether these are modulated by the presence of UL33. Such an analysis might also allow specific defects of the UL33 insertion mutants to be identified.

A major step forward would be the development of a cell-free system for HSV-1 DNA

packaging similar to those reported for several dsDNA bacteriophage (Hwang *et al.*, 1996; Leffers & Rao, 2000; Smith *et al.*, 2001). Such a system would include procapsids, concatemeric DNA, terminase and other essential viral (and host) proteins. It might be developed from extracts from HSV-1-infected cells, or from individual components, for example expressed by recombinant baculoviruses. The availability of an *in vitro* packaging system would allow rigorous demonstration that UL33 is an obligatory component of the terminase, and enable the packaging process to be broken down into component reactions e.g. recognition of DNA by the terminase; assembly of a prepackaging complex; cleavage of the DNA; DNA insertion into the capsid; cleavage to terminate packaging. This would facilitate a much more detailed analysis of the mutated UL33 proteins, and hopefully allow their defects to be pinpointed.

References

- Abbotts, A. P., Preston, V. G., Hughes, M., Patel, A. H. & Stow, N. D. (2000). Interaction of the herpes simplex virus type 1 packaging protein UL15 with full length and truncated forms of UL28. *Journal of General Virology* **81**, 2999-3009.
- Addison, C., Rixon, F. J., Palfreyman, J. W., O'Hara, M. & Preston, V. G. (1984). Characterisation of herpes simplex virus type 1 mutant which has a temperature-sensitive defect in penetration of cells and assembly of capsids. *Virology* **138**, 246-259.
- Addison, C., Rixon, F. J. & Preston, V. G. (1990). Herpes simplex virus type 1 UL28 gene product is important for the formation of mature capsids. *Journal of General Virology* **71**, 2377-2384.
- Adelman, K., Salmon, B. & Baines, J. (2001). Herpes simplex virus packaging sequences adopt novel structures that are specifically recognised by a component of the cleavage and packaging machinery. *PNAS USA* **98**, 3086-3091.
- Agirrezabala, X., Martin-Benito, J., Caston, J. R., Miranda, R., Valpuesta, J. M. & Carrascosa, J. L. (2005b). Maturation of phage T7 involves structural modification of both shell and inner core components. *EMBO Journal* **24**, 3820-3829.
- Agirrezabala, X., Martin-Benito, J., Valle, M., Gonzalez, J. M., Valencia, A., Valpuesta, J. M. & Carrascosa, J. L. (2005a). Structure of the connector of bacteriophage T7 at 8 Å resolution: structural homologies of a basic component of a DNA translocating machinery. *Journal of Molecular Biology* **347**, 895-902.
- Albrecht, J. C., Nicholas, J., D., B., Cameron, K. R., Biesinger, B., Newman, C., Wittmann, S., Craxton, M., Coleman, H., Fleckenstein, B. & Honess, R. W. (1992). Primary structure of the herpesvirus saimiri genome. *Journal of Virology* **66**, 5047-5058.
- Al-Kobaisi, M. F., Rixon, F. J., McDougall, I. & Preston, V. G. (1991). The herpes simplex virus UL33 gene product is required for the assembly of full capsids. *Virology* **180**, 380-388.
- Arzul, I., Nicolas, J.-L., Davison, A. J. & Renault, T. (2001). French scallops: a new host for ostreid herpesvirus-1. *Virology* **290**, 342-349.
- Baines, J. D., Cunningham, C., Nalwanga, D. & Davison, A. J. (1997). The UL15 gene

- of herpes simplex virus type 1 contains within its second exon a novel open reading frame that is translated in frame with the UL15 gene product. *Journal of Virology* **71**, 2666-2673.
- Baines, J. D., Poon, A., Rovnak, R. & Roizman, B. (1994). The herpes simplex virus 1 UL15 gene encodes two proteins and is required for cleavage of genomic viral DNA. *Journal of Virology* **68**, 8118-8124.
- Baines, J. D. & Roizman, B. (1991). The open reading frames UL3, UL4, UL10, and UL16 are dispensable for the replication of herpes simplex virus 1 in cell culture. *Journal of Virology* **65**, 938-944.
- Baines, J. D. & Roizman, B. (1992). The cDNA of UL15, a highly conserved herpes simplex virus 1 gene, effectively replaces the two exons of the wild-type virus. *Journal of Virology* **66**, 5621-5626.
- Baines, J. D. & Weller, S. K. (2005). Cleavage and packaging of herpes simplex virus 1 DNA. In *Viral Genome Packaging Machines: Genetics, Structure, and Mechanism*, pp. 135-150. Edited by C. Catalano. New York: Kluwer Academic/Plenum Publishers.
- Baker, M. L., Jiang, W., Rixon, F. J. & Chiu, W. (2005). Common ancestry of herpesviruses and tailed DNA bacteriophages. *Journal of Virology* **79**, 14967-14970.
- Balliet, J. W., Min, J. C., Cabatingan, M. S. & Schaffer, P. A. (2005). Site-directed mutagenesis of large DNA palindromes: construction and in vitro characterisation of herpes simplex virus type 1 mutants containing point mutations that eliminate oriL or oriS initiation function. *Journal of Virology* **79**, 12783-12797.
- Barnard, E. C., Brown, G. & Stow, N. D. (1997). Deletion mutants of the herpes simplex virus type 1 UL8 protein: effect on DNA synthesis and ability to interact with and influence the intracellular localization of the UL5 and UL52 proteins. *Virology* **237**, 97-106.
- Baumann, R. G. & Black, L. W. (2003). Isolation and characterization of T4 bacteriophage gp17 terminase, a large subunit multimer with enhanced ATPase activity. *Journal of Biological Chemistry* **278**, 4618-4627.
- Baumann, R. G., Mullaney, J. & Black, L. W. (2006). Portal fusion protein constraints on function in DNA packaging of bacteriophage T4. *Molecular Microbiology* **61**, 16-32.

- Beard, P. M. & Baines, J. D. (2004). The DNA cleavage and packaging protein encoded by the UL33 gene of herpes simplex virus 1 associates with capsids. *Virology* **324**, 475-482.
- Beard, P. M., Taus, N. S. & Baines, J. D. (2002). DNA cleavage and packaging proteins encoded by the genes UL15, UL28 and UL33 of herpes simplex virus type 1 form a complex in infected cells. *Journal of Virology* **76**, 4785-4791.
- Bender, F. C., Whitbeck, J. C., Lou, H., Cohen, G. H. & Eisenberg, R. J. (2005). Herpes simplex virus glycoprotein B binds to cell surfaces independently of heparan sulphate and blocks virus entry. *Journal of Virology* **79**, 11588-11597.
- Benson, P. M., Malane, S. L., Banks, R., Hicks, C. B. & Hilliard, J. (1989). B virus (*Herpesvirus simiae*) and human infection. *Archives of Dermatology* **125**, 1247-1248.
- Bhella, D., Rixon, F. J. & Dargan, D. (2000). Cryomicroscopy of human cytomegalovirus virions reveals more densely packed genomic DNA than in herpes simplex virus type 1. *Journal of Molecular Biology* **295**, 155-161.
- Bjerke, S. L. & Roller, R. J. (2006). Roles for herpes simplex virus type 1 UL34 and US3 proteins in disrupting the nuclear lamina during herpes simplex virus type 1 egress. *Virology* **347**, 261-276.
- Boemher, P. E. & Lehman, I. R. (1997). Herpes simplex virus DNA replication. *Annual Review of Biochemistry* **66**, 347-384.
- Bogner, E. (1999). Human cytomegalovirus (HCMV) nuclease: implications for new strategies in gene therapy. *Gene Therapy and Molecular Biology* **3**, 75-78.
- Bogner, E., Radsak, K. & Stinski, M. (1998). The gene product of human cytomegalovirus open reading frame UL56 binds the *pac* motif and has specific nuclease activity. *Journal of Virology* **72**, 2259-2264.
- Bogner, E., Reschke, M., Reis, B., Mockenhaupt, T. & Radsak, K., . (1993). Identification of the gene product encoded by ORF56 of the human cytomegalovirus genome. *Virology* **196**, 290-293.
- Booy, F., Newcomb, W. W., Trus, B. L., Brown, J. C., Baker, T. S. & Steven, A. C. (1991). Liquid-crystalline, phage-like packaging of encapsidated DNA in herpes simplex virus. *Cell* **64**, 1007-1015.
- Booy, F. P., Trus, B. L., Davison, A. J. & Steven, A. C. (1996). The capsid architecture of channel catfish virus, an evolutionarily distant herpesvirus, is largely conserved in the absence of discernible sequence homology with herpes

- simplex virus. *Virology* **215**, 134-141.
- Bowman, B. R., Welschhans, R. L., Jayaram, H., Stow, N. D., Preston, V. G. & Quioco, F. A. (2006). Structural characterization of the UL25 DNA-packaging protein from herpes simplex virus type 1. *Journal of Virology* **80**, 2309-2317.
- Brandon Chen, I.-H., Li, L., Silva, L. & Sandri-Goldin, R. M. (2005). ICP27 recruits Aly/REF but not TAP/NXF1 to herpes simplex virus type 1 transcription sites although TAP/NXF1 is required for ICP27 export. *Journal of Virology* **79**, 3949-3961.
- Brown, J. C., McVoy, M. A. & Homa, F. L. (2002). Packaging DNA into herpesvirus capsids. In *Structure-Function Relationships of Human Pathogenic Viruses*, pp. 111-153. Edited by A. Holzenburg & E. Bogner. New York: Kluwer Academic/Plenum Publishers.
- Burch, A. D. & Weller, S. K. (2004). Nuclear sequestration of cellular chaperone and proteasomal machinery during herpes simplex virus type 1 infection. *Journal of Virology* **78**, 7175-7185.
- Butcher, S. J., Aitken, J., Mitchell, J., Gowen, B. & Dargan, D. (1998). Structure of the human cytomegalovirus B capsid by electron cryomicroscopy and image reconstruction. *Journal of Structural Biology* **124**, 70-76.
- Calderwood, M. A., Venkatesan, K., Xing, L., Chase, M. R., Vasquez, A., Holthaus, A. M., Ewence, A. E., Li, N., Hirozane-Kishikawa, T., Hill, D. E., Vidal, M., Kieff, E. & Johannsen, E. (2007). Epstein-Barr virus and virus human protein interaction maps. *PNAS USA* **104**, 7606-7611.
- Cardone, G., Winkler, D. C., Trus, B. L., Cheng, N., Heuser, J. E., Newcomb, W. W., Brown, J. C. & Steven, A. C. (2007). Visualization of the herpes simplex virus portal *in situ* by cryo-electron tomography. *Virology* **361**, 426-434.
- Catalano, C. (2000). The terminase enzyme from bacteriophage lambda: a DNA packaging machine. *Cell and Molecular Life Sciences* **57**, 128-148.
- Cavalcoli, J. D., Baghian, A., Homa, F. L. & Kousoulas, K. G. (1993). Resolution of phenotypic and genotypic properties of herpes simplex virus type 1 temperature-sensitive mutant (KOS) tsZ47: evidence for allelic complementation in the UL28 gene. *Virology* **197**, 23-34.
- Cebra, J., Berthelot, N. & Laither, M. (1989). Genome structure of cottontail rabbit herpesvirus. *Journal of Virology* **63**, 523-531.

- Cerritelli, M. E., Cheng, N., Rosenberg, A. H., McPherson, C. E., Booy, F. & Steven, A. C. (1997). Encapsidated conformation of bacteriophage T7 DNA. *Cell* **91**, 271-280.
- Chang, J. T., Schmid, M. F., Rixon, F. J. & Chiu, W. (2007). Electron cryotomography reveals the portal in the herpesvirus capsid. *Journal of Virology* **81**, 2065-2068.
- Chang, Y. E., Poon, A. W. P. & Roizman, A. (1996). Properties of the protein encoded by the UL32 open reading frame of herpes simplex virus type 1. *Journal of Virology* **70**, 3938-3946.
- Chelbi-Alix, M. K. & de The, H. (1999). Herpes virus induced proteasome-dependent degradation of the nuclear bodies-associated PML and Sp100 proteins. *Oncogene* **18**, 935-941.
- Chen, Y. M. & Knipe, D. M. (1996). A dominant mutant form of the herpes simplex virus ICP8 protein decreases viral late gene transcription. *Virology* **221**, 281-290.
- Cheshenko, N., Liu, W., Satlin, L. M. & Herold, B. C. (2005). Focal adhesion kinase plays a pivotal role in herpes simplex virus entry. *Journal of Biological Chemistry* **280**, 31116-31125.
- Coller, K. E., Lee, J. I.-H., Ueda, A. & Smith, G. A. (2007). The capsid and tegument of the alphaherpesviruses are linked by an interaction between the UL25 and VP1/2 protein. *Journal of Virology* **81**, 11790-11797.
- Conner, J., Rixon, F. J. & Brown, S. M. (2005). Herpes simplex virus type 1 strain HSV1716 grown in baby hamster kidney cells has altered tropism for nonpermissive chinese hamster ovary cells compared to HSV1716 grown in Vero cells. *Journal of Virology* **79**, 9770-9781.
- Cousens, D. J., Greaves, R., Goding, C. R. & O'Hare, P. (1989). The C-terminal 79 amino acids of the herpes simplex virus regulatory protein, Vmw65, efficiently activate transcription in yeast and mammalian cells in chimeric DNA-binding proteins. *EMBO Journal* **8**, 2337-2342.
- Cunningham, C. & Davison, A. J. (1993). A cosmid-based system for constructing mutants of herpes simplex virus type 1. *Virology* **197**, 116-124.
- Cunningham, C., Davison, A. J., MacLean, A. R., Taus, N. S. & Baines, J. D. (2000). Herpes simplex virus type 1 gene UL14: phenotype of a null mutant and identification of the encoded protein. *Journal of Virology* **74**, 33-41.
- Dasgupta, A. & Wilson, D. W. (1999). ATP depletion blocks herpes simplex virus DNA packaging and capsid maturation. *Journal of Virology* **73**, 2006-2015.

- Davison, A. J. (1992). Channel catfish virus: A new type of herpesvirus. *Virology* **186**, 9-14.
- Davison, A. J. (2002). Evolution of the herpesviruses. *Veterinary Microbiology* **86**, 69-88.
- Davison, A. J. & Davison, M. D. (1995). Identification of structural proteins of Channel Catfish virus by mass spectrometry. *Virology* **206**, 1035-1043.
- Davison, A. J. & Scott, J. E. (1986). The complete DNA sequence of varicella-zoster virus. *Journal of General Virology* **67**, 1759-1816.
- Davison, A. J., Trus, B. L., Cheng, N., Steven, A. C., Watson, M., Cunningham, C., Le Deuff, R.-M. & Renault, T. (2005). A novel class of herpesvirus with bivalve hosts. *Journal of General Virology* **86**, 41-53.
- de Beer, T., Fang, J., Ortega, M. E., Yang, Q., Maes, L., Duffy, C., Berton, N., Sippy, J., Overduin, M., Feiss, M. & Catalano, C. E. (2002). Insights into specific DNA recognition during the assembly of a viral genome packaging machine. *Molecular Cell* **9**, 981-991.
- de Bruyn Kops, A., Uprichard, S. L., Chen, M. & Knipe, D. M. (1998). Comparison of the intracellular distributions of herpes simplex virus proteins involved in various viral functions. *Virology* **252**, 162-178.
- de Zarate, I. B. O., Kaelin, K. & Rozenburg, F. (2004). Effects of mutations of herpes simplex virus type 1 glycoprotein B on intracellular transport and infectivity. *Journal of Virology* **78**, 1540-1551.
- Deeds, E. J., Asheburg, O. & I, S. E. (2006). A simple physical model for scaling in protein-protein interaction networks. *PNAS USA* **103**, 311-316.
- Deiss, L. P., Chou, J. & Frenkel, N. (1986). Functional domains within the *a* sequence involved in the cleavage-packaging of herpes simplex virus DNA. *Journal of Virology* **59**, 605-618.
- Deng, B., O'Connor, C. M., Kedes, D. H. & Hong Zhou, Z. (2007). Direct visualization of the putative portal in the Kaposi's Sarcoma-associated herpesvirus capsid by cryoelectron tomograph. *Journal of Virology* **81**, 3640-3644.
- Deng, H., Chu, J. T., Park, N.-H. & Sun, R. (2004). Identification of *cis* sequences required for lytic DNA replication and packaging of murine gammaherpesvirus 68. *Journal of Virology* **78**, 9123-9131.
- Deng, H. & Dewhurst, S. (1998). Functional identification and analysis of *cis*-acting sequences which mediate genome cleavage and packaging in human herpesvirus 6. *Journal of Virology* **72**, 320-329.

- Dhar, A. & Feiss, M. (2004). Bacteriophage λ terminase: alterations of the high-affinity ATPase affect viral DNA packaging. *Journal of Molecular Biology* **347**, 71-80.
- Dittmer, A. & Bogner, E. (2006). Specific short hairpin RNA-mediated inhibition of viral DNA packaging of human cytomegalovirus. *FEBS Letters* **580**, 6132-6138.
- Dittmer, A., Drach, J. C., Townsend, L. B., Fischer, A. & Bogner, E. (2005). Interaction of the putative human cytomegalovirus portal protein pUL104 with the large terminase subunit pUL56 and its inhibition by benzimidazole-D-ribonucleosides. *Journal of Virology* **79**, 14660-14667.
- Dohner, K., Wolfstein, A., Prank, U., Echeverri, C., Dujardin, D., Vallee, R. & Sodeik, B. (2002). Function of Dynein and Dynactin in Herpes Simplex Virus Capsid Transport. *Molecular Biology of the Cell* **13**, 2795-2809.
- Dolan, A., Jamieson, F. E., Cunningham, C., Barnett, B. C. & McGeoch, D. J. (1998). The genome sequence of herpes simplex virus type 2. *Journal of Virology* **72**, 2010-2021.
- Efstathiou, S. & Preston, C. (2005). Towards an understanding of the molecular basis of herpes simplex virus latency. *Virus Research* **111**, 108-119.
- Everett, R. D. (2000). ICP0, a regulator of herpes simplex virus during lytic and latent infection. *BioEssays* **22**, 761-770.
- Everett, R. D. (2006). Interactions between DNA viruses, ND10 and the DNA damage response. *Cellular Microbiology* **8**, 365-374.
- Everett, R. D., Freemont, P., Saitoh, H., Dasso, M., Orr, A., Kathoria, M. & Parkinson, J. (1998). The disruption of ND10 during herpes simplex virus infection correlates with a Vmw110- and proteasome-dependent loss of several PML isoforms. *Journal of Virology* **72**, 2661-2672.
- Everett, R. D. & Murray, J. (2005). ND10 components relocate to sites associated with herpes simplex virus type 1 nucleoprotein complexes during virus infection. *Journal of Virology* **79**, 5078-5089.
- Everett, R. D., Parada, C., Gripon, P., Sirma, H. & Orr, A. (2007). Replication of ICP0 null mutant herpes simplex virus type 1 is restricted by both PML and Sp100. *Journal of Virology* **82**, 2661-2672.
- Everett, R. D., Sourvinos, G., Leiper, C., Clements, J. B. & Orr, A. (2004). Formation of nuclear foci of the herpes simplex virus type 1 regulatory protein ICP4 at early times of infection: localization, dynamics, recruitment of ICP27, and evidence for the de novo induction of ND10-like complexes. *Journal of Virology*

78, 1903-1917.

- Farnsworth, A. & Johnson, D. C. (2006). Herpes simplex virus gE/gI must accumulate in the *trans*-Golgi network at early times and then redistribute to cell junctions to promote cell-cell spread. *Journal of Virology* **80**, 3167-3179.
- Farnsworth, A., Wisner, T. W. & Johnson, D. C. (2007). Cytoplasmic residues of herpes simplex virus glycoprotein gE required for secondary envelopment and binding to the tegument proteins VP22 and UL11 to gE and gD. *Journal of Virology* **81**, 319-331.
- Feederle, R., Shannon-Lowe, C., Baldwin, G. & Delecluse, H. J. (2005). Defective infectious particles and rare packaged genomes produced by cells carrying terminal-repeat-negative Epstein-Barr virus. *Journal of Virology* **79**, 7641-7647.
- Feiss, M. & Catalano, C. (2005). Bacteriophage lambda terminase and the mechanisms of viral DNA packaging. In *Viral Genome Packaging Machines: Genetics, Structure, and Mechanism*, pp. 5-39. Edited by C. Catalano. New York: Kluwer Academic/Plenum Publishers.
- Fokine, A., Chipman, P. R., Leiman, P. G., Mesyanzhinov, V. V., Rao, V. B. & Rossmann, M. G. (2004). Molecular architecture of the prolate head of bacteriophage T4. *PNAS USA* **101**, 6003-6008.
- Fontaine-Rodriguez, E. C., Taylor, T. J., Olesky, M. & Knipe, D. M. (2004). Proteomics of herpes simplex virus infected cell protein 27: association with translation initiation factors. *Virology* **330**, 487-492.
- Forest, T., Barnard, S. & Baines, J. D. (2005). Active intracellular movement of herpesvirus capsids. *Nature Cell Biol.* **7**, 429-431.
- Fujisawa, H. & Morita, M. (1997). Phage DNA packaging. *Genes to Cells* **2**, 537-545.
- Furlong, D., Swift, H. & Roizman, B. (1972). Arrangement of herpesvirus deoxyribonucleic acid in the core. *Journal of Virology* **10**, 1071-1074.
- Garber, D. A., Beverley, S. M. & Coen, D. M. (1993). Demonstration of circularization of herpes simplex virus DNA following infection using pulsed field gel electrophoresis. *Virology* **197**, 459-462.
- Gasteiger, E., Gattiker, A., Hoogland, C., Ivanyi, I., Appel, R. D. & Bairoch, A. (2003). ExpPASy: The proteomics server for in-depth protein knowledge and analysis. *Nucleic Acids Research* **31**, 3784-3788.
- Gaussier, H., Ortega, M. E., Maluf, N. K. & Catalano, C. E. (2005). Nucleotides regulate the conformational state of the small terminase subunit from

- bacteriophage lambda: implications for the assembly of a viral genome-packaging motor. *Biochemistry* **44**, 9645-9656.
- Geisen, K., Radnak, K. & Bogner, E. (2000a). Targeting of the gene product encoded by ORF UL56 of human cytomegalovirus into viral replication centers. *FEBS Letters* **471**, 215-218.
- Geisen, K., Radnak, K. & Bogner, E. (2000b). The potential terminase subunit of human cytomegalovirus, pUL56, is translocated into the nucleus by its own nuclear localisation signal and interacts with importin α . *Journal of General Virology* **81**, 2234-2241.
- Gerster, T. & Roeder, R. G. (1988). A Herpesvirus Trans-Activating Protein Interacts with Transcription Factor OTF-1 and Other Cellular Proteins. *Proceedings of the National Academy of Sciences* **85**, 6347-6351.
- Gibson, W. & Roizman, B. (1971). Compartmentalization of spermine and spermidine in the herpes simplex virion. *PNAS USA* **68**, 2818-2821.
- Given, D. & Kieff, E. (1979). DNA of Epstein-Barr virus. VI. Mapping of the internal tandem reiteration. *Journal of Virology* **31**, 315-324.
- Gompels, U. A., Nicholas, J., Lawrence, G., Jones, M., Thomson, B. J., Martin, M. E. D., Efstathiou, S., Craxton, M. & Macaulay, H. A. (1995). The DNA sequence of human herpesvirus-6: structure, coding content, and genome evolution. *Virology* **209**, 29-51.
- Granzow, H., Klupp, B. G. & Mettenleiter, T. C. (2005). Entry of pseudorabies virus: an immunogold-labeling study. *Journal of Virology* **79**, 3200-3205.
- Grondin, B. & DeLuca, N. A. (2000). Herpes simplex virus type 1 ICP4 promotes transcription preinitiation complex formation by enhancing the binding of TFIID to DNA. *Journal of Virology* **74**, 11504-11510.
- Hafezi, W., Bernard, E., Cook, R. & Elliott, G. (2005). Herpes simplex virus tegument protein VP22 contains an internal VP16 interaction domain and a C-Terminal domain that are both required for VP22 assembly into the virus particle. *Journal of Virology* **79**, 13082-13093.
- Hagglund, R. & Roizman, B. (2004). Role of ICP0 in the strategy on conquest of the host cell by herpes simplex virus 1. *Journal of Virology* **78**, 2169-2178.
- Hang, J. Q., Tack, B. F. & Feiss, M. (2000). ATPase center of bacteriophage λ terminase involved in post-cleavage stages of DNA packaging: identification of ATP-interactive amino acids. *Journal of Molecular Biology* **302**, 777-795.

- Harrison, S. C. (1983). Packaging of DNA into bacteriophage heads: a model. *Journal of Molecular Biology* **171**, 577-580.
- Heine, J. W., Honess, R. W., Cassai, E. & Roizman, B. (1974). Proteins Specified by Herpes Simplex Virus XII. The Virion Polypeptides of Type 1 Strains. *Journal of Virology* **14**, 640-651.
- Hendrix, R. W. (1978). Symmetry mismatch and DNA packaging in large bacteriophages. *PNAS USA* **75**, 4779-4783.
- Hodge, P. D. & Stow, N. D. (2001). Effects of mutations within the herpes simplex virus type 1 DNA encapsidation signal on packaging efficiency. *Journal of Virology* **75**, 8977-8986.
- Homa, F. L. & Brown, J. C. (1997). Capsid assembly and DNA packaging in herpes simplex virus. *Reviews in Medical Virology* **7**, 107-122.
- Hugel, T., Michealis, J., Hetherington, C. L., Jardine, P. J., Grimes, S., Walter, J. M., W., F., Anderson, D. L. & Bustamante, C. (2007). Experimental test of connector rotation during DNA packaging into bacteriophage phi29 capsids. *PLoS Biology* **5**, 558-567.
- Hwang, J.-S. & Bogner, E. (2002). ATPase activity of the terminase subunit UL56 of human cytomegalovirus. *Journal of Biological Chemistry* **277**, 6943-6948.
- Hwang, Y., Catalano, C. E. & Feiss, M. (1996). Kinetic and mutational dissection of the two ATPase activities of terminase, the DNA packaging enzyme of bacteriophage λ . *Biochemistry* **35**, 2796-2803.
- Jackson, S. A. & DeLuca, N. A. (2003). Relationship of herpes simplex virus genome configuration to productive and persistent infections. *PNAS USA* **100**, 7871-7876.
- Jacobson, J. G., Yang, K., Baines, J. D. & Homa, F. L. (2006). Linker insertion mutations in the herpes simplex virus type 1 UL28 gene: effects on UL28 interaction with UL15 and UL33 and identification of a second-site mutation in the UL15 gene that suppresses a lethal UL28 mutation. *Journal of Virology* **80**, 12312-12323.
- Jenkins, F. J. & Roizman, B. (1986). Herpes simplex virus 1 recombinants with noninverting genomes frozen in different isomeric arrangements are capable of independent replication. *Journal of Virology* **59**, 494-499.
- Jiang, W., Chang, J., Janaka, J., Weigele, P., King, J. & Chiu, W. (2006). Structure of epsilon15 bacteriophage reveals genome organization and DNA

- packaging/injection apparatus. *Nature* **439**, 612-616.
- Johnson, D. C. & Huber, M. T. (2002). Directed egress of animal viruses promotes cell-to-cell spread. *Journal of Virology* **76**, 1-8.
- Jones, D. T. (1999). Protein secondary structure prediction based on position-specific scoring matrices. *Journal of Molecular Biology* **292**, 195-202.
- Kanamaru, S., Kondabagil, K. R., Rossmann, M. G. & Rao, V. B. (2004). The functional domains of bacteriophage T4 terminase. *Journal of Biological Chemistry* **279**, 40795-40801.
- Kirkitadze, M. D., Barlow, P. N., Price, N. C., Kelly, S. M., Boutell, C. J., Rixon, F. J. & McClelland, D. A. (1998). The herpes simplex virus triplex protein, VP23, exists as a molten globule. *Journal of Virology* **72**, 10066-10072.
- Koch, H.-G., Delius, H., Matz, B., Flugel, R. M., Clarke, J. & Darai, G. (1985). Molecular cloning and physical mapping of the tupaia herpesvirus genome. *Journal of Virology* **55**, 86-95.
- Kondabagil, K. R., Zhang, Z. & Rao, V. B. (2006). The DNA translocating ATPase of bacteriophage T4 packaging motor. *Journal of Molecular Biology* **363**, 786-799.
- Koslowski, K. M., Shaver, P. R., Casey, J. T. I., Wilson, T., Yamanaka, G., Sheaffer, A. K., Tenney, D. J. & Pedersen, N. E. (1999). Physical and functional interactions between the herpes simplex virus UL15 and UL28 DNA cleavage and packaging proteins. *Journal of Virology* **73**, 1704-1707.
- Koslowski, K. M., Shaver, P. R., Wang, X.-Y., Tenney, D. J. & Pedersen, N. E. (1997). The pseudorabies virus protein UL28 enters the nucleus after co-expression with the herpes simplex virus UL15 protein. *Journal of Virology* **71**, 9118-9123.
- Kristensson, K., Lycke, E., Roytta, M., Svennerholm, B. & Vahlne, A. (1986). Neuritic Transport of Herpes Simplex Virus in Rat Sensory Neurons in vitro. Effects of Substances Interacting with Microtubular Function and Axonal Flow [Nocodazole, Taxol and Erythro-9-3-(2-hydroxynonyl)adenine]. *Journal of General Virology* **67**, 2023-2028.
- Kristie, T. M. & Roizman, B. (1987). Host Cell Proteins Bind to the Cis-Acting Site Required for Virion-Mediated Induction of Herpes Simplex Virus 1 alpha Genes. *Proceedings of the National Academy of Sciences* **84**, 71-75.
- Krosky, P. M., Underwood, M. R., Turk, S. R., Feng, K. W.-H., Jain, R. K., Ptak, R. G., Westerman, A. C., Biron, K. K., Townsend, L. B. & Drach, J. C. (1998). Resistance of human cytomegalovirus to benzimidazole ribonucleosides maps

- to two open reading frames: UL89 and UL56. *Journal of Virology* **72**, 4721-4728.
- LaBoissiere, S. & O'Hare, P. (2000). Analysis of HCF, the cellular cofactor of VP16, in herpes simplex virus-infected cells. *Journal of Virology* **74**, 99-109.
- Lamberti, C. & Weller, S. K. (1998). The herpes simplex virus type 1 cleavage/packaging protein, UL32, is involved in efficient localisation of capsids to replication compartments. *Journal of Virology* **72**, 2463-2473.
- Lander, G. C., Tang, L., Casjens, S. R., Gilcrease, E. B., Prevelige Jr, P. E., Poliakov, A., Potter, C. S., Carragher, B. & Johnson, J. E. (2006). The structure of an infectious P22 virion shows the signal for headful DNA packaging. *Science* **312**, 1791-1795.
- Lebedev, A. A., Krause, M. H., Isidro, A. L., Vagin, A. A., Orlova, E. V., Turner, J., Dodson, E. J. & Antson, A. A. (2007). Structural framework for DNA translocation via the viral portal protein. *EMBO Journal* **26**, 1984-1994.
- Leffers, G. & Rao, V. B. (2000). Biochemical characterization of an ATPase activity associated with the large packaging subunit gp17 from bacteriophage T4. *Journal of Biological Chemistry* **275**, 37127-37136.
- Lehman, I. R. & Boemher, P. E. (1999). Replication of herpes simplex virus DNA. *Journal of Biological Chemistry* **274**, 28059-28062.
- Leopardi, R., Michael, N. & Roizman, B. (1995). Repression of the herpes simplex virus 1 alpha 4 gene by its gene product (ICP4) within the context of the viral genome is conditioned by the distance and stereoaxial alignment of the ICP4 DNA binding site relative to the TATA box. *Journal of Virology* **69**, 3042-3048.
- Leuzinger, H., Zeigler, U., Schraner, E. M., Fraefel, C., Glauser, D. L., Heid, I., Ackermann, M., Mueller, M. & Wild, P. (2005). Herpes simplex virus type 1 envelopment follows two diverse pathways. *Journal of Virology* **79**, 13047-13059.
- Liang, L. & Baines, J. D. (2005). Identification of an essential domain in the herpes simplex virus 1 UL34 protein that is necessary and sufficient to interact with UL31 protein. *Journal of Virology* **79**, 3797-3806.
- Linding, R., Russell, R. B., Neduva, V. & Gibson, T. J. (2003). GlobPlot: exploring protein sequences for globularity and disorder. *Nucleic Acids Research* **31**, 3701-3708.
- Lohman, T. M. (1993). Helicase-catalyzed DNA unwinding. *Journal of Biological Chemistry* **268**, 2269-2272.
- Lynch, T. W., Read, E. K., Mattis, A. N., Gardner, J. F. & Rice, P. A. (2003).

- Integration host factor: putting a twist on protein-DNA recognition. *Journal of Molecular Biology* **330**, 493-502.
- Mabit, H., Nakano, M. Y., Prank, U., Saam, B., Dohner, K., Sodeik, B. & Greber, U. F. (2002). Intact Microtubules Support Adenovirus and Herpes Simplex Virus Infections. *Journal of Virology* **76**, 9962-9971.
- Malik, A. K., Shao, L., Shanley, J. D. & Weller, S. K. (1996). Intracellular localization of the herpes simplex virus type-1 origin binding protein, UL9. *Virology* **224**, 380-389.
- Maluf, N. K., Gaussier, H., Bogner, E., Feiss, M. & Catalano, C. E. (2006). Assembly of bacteriophage lambda terminase into a viral DNA maturation and packaging machine. *Biochemistry* **45**, 15259-15268.
- Martinez, R., Sarisky, R. T., Weber, P. C. & Weller, S. K. (1996). Herpes simplex virus type 1 alkaline nuclease is required for efficient processing of viral DNA replication intermediates. *Journal of Virology* **70**, 2075-2085.
- McClelland, D. A., Aitken, J. D., Bhella, D., McNab, D., Mitchell, J., Kelly, S. M., Price, N. C. & Rixon, F. J. (2002). pH reduction as a trigger for dissociation of herpes simplex virus type 1 scaffolds. *Journal of Virology* **76**, 7407-7417.
- McGeoch, D. J. (2001). Molecular evolution of the gamma-herpesvirinae. *Philos. Trans. R. Soc. Lond. B. Biol. Sci.* **356**, 421-435.
- McGeoch, D. J., Dalrymple, M. A., Davison, A. J., Dolan, A., Frame, M. C., McNab, D., Perry, L. J., Scott, J. E. & Taylor, P. (1988). The complete DNA sequence of the long unique region in the genome of herpes simplex virus type 1. *Journal of General Virology* **69**, 1531-1574.
- McGeoch, D. J., Dolan, A. & Ralph, A. C. (2000). Towards a comprehensive phylogeny for mammalian and avian herpesviruses. *Journal of Virology* **74**, 10401-10406.
- McGeoch, D. J. & Gatherer, D. (2005). Integrating reptilian herpesviruses into the family herpesviridae. *Journal of Virology* **79**, 725-731.
- McGeoch, D. J., Rixon, F. J. & Davison, A. J. (2006). Topics in herpesvirus genomics and evolution. *Virus Research* **117**, 90-104.
- McGuffin, L. J., Bryson, K. & Jones, D. T. (2000). The PSIPRED protein structure prediction server. *Bioinformatics* **16**, 404-405.
- McLauchlan, J., Addison, C., Craigie, M. C. & Rixon, F. J. (1992). Noninfectious L-particles supply functions which can facilitate infection by HSV-1. *Virology* **190**,

682-688.

- McLean, G. W., Abbotts, A. P., Parry, M. E., Marsden, H. S. & Stow, N. D. (1994). The herpes simplex virus type 1 origin-binding protein interacts specifically with the viral UL8 protein. *Journal of General Virology* **75**, 2699-2706.
- McNab, A. R., Desai, P., Person, S., Roof, L. L., Thomsen, D. R., Newcomb, W. W., Brown, J. C. & Homa, F. L. (1998). The product of the herpes simplex virus type 1 UL25 gene is required for encapsidation but not cleavage of replicated viral DNA. *Journal of Virology* **72**, 1060-1070.
- McVoy, M. A. & Nixon, D. E. (2005). Impact of 2-Bromo-5,6-Dichloro-1- β -D-Ribofuranosyl Benzimidazole Riboside and inhibitors of DNA, RNA, and protein synthesis on human cytomegalovirus genome maturation. *Journal of Virology* **79**, 11115-11127.
- McVoy, M. A., Nixon, D. E., Adler, S. P. & Mocarski, E. S. (1998). Sequences within the herpesvirus conserved *pac1* and *pac2* motifs are required for cleavage and packaging of the murine cytomegalovirus genome. *Journal of Virology* **72**, 48-56.
- Mears, W. & Rice, S. (1996). The RGG box motif of the herpes simplex virus ICP27 protein mediates an RNA-binding activity and determines in vivo methylation. *J. Virol.* **70**, 7445-7453.
- Mettenleiter, T. C. (2002). Herpesvirus assembly and egress. *Journal of Virology* **76**, 1537-1547.
- Mettenleiter, T. C. (2004). Budding events in herpesvirus morphogenesis. *Virus Research* **106**, 167-180.
- Mettenleiter, T. C. & Minson, T. (2006). Letter to the Editor: Egress of alphaherpesviruses. *Journal of Virology* **80**, 1610-1612.
- Mettenleiter, T. C., Saalmuller, A. & Weiland, F. (1993). Pseudorabies virus protein homologous to herpes simplex virus type 1 ICP18.5 is necessary for capsid maturation. *Journal of Virology* **67**, 1236-1245.
- Milne, R. S. B., Vicola, A. V., Whitbeck, J. C., Eisenberg, R. J. & Cohen, G. H. (2005). Glycoprotein D receptor-dependent, low-pH-independent endocytic entry of herpes simplex virus type 1. *Journal of Virology* **79**, 2655-2663.
- Mitchell, M. S. & Rao, V. B. (2004). Novel and deviant Walker A ATP-binding motifs in bacteriophage large terminase-DNA packaging proteins. *Virology* **321**, 217-221.
- Mocarski, E. S. & Roizman, B. (1982). Structure and role of the herpes simplex virus

- DNA termini in inversion, circularization and generation of virion DNA. *Cell* **31**, 89-97.
- Mouzakitis, G., McLauchlan, J., Barreca, C., Kueltzo, L. & O'Hare, P. (2005). Characterisation of VP22 in herpes simplex virus-infected cells. *Journal of Virology* **79**, 12185-12198.
- Muylaert, I. & Elias, P. (2007). Knock-down of DNA ligase IV/ XRCC4 by RNAi inhibits herpes simplex virus type I DNA replication. *Journal of Biological Chemistry* **282**, 10865-10872.
- Nasseri, M. & Mocarski, E. S. (1988). The cleavage recognition signal is contained within sequences surrounding an a-a junction in herpes simplex virus DNA. *Virology* **167**, 25-30.
- Nellissery, J. K., Szczepaniak, R., Lamberti, C. & Weller, S. K. (2007). A putative leucine zipper within the herpes simplex virus type 1 UL6 protein is required for portal ring formation. *Journal of Virology* **81**, 8868-8877.
- Newcomb, W. W. & Brown, J. C. (2002). Inhibition of herpes simplex virus replication by WAY-150138: assembly of capsids depleted of the portal and terminase proteins involved in DNA encapsidation. *Journal of Virology* **76**, 10084-10088.
- Newcomb, W. W., Homa, F. L. & Brown, J. C. (2005). Involvement of the portal at an early step in herpes simplex virus capsid assembly. *Journal of Virology* **79**, 10540-10546.
- Newcomb, W. W., Homa, F. L. & Brown, J. C. (2006). Herpes simplex virus capsid structure: DNA packaging protein UL25 is located on the external surface of the capsid near the vertices. *Journal of Virology* **80**, 6286-6294.
- Newcomb, W. W., Homa, F. L., Thomsen, D. R., Booy, F., Trus, B. L., Steven, A. C., Spencer, J. V. & Brown, J. C. (1996). Assembly of the herpes simplex virus capsid: characterisation of intermediates observed during cell-free capsid formation. *Journal of Molecular Biology* **263**, 432-446.
- Newcomb, W. W., Homa, F. L., Thomsen, D. R., Trus, B. L., Cheng, N., Steven, A., Booy, F. & Brown, J. C. (1999). Assembly of the herpes simplex virus procapsid from purified components and identification of small complexes containing the major capsid and scaffold proteins. *Journal of Virology* **73**, 4239-4250.
- Newcomb, W. W., Juhas, R. M., Thomsen, D. R., Homa, F. L., Burch, A. D., Weller, S. K. & Brown, J. C. (2001). The UL6 gene product forms the portal for entry of

- DNA into the herpes virus capsid. *Journal of Virology* **75**, 10923-10932.
- Nicola, A. V. & Straus, S. E. (2004). Cellular and viral requirements for rapid endocytic entry of herpes simplex virus. *Journal of Virology* **78**, 7508-7517.
- Nixon, D. E. & McVoy, M. A. (2004). Dramatic effects of 2-Bromo-5,6-Dichloro-1- β -D-Ribofuranosyl benzimidazole riboside on the genome structure, packaging, and egress of guinea pig cytomegalovirus. *Journal of Virology* **78**, 1623-1635.
- Nozawa, N., Kawaguchi, Y., Tanaka, M., Kato, A., Kato, A., Kimura, H. & Nishiyama, Y. (2005). Herpes simplex virus type 1 UL51 protein is involved in maturation and egress of virus particles. *Journal of Virology* **79**, 6947-6956.
- Ogasawara, M., Suzutani, T., Yoshida, I. & Azuma, M. (2001). Role of the UL25 gene product in packaging DNA into the herpes simplex virus capsid: location of UL25 product in the capsid and demonstration that it binds DNA. *Journal of Virology* **75**, 1427-1436.
- O'Hare, P., Goding, C. R. & Haigh, A. (1988). Direct combinatorial interaction between a herpes simplex virus regulatory protein and a cellular octamer-binding factor mediates specific induction of virus immediate-early gene expression. *EMBO Journal* **7**, 4231-8.
- Orlova, E. V., Gowen, B., Droge, A., Stiege, A., Weise, F., Lurz, L., van Heel, M. & Tavares, P. (2003). Structure of a viral DNA gatekeeper at 10Å resolution by cryo-electron microscopy. *EMBO Journal* **22**, 1255-1262.
- Ortega, M. E. & Catalano, C. E. (2006). Bacteriophage lambda gpNu1 and Escherichia coli IHF proteins cooperatively bind and bend viral DNA: implications for the assembly of a genome-packaging motor. *Biochemistry* **45**, 5180-5189.
- Patel, A. H. & MacLean, J. B. (1995). The product of the UL6 gene of herpes simplex virus type 1 is associated with virus capsids. *Virology* **206**, 465-478.
- Patel, A. H., Rixon, F. J., Cunningham, C. & Davison, A. J. (1996). Isolation and characterisation of herpes simplex virus type 1 mutants defective in the UL6 gene. *Virology* **217**, 111-123.
- Perez, A., Li, Q.-X., Perez-Romero, P., DeLassus, G., Lopez, S. R., Sutter, S., McLaren, N. & Fuller, A. O. (2005). A new class of receptor for herpes simplex virus has heptad repeat motifs that are common to membrane fusion proteins. *Journal of Virology* **79**, 7419-7430.
- Phelan, A., Dunlop, J., Patel, A. H., Stow, N. D. & Clements, J. B. (1997). Nuclear sites of herpes simplex virus type 1 DNA replication and transcription colocalize at

- early times postinfection and are largely distinct from RNA processing factors. *Journal of Virology* **71**, 1124-1132.
- Poffenberger, K. L. & Roizman, B. (1985). A noninverting genome of a viable herpes simplex virus 1: presence of head-to-tail linkages in packaged genomes and requirements for circularization after infection. *Journal of Virology* **53**, 587-595.
- Ponchon, L., Boulanger, P., Labesse, G. & Letellier, L. (2006). The endonuclease domain of bacteriophage terminases belongs to the resolvase/integrase/ribonuclease H superfamily. *Journal of Biological Chemistry* **281**, 5829-5836.
- Poon, A. & Roizman, B. (1993). Characterization of a temperature-sensitive mutant of the UL15 open reading frame of herpes simplex virus 1. *Journal of Virology* **67**, 4497-4503.
- Porter, I. & Stow, N. D. (2004a). Virus particles produced by the herpes simplex type 1 alkaline nuclease null mutant ambUL12 contains abnormal genomes. *Journal of General Virology* **85**, 583-591.
- Porter, I. & Stow, N. D. (2004b). Replication, recombination and packaging of amplicon DNA in cells infected with the herpes simplex virus type 1 alkaline nuclease null mutant ambUL12. *Journal of General Virology* **85**, 3501-3510.
- Preston, V. G., Coates, J. A. & Rixon, F. J. (1983). Identification and characterization of a herpes simplex virus gene product required for encapsidation of virus DNA. *Journal of Virology* **45**, 1056-1064.
- Przech, A. J., Yu, D. & Weller, S. K. (2003). Point mutations in exon 1 of the herpes simplex virus putative terminase subunit, UL15, indicate that most conserved residues are essential for cleavage and packaging. *Journal of Virology* **77**, 9613-9621.
- Quinlan, M. P., Chen, L. B. & Knipe, D. M. (1984). The intranuclear location of a herpes simplex virus DNA-binding protein is determined by the state of viral DNA replication. *Cell* **36**, 857-868.
- Randall, R. E. & Dinwoodie, N. (1986). Intranuclear localization of herpes simplex virus immediate-early and delayed-early proteins: evidence that ICP4 is associated with progeny virus DNA. *Journal of General Virology* **67**, 2163-2177.
- Rao, V. B. & Black, L. W. (2005). DNA packaging in bacteriophage T4. In *Viral Genome Packaging Machines: Genetics, Structure, and Mechanism*, pp. 40-58. Edited by C. Catalano. New York: Kluwer Academic/Plenum Publishers.

- Reuven, N. B., Staire, A. E., Myers, R. S. & Weller, S. K. (2003). The herpes simplex virus type 1 alkaline nuclease and single-stranded DNA binding protein mediate strand exchange *in vitro*. *Journal of Virology* **77**, 7425-7433.
- Reuven, N. B. & Weller, S. K. (2005). Herpes simplex virus type 1 single-strand DNA binding protein ICP8 enhances the nuclease activity of the UL12 alkaline nuclease by increasing its processivity. *Journal of Virology* **79**.
- Reynolds, A. E., Fan, Y. & Baines, J. D. (2000). Characterisation of the UL33 gene product of herpes simplex virus 1. *Virology* **266**, 310-318.
- Reynolds, A. E., Wills, E. G., Roller, R. J., Ryckman, B. J. & Baines, J. D. (2002). Ultrastructural localization of the herpes simplex virus type 1 UL31, UL34, and US3 proteins suggests specific roles in primary envelopment and egress of nucleocapsids. *Journal of Virology* **76**, 8939-8952.
- Richards, K. E., Williams, R. C. & Calendar, R. (1973). Mode of DNA packing within bacteriophage heads. *Journal of Molecular Biology* **78**, 255-259.
- Rixon, F. J. (1993). Structure and assembly of herpesviruses. *Seminars in Virology* **4**, 135-144.
- Roizman, B. (1979). The structure and isomerization of herpes simplex virus genomes. *Cell* **16**, 481-494.
- Romero, P., Obradovic, Z. & K., D. A. (2004). Natively disordered proteins: functions and predictions. *Applied Bioinformatics* **3**, 105-13.
- Rosenthal, K. S., Leuther, M. D. & Barisas, B. G. (1984). Herpes simplex virus binding and entry modulate cell surface protein mobility. *Journal of Virology* **49**, 980-983.
- Salmon, B. & Baines, J. D. (1998). Herpes simplex virus DNA cleavage and packaging: association of multiple forms of UL15-encoded proteins with B capsids requires at least UL6, UL17 and UL28 genes. *Journal of Virology* **72**, 3045-3050.
- Salmon, B., Nalwanga, D., Fan, Y. & Baines, J. D. (1999). Proteolytic cleavage of the amino terminus of the UL15 gene product of herpes simplex virus type 1 is coupled with maturation of viral DNA into unit-length genomes. *Journal of Virology* **73**, 8338-8348.
- Sandri-Goldin, R. M. (1998). ICP27 mediates HSV RNA export by shuttling through a leucine-rich nuclear export signal and binding viral intronless RNAs through an RGG motif. *Genes & Development* **12**, 868-879.
- Sandri-Goldin, R. M. (2004). Viral regulation of mRNA export. *Journal of Virology* **78**, 4389-4396.

- Savva, C. W. G., Holzenburg, A. & Bogner, E. (2004). Insights into the structure of human cytomegalovirus large terminase subunit pUL56. *FEBS Letters* **563**, 135-140.
- Schaffer, P. A., Aron, G. M., N., B. & Benyesh-Melnick, M. (1973). Temperature-sensitive mutants of herpes simplex virus type 1: isolation, complementation and partial characterization. *Virology* **52**, 57-71.
- Scheffczik, H., Savva, C. W. G., Holzenburg, A., Kolensnikova, L. & Bogner, E. (2002). The terminase subunits pUL56 and pUL89 of human cytomegalovirus are DNA-metabolising proteins with toroidal structure. *Nucleic Acids Research* **30**, 1695-1703.
- Schildgen, O., Graper, S., Blumel, J. & Matz, B. (2005). Genome replication and progeny virion production of herpes simplex virus type 1 mutants with temperature-sensitive lesions in the origin-binding protein. *Journal of Virology* **79**, 7273-7278.
- Scholz, B., Rechter, S., Drach, J. C., Townsend, L. B. & Bogner, E. (2003). Identification of the ATP-binding site in the terminase subunit pUL56 of human cytomegalovirus. *Nucleic Acids Research* **31**, 1426-1433.
- Schrag, J. D., Prasad, B. V., Rixon, F. J. & Chiu, W. (1989). Three-dimensional structure of the HSV 1 nucleocapsid. *Cell* **56**, 651-660.
- Serwer, P. (1988). The source of energy for bacteriophage DNA packaging: an osmotic pump explains the data. *Biopolymers* **27**, 165-169.
- Serwer, P. (2003). Models of bacteriophage DNA packaging motors. *Journal of Structural Biology* **141**, 179-188.
- Shahin, V., Hafezi, W., Oberleithner, H., Ludwig, Y., Windoffer, B., Schillers, H. & Kuhn, J. E. (2006). The genome of HSV-1 translocates through the nuclear pore as a condensed rod-like structure. *Journal of Cell Science* **119**, 23-30.
- Shao, L., Rapp, L. M. & Weller, S. K. (1993). Herpes simplex virus type 1 alkaline nuclease is required for efficient egress of capsids from the nucleus. *Virology* **196**, 146-162.
- Sheaffer, A. K., Newcomb, W. W., Gao, M., Yu, D., Weller, S. K., Brown, J. C. & Tenney, D. J. (2001). Herpes simplex virus DNA cleavage and packaging proteins associate with the procapsid prior to its maturation. *Journal of Virology* **75**, 687-698.
- Sherman, G. & Bachenheimer, S. L. (1987). DNA processing in temperature-sensitive

- morphogenic mutants of HSV-1. *Virology* **158**, 427-430.
- Sherman, G. & Bachenheimer, S. L. (1988). Characterisation of intranuclear capsids made by ts morphogenic mutants of HSV-1. *Virology* **163**, 471-480.
- Shibata, H., Fujisawa, H. & Minigawa, T. (1987). Characterization of the bacteriophage T3 DNA packaging reaction in vitro in a defined system. *Journal of Molecular Biology* **196**, 845-851.
- Simpson, A. A., Tao, Y., Leiman, P. G., Badasso, M. O., He, Y., Jardine, P. J., Olson, N. H., Morais, M. C., Grimes, S., Anderson, D. L., Baker, T. S. & Rossmann, M. G. (2000). Structure of the bacteriophage phi29 DNA packaging motor. *Nature* **408**, 745-750.
- Simpson-Holley, M., Colgrove, R. C., Nalepa, G., Harper, J. W. & Knipe, D. M. (2005). Identification and functional evaluation of cellular and viral factors involved in the alteration of nuclear architecture during herpes simplex virus type 1 infection. *Journal of Virology* **79**, 12840-12851.
- Sinclair, J. & Sissons, P. (2006). Latency and reactivation of human cytomegalovirus. *Journal of General Virology* **87**, 1163-1179.
- Singer, G. P., Newcomb, W. W., Thomsen, D. R., Homa, F. L. & Brown, J. C. (2005). Identification of a region in the herpes simplex virus scaffolding protein required for interaction with the portal. *Journal of Virology* **79**, 132-139.
- Smiley, J. R., Duncan, J. & Howes, M. (1990). Sequence requirements for DNA rearrangements induced by the terminal repeat of herpes simplex virus type 1 KOS DNA. *Journal of Virology* **64**, 5036-5050.
- Smith, A. E. & Helenius, A. (2004). How viruses enter animal cells. *Science* **304**, 237-242.
- Smith, D. E., Tans, S. J., Smith, S. B., Grimes, S., Anderson, D. L. & Bustamante, C. (2001). The bacteriophage phi29 portal motor can package DNA against a large internal force. *Nature* **413**, 748-752.
- Sodeik, B., Ebersold, M. W. & Helenius, A. (1997). Microtubule-mediated Transport of Incoming Herpes Simplex Virus 1 Capsids to the Nucleus. *Journal of Cell Biology* **136**, 1007-1021.
- Spaete, R. R. & Frenkel, N. (1985). The herpes simplex virus amplicon: analyses of cis-acting replication functions. *PNAS USA* **82**, 694-698.
- Spear, P. G. & Longnecker, R. (2003). Herpesvirus entry: an update. *Journal of Virology* **77**, 10179-10185.

- Spear, P. G. & Roizman, B. (1972). Proteins Specified by Herpes Simplex Virus V. Purification and Structural Proteins of the Herpesvirion. *Journal of Virology* **9**, 143-159.
- Stirling, P. C., Lundin, V. F. & Leroux, M. R. (2003). Getting a grip on non-native proteins. *EMBO Reports* **4**, 565-570.
- Stow, N. D., Brown, G., Cross, A. M. & Abbotts, A. P. (1998). Identification of residues within the herpes simplex virus type 1 origin-binding protein that contribute to sequence-specific DNA binding. *Virology* **240**, 183-192.
- Stow, N. D., Hammersten, O., Arbuckle, M. I. & Elias, P. (1993). Inhibition of herpes simplex virus type 1 DNA replication by mutant forms of the origin-binding protein. *Virology* **196**, 413-418.
- Stow, N. D., McMonagle, E. C. & Davison, A. J. (1983). Fragments from both termini of the herpes simplex virus type 1 genome contain signals required for the encapsulation of viral DNA. *Nucleic Acids Research* **11**, 8205-8220.
- Stow, N. D. & Wilkie, N. M. (1976). An improved technique for obtaining enhanced infectivity with herpes simplex virus type 1 DNA. *Journal of General Virology* **33**, 447-458.
- Strang, B. L. & Stow, N. D. (2005). Circularisation of the herpes simplex virus type 1 genome upon lytic infection. *Journal of Virology* **79**, 12487-12494.
- Strang, B. L. & Stow, N. D. (2007). Blocks to herpes simplex virus type 1 replication in a cell line, tsBN2, encoding a temperature sensitive RCC1 protein. *Journal of General Virology* **88**, 376-383.
- Sun, S., Kondabagil, K. R., Gentz, P. M., Rossmann, M. G. & Rao, V. B. (2007). The structure of the ATPase that powers DNA packaging into bacteriophage T4 procapsids. *Molecular Cell* **25**, 943-949.
- Talcott, B. & Moore, M. S. (1999). Getting across the nuclear pore complex. *Trends in Cell Biology* **9**, 312-318.
- Tang, L., Marion, W. R., Cingolani, G., Prevelige Jr, P. E. & Johnson, J. E. (2005). Three-dimensional structure of the bacteriophage P22 tail machine. *EMBO Journal* **24**, 2087-2095.
- Taus, N. S., Salmon, B. & Baines, J. D. (1998). The herpes simplex virus 1 UL17 gene is required for localisation of capsids and major and minor capsid proteins to intranuclear sites where viral DNA is cleaved and packaged. *Virology* **252**, 115-125.

- Tengelsen, L. A., Pederson, N. E., Shaver, P. R., Wathen, M. W. & Homa, F. L. (1993). Herpes simplex virus type 1 DNA cleavage and encapsidation require the product of the UL28 gene: isolation and characterization of two UL28 deletion mutants. *Journal of Virology* **67**, 3470-3480.
- Thoma, C., Borst, E., Messerle, M., Rieger, M., Hwang, J.-S. & Bogner, E. (2006). Identification of the interaction domain of the small terminase subunit pUL89 with the large subunit pUL56 of human cytomegalovirus. *Biochemistry* **45**, 8855-8863.
- Thurlow, J. K., Murphy, M., Stow, N. D. & Preston, V. G. (2006). Herpes simplex virus type 1 DNA-packaging protein UL17 is required for efficient binding of UL25 to capsids. *Journal of Virology* **80**, 2118-2126.
- Thurlow, J. K., Rixon, F. J., Murphy, M., Targett-Adams, P., Hughes, M. & Preston, V. G. (2005). The herpes simplex virus type 1 DNA packaging protein UL17 is a virion protein that is present in both the capsid and the tegument compartments. *Journal of Virology* **79**, 150-158.
- Trus, B. L., Cheng, N., Newcomb, W. W., Homa, F. L., Brown, J. C. & Steven, A. C. (2004). Structure and polymorphism of the UL6 portal protein of herpes simplex virus type 1. *Journal of Virology* **78**, 12668-12671.
- Turcotte, S., Letellier, J. & Lippe, R. (2005). Herpes simplex virus type 1 capsids transit by the *trans*-Golgi network, where viral glycoproteins accumulate independently of capsid egress. *Journal of Virology* **79**, 8847-8860.
- Twigg, A. J. & Sherratt, D. (1980). Trans-complementable copy-number mutants of plasmid ColE1. *Nature* **282**, 216-218.
- Uetz, P., Dong, Y.-A., Zeretzke, C., Atzler, C., Baiker, A., Berger, B., Rajagopala, S. V., Roupelieva, M., Rose, D., Fossum, E. & Haas, J. (2006). Herpesviral protein networks and their interaction with the human proteome. *Science* **311**, 239-242.
- Ushijima, Y., Luo, C., Goshima, F., Yamauchi, Y., Kimura, H. & Nishiyama, Y. (2007). Determination and analysis of the DNA sequence of highly attenuated herpes simplex virus type 1 mutant HF10, a potential oncolytic virus. *Microbes and Infection* **9**, 142-149.
- van Zeijl, M., Fairhurst, J., Jones, T. R., Vernon, S. K., Morin, J., LaRocque, J., Feld, B., O'Hara, B., Bloom, J. D. & Johann, S. V. (2000). Novel class of thiourea compounds that inhibit herpes simplex virus type 1 DNA cleavage and encapsidation: resistance maps to the UL6 gene. *Journal of Virology* **74**, 9054-

9061.

- Vellani, T. S. & Myers, R. S. (2003). Bacteriophage SPP1 Chu is an alkaline exonuclease in the SynExo family of viral two-component recombinases. *Journal of Bacteriology* **185**, 2465-2474.
- Visalli, R. J. & van Zeijl, M. (2003). DNA encapsidation as a target for anti-herpesvirus drug therapy. *Antiviral Research* **59**, 73-87.
- Vlazny, D. A., Kwong, A. & Frenkel, N. (1982). Site-specific cleavage/packaging of herpes simplex virus DNA and the selective maturation of nucleocapsids containing full-length viral DNA. *PNAS USA* **79**, 1423-1427.
- Vossen, M. T., Westerhout, E. M., Soderburg-Naucler, C. & Wiertz, E. J. (2002). Viral immune evasion: a masterpiece of evolution. *Immunogenetics* **54**, 527-542.
- Walker, J. E., Saraste, M., Runswick, M. J. & Gay, N. J. (1982). Distantly related sequences in the α - and β -subunits of ATP synthase, myosin, kinases and other ATP-requiring enzymes and a common nucleotide binding fold. *EMBO Journal* **1**, 945-951.
- Ward, P., Ogle, W. & Roizman, B. (1996). Assemblons: nuclear structures defined by aggregation of immature capsids and some tegument proteins of herpes simplex virus 1. *Journal of Virology* **70**, 4623-4631.
- Weir, J. P. (2001). Regulation of herpes simplex virus gene expression. *Gene* **271**, 117-130.
- Whitbeck, J. C., Y., Z., Milne, R. S. B., Cohen, G. H. & Eisenberg, R. J. (2006). Stable association of herpes simplex virus with target membranes is triggered by low pH in the presence of the gD receptor, HVEM. *Journal of Virology* **80**, 3773-3780.
- White, C. A., Stow, N. D., Patel, A. H., Hughes, M. & Preston, V. G. (2003). Herpes simplex virus type 1 portal protein UL6 interacts with putative terminase subunits UL15 and UL28. *Journal of Virology* **77**, 6351-6358.
- Wilkinson, D. E. & Weller, S. K. (2003). The role of DNA recombination in herpes simplex virus DNA replication. *IUBMB Life* **55**, 451-458.
- Xiang, Y., Morais, M. C., Battisti, A. J., Grimes, S., Jardine, P. J., Anderson, D. L. & Rossmann, M. G. (2006). Structural changes of bacteriophage phi29 upon DNA packaging and release. *EMBO Journal* **25**, 5229-5239.
- Yamauchi, Y., Kiriya, K., Kubota, N., Kimura, H., Usukura, J. & Nishiyama, Y. (2008). The UL14 tegument protein of herpes simplex virus type 1 is required

- for efficient nuclear transport of the alpha transinducing factor VP16 and viral capsids. *Journal of Virology* **82**, 1094-1106.
- Yamauchi, Y., Wada, K., Goshima, F., Daikoku, T., Ohtsuka, K. & Nishiyama, Y. (2002). Herpes simplex virus type 2 UL14 gene product has heat-shock protein (HSP)-like functions. *Journal of Cell Science* **115**, 2517-2527.
- Yamauchi, Y., Wada, K., Goshima, F., Takakuwa, H., Daikoku, T., Yamada, M. & Nishiyama, Y. (2001). The UL14 protein of herpes simplex virus type 2 translocates the minor capsid protein VP26 and the DNA cleavage and packaging UL33 protein into the nucleus of coexpressing cells. *Journal of General Virology* **82**, 321-330.
- Yang, K., Homa, F. & Baines, J. D. (2007). Putative terminase subunits of herpes simplex virus 1 form a complex in the cytoplasm and interact with portal protein in the nucleus. *Journal of Virology* **81**, 6419-6433.
- Yang, K., Poon, A. P., Roizman, B. & Baines, J. D. (2008). Temperature-sensitive mutations in the putative herpes simplex virus type 1 terminase subunits pUL15 and pUL33 preclude viral DNA cleavage/packaging and interaction with pUL28 at the nonpermissive temperature. *Journal of Virology* **82**, 487-494.
- Yang, Q. & Catalano, C. (2003). Biochemical characterization of bacteriophage lambda genome packaging *in vitro*. *Virology* **305**, 276-287.
- Yang, Q. & Catalano, C. E. (2004). A minimal kinetic model for a viral DNA packaging machine. *Biochemistry* **43**, 289-299.
- Yu, D., Sheaffer, A. K., Tenney, D. J. & Weller, S. K. (1997). Characterisation of ICP6::lacZ insertion mutants of the UL15 gene of herpes simplex virus type 1 reveals the translation of two proteins. *Journal of Virology* **71**, 2656-2665.
- Yu, D. & Weller, S. K. (1998a). Genetic analysis of the UL15 locus for the putative terminase of herpes simplex virus type 1. *Virology* **243**, 32-44.
- Yu, D. & Weller, S. K. (1998b). Herpes simplex virus type 1 cleavage and packaging proteins are associated with B but not A capsids during packaging. *Journal of Virology* **72**, 7428-7439.
- Zhang, Z., Greene, B., Thuman-Commike, P. A., Janaka, J., Prevelige Jr, P. E., King, J. & Chiu, W. (2000). Visualization of the maturation transition in bacteriophage P22 by electron cryomicroscopy. *Journal of Molecular Biology* **297**, 615-626.
- Zhou, Z. H., Chen, D. H., Jakana, J., Rixon, F. J. & Chiu, W. (1999). Visualization of tegument-capsid interactions and DNA in intact herpes simplex virus type 1

virions. *Journal of Virology* **73**, 3210-3218.